Universidade do Minho
Escola de Ciências

Sara Margarida Araújo Ferreira

^{99m}Tc-PEI-MP and ^{188}Re-PEI-MP for Imaging and Therapy of the Bladder Malignant Tumours – An Experimental Study

abril de 2015

Universidade do Minho
Escola de Ciências

Sara Margarida Araújo Ferreira

^{99m}Tc-PEI-MP and ^{188}Re-PEI-MP for Imaging and Therapy of the Bladder Malignant Tumours – An Experimental Study

Programa Doutoral em Biologia Molecular e Ambiental
Especialidade em Biologia Celular e Saúde

Trabalho realizado sob a orientação da
Professora Doutora Maria Filomena Botelho
da
Professora Doutora Irene Dormehl
e da
Professora Doutora Célia Pais

abril de 2015

DECLARAÇÃO

Nome: Sara Margarida Araújo Ferreira

Endereço electrónico: saramaferreira@gmail.com

Título da tese de doutoramento: ^{99m}Tc-PEI-MP and ^{188}Re-PEI-MP for Imaging and Therapy of the Bladder Malignant Tumours – An Experimental Study

Orientadores: Professora Doutora Maria Filomena Botelho**,** Professora Doutora Irene Dormehl e Professora Doutora Célia Pais

Ano de conclusão: 2015

Designação do doutoramento: Programa Doutoral em Biologia Molecular e Ambiental, Especialidade em Biologia Celular e Saúde

Universidade do Minho, ____ / ____ / _____

Assinatura: _____

STATEMENT OF INTEGRITY

I hereby declare having conducted my thesis with integrity. I confirm that I have not used plagiarism or any form of falsification of results in the process of the thesis elaboration.

I further declare that I have fully acknowledged the Code of Ethical Conduct of the University of Minho.

University of Minho, _____

Full name: _____

Signature: _____

Acknowledgments

Although a doctorate thesis is an individual work, many were those who directly or indirectly contributed to the completion of this work that I engaged myself, and to which I owe my thanks.

To Professor Maria Filomena Botelho, director of the Biophysics Unit, of the Faculty of Medicine of the University of Coimbra, the supervisor of this project, my thanks for having me integrated within his research group, for the support and dedication throughout the development of this project, for comments, suggestions and always timely advice in reviewing this manuscript, and finally, but not last, by the sharing of knowledge and scientific experience.

To Professor Irene Dormehl, co-advisor of this project, that despite the distance was always available to share its scientific knowledge, and my thanks for the advice and constructive criticism and dedication shown throughout this work.

To Professor Célia Pais, co-advisor of this project, I'm thankful for its availability and for their help on the development of this project.

To the Doctors Werner Louw and Jan Zeevaart, from the department of Radiochemistry of NECSA in South Africa, my thanks for the synthesis of the polymer PEI-MP, and for their help in knowing the polymer. To the professionals and the departments of Nuclear Medicine of the Oncology Institute and of the University Hospitals of Coimbra, my thanks for providing the ^{99m}Tc-Pertechnetate, without which it would not be possible to complete this work.

To Professor Margarida Abrantes and Master Mafalda Laranjo thank you for the examples of work and dedication, for the cooperation in various tasks, for the teachings and availability demonstrated throughout these years of work.

To my cabinet, laboratory colleagues and friends, the Masters Catarina, Ana, Salomé, Fernando and Siri, my thanks for the words of support, for the company, for the sharing of knowledge and cooperation.

To Master João Casalta, for the availability and valuable help in the statistical analysis of the results of this work. To Professor Ana Bela Sarmento Ribeiro

and Master Cristina Gonçalves for the availability and valuable help in the flow cytometry studies.

To all the other laboratory colleagues who directly or indirectly contributed to the development of this work, and by cooperation, mutual support and friendship environment. To my colleagues of the Nuclear Medicine Course of the High Institute of Allied Health Technologies of Porto's Polytechnic Institute, for the words of support and incentive, and for being the springboard to propel me in this adventure. To Cláudia Caridade I appreciate the friendliness and availability.

To Marco I appreciate the support and affection, the love and patience in less good days, for the joy on good days and for being part of my life. To my parents, my baby sister and my grandparents, I thank their love and affection, their wise counsel and inexhaustible understanding.

To God who certainly has guided all my steps, who put these people in my way and other people which, not having been mentioned, were definitely not forgotten.

"To be great, be whole;

Exclude nothing, exaggerate nothing that is not you.

Be whole in everything. Put all you are

Into the smallest thing you do.

So in each lake, the moon shines with splendour

Because it blooms up above."

Fernando Pessoa

Abstract

^{99m}Tc-PEI-MP and ^{188}Re-PEI-MP for Imaging and Therapy of the Bladder Malignant Tumours – An Experimental Study

Bladder cancer is the most common malignancy of the urinary tract, and is the fifth most common tumour world-wide, being responsible for about 2% of all cancer deaths. Current methods of diagnosis of the bladder cancer are mainly morphologic imaging techniques, while physiological imaging techniques, like nuclear medicine imaging that would enable to detect the disease in a very early stage, is not being fully availed for this type of cancer. The main methods to treat bladder cancer are aggressive and invasive to the patient, in a time where conservative management, with organ preservation, is now the standard of care in numerous malignancies. There is no reference to the use of radiopharmaceuticals for bladder cancer therapy, nevertheless, the existence of a specific radiopharmaceutical to bladder cancer could enable the delivery of high doses of radiation to the target tissue with minimal side effects, and some current therapy modalities could be substituted. Searching for a molecule for use in the palliative therapy of bone metastasis, the water soluble polymer polyethyleneiminomethyl phosphonic acid (PEI-MP), was synthesized. Pre-clinical studies performed with PEI-MP labelled with several radionuclides, demonstrated the high value of accumulation and retention by the bladder wall, which could demonstrate some affinity of PEI-MP to bladder cells, and possibly by bladder cancer cells. Thus, the aim of this work was to explore *in vitro* and *in vivo* the potential of PEI-MP radiolabelled with ^{99m}Tc or ^{188}Re, for imaging and radionuclide therapy of bladder cancer. In a first stage it was prepared the PEI-MP kits for a quick and easy radiolabelling with ^{99m}Tc or ^{188}Re, and to ensure high radiochemical purity. For *in vitro* studies, the cell lines of human bladder carcinoma (HT-1376) and human osteosarcoma (MNNG/HOS) were used. The osteosarcoma cells were used considering the original intent of using PEI-MP, and in order to make comparisons. Considering that PEI-MP should act only as a carrier for nuclear medicine imaging and therapy, cellular cytotoxicity of PEI-MP was analysed by the evaluation of the cellular metabolic activity and viability through spectrophotometry and flow cytometry. Cellular uptake and retention

studies of ^{99m}Tc-PEI-MP and ^{188}Re-PEI-MP were also performed. *In vivo* and *ex vivo* studies consisted on imaging and biodistribution studies performed in balb/c mice and balb/c n/nu mice with xenografts of bladder carcinoma and osteosarcoma, after the administration of ^{99m}Tc-PEI-MP and ^{188}Re-PEI-MP. The PEI-MP kits demonstrated to be suitable for radiolabelling, allowing to achieve a high radiochemical purity over 5 hours, revealing the stability of the kit formulation. PEI-MP didn't inhibit the metabolic activity or decreased the cell viability significantly and therefore would act as a carrier. Cellular uptake studies demonstrated that the uptake and retention of ^{99m}Tc-PEI-MP was, respectively, at least 5 and 4 times superior than the ^{99m}Tc-Pertechenetate for both cell lines. The same studies demonstrated that the uptake and retention of ^{188}Re-PEI-MP was, respectively, at least 62 and 194 times superior than the ^{188}Re-Perrhenate for both cell lines. These studies demonstrated the specificity of PEI-MP. *In vivo* and *ex vivo* studies demonstrated that ^{99m}Tc-PEI-MP and ^{188}Re-PEI-MP were mainly excreted through the renal system and a small amount by enterohepatic circulation. Also it was confirmed the uptake of ^{99m}Tc-PEI-MP and ^{188}Re-PEI-MP by lungs. The uptake of ^{99m}Tc-PEI-MP and ^{188}Re-PEI-MP by the xenografts of bladder carcinoma or osteosarcoma, that demonstrated to be superior to 1 in relation to muscle, may be related not only with the blood perfusion to the tumour or the enhanced permeability and retention effect associated with PEI-MP, but also with the presence of specific membrane receptors in the case of bladder carcinoma and high concentrations of Ca^{2+} in both tumour types. Tumour/bladder, tumour/liver, tumour/lung and tumour/bone were always inferior to one. These results demonstrated that for diagnostic nuclear medicine a bladder carcinoma and its metastases would present as cold lesions allowing identifying them in the images. One the other hand the therapy of bladder carcinoma and its metastasis seem not to be feasible if administered intravenously, considering the high dosimetry to other organs.

Resumo

^{99m}Tc-PEI-MP e ^{188}Re-PEI-MP para Imagiologia e Terapia de Tumores Malignos da Bexiga – Um Estudo Experimental

O cancro da bexiga é a neoplasia maligna mais comum do trato urinário, e é o quinto tumor mais comum em todo o mundo, sendo responsável por cerca de 2% de todas as mortes relacionadas com o cancro. Os métodos actuais de diagnóstico para o cancro da bexiga são principalmente técnicas de imagem morfológicas, sendo que as técnicas de imagem fisiológicas, como as da medicina nuclear que permitiriam detectar a doença numa fase inicial, não estão ser totalmente aproveitadas para este tipo de cancro. Os principais métodos de terapia para o cancro da bexiga são agressivos e invasivos para o doente, numa época em que o tratamento conservador, com preservação de órgãos, é agora o padrão para o tratamento de diversas neoplasias. Não há nenhuma referência à utilização de radiofármacos para a terapia do cancro da bexiga, no entanto, a existência de um radiofármaco específico pode permitir a entrega de elevadas doses de radiação ao tecido alvo e com mínimos efeitos secundários, e algumas modalidades de tratamento actuais poderão vir a ser substituídas. Na procura de uma molécula para o tratamento paliativo de metástases ósseas, o ácido fosfónico solúvel em água polietilenoiminometil (PEI-MP), foi sintetizado. Estudos pré-clínicos realizados com o PEI-MP marcado com vários radionuclídeos, demonstraram uma elevada captação e retenção pela parede da bexiga, evidenciando a possível afinidade do PEI-MP para as células da bexiga e possivelmente para células de cancro da bexiga. Assim, o objetivo deste trabalho foi explorar *in vitro* e *in vivo* o potencial do PEI-MP radiomarcado com ^{99m}Tc ou ^{188}Re, para a imagiologia e terapia com radionuclídeos do cancro da bexiga. Numa primeira fase, foram preparados os kits de PEI-MP para uma radiomarcação rápida e fácil com o ^{99m}Tc ou ^{188}Re, e para assegurar a alta pureza radioquímica. Para os estudos *in vitro*, foram utilizadas as linhas celulares humanas de carcinoma da bexiga (HT-1376) e de osteossarcoma (MNNG/HOS). As células de osteossarcoma foram usadas tendo em conta a intenção inicial do PEI-MP, e de modo a fazer comparações. Considerando que o PEI-MP deve servir apenas como um veículo para a

imagiologia e terapia de medicina nuclear, a citotoxicidade celular do PEI-MP foi analisada avaliando a actividade metabólica e viabilidade celular através da espectrofotometria e citometria de fluxo. Também foram realizados estudos de captação e retenção celulares do ^{99m}Tc-PEI-MP e ^{188}Re-PEI-MP. Os estudos *in vivo* consistiram na realização de imagens e na análise da biodistribuição em ratinhos balb/c e balb/c nu/nu com xenoenxertos de carcinoma da bexiga e osteossarcoma após a administração de ^{99m}Tc-PEI-MP e ^{188}Re-PEI-MP. Os kits de PEI-MP mostraram-se adequados para a marcação radioactiva, permitindo obter um elevado grau de pureza radioquímica 5 horas após a marcação, revelando a estabilidade da formulação do kit. O PEI-MP não inibiu a actividade metabólica ou diminuiu de forma significativa a viabilidade celular, podendo assim ser usado como um veículo. Os estudos de captação celular demonstraram que a captação e retenção do ^{99m}Tc-PEI-MP foi, respecivamente, 5 e 4 vezes superior à do ^{99m}Tc-pertecnetato para ambas as linhas celulares. Os mesmos estudos demonstraram que a captação e retenção do ^{188}Re-PEI-MP foi, respectivamente, 62 e 194 vezes superior à do ^{188}Re-perrenato para ambas a linhas celulares. Estes estudos demonstraram a especificidade de PEI-MP. Os estudos *in vivo* e *ex vivo* demonstraram que o ^{99m}Tc-PEI-MP e ^{188}Re-PEI-MP são excretados maioritariamente por via renal e uma pequena quantidade pela circulação entero-hepática. A captação do ^{99m}Tc-PEI-MP e ^{188}Re-PEI-MP pelos xenotransplantes de carcinoma da bexiga ou osteosarcoma, que demonstrou ser superior ao valor de um em relação ao músculo, pode estar relacionada não só com a perfusão sanguínea para o tumor ou o efeito do aumento da permeabilidade e retenção associado ao PEI-MP, mas também com a presença de receptores de membrana específicos, no caso de carcinoma da bexiga e de concentrações elevadas de Ca^{2+} em ambos os tipos de tumores. As razões tumor/bexiga, tumor/fígado, tumor/pulmão e tumor/osso foram sempre inferiores ao valor de um. Estes resultados demonstraram que para o diagnóstico de carcinoma da bexiga e suas metástases em medicina nuclear, o tumor e as metástases surgiriam nas imagens como lesões frias, permitindo a sua identificação. Por outro lado, a terapia de carcinoma da bexiga e suas metástases parece não ser viável se administrado por via intravenosa, considerando a dosimetria elevada para outros órgãos.

Table of Contents

List of Symbols, Abbreviations, Expressions and Chemical Formulas

µCi//µg – Microcurie per microgram

µl – Microliters

µm – Micrometer

µM – Micromolar

$^{111/114}$**In** – Indium-111/114

^{115m}**In** – Indium-115 metastable

$^{131/123/124/126}$**I** – Iodine-131/123/124/126

^{153}**Sm** – Samarium-153

$^{161/149}$**Tb** – Terbium-161/149

^{166}**Ho** – Holmium-166

^{167}**Tm** – Thulium-167

^{177}**Lu** – Lutetium-177

$^{188/186}$**Re** – Rhenium-188/186

^{188}**ReO$_2$** – Reduced-hydrolysed rhenium-188

^{188}**W** – Tungsten-188

^{18}**F** – Fluorine-18

$^{193/195m}$**Pt** – Platinum-193/195 metastable

^{201}**Tl** – Thalium-201

^{203}**Pb** – Lead-203

^{211}**At** – Astatine-211

$^{213/212}$**Bi** – Bismuth-213/212

$^{224/223}$**Ra** – Radium-224/223

^{225}**Ac** – Actinium

^{226}**Th** – Thorium-226

^{32}**P** – Phosphorus-32

^{51}**Cr** – Chromium-51

^{67}**Cu** – Copper-67

^{67}**Ga** – Gallium-67

$^{76/77}$**As** – Arsenic-76/77

^{77}**Br** – Bromine-77

^{89}**Sr** – Strontium-89

^{90}Y – Yttrium-90

$^{94/99}$Tc – Technetium-94/99

^{99}Mo – Molybdenum-99

^{99m}Tc – Technetium-99 metastable

$^{99m}TcO_2$ – Reduced-hydrolysed techetium-99 metastable

$^{99m}TcO_4^-$ – Anionic pertechnetate

^{99}Ru – Ruthenium-99

AJCC – American joint committee on cancer

Al_2O_3 – Aluminium oxide

ALSYMPCA – Alpharadin in symptomatic prostate cancer

ANOVA – Analysis of variance

APD – 3-amino-1-hydroxypropylidene-1,1-diphosphonate

APDDMP – N,N,-dimethylene-phosphonate-1-hydroxy-4- aminopropylidene-diphosphonate

ATCC – American type culture collection

ATP – Adenosine triphosphate

AV/PI – Annexin-V/propidium iodide

BAK – Bcl-2 homologous antagonist killer

BAX – Bcl-2-associated X protein

BCG – Bacillus calmette-guérin

BCL-2 – B-cell Lymphoma 2 Protein

BCL-W – Bcl-2-like protein 2

BCL-XL – B-cell lymphoma-extra large

BID – BH3 interacting domain death agonist

BIM – Bcl-2-like protein 11

CDK – Cyclin-dependent kinase

CDKN2A – Cyclin-dependent kinase inhibitor 2A gene

CDKN2B – Cyclin-dependent kinase 4 Inhibitor B protein

CHEK2 – Checkpoint kinase 2 gene

CIP1 – Cyclin-dependent kinase inhibitor 1

cm – Centimeters

c-MYC – Myelocytomatosis oncogene

CPM – Counts per minute

CT – Computed tomography

CXCR4/12 – C-X-C chemokine receptor type 4/12

DCF – Dichlorofluorescien

DCFH2 – 2,7-dichlorodihydrofluorescein

DCFH2-DA – 2,7-dichlorodihydrofluorescein diacetate

DHE – Dihydroethidium

DMEM – Dulbecco´s modified eagle´s medium

DMSO – Dimethyl sulfoxide

DNA – Deoxyribonucleic acid

DOTA – 1,4,7,10-tetraazacyclododecane-1,4,7,10-tetraacetic acid

DOTMP – 1,4,7,10-tetraazacyclododecane-1,4,7,10-tetramethylene phosphonate

DTPA – Diethylene triamine pentaacetic acid

e^- – Electron

EBRT – External-beam radiation therapy

EC – Electron capture

E-cadherin – Calcium-dependent adhesion

EDTA – Ethylenediamine tetraacetic acid

EDTMP – Ethylene-diamine-tetramethylene-phosphonate

ELISA – Enzyme linked immunosorbent assay

EPR effect – Enhanced permeability and retention effect

EXT1/2/3 – Exostosin-1/2/3 genes

FAS – Type-II transmembrane protein

FDG – Fluorodeoxyglucose

FGFR3 – Fibroblast growth factor receptor 3 gene

g – Gram

G force – Gravitational force

GBq/µg – Gigabecquerel per microgram

GLUT1 – Glucose transporter 1

GSH – Reduced glutathione or L-glutamyl-L-cysteinyl-glycine

GSSG – Glutathione disulfide

GSTM1 – S-transferase mu 1

Gy – Gray

H_2O – Chemical formula of water

H_2O^+ – Chemical formula of ion radical of water

H_2O_2 – Hydrogen peroxide

HBP – 4-amino-1-hydroxybutylidene-1,1-bisphosphonate

HCl – Hydrochloric acid

HEDP – 1-hydroxy-ethylene-diphosphonic acid

HIF1α/2α – Hypoxia-Inducible factors 1-alpha/2-alpha

HNO_3 – Nitric acid

HO_2 – Hydroperoxyl

$HReO_4$ – Perrhenic acid

HT-1376 – Bladder transitional cell carcinoma cell line

HTRA2 – HtrA serine peptidase 2

IL-6/8 – Interleukin 6/8

IT – isomeric transition

ITLC – Instant thin layer chromatography

ITLC-SA – Instant thin layer chromatography-silicic acid

ITLC-SG – Instant thin layer chromatography-silica gel

IVU – Intravenous urography

JC-1 – 5,5´,6,6´-tetrachloro-1,1´,3,3´-tetraethylbenzimidazol-carbocyanine iodide

kDa – Kilodalton

keV – Kilo electronvolt

keV/µm – Kilo electronvolt per micrometre

KLH – Keyhole-limpet hemocyanin

LET – Linear energy transfer

log Po/w – Partition coefficient

mAbs – Monoclonal antibodies

MDP – Methylene-diphosphonic acid

MEK – Methyl ethyl ketone

MeV – Mega electronvolt

Mg^{2+} – Magnesium ion

mGy – Milligray

mHg – Milimeters of mercurie

MIBG – Meta-iodobenzylguanidine

ml – Milliliter

mm – Millimetre

MNNG/HOS – Human osteosarcoma cell line

MRI – Magnetic resonance imaging

mSv – Millisievert

MTT – 3-(4,5-dimethylthiazolyl-2)2,5-diphenyltetrazolium bromide

Na(Tl) crystal – Sodium iodide doped with thallium scintillator crystal

$Na^{188}ReO_4$ – Sodium perrhenate

$Na^{99m}TcO_4$ – Sodium pertechnetate

NAT2 – acetylator N-acetyltransferase 2

NOXA – Phorbol-12-myristate-13-acetate-induced protein 1

O^{2-} – Superoxide anion

$O2^{2-}$ – Peroxide

ºC – Degree celsius

OER - Oxygen enhancement radio

OH• - Hydroxyl radical

p34cdc2 - Cyclin-dependent kinase 1 also known as CDK1

***P53*/P53** - Tumour supressor 53 gene/protein

PBS - Phosphate buffered saline

PEI - Polyethyleneimine

PEI-MP - Polyethyleneiminomethyl phosphonic acid

PET - Positron emission tomography

PI3K-PKB - Phosphoinositide 3-kinase and protein kinase B

PUMA - P53 upregulated modulator of apoptosis

PUNLMP - Papillary urothelial neoplasm of low malignant potential

***RAS*/RAS** - Rat sarcoma gene/protein

RBE - Relative biologic effect

REQL4 - ATP-dependent DNA helicase Q4 gene

RIA - Radioimmunoassay

rmp - Rotations per minute

RNA - Ribonucleic acid

RNS - Reactive species of nitrogen

ROI - Region of interest

ROS - Reactive oxygen species

SEER - Surveillance, epidemiology, and end results program

SF - Solvent front

Si-OH - Silanol

Si-O-Si - Siloxane

SMAD4 - Mothers against decapentaplegic homolog 4

$SnCl_2$ - Stannous chloride

SPECT - Single photon emission tomography

SPSS - Statistical package for the social sciences

SRC - Subrenal capsule

$T½_b$ - Biological half-life

$T½_e$ - Effective half-life

$T½_f$ - Physical half-life

TGFβ - Transforming growth factor beta

TSC1/2 - Tuberous sclerosis 1/2 genes

UICC - Union international contre le cancer

US - Ultrasonography

VEGF - Vascular endothelial growth factor

W3MM - Whatman® cellulose chromatography papers 3MM chr sheets

WHO - World health organization

α - Alpha

$β^-$ - Beta negative

$β^+$ - Positron

List of Figures

List of Tables

List of Equations

Section I. Preamble

The following work corresponds to the doctoral thesis, carried out under the Doctoral Program in Molecular and Environmental Biology of the School of Science in the University of Minho.

The experimental work was developed in the Biophysics unit of the Faculty of Medicine of the University of Coimbra, under the supervision of Professor Maria Filomena Botelho (MD, PhD), Full Professor of the Faculty of Medicine of the University of Coimbra. The work also included the co-orientation of the Professor Irene Dormehl (DSc, PhD), Emeritus Professor of the University of Pretoria and Professor Extraordinary of the North-West University in South Africa, and of Professor Célia Pais (DSc, PhD), Associate Professor of the School of Sciences in the University of Minho.

The following work resulted in the publication of an article in an international journal and a number of abstracts in international and national journals. The article and abstracts published here are listed:

Papers in periodics with scientific refereeing (Articles):

1. **Ferreira S**, Dormehl I, Botelho MF: Radiopharmaceuticals for bone metastasis therapy and beyond: a voyage from the past to the present and a look to the future. Cancer biotherapy & radiopharmaceuticals 2012, 27(9):535-551 (doi:10.1089/cbr.2012.1258)

   SCImago Journal Rank (SJR): Q2

   Citations: 5

Papers in conference proceedings with scientific refereeing (Abstracts):

1. **SM Ferreira**, AM Abrantes, M Laranjo, *et al*; Evaluation of the potential of ^{99m}Tc-PEI-MP for diagnosis and follow-up, in a comparative study using in vivo models of bladder cancer and osteosarcoma; Eur J Nucl Med Mol

Imaging 2014; 41 (Suppl 2): S151-S705 *(work presented in the 27th Annual Congress of the European Association of Nuclear Medicine, Gothenburg)*

2. **S Ferreira**, AM Abrantes, AF Brito, *et al*; Radiolabeled polyethyleneiminomethyl phosphonic acid as a molecule with potential for diagnosis and therapy. Comparative study on models of bladder cancer and osteosarcoma; Eur J Nucl Med Mol Imaging 2013; 40 (Suppl 2): S89-S567 *(work presented in the 26th Annual Congress of the European Association of Nuclear Medicine, Lyon)*
3. **Ferreira S**, Abrantes AM, Brito A, *et al*; A new possible approach for therapy and follow up of bladder cancer; Rev Port Pneumol. 2013;19 (Esp Cong 2):9-36; P55 *(work presented in the Updates in Oncology/2nd Congress of CIMAGO, Coimbra)*
4. Tavares-Silva E, **Ferreira S**, Abrantes AM, *et al*; Una posible nueva molécula para el diagnóstico y seguimiento del cáncer de vejiga: el polímero radiomarcado ^{99m}Tc-PEI-MP; Actas Urológicas Españolas 2013; 37(S1): pág. 190 *(work presented in the LXXVIII Congreso Nacional de Urología, Granada)*
5. **S Ferreira**, M Laranjo, AM Abrantes, *et al*; The potential of ^{99m}Tc-PEI-MP for diagnosis and ^{188}Re-PEI-MP for therapy of bladder carcinoma; Eur J Nucl Med Mol Imaging 2012; 39 (Suppl 2): S384-S497 *(work presented in the 25th Annual Congress of the European Association of Nuclear Medicine, Milan)*
6. **S Ferreira**, M Laranjo, AM Abrantes, *et al*; An *in vivo* study to analyse the potential of ^{188}Re-PEI-MP for metabolic radiotherapy of bladder carcinoma; Annals of Oncology 23 (Supplement 1): i26–i44, 2012 (doi:10.1093/annonc/mds018) *(work presented in the 25th TAT 2012 - Targeted Anticancer Therapies 2012, Amsterdam)*
7. **S Ferreira**, M Laranjo, AM Abrantes, *et al*; An *in vivo* evaluation of the potential of 188Re-PEI-MP for therapy of bladder carcinoma and ^{99m}Tc-PEI-MP for diagnosis and follow up; European Journal of Cancer; Vol.48 July, 2012, p.S272, Supplement 5 *(work presented in the European Association Cancer Research Congress, Dublin)*
8. **Ferreira S**M, Laranjo M, Brito A, *et al*; The potential of ^{188}Re-PEI-MP for metabolic radiotherapy of bone tumors; Acta Médica Portuguesa;

Suplemento nº1/2011, Dezembro 2011 *(work presented in the Updates in Oncology 2011, Coimbra)*

9. **SM Ferreira**, AM Abrantes, LF Metello, *et al*; ^{188}Re-PEI-MP as a potential agent for metabolic radiotherapy; Eur J Nucl Med Mol Imaging 2011, Vol 38, Suppl 2: S93-S228 *(work presented in the 24th Annual Congress of the European Association of Nuclear Medicine, Birmingham)*

A research article was submitted to an international journal and is waiting for revision, and is expected to compose and submit another research article until the beginning of next year.

This work is organized in sections starting with the preamble, followed by the literature review, the experimental studies, the discussion and conclusions and finally the bibliography. The literature review, or section II, is organized in chapter 1 to 4, where general topics are reviewed such as what is cancer and what is implied and the current diagnostic and therapy techniques, following by more specific revisions in order to know the history of PEI-MP and be familiar with the particularities of bladder cancer and what are the current methods of diagnosis and therapy. The section III, dedicated to the experimental studies is organized in chapter 5 and 6, where are presented the material and methods, results, and discussion of the experimental studies carried out *in vitro* and *in vivo*/*ex vivo*.

Considering that it was not possible to obtain a second generator of ^{188}W/^{188}Re, some studies were not concluded, especially with respect to the *in vitro* studies. Despite this situation the studies with ^{188}Re allowed to draw final conclusions.

Section II. Literature Review

Chapter 1.Cancer

1.1. Introduction

Development, differentiation, and the maintenance of vital functions involve exact regulation of the time and location of the cell divisions and self-elimination programmed cell death, or apoptosis. A tumour arises as a result of uncontrolled cell division and failure of programmed cell death [1, 2].

Most tumours can be classified clinically as benign or malignant [3, 4]. The cells of the malignant tumours are pleomorphic, varying in size and shape. Furthermore, these cells are less differentiated, or anaplastic, then their benign counterparts [4]. Malignant tumours occur as a result of mutations in three basic types of genes: DNA (Deoxyribonucleic acid) repair genes, tumour suppressor genes, and proto-oncogenes. Alterations in these genes are responsible for the deregulated control mechanisms, that are the hallmarks of cancer cells [1, 2, 5].

1.2. Hallmarks of cancer

Cells must acquire a series of traits in order to become malignant. These traits have been grouped in categories, as represented in fig. 1 [6, 7].

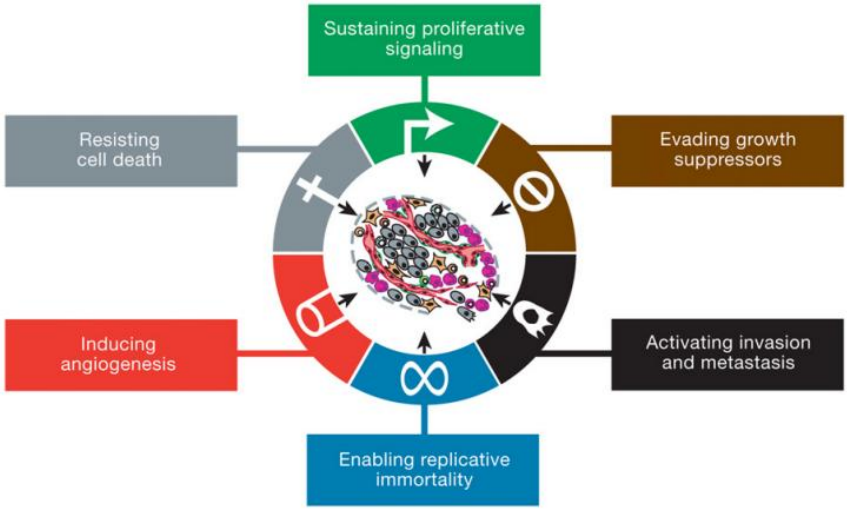

Figure 1. The hallmarks of cancer, organized in six categories, namely the sustaining proliferative signals, evading growth suppressors, resisting cell death, replicative immortality, angiogenesis, invasion and metastasis (Hanahan D. *et al.*, 2011).

1.2.1. Sustaining proliferative signalling

Normal tissues control the production and release of growth-promoting signals, giving instructions for the progression through the cell growth-and-division cycle, ensuring the maintenance of cell number and of normal tissue architecture and function [6]. These signals are transmitted into the cell by transmembrane receptors that bind to unique classes of signalling molecules, namely diffusible growth factors, extracellular matrix components and cell-to-cell adhesion/interaction molecules.

Such behaviour contrasts strongly with that of tumour cells. Tumour cells generate many of their own growth signals, thus reducing their dependence on stimulation from their normal tissue microenvironment [7].

Cancer cells can acquire the capability to maintain proliferative signalling in a number of different ways, namely producing growth factor ligands (to which they can respond *via* the expression of cognate receptors, resulting in autocrine proliferative stimulation) and sending signals to stimulate normal cells within the supporting tumour-associated stroma, which respond by supplying the cancer cells with a variety of growth factors [6].

Growth factor receptors, often carrying tyrosine kinase activity in their cytoplasmic domains, are over-expressed in many cancers. Receptor over-expression may facilitate the cancer cell to become hyper-responsive to normal levels of growth factors that usually would not trigger proliferation [6, 7].

Cancer cells also control the expression of the types of extracellular matrix receptors (integrins), favouring ones that transmit pro-growth signals. The successful binding to specific moieties of the extracellular matrix, enable the transduction of signals into the cytoplasm by the integrin receptors, that influence cell behaviour, ranging from quiescence to motility in normal tissue, resistance to apoptosis, and entrance into the cell cycle. On the other hand, the failure of integrins to build these extracellular links can prejudice cell motility, induce apoptosis, or cause cell cycle arrest [6, 7].

1.2.2. Evading growth suppressors

Multiple anti-proliferative signals operate to maintain cellular quiescence and tissue homeostasis in normal tissue. Both soluble growth inhibitors and immobilized inhibitors embedded in the extracellular matrix and on the surfaces of nearby cells are anti-proliferative signals [7].

Antigrowth signals can block proliferation by two distinct mechanisms:

– cells may be forced out of the proliferative cycle into the quiescence state (G_0) from which they may remerge when extracellular signals allow;
– cells may be induced to permanently give up their proliferative potential by being induced to enter into post-mitotic states, typically associated with acquisition of particular differentiated-associated traits [7].

To prosper, cancer cells must evade these anti-proliferative signals. Much of the circuitry that enables normal cells to respond to antigrowth signals is linked with the cell cycle clock, particularly the component governing the transit of the cell through the G_1 phase. At the molecular level, many of the anti-proliferative signals are funnelled through the retinoblastoma protein and its two relatives, the retinoblastoma-like protein 1 and 2 [7]. When in a hypophosphorylated

state, retinoblastoma protein blocks proliferation by sequestering and changing the function of transcription factor family that control the expression of banks of genes, that are essential to the progression from G_1 into S phase [8].

Disruption of the retinoblastoma protein pathway liberates transcription factors and consequently allows cell proliferation, turning cells insensible to antigrowth factors that operate along this pathway to block advance through the G_1 phase of the cell cycle. The soluble signalling molecule TGFβ (Transforming growth factor beta) acts in a number of ways to stop the phosphorylation that inactivates retinoblastoma protein, blocking the advance through G_1. In some cell types, TGFβ suppresses expression of the *c-MYC* (Myelocytomatosis oncogene) gene, which regulates the G_1 cell cycle apparatus [7]. Also, TGFβ causes synthesis of the CDKN2B (Cyclin-dependent kinase 4 inhibitor B Protein) and CIP1 (Cyclin-dependent kinase Inhibitor 1) proteins, which block the CDK (Cyclin-dependent kinase) complexes responsible for the retinoblastoma protein phosphorylation [9].

Some lose responsiveness to TFGβ, through down regulation of their receptors, while others display dysfunctional receptors. The cytoplasmic SMAD4 (Mothers against decapentaplegic homolog 4) protein, responsible for the transduction of signals from ligand-activated TFGβ receptors to downstream targets, may be eliminated through mutation of its encoding gene [10]. The locus encoding CDKN2B may be deleted. Alternatively, the immediate downstream targets of its actions may become unresponsive to the inhibitory actions of CDKN2B given to mutations that create amino acid substitutions. The resulting CDK complexes are then given a free hand to inactivate retinoblastoma protein by hyperphosphorilation. Finally, functional retinoblastoma protein, may be lost through mutations of this gene [7].

1.2.3. Resisting cell death

The capability of tumour cell populations to increase in number is determined not only by the rate of cell proliferation but also by the rate of cell attrition. Apoptosis represents the major source of this attrition [7].

The apoptotic machinery is composed of both upstream and downstream effectors components [11]. The regulators, in turn, are divided into two major circuits, one receiving and processing extracellular death-inducing signals (the extrinsic apoptotic program, involving the FAS (Type-II transmembrane protein) ligand/FAS receptor, and the other sensing and integrating a variety of signals of intracellular origin (the intrinsic program).

Each of these programs culminates in the activation of caspases 8 and 9, which proceeds to initiate a cascade of proteolysis involving effectors caspases that are responsible for running apoptosis, in which the cell is progressively disassembled and then consumed, both by its neighbours and by phagocyte cells. Currently, the intrinsic apoptotic program is more widely implicated as a barrier to cancer pathogenesis [6, 7].

Many of the signals that elicit apoptosis converge on the mitochondria, which in turn respond to pro-apoptotic signals by releasing cytochrome C, that is a potent catalyst of apoptosis [7]. The “apoptotic trigger” that conveys signals between the regulators and effectors is controlled by counterbalancing pro- and anti-apoptotic members of the BCL-2 (B-cell lymphoma 2 protein) family of regulatory proteins [11]. Members of the BCL-2 family, whose members have either pro-apoptotic (BAX, BAK, BID, BIM) or anti-apoptotic (BCL-2, BCL-XL, BCL-W) function, act partly by governing mitochondrial death signalling through cytochrome C release. The release of cytochrome C, activates a cascade of caspases that act via their proteolytic activities, inducing the multiple cellular changes associated with the apoptotic program [6, 7]. Several abnormality sensors that play key roles in tumour development have been identified [11, 12]. Most prominent is a DNA-damage sensor that functions via the *P53* tumour suppressor gene [13]. *P53* induces apoptosis by up-regulating expression of the NOXA (Phorbol-12-myristate-13-acetate-induced protein 1) and PUMA (P53 upregulated modulator of apoptosis) proteins, in response to substantial levels of DNA breaks and other chromosomal abnormalities [6].

The most frequently occurring loss of a pro-apoptotic regulator through mutation involves the *P53* tumour suppressor gene. The resulting functional inactivation of its product, the P53 protein, is seen in more than 50% of human cancers and

results in the deletion of a key component of the DNA damage sensor that can induce the apoptotic effectors cascade [14]. Signal evoked by other abnormalities, including hypoxia and oncogene hyper-expression, result in part *via TP53* to the apoptotic machinery. These two are impaired at eliciting apoptosis when P53 function is lost [15]. Additionally the PI3K-PKB (Phosphoinositide 3-kinase and protein kinase B) pathway, which transmits anti-apoptotic survival signals, is probably involved with apoptosis in a substantial fraction of human tumours [7].

1.2.4. Enabling replicative immortality

A decade ago, it was widely accepted that cancer cells require infinite replicative potential in order to produce tumours. This capability is a marked contrast comparatively with “normal cells”, which are able to pass through only a limited number of cell growth-and-division cycles. This limitation has been associated with two different barriers to proliferation: senescence and crises. Senescence is an irreversible entrance into a non proliferative but viable state, and crisis involves cell death. Accordingly, when cells are propagated in culture, repeated cycles of cell division lead to senescence and after, the cells that succeed in circumventing this barrier, progresses to crisis phase in which the great majority of cells die. On rare occasions, cells emerge from a population in crisis and exhibit unlimited replicative potential. This transition has been called immortalization, an attribute that most established cell lines possess since they can proliferate in culture without evidence of either senescence or crisis [6, 7].

Multiple evidences indicate that telomeres who protecting the ends of chromosomes, have a pivotal role on the capability for unlimited proliferation [16]. In fact, telomere length underlies the number of times a cell can have successive division. In each cell division, the telomeres decrease the length which means that they lose their function of protection causing cell death [6].

The telomerase is an enzyme that adds, to the end of the telomere, repetitive DNA sequences. Without telomerase, the cells can only divide 50 to 70 times, but after they become senescent and stop the cell division. This is what

happens in the normal cells, non-immortalized. If telomerase is present, any cell can divide without limit. This is what happens in immortalized cells that include cancer cells. In fact, cancer cells can spontaneously become immortalized. By extending telomeric DNA, telomerase is able to respond to the progressive telomere erosion that would otherwise occur in its absence. The presence of telomerase activity, both in spontaneously immortalized cells or in the context of cells engineered to express the enzyme, is correlated with a resistance to the induction of both senescence and crisis. Conversely, suppression of telomerase activity leads to telomere shortening and to the activation of one or more of these proliferative barriers [6, 7].

1.2.5. Inducing angiogenesis

For the cell function and survival, the oxygen and nutrients supplied by the vasculature are crucial. Therefore, virtually all cells in a tissue should reside within 100 µm of a capillary blood vessel. This closeness is ensured during organogenesis, by coordinated growth of vessels and parenchyma. Once a tissue is formed, the angiogenesis (growth of new blood vessels) is transitory and carefully regulated [7]. However, if the cells are within aberrant proliferative lesions, initially they lack angiogenic ability, which reduces their capability for expansion [17].

The dominance of positive or negative signals determines the promotion or the blocking of angiogenesis. Some of these signals are transmitted by soluble factors who bind to receptors located on the surface of endothelial cells. In this context, also integrins and some adhesion molecules who mediate cell-matrix and cell-cell relations have a critical role. The initiation signals of angiogenesis are due to the vascular endothelial growth factor (VEGF) and acidic and basic fibroblast growth factors which bind to transmembrane tyrosine kinase receptors in the endothelial cells [18]. A typical example of an angiogenesis inhibitor is the thrombospondin-1, which binds to cluster of differentiation 36, a transmembrane receptor on endothelial cells coupled to intracellular sarcoma-like tyrosine kinases [7].

Like any tissue, tumours need oxygen and nutrients as well as eliminate carbon dioxide and metabolic waste. These two functions are achieved by the neovasculature associated with the tumour. During embryogenesis, two processes are involved in the vasculature development, the vasculogenesis and the angiogenesis. The vasculogenesis is the appearing of new endothelial cells and their combinations to form the tubular system whereas the angiogenesis determines the appearance of new vessels from existing ones. After this stage, the normal vasculature becomes virtually quiescence, except in cases of a wound healing and female reproductive cycling, where angiogenesis is turned on transiently [6]. Oppositely during tumour progression, the process of angiogenesis remains switched on and new vessels are continually generated, helping to maintain the expanding growth [17].

Many tumours produce growth factors that stimulate angiogenesis whereas others are able to induce surrounding normal cells to synthesize and to secrete such factors [5]. The blood vessels produced inside the tumours as a result of the angiogenenic process are typically aberrant. In fact, the tumour neovasculature is marked by precocious capillary development, convoluted and excessive vessel branching, deformed and enlarged vessels, erratic blood flow, leakiness, and abnormal levels of endothelial cell proliferation and apoptosis [19]. The fundamental role of angiogenesis is also demonstrated by the effect of a large number of increasing catalogue of angiogenic substances to impair the growth of tumour cells inoculated subcutaneously in mice. Tumours arising in cancer-prone transgenic mice are similarly susceptible to angiogenic inhibitors [20].

1.2.6. Activating invasion and metastasis

At least for a time some malignant tumours remain localized and encapsulated, but eventually they gain the ability to progress, and the cells may invade the surrounding tissues, or even get into the body's circulatory system establishing secondary areas of proliferation (metastasis) [4, 5].

The metastases arise as amalgams of cancer cells and normal supporting cells from the host tissue. Successful invasion and metastasis depend upon all of the hallmarks capabilities [7].

Invasion of new tissues is non-random, and depends on the nature of the metastasizing cell and the invaded tissue. If the cells produce growth factors and angiogenesis factors, metastasis is facilitated. Tissues under attack are most vulnerable if they also produce growth factors, and are more resistant if they produce anti-proliferative factors, inhibitors of proteolytic enzymes, and anti-angiogenesis factors [5].

To disseminate widely in the body, the cells of a typical solid tumour must lose the adhesion to their original neighbours, escape from the tissue of origin, burrow through other tissues until they reach a blood or a lymphatic vessel. Reaching the blood vessel the cells must cross the basal lamina and endothelial lining of the vessel to enter in the circulation, enabling the cells to reach anywhere in the body. Each of these steps requires different properties. For example, in a variety of carcinomas, loss of adhesion to neighbouring cells in an epithelium depends on loss of expression of the epithelial cell-cell adhesion molecule E-cadherin (Calcium-dependent adhesion). However the ability to burrow through tissues seems to depend on the production of proteolytic enzymes that are able to break down extracellular matrix. The frequently observed down-regulation and occasional mutational inactivation of E-cadherin in human carcinomas demonstrated its key role as a suppressor of this hallmark capability [21]. By E-cadherin bridges is possible the coupling between adjacent cells, that in turn results in the transmission of antigrowth and other signals *via* cytoplasmic contacts with β-catenin to intracellular signalling circuits, including the lymphoid enhancer-binding transcription factor [7].

Cancer cells have a complex relation to the extracellular and basal lamina. The cells must degrade the basal lamina to penetrate it and metastasize, however in some cases cells may migrate along the lamina. Many tumour cells secrete a protein plasminogen to the active protease plasmin. This increased plasmin activity promotes metastasis by digesting the basal lamina, consequently allowing its penetration by tumour cells [5, 22].

Matrix-degrading proteases are typically associated with the cell surface, by synthesis with a transmembrane domain, binding to specific protease receptors, or association with integrins [23, 24].

Changes in integrin expression are also present in invasive and metastatic cells. Successful colonization of these new sites demand adaptation, which is achieved through shifts in the spectrum of integrin α or β subunits that are presented by the migrating cells [7].

The final steps in metastasis are probably the most difficult. Many tumours release large numbers of cells into the circulation, but fewer than 1 in 10000 cells that escape the primary tumour survive to colonize another tissue and form metastatic tumour. More than escaping from the original tumour and enter the blood, tumour cells must adhere to an endothelial cell lining a capillary and then migrate across or through it into the underlying tissue [5, 22].

Additionally to important changes in cell-surface proteins, dramatic changes occur in the cytoskeleton during tumour cell formation and metastasis. These alterations can result from changes in the expression of genes encoding rhodopsin and other small hydrolyzed guanosine triphosphate enzymes that regulate the actin cytoskeleton. For instance, tumour cells have been found to over-express the rhodopsin gene, and this increased activity stimulates metastasis [5].

1.2.7. Emerging hallmarks of cancer

New concepts for the formation and development of cancer have emerged. The chronic and often uncontrolled cell proliferation that represents the essence of neoplastic disease involves not only deregulated control of cell proliferation but also adjustments of energy metabolism in order to fuel cell growth and decision. Also, tumour formation involves the immune system that play a role in resisting or eradicating formation and progression of incipient neoplasias, late-stage tumours, and micrometastases [6].

1.2.7.1. Reprogramming energy metabolism

Normal cells, under aerobic conditions, process glucose, primary to pyruvate *via* glycolysis in the cytosol and subsequently to carbon dioxide in the mitochondria. Under anaerobic conditions, glycolysis is favoured and little pyruvate is dispatched to the oxygen-consuming mitochondria. Cancer cells, even in the presence of oxygen, can reprogram their glucose metabolism by limiting their energy metabolism to glycolysis, leading to a state that is called “aerobic glycolysis” [6].

This reprogramming of energy metabolism is apparently counterintuitive, given the fact that cancer cells must compensate the approximately 18-fold lower efficiency of adenosine triphosphate (ATP) production obtained by glycolysis in compared to mitochondrial oxidative phosphorylation. This is possible in part by up-regulating glucose transporters, particularly GLUT1 (Glucose transporter 1), which increases substantially glucose import into the cytoplasm [25, 26]. This markedly increased uptake and utilization of glucose, was documented in many human tumour types by noninvasively visualization glucose uptake using positron emission tomography (PET) with a radiolabelled analogue of glucose (^{18}F-fluorodeoxyglucose, FDG) [6].

The glycolytic fuelling has been shown to be connected with activated oncogenes such as *RAS*, or *MYC,* and mutant tumour suppressors such as *TP53* [25, 26]. This dependence on glycolysis can be further accentuated under the hypoxic conditions that operate within many tumours. The hypoxia response system acts pleiotropically to up-regulate glucose transporters and multiple enzymes of the glycolytic pathway [25-27]. Therefore, both the RAS oncoprotein and hypoxia can independently increase the levels of the HIF1α/2α (Hypoxia-Inducible factors 1-alpha/2-alpha) transcription factors, which in turn up-regulate glycolysis [28].

Curiously, some tumours have shown to contain two subpopulations of cancer cells that differ in their energy-generating pathways, but that function symbiotically. One subpopulation consists of glucose-dependent cells that secrete lactate, whereas cells of the second subpopulation preferentially import and utilize the lactate produced by their neighbours as their main energy

source, employing part of the citric acid cycle to do so [29]. Additionally, oxygenation ranging from normoxia to hypoxia, is not necessarily static in tumours but instead fluctuates temporally and regionally [30]. This situation may be a result of the instability and chaotic organization of the tumour neovasculature.

1.2.7.2. Evading immune destruction

The immune system plays a role in resisting or eradicating formation and progression of early neoplasias, late-stage tumours, and micrometastases. Therefore, according to this logic, solid tumours that appear have somehow managed to avoid detection by the immune system or have been able to limit the attack of the immunological defences, thereby evading eradication [6].

The role of defective immunological monitoring of tumours is validated by the striking increase of certain cancers in immunocompromised individuals [31]. However the great majority of these are virus-induced cancers, suggesting that much of the control of this class of cancers depends on the reduction of viral burden in infected individuals, partly through eliminating virus infected cells. These observations shed a little light on the possible role of the immune system in limiting formation of at least 80% of tumours of nonviral aetiology.

In recent years, studies using genetically engineered mice and the clinical epidemiology, suggested that the immune system operates as a significant barrier to tumour formation and progression, at least in some forms of non-virus-induced cancer. As an example, when mice genetically engineered to be immunocompromised were assessed for the development of carcinogen-induced tumours, it was observed that tumours arose more frequently and/or grew more rapidly in the immunodeficient mice relative to immunocompetent controls. In particular, deficiencies in the development or function of the cluster of differentiation 8 positive cytotoxic T lymphocytes, cluster of differentiation 4 positive T helper 1 cells, or natural killer cells each led to demonstrable increases in tumour incidence. Moreover, mice with combined immunodeficiencies in both T cells and natural killer cells were even more susceptible to cancer development. The result indicate that, at least in certain

experimental models, both the innate and adaptative cellular arms of the immune system are able to contribute significantly to immune surveillance and thus tumour eradication [32, 33].

1.3. Tumour grading and staging

The most widely used staging system is called the TNM system. It is based on the size and/or extent of the primary tumour (T), the extent of spread to lymph nodes (N), and presence of metastases (M) [3, 4]. The TNM system is currently used worldwide, enabling clinical scientists from various institutions to standardize the staging of tumours and compare the therapeutic results. The TNM system is resumed in the table 1 [4, 34].

Table 1. The TNM system (McKinnell R.G. *et al.*, 2006; AJCC, 2010).

Primary tumour (T)	
TX	Primary tumour cannot be evaluated.
T0	No evidence of primary tumour.
Tis	Carcinoma in situ.
T1-T4	Size and/or extent of the primary tumour.
Regional lymph nodes (N)	
NX	Regional lymph nodes cannot be evaluated.
N0	No regional lymph node involvement.
N1-N3	Degree of regional lymph node involvement.
Distant metastasis (M)	
MX	Distant metastasis cannot be evaluated.
M0	No distant metastasis.
M1	Distant metastasis present.

Legend: The TNM system is organized in three categories, namely the size and/or extent of the primary tumour (T), the extent of spread to lymph nodes (N), and presence of metastases (M). For each of these categories, subdivisions can be made according with the extent, for example, the size of the tumour, the grade of invasion to lymph nodes and metastases. Therefore, for Tx, Nx or Mx, the primary tumour, regional lymph nodes or metastasis cannot be evaluated. For T0, N0 or M0, there is no evidence of tumour, regional lymph node involvement or metastasis. From the moment in which is assigned a number, in a growing sequence (1, 2, 3...), to T, N or M, the size of the tumour, the involvement of lymph nodes and the presence of metastasis increases to, and the prognosis deteriorates.

The patient's prognosis deteriorates progressively if the tumour has invaded the stroma of an organ but has not penetrated it. It is worse if the wall is penetrated and even worse if its spreads to lymph nodes. It is dismal if there are distant metastases [4]. For many cancers, TNM combinations correspond to one of five stages resumed in table 2 [34].

Table 2. Stages of cancer (AJCC, 2010).

Stage	**Definition**
Stage 0	Carcinoma in situ (early cancer that is present only in the layer of cells in which it began).
Stage I, II and III	Higher numbers indicate more extensive disease: greater tumour size, and/or spread of the cancer to nearby lymph nodes and/or organs adjacent to the primary tumour.
Stage IV	The cancer has spread to distant tissues or organs.

Legend: The combinations from the TNM system can result in five stages of cancer, starting from stage 0, representing the most benign stage, where the tumour is still *in situ*, and then progressing to stages I, II and III. In these last stages the tumour starts to invade the lymph nodes and adjacent organs. The last stage, and the worst, is the stage IV, where the cancer has spread to distant organs and tissues.

Tumour grading is based on histological examination of tumours and is a semi-quantitative assessment of the malignancy of each tumour. In this process, the pathologist will assess the individual cells and the architectural organization of the tumour tissue. In most instances, the tumours can be graded on scale from 1 to 4, and are designated as well differentiated (grade 1), moderately well differentiated (grade 2), poorly differentiated (grade 3), or undifferentiated (grade 4) [3, 4].

In clinical practice, the tumour grading and tumour staging data are combined before additional therapy is recommended. The stage of the tumour at the time of diagnosis is also the most important prognostic parameter for most human tumours, and it can generally predict whether a tumour can be cured or not [3, 4].

1.4. Classification and nomenclature

The cells of the benign tumours and many malignant ones retain some microscopic features of the tissue of their origin. Therefore, the tumours are classified according to the tissue and cell type from which they arise, and then a suffix is add to denote whether the tumour is benign or malignant. Some examples of benign and malignant tumours and its nomenclature is represented in table 3 [3, 22].

Table 3. Classification and nomenclature of some benign and malignant tumours (Damjanov I., 2000; McKinnell R.G. *et al.*, 2006; Alberts D. *et al.*, 2008).

Tumour	**Suffix**	**Examples**	**Tissue and/or Origin**
Benign	Oma	Fibroma	Fibrous connective
		Lipomas	Fat
		Chondromas	Cartilage
		Neuromas	Nervous
		Osteoma	Bone
		Adenomas	Epithelial
Malignant	Carcinoma	Carcinoma of the lung	Epithelial
		Adenocarcinoma of breast	
	Sarcoma	Osteosarcoma	Mesenchymal tissues
		Chondrosarcoma	
	Blastoma	Neuroblastoma	Embryonic cells
		Nephroblastomas	

Legend: The tumours can be classified as benign or malignant. In order to distinguish them is attributed a suffix, the “oma” for benign tumours, and the suffix “carcinoma”, “sarcoma” or “blastoma” for malignant tumours, depending on the tissue of origin. If the malignant tumour has its origin in epithelial cells is attributed the suffix “carcinoma”, if had its origin in mesenchymal cells is attributed the suffix “sarcoma”, and finally if has its origin from embryonic cells is attributed the suffix “blastoma”.

Some malignant tumours cannot be classified as carcinomas, sarcomas, or blastomas. Most important among these are brain tumours which originate from glia cells and are thus called gliomas. Due to their location inside the brain these tumours cannot be completely removed and thus all gliomas are considered clinically malignant [4, 22].

Some tumours of the same name can be either benign or malignant. For example, islet cell tumours of the pancreas can be either benign or malignant.

Because the distinction cannot made clearly on histological examination, the noncommittal term islet cell tumour is used for most of these tumours. However, if such a tumour is accompanied by metastases, it is clearly malignant and so is designated a malignant islet cell tumour. Malignant tumours originating from lymphocytes are called lymphomas. Although their name sounds deceptively benign, it is worth notice that there are no benign lymphomas, and all tumours in this category should be considered malignant. Likewise, germ cell tumours composed of cell resembling the seminal cells of the testis have a benign-sounding name-seminoma, but all of them are malignant. Malignant melanoma, a common malignant tumour of pigmented cells of the skin (melanocytes) is colloquially known as “melanoma” [3, 4, 22].

Sometimes, some tumours have eponym names, that is, are known under the name of the physician who has described first. Ewing’s sarcoma is a poorly differentiated sarcoma of bones and soft tissue. Since the cell of origin of Ewing’s sarcoma has not been identified, there are no alternative names for this neoplasm. On the other hand, Wilm’s tumour is a widely used name for nephroblastoma, a childhood renal tumour. In some cases, these medical eponyms are a godsend. As an example, Kaposi’s sarcoma is easier to remembered and pronounced than the original proposed name, attributed by the famous nineteenth-century Viennese dermatologist who described and named it in Latin as “idiopathic pigmented hemorrhagic sarcoma” [3, 4].

Section II. Literature Review

Chapter 2.Diagnosis and Therapy of Cancer

2.1. Introduction

The main goals of cancer diagnosis and treatment is to cure or prolong considerably the life of patients and to ensure the best possible quality of life to cancer survivors [35].

Cancer is easier to treat and cure, and as a result mortality can be reduced, if it is diagnosed early. Therefore, a huge amount of effort was done to the development of ways to detect early signs of the disease. The most effective treatment programmes are those that are provided in a sustained and equitable way, linked to early detection and that adhere to evidence-based standards of care and a multidisciplinary approach [35, 36].

Cancer diagnosis methods include imaging, endoscopy, biopsy, blood tests and other samples, etc.

Driven by the diversity of genomic alterations involved in malignancy, a variety of assays had been developed with the purpose of complete tumour profiling. New molecular diagnostics, integrated into existing histomorphological classifications in surgical pathology, provides added stratification for a more accurate cancer prognosis [37]. Personalized treatment approaches are being developed based on the cancer diagnostic biomarkers [38]. These molecular markers can be products of altered genes/DNA or abnormal pathways. Some of the techniques involved in this group are: Fluorescence in situ hybridization technique, that uses probes to confirm the presence or absence of specific DNA sequences on chromosomes; Polymerase Chain Reaction, that permits amplification and analysis of target DNA regions in tumour samples; DNA microarray analysis is equipped to measure the expression levels of large number of genes concurrently; Immunocytochemistry used to detect antigens or protein expression on a fixed tissue section by means of an antibody that is specific for the antigen/protein; Flow cytometry to examine and differentiate

cells based on certain physical and chemical properties; Electron microscopy, used when specific cellular or intracellular structures need to be examined [37].

Histological diagnosis is still essential to establish the diagnosis of cancer. However, a well designed imaging strategy is important in the management of a patient with cancer. Imaging in oncology is used for screening, detection, diagnosis, treatment and to follow the response to treatment. Imaging techniques enable doctors to create detailed pictures of what is going on in our bodies non-invasively. Some of the imaging techniques that can be used for the diagnosis of cancer are the morphological imaging techniques X-rays, CT (Computed tomography) scans, MRI (Magnetic resonance imaging) scans and ultrasound, and the physiological imaging techniques SPECT (Single photon emission tomography) and PET scans [37, 39].

Once the diagnosis and degree of spread of the tumour have been established, a decision have to be made regarding the most effective cancer treatment in the given socioeconomic setting [35].

This requires a careful selection of one or more of the major treatment modalities, such as surgery, radiotherapy and systemic therapy. This selection should be based on evidence of the best existing treatment given the resources available. Given that each patient and each cancer is different, treatment must be individualized. Therefore, the choice of the exact treatment or combination of treatments will depend on the patient, the disease and the stage of the disease as well as other considerations such as performance status, and comorbid conditions [37].

When tumour is localized and small in size, sometimes, surgery or radiotherapy alone is only likely to be highly successful. Surgery plays a vital role in the prevention, diagnosis, staging, cure and palliation. Many premalignant lesions are frequently surgically removed, preventing the progression to cancer. Surgery forms the basis of therapy for early cancer, being applied for local treatment of small tumours, to reduce the bulk of the disease, and for removal of metastatic tumours. Although late stage cancers are generally treated by chemotherapy, surgery could offer palliation in advanced cancers [37].

Chemotherapy alone can be effective for a small number of cancers, such as haematological neoplasm's (leukaemia and lymphomas) [35-37]. As mentioned before, chemotherapeutic agents are used as primary treatment for advanced disease, but also as neoadjuvant to surgery/radiation for localized disease or as adjuvant therapy (with surgery and/or radiation) [37].

Recent advances in genetics and molecular cellular biology has led to an increase in the understanding of the molecular events that either initiate or sustain cancer growth. Traditional chemotherapeutic agents do not distinguish normal and cancer cells. However these new biological agents target specific molecular pathology (pathways and aberrant genes) in cancer cells. Target therapeutics can be monoclonal antibodies or small molecules, that can be used alone or in combination with other chemotherapeutics, surgery or radiation therapy [37].

Radiation therapy is the administration of ionizing radiation to a cancer patient with the purpose of cure, to provide palliation or as an adjunct to surgical treatment. Radiation therapy uses high-energy radiation to reduce the size of tumours and kill cancer cells. X-rays, gamma rays, and charged particles are types of radiation used for cancer treatment. In radiotherapy, radiation may be delivered by a machine outside the body (external-beam radiation therapy), it may come from radioactive material placed in the body near cancer cells (brachytherapy), or it may come by systemic administration of radioactive substances, that travel in the blood to kill cancer cells (therapy with radionuclides) [37, 40].

Radiation therapy is often used in conjunction with surgery for eradication of small and limited cancers. Preoperatively, radiation therapy may be given to reduce the size of inoperable tumours or to destroy unrecognized peripheral projections of the tumour. In addition, radiation therapy may be given to reduce the size of a tumour so it can be removed by surgery and be less likely to return. Radiation therapy given during surgery is called intraoperative radiation therapy. Alternatively, radiation therapy can be given post operatively to eradicate residual. Radiation therapy is also used for palliation (to relieve symptoms and reduce suffering) in cases where there is no cure possible, for example in cancers of the central nervous system and pathological metastasis to the bones [37, 40].

Despite conventional or external beam radiotherapy play a vital role in treatment of cancers, it is not effective for treatment of metastasis outside the treatment area. In contrast, systemic administration of radiopharmaceuticals that are designed for site specific localization, or radionuclides that have a natural affinity for some tissues, provides the opportunity for treatment of widely disseminated disease. Ideally, therapeutic radiopharmaceuticals should locate with high specificity at cancerous foci, even when the location of the tumour in the body is unknown, while producing minimal or tolerable radiation damage to normal and healthy tissues [41].

Even though radionuclide therapy has been available for many years, few are the methods routinely used on a large scale. The exceptions are for example ^{131}I iodide for the therapy of thyroid cancer [42, 43], ^{32}P-orthophosphate for therapy of polycythemia and thrombocythemia [44, 45], Bexxar (Iodine-131) and Zevalin (Yttrium-90) for therapy of lymphomas with anti-B-lymphocyte antigen antibodies [46, 47], ^{131}I labelled MIBG (meta-iodobenzylguanidine) for the treatment of pheochromocytoma and neuroblastoma [48-50] and Lutelium-177 labelled somatostatin analogues for treatment of neuroendocrine tumours [51-53].

Gene therapy is one of the new methods for cancer therapy, and is anchored on the premise that many cancers are due to genetic alterations that eventually lead to malignant changes in tissues. Gene therapy involves the transfer of genetic material into a cell that in turn alters the cellular phenotype transiently or permanently. Different vectors exist for gene delivery into cancerous cells. Viruses (such as retroviruses) serve as a perfect tool for gene transfer [37].

2.2. Nuclear Medicine Imaging and Therapy

A unique capability of the nuclear medicine is the imaging of organ function and disease states, using specific radiotracers called radiopharmaceuticals. Unlike other imaging modalities such as CT, MRI and Ultrasonography (US), nuclear medicine procedures are capable of mapping physiological function and metabolic activity, giving more precise information about the organ function and dysfunction. These images of functional morphology of organs, obtained after

the distribution *in vivo* of a radiopharmaceutical plays an important role in the diagnosis of many common diseases (malfunction organs or certain type of cancers) in a non-invasive manner [54].

Nuclear medical imaging is based on the detection of emissions from a radionuclide, associated or not with a molecule, which has been infiltrated in the metabolism of the body. Imaging in nuclear medicine is done by scintigraphy (two-dimensional images), SPECT or by PET (three-dimensional images). Both in scintigraphy and SPECT are detected gamma ray with energies ranging 100 to 200 keV, which are emitted by radionuclides during its radioactive decay. The sensitivity and resolution of currently used gamma-cameras has been optimized for these gamma-ray energies, that is a consequence of the properties of ^{99m}Tc as the dominating radiolabel for non-PET diagnostics [55].

PET is a nuclear imaging technique that uses radionuclides that decay by positron emission. The principal behind PET imaging is the simultaneous detection of two gamma ray photons of 511 keV that are emitted in opposite directions, that results of the annihilation of the positron with an electron. To minimize the distance between the emission and the annihilation sites of the positron, the energy of the emitted positrons should be as small as possible [56].

In diagnostic applications, tiny concentrations of molecules are added to the biological system as a tracer, which are detectable due to the emissions from their radioactive labels. The concentration of the radiolabelled tracer added to the biological system is so small that in principle it will not alter the properties of the process under investigation. This presumes that the radiolabelling of a molecule does not alter its physiological and biochemical properties, and the radiotracer have to behave in the system exactly as the native non-labelled molecule. The difference between the labelled and non-labelled molecule is that the first will allow a mapping of the physiological function and metabolism of a tissue, allowing to draw conclusions on tissue function or dysfunction [41, 54, 55].

The development and availability of a rapidly increasing number of specific radiopharmaceuticals (currently more than 100) [54] and the availability of

suitable radionuclides produced in research reactors [57] or with accelerators [58], lead to the widespread utilization and growing demand for these techniques.

In spite of all recent and future developments, the challenge in radiopharmaceutical development and production will remain finding the proper combination of a carrier molecule with a radionuclide that meets all requirements [41, 59].

Targeted radionuclide therapy involves the use of radiopharmaceuticals to selectively deliver therapeutic doses of ionizing radiation to specific diseases sites. In therapeutic applications is administered high radiation activity with the intention of destroying the target tissue. It is known that for a specific tissue of an individual, the biological radiotherapeutic effect is greater the higher the absorbed dose. Also is known that the same dose absorbed by different tissues from the same individual or different individuals of corresponding tissues, can cause uneven effects, reflecting a difference in radiosensitivity. For an effective therapy, there must be a high relationship between radiation dose to target organ and surrounding healthy tissues, thus allowing to reduce the side effects that can come from therapy [1, 41, 59].

Ionizing radiation is energy transmitted via x-rays, gamma rays, beta particles, alpha particles, neutrons, protons, and other heavy ions. The physical factors affecting cell response to a specific radiation include the linear energy transfer (LET), the relative biologic effect (RBE) and the oxygen enhancement radio (OER). LET describes a measure of the rate at which energy is deposited as a charged particle travel through matter, and it is also a function of the physical characteristics of radiation, that is, mass and charge, therefore particles with charge and mass have a higher LET. Radiations that cause dense ionization along their track are called high-linear-energy-transfer (high-LET) radiation (ex. α particles, neutrons). Low-LET radiations produce ionizations only sparsely along their track (ex. gamma and x-rays, electrons). The higher LET of a radiation, the greater the chance for a biologic interaction. Thus, high-LET radiations are more destructive to biological material than low-LET radiations, because at the same dose, considering that high-LET radiations transfer most

of their energy to a small region of the cell. The localized DNA damage caused by high-LET radiations is more difficult to repair than the diffuse DNA damage caused by the sparse ionizations from low-LET radiations [1, 60].

The relative effect of LET is quantitatively described by RBE. The OER is a numerically description of the biological response to radiation in the presence of oxygen. There is a strong evidence that DNA is the principal target for the biologic effects of radiation, including cell killing, carcinogenesis, and mutation. Radiation-induced ionizations may act directly on the cellular component molecules or indirectly on water molecules, causing water-derived radicals. The atoms of the target itself may be ionized or excited, thus initiating the chain of events that leads to a biologic change. This is called direct action of radiation, which is the dominant process if radiations with high LET are considered. On the other hand, the radiation may interact with other atoms or molecules in the cell, particularly water that may become ionized, to produce free radicals that are able to diffuse far enough to reach and damage the critical targets, namely DNA. This is called indirect action of radiation, which is the dominant process if radiations with low LET are considered [1, 60]. A free radical is an atom or molecule carrying an unpaired orbital electron in the outer shell, which is a state of high degree of chemical reactivity. This may be expressed as:

$$H_2O + \gamma \rightarrow H_2O^+ + e^-$$

H_2O^+ is an ion radical with an extremely short life-time (10-10 second). They decay or react with other molecules of water to form free radicals, which are not charged but still have an unpaired electron, namely hydroxyl radical ($OH^{\cdot}$) [1, 60].

The hydroxyl radical is a highly reactive free radical which can spread quickly over a short distance allowing to reach a critical target in the cell. The hydroxyl radicals can recombine with each other, and form hydrogen peroxide (H_2O_2), which together with $OH^{\bullet}$ radical are responsible for about two-thirds of all radiation injuries following the water radiolysis [1, 60].

Considering the indirect effects of radiation in the cell which are related with the free radicals produced, they are able to increase the cell damage if molecular

oxygen is present, allowing its reaction with the DNA. The DNA damaged by this route, can be chemically restored by reacting with an SH group. However if HO_2 (hydroperoxyl) is formed instead of hydroxyl radical, that is an organic peroxide, the lesions occurred in the target material are non-restorable. Thus, a change in the chemical composition of the material occurs, resulting in cell death [1, 60].

The major effect in cells is DNA breaks, and since DNA is formed by two complementary double strands, breaks of either a single strand or both strands can occur. Most single-strand breaks can be repaired by the normally mechanisms of cell repair, due to the complementary nature of the two strands, being the intact strand a template for repair the damaged opposite strand. If double-strand breaks occur, the repair is not only more difficult but also an erroneous re-arranje of the broken ends may occur. These misrepairs result in induction of mutations, chromosomal aberrations, or cell death [1, 60].

The development of molecular carriers and the availability of radionuclides with high purity and adequate specific activity can contribute to the successful application of radionuclide therapy [54].

2.2.1. ***Radionuclides for Imaging and Therapy***

Radioisotopes (or radionuclides) are contributing significantly to improving health care in most countries. Globally there is a growth in the number of medical procedures involving the use of radionuclides, and with this the growth in the number of procedures requiring different radionuclides, for example in diagnostic nuclear medicine and radionuclide therapy [54].

A radionuclide is an element with an unstable combination of protons and neutrons (nucleons). When trying to reach stability is emitted radiation (radioactive decay or radioactivity). It entails a change from an unstable combination of neutrons and protons in the nucleus to a stable or more stable combination. The type of decay determines whether the ratio of neutrons to protons will increase or decrease to reach a more stable configuration, and also determines the type of radiation emitted [61].

Radionuclides used in nuclear medicine are primarily produced in a cyclotron or a reactor. The type of radionuclide produced in a cyclotron or a reactor depends on the irradiating particle, its energy, and the target nuclei. The use of radionuclides with short half-life has grown considerably, and this has led to the development of radionuclide generators [61].

In radionuclide generators a relatively long-lived parent radionuclide decays into a daughter radionuclide with a shorter half-life. Due to the different chemical properties of parent and daughter nuclide, the daughter can be chemically separated [55, 59].

A radionuclide generator consists of a glass column filled with an absorbent material such as aluminium oxide or an ion-exchange resin to which the parent nuclide is bound. The column is filled with a filter at the outlet to retain particulate matter. On top is the elution platform, where an evacuated sterile vial is connected with the outlet of the column though which saline or another suitable eluent is drawn from the eluent reservoir [55].

Radionuclide generators serve as a convenient source of radionuclides with short half-life for medical application. The lifetime of a generator system depends on the half-life of the parent nuclide, therefore, the longer the half-life of the parent, the longer can the daughter radionuclide be eluted in adequate amounts. This condition is favourable for both transport and the use of radionuclides with short half-life in diagnostic nuclear medicine [62].

There are various radionuclides that emit gamma-rays and are used for scintigraphy and SPECT. Some of these radionuclides, and its characteristics are organized in table 4.

Table 4. Most frequently used radionuclides for scintigraphy and SPECT imaging and their most relevant physical properties (Cantone M. *et al.*, 2011).

Nuclide	Half-life	Preferentially imaged γ-energy (keV)	Yield (%)	Decay mode	Source
^{67}Ca	78.28 hours	93.3 184.6 300.2	38.81 21.41 16.64	EC	Cyclotron
^{81m}Kr	13.10 hours	190.5	64.9	IT	Generator
^{99m}Tc	6.015 hours	140.5	89.06	IT	Generator
^{111}In	67.31 hours	171.3 245.4	90.7 94.1	EC	Cyclotron
^{123}I	13.22 hours	159.0	83.3	EC	Cyclotron
^{131}I	8.025 days	364.5	81.5	β^-	Reactor
^{133}Xe	5.243 days	81.0	38.0	β^-	Reactor
^{201}Tl	73.01 hours	167.4	10.0	EC	Cyclotron

Legend: Most frequent radionuclides for scintigraphy and SPECT imaging, and its physical characteristics, namely the physical half-life, the mode of radioactive decay (EC - Electron Capture; IT – Isomeric Transition; β^- - Beta negative), how it is produced, and the energy of the gamma rays used for imaging.

Technetium-99m (^{99m}Tc) is the most widely used radioisotope in diagnostic nuclear medicine. It has been estimated that over 80% of the nearly 25 million diagnostic nuclear medicine studies carried out annually are done with this single isotope [54]. It can be easily eluted at the hospital from a ^{99}Mo/^{99m}Tc generator, making it widely available [55].

The convenience of having a radionuclide generator that can be used for one week promoted the development of ^{99m}Tc radiochemistry and cold kits (so called because they do not contain radioactivity). Cold kits are an efficient way to formulate ^{99m}Tc-labelled radiopharmaceuticals from sodium pertechnetate ($Na^{99m}TcO_4$) solution eluted from a ^{99m}Tc-generator [54].

The evolution of Positron Emission Tomography (PET) as a clinically useful imaging modality has its origin in the synthesis of the positron emitting radioisotope fluorine-18 radiolabelling fluorodeoxyglucose (^{18}F-FDG) in 1976 at the Brookhaven National Laboratory, with the intention of applying ^{18}F-FDG for mapping glucose metabolism in the brain, to understand and monitor neurological diseases. While it is also useful for studying myocardial viability, due to the greater utilization of glucose by the proliferating cells, the major use

of ^{18}F-FDG subsequently emerged in the detection, staging and treatment follow up of various types of cancers [54, 55].

Currently PET studies using ^{18}F-FDG account for 10% of all nuclear medicine imaging. A number of other fluorine-18 labelled radiopharmaceuticals are being developed and a few of them are under clinical investigation [54].

Also fluorine-18 is the radionuclide most used in PET, other radionuclides are being used. Some of these radionuclides and its characteristics are organized in table 5.

Table 5. Most important PET radionuclides (Cantone M. *et al.*, 2011).

Nuclide	Half-life	Average β^+-energy (MeV)	Mean range in tissue (mm)	β^+-yield (%)
^{11}C	20.385 min	0.386	0.3	99.75
^{13}N	9.965 min	0.492	1.4	99.80
^{15}O	2.037 min	0.735	1.5	99.90
^{18}F	109.77 min	0.250	0.2	96.73
^{62}Cu	9.673 min	1.314	2.3	97.43
^{64}Cu	12.701 h	0.278	0.2	17.60
^{68}Ga	67.71 min	0.830	1.9	89.14
^{82}Rb	76.38 s	1.479	2.6	95.43
^{86}Y	14.74 h	0.660	0.7	31.90
^{89}Zr	78.41 h	0.396	0.3	22.74
^{124}I	4.176 days	0.820	0.8	22.70

Legend: Most important PET radionuclides, and its physical characteristics, namely the physical half-life, and the energy and range (mm) in tissues of β^+ particles.

The primary role of radiopharmaceuticals in cancer treatment will be towards the follow-up of patients with a known disease. Radiopharmaceuticals can provide useful information about the function and molecular biology of the tumour by measuring several of the causal factors of the tumour [54].

When planning radionuclide therapy, key factors should be considered for the selection of an effective radionuclide are: (i) the half-life; (ii) the radiation characteristics; (iii) the ability to produce the radionuclide with high specific activity (e.g. high amount of radioactivity per unit mass) and (iv) the radionuclide purity [63, 64].

The physical half-life of the chosen radionuclide for therapeutic applications, should be ideally about two or three times longer than the time required for achieving maximum uptake of the radiopharmaceutical in the target tissue [55].

An excessively long physical half-life increases the amount of radiation that is delivered to tumour cells to achieve therapeutic level before excretion, but also can create problems related with environmental safety in case of spill or early death of the patient [59, 65].

On the other hand, an extremely short physical half-life may not allow enough time for the tumour-targeting process to take place, resulting that the majority of the radioactive decays occurs in the vicinity of or even in the health tissues [59, 65].

Incorporated radionuclides are also characterized by their biological half-life, which is given by the time required to excrete half of the substance from the organism. The biological half-life depends also from the chemical form in which the radionuclide is present and that affects the metabolic pathways of excretion. The combined effect is described by the effective half-life, defined as in the equation 1 [55]:

$$T½_e = \frac{T½_b \,.\, T½_f}{T½_b + T½_f}$$

Equation 1. Equation for calculating the effective half-life, being $T½_e$ the effective half-life, $T½_b$ the biological half-life and $T½_f$ the physical half-life (Cantone M. *et al.*, 2011).

If the travelling time of the carrier molecules in the body is too long, and the physical half-life of the radionuclide is short, the molecules will reach their targets after the radionuclide has already decayed. As a consequence, this will cause an unspecific, unacceptable radiation dose to healthy tissues. If the same carrier molecule is labelled with a radionuclide with a longer half-life, practically all carriers would deliver their radioactive charge to the target cells, but the dose rate might be too low for achieving a therapeutic effect [55, 61]. Therefore, the physical half-life of the radionuclides should preferably be of the same order of

magnitude as the biological half-life of the radionuclide or the radionuclide conjugate [59].

The characteristics of the radiation emitted during radionuclide decay are also an important point to be considered. If the radionuclide during its decay emits gamma photons with an appropriate energy to perform images, it could be useful to monitor the distribution of the radiopharmaceutical in the patient for assessing dosimetry [41].

Radionuclides must be available with high purity, high activity concentration, and high specific activity (i.e. Ci/µg or GBq/µg). Radiolabelled compounds should be prepared as high specific activity drugs since they target low-capacity systems [41, 66]. For example, the therapeutic efficacy of a radiolabelled ligand may be compromised by molecules with improper labels that will competitively bind to the receptor site and may obscure the binding of the radiolabelled ligand, since the capacity to targeted receptors on malignant cells may be as low as a few nanomoles. Thus, specific activities ≥ 70-200 GBq/µg are required [41].

To meet the requirements, a radionuclide to use for therapy, should have some physical properties:

– The radionuclide should emit alpha (α) or beta negative (β^-) particles, Auger and/or conversion electrons in sufficient abundance to induce tumour cell death;

– High abundance of high-energy gamma rays is undesirable since it gives whole-body irradiation; however, low abundance photons of 100 to 200 keV might be of advantage for imaging and therapy monitoring using a gamma-camera;

– A physical half-life of 1 to 14 days, depending on *in vivo* pharmacokinetics of the targeting agent, seems to be optimal to ensure the therapeutic effect;

– To produce the radionuclide with a high specific radioactivity;

– To produce the radionuclide in a cost-effective way, allowing it to be more available;

– High-yield labelling of proteins and peptides and provide a conjugate which is stable in the blood circulation, enabled by the chemical properties of the radionuclide;

– To avoid the accumulation of radiocatabolites in normal organs or tissues they should be quickly excreted from the body [59, 67].

Radionuclides that decay by β^--particle emission, α-particle emission, and Auger-electron are effective for delivering localized cytotoxic doses of ionizing radiation [41, 66]. Each type of these particles has different effective range, LET and RBE. The type of particle emission that is applicable will depend on the size of the tumour, intra-tumour distribution (i.e., degree of heterogeneity of radiotracer deposition), pharmacokinetics of the tracer, etc. Gamma-ray emission may be or may be not accompany the particle emission process and little will contribute to the therapeutic effectiveness, however will augment irradiation to non-target tissues. On the other hand, in cases where the gamma-ray energy is in diagnostically useful range, is feasible to perform radionuclide imaging of tracer biodistribution.

As referred before, the biological effect of radiation is directly related to the LET, which is the average energy deposited by a particle per unit track length (keV/µm). High-LET radiation like α-particle radiation (25-230 keV/µm) [59] can destroy cells even by single hits, whereas low β-radiation (LET ~1 keV/µm) is much less efficient. Auger emitters may reach the LET values of α-particles but confined in a range of about 10 nm, which explains why they should be targeted directly to DNA [59, 68].

The beta negative particles are high energy electrons emitted from the nucleus as a spectrum or continuum of energies (and ranges) up to a maximum value. The range of these high-energy electrons is much greater than α particles, and the low ionization density along their tracks accounts for their low LET [41, 66]. Radionuclides that decay by β^--particle emission are used most extensively for radiotherapeutic applications in current clinical practice. Utilization of β^--particle emitters provides a mechanism to produce a highly homogeneous radiation

dose even though their deposition is heterogeneously distributed in target tissues, considering their range. Therefore, these radionuclides are useful for treatment of bulky tumours and therefore, the long range can compensate the poor penetration of the targeting molecule into a tumour mass and overcome a possible heterogeneity of target expression. On the other hand, high energy beta negative particles are inefficient for destroying single cancer cells or small micrometastases, because most of the energy associated with the radionuclide decay is deposited outside the malignant cell [41, 59]. This means that considerable cross-fire will occur with possible sterilization of untargeted neoplastic cells from radioisotopes deposited on neighbouring tumour cells. Table 6 provides a list of β^--particle emitting radionuclides with therapeutic potential [67, 69].

Table 6. Physical properties of some β^--emitting radionuclides considered for radionuclide therapy (Ferreira S. *et al.*, 2012; Palmedo H., 2007).

Nuclide	Half-life (days)	Average β energy (MeV)	Average range (mm)	Photon radiation (keV)
High-energy beta-particles				
^{188}**Re**	0.7	0.744	3.5	155 (15%)
^{166}**Ho**	1.1	0.666	3.2	80.5 (6.7%)
^{90}**Y**	2.7	0.935	3.9	_
^{76}**As**	1.1	1.0	5.0	559 (45%); 657 (6.2%)
^{89}**Sr**	52	1.4	6.6	_
^{32}**P**	1.4	1.7	8.1	_
Medium-energy beta-particles				
^{77}**As**	1.6	0.228	1.2	_
^{153}**Sm**	1.9	0.229	1.2	103 (30%)
^{186}**Re**	3.7	0.362	1.8	137 (9.4%)
Low-energy beta-particles				
^{67}**Cu**	2.6	0.141	0.71	91 (7%); 93 (16%); 185 (49%)
^{131}**I**	8.0	0.181	0.91	364 (82%)
^{161}**Tb**	6.9	0.154	0.77	75 (10%)
^{177}**Lu**	6.7	0.133	0.67	113 (6%); 208 (11%)

Legend: Some radionuclides considered for β^- therapy, arranged according to the energy of β^- particles as high-energy (0.666 to 1.7 MeV), medium-energy (0.228 to 0.362 MeV) and low-energy (0.133 to 0.181 MeV).[1]

[1] The Table 6 is a modified version of the Table 3 of the following publication: Ferreira S, Dormehl I, Botelho MF: Radiopharmaceuticals for bone metastasis therapy and beyond: a voyage from the past to the present and a look to the future. Cancer biotherapy & radiopharmaceuticals 2012, 27(9):535-551.

Alpha particles are high-energy helium nuclei that produce high densities of ionization along their linear tracks and therefore are classified as high LET radiation. The alpha particles deposit their energy over short ranges (i.e. usually between 40 μm to 100 μm) [41, 66].

Because of their relatively short range and high LET, alpha particles have the capability for producing a high degree of tumoricidal activity while normal surrounding tissues are spared [41, 66].

The high LET of alpha particles limits the ability of cells to repair damage to DNA and is effective in killing cells in hypoxic conditions. The high RBE of this type of radiation results in inactivation of cells with few alpha particles in contrast to gamma radiation or beta particles. On the other hand, a disadvantage of alpha emitters is that they require binding of the carrier to most cancer cells in a tumour or to their near neighbours for irradiation of all cells [41, 66]. In contrast to β^--particle emitters, α-particle emitters are more compatible for use in treatment of tumours with small diameters (like metastasis) and where their localization within the tumour is more spatially homogeneous. Although more than 100 radionuclides exist which decay by the emission of alpha particles, the vast majority have half-lives that are too long to be compatible with *in vivo* applications, and are difficult to produce in large quantities with acceptable radionuclidic purity [41]. Table 7 provides a list of α-particle emitting radionuclides with therapeutic potential.

Table 7. Some α-particle emitting radionuclides for radionuclide therapy (Cantone M. *et al.*, 2011; Stigbrand T., 2008).

Nuclide	Half-life	Average α energy (MeV)	Average range (μm)	Photon radiation (keV)
^{213}**Bi**	45.6 min	8.320	85	440.5 (25.9%)
^{212}**Bi**	60.6 min	7.738	82	None
^{211}**At**	7.2 hours	6.746	65	None
^{149}**Tb**	4.1 hours	3.967	28	165 (26.4%)
^{226}**Th**	30.6 min	6.917	70	None
^{225}**Ac**	10.0 days	6.867	69	218.1 (11.4%); 440 (25.9%)
^{224}**Ra**	87.8 hours	6.566	64	241 (4.1%); 238.6 (43.6%)
^{223}**Ra**	11.4 days	5.668	53	269.5 (13.9%); 351 (12.9%)

Legend: Some radionuclides considered for α therapy, and its physical characteristics, namely the physical half-life, the energy and range of α particles. Also is indicated if the radionuclides represented in the table are as well emitters of gamma radiation or not.

Low-energy Auger electrons, which are emitted during electron capture or isomeric transition decay, are also considered suitable particles for inactivation of single spread malignant cells. These particles, due to their high yield per decay, are extremely radiotoxic if they hit DNA, considering the high probability to induce a severe double-strand break, and, hence, inactivate the cell [70]. This is the result of the deposition of a concentrated amount of energy, emitted in the form of a shower of Auger electrons with energies ranging from a few to several hundred electron volts, into an extremely small volume within the nuclear DNA [41, 66].

This type of radiation exposure produces decreasing survival curves with no shoulder at low doses and is relatively independent of oxygen effects. Since these auger electron emitter's radionuclides are less cytotoxic if they are present in the cytoplasm or on the surface of target cells, they must be incorporated into the nucleus of cells [41, 66].

In vivo and *in vitro* studies demonstrated that the toxicity of Auger electron emitters approximates that for low LET radiation when the emitter is localized in the cytoplasm and, on the other hand when Auger-electron emitter is covalently bound to DNA in the cellular nucleus, they approximates that for high LET radiation. Therefore, in order to complete eradication of cancer cells in a tumour, the Auger-emitting radiopharmaceuticals must be capable of localizing in all of the targeted cells [41].

While efforts are being made in designing therapeutic radiopharmaceuticals with several promising Auger-electron emitters, the design of effective Auger-emitting targeting agents for *in vivo* targeting and treatment of cancers remains a challenge [41].

Table 8 provides a list of Auger and conversion electron emitters with therapeutic potential.

Table 8. Compilation of Auger and conversion electron emitters in use or in discussion for radionuclide therapy (Cantone M. *et al.*, 2011; Stigbrand T., 2008).

Nuclide	Half-life	Average e^- properties		Decay Mode
		Energy (keV)	e^-/decay	
^{51}**Cr**	20.70 days	3.97	4.68	EC
^{67}**Ga**	78.28 hours	7.07	7.03	EC
^{77}**Br**	57.04 hours	4.13	4.96	EC, β^+
^{94}**Tc**	4.88 hours	5.17	6.42	EC
^{99m}**Tc**	6.01 hours	0.96	4.67	IT
^{111}**In**	2.82 days	6.51	6.05	EC
^{114}**In**	49.51 days	4.15	7.74	EC
^{115m}**In**	4.49 hours	2.85	5.04	IT, β^-
^{123}**I**	13.20 hours	7.33	12.60	EC
^{124}**I**	4.18 days	4.87	8.60	EC, β^+
^{125}**I**	59.40 days	11.90	21.00	EC
^{167}**Tm**	9.25 days	13.60	11.40	EC
^{193m}**Pt**	4.33 days	10.90	20.30	IT
^{195m}**Pt**	4.01 days	21.80	31.5	IT
^{201}**Tl**	73.01 hours	15.27	36.9	EC
^{203}**Pb**	51.92 hours	11.63	23.3	EC

Legend: Some radionuclides considered for auger and conversion electron therapy, and its physical characteristics, namely the physical half-life, the energy of auger and conversion electrons, and the type of radioactive decay (EC - Electron Capture; IT - Isomeric Transition).

2.2.2. ***Physical and chemical characteristics of Technetium-99m***

Technetium-99m (^{99m}Tc) is the most commonly used isotope for nuclear imaging due to favourable physical properties for scintigraphy and its versatile chemistry that allows the incorporation of the label into a manifold of ligands. Technetium-99m decays with a half-life of 6.02 hours by isomeric transition and emission of gamma-rays of 140 keV, which is ideal for gamma-camera detection. The short half-life and the energy of the gamma-rays allow the use of significantly higher doses compared to other radioisotopes, resulting in higher count rates, contributing for the increase in the temporal resolution for dynamic studies. On the other hand, the lifetime is long enough to allow for target-specific applications. Large amounts of radioactivity may be used with the SPECT technology, producing high-contrast images with the gamma-camera [71]. Technetium-99m is generator-produced from molybdenum-99 (^{99}Mo),

which allows the general availability of the tracer. Molybdenum-99, with a half-life of 66.02 hours, decays by several β-particle transitions producing metastable ^{99m}Tc with 87.5% intensity, while 12.5% decay directly to long-lived technetium-99 (^{99}Tc). Subsequently, metastable ^{99m}Tc decays by isomeric transition to ^{99}Tc. ^{99}Tc decays with a half-life of 212000 years to stable ruthenium-99 (^{99}Ru). The process of radioactive decay of ^{99}Mo is represented in fig. 2 [72].

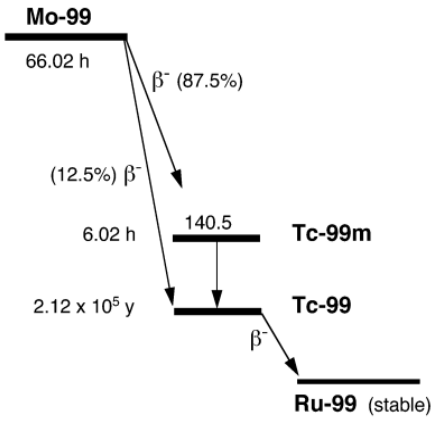

Figure 2. Decay scheme of parent ^{99}Mo to stable ^{99}Ru (Cantone M. *et al.*, 2011).

The parent radionuclide ^{99}Mo can be prepared in abundant quantities by the fission of uranium-235 in a nuclear reactor with a fission yield of about 6%. There are only a limited number of industrial companies producing ^{99}Mo from fission products, but collectively they have adequate capacity to meet the world's demand for ^{99}Mo [54].

^{99}Mo/^{99m}Tc generators produced for worldwide application have a sophisticated system for safe elution of the daughter radionuclide. The generator column is well shielded with lead, and the whole system must be adequately shielded to reduce radiation exposure of the operator to a permissible level [55].

Parent ^{99}Mo and the daughter with shorter half-life, ^{99m}Tc, reach the transient equilibrium, characterized by the decay of both parent and daughter radionuclides with one apparent half-life, namely that of the ^{99}Mo. Transient equilibrium is established when the half-life of parent is long with respect to daughter radionuclide, but parent activity changes perceptibly during the period

under consideration. Build-up of daughter ^{99m}Tc activity occurs until a maximum is reached, and then the “effective” half-life of the daughter activity will be essentially equal to the parent half-life, as long as parent activity continues to produce the daughter radionuclide. The ratio of daughter activity to parent activity is unchanging with respect to time, but the activity of each is declining with respect to time [55, 72].

Several methods have been used to separate the daughter nuclide ^{99m}Tc from parent ^{99}Mo, the three most common methods are column chromatography, solvent extraction, and sublimation [72, 73]. The ^{99}Mo/^{99m}Tc generator used in nuclear medicine is based on the chromatographic separation of ^{99m}Tc-pertechnetate, where ^{99}Mo is bound strongly to a bed of chromatographic-grade alumina. The daughter radionuclide ^{99m}Tc is eluted with sodium chloride from aluminium oxide (Al_2O_3) column, being obtained sodium pertechnetate ($Na^{99m}TcO_4$). A general representation of the components that constitutes a ^{99}Mo/^{99m}Tc generator is represented in fig. 3 [55].

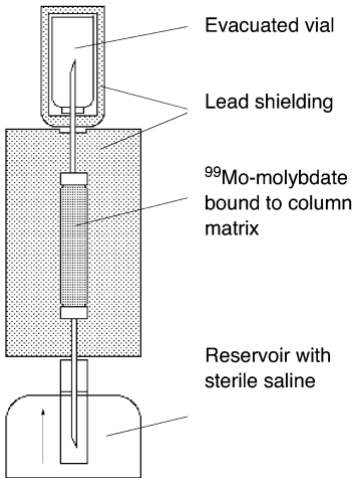

Figure 3. Components of the ^{99}Mo/^{99m}Tc generator system (Cantone M. *et al.*, 2011).

Technetium-99m chemistry is primarily the chemistry of anionic pertechnetate ($^{99m}TcO_4^-$), obtained from the ^{99}Mo/^{99m}Tc generator with high specific activity. Anionic pertechnetate is no-carrier-added because ^{99m}Tc activity is present in the radiopharmaceutical kit at 10^{-8} to 10^{-9} M [74].

The element technetium belongs to the second-row elements of the group VIIB of the periodic table, between manganese and rhenium. The atomic radius of technetium is similar to rhenium, and thus, many similarities are found in the chemistry between these two elements. Technetium can exist in eight oxidation states, varying from (VII) to (-I). The most stable states are (VII), (V), (IV), (III), (I) and 0. The most difficult states to stabilize are (VI), (II) and (-I) [75].

The highest oxidation state (VII) is occupied by the pertechnetate anion (TcO_4^-). The representation of the chemical structure of the pertechnetate anion is represented in fig. 4 [74].

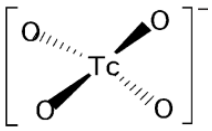

Figure 4. Pertechnetate anion (Mazzi U., 2007).

The chemical reactivity of the pertechnetate anion is negligible, therefore it does not bind directly to any ligand. Consequently, for the production of ^{99m}Tc pharmaceuticals, reduction to a lower oxidation state in the presence of a suitable ligand is a prerequisite for the synthesis of ^{99m}Tc-labelled molecules. During reduction, the ligand stabilizes the lower oxidation state, otherwise, colloidal TcO_2 is formed in aqueous media [74].

The so-called coordination complexes of technetium (central metal) are formed by means of bonds between technetium acting as Lewis acid, and atoms or functional groups, acting as Lewis bases (donate electron pairs). Typical ligands for technetium complex formation may have one donor group (monodendate) such as amine, amide, thiol, phosphine, oxime, or isonitrile. With two donor groups, the complex is bidentate, where more than two groups form a single molecule bind to one Tc core, being designated chelate [74].

2.2.3. ***Physical and chemical characteristics of Rehnium-188***

Rhenium-188 (^{188}Re) is a β^- particle emitter, and is an excellent candidate for radionuclide therapy [76, 77]. This radionuclide is easily obtained carrier free as

perrhenate ion (ReO_4^-) in normal saline solution [78] or perrhenic acid ($HReO_4$) in aqueous HCl or HNO_3 [79] from a rugged and economical alumina based tungsten-188/rhenium-188 ($^{188}W/^{188}Re$) generator system. The alumina-based $^{188}W/^{188}Re$ generator is completely analogous to the $^{99}Mo/^{99m}Tc$ generator, nevertheless, the $^{188}W/^{188}Re$ generator system has a greater shelf life, since ^{188}W has a much longer physical half-life (69 days) than ^{99}Mo (66 hours) [61, 79, 80]. ^{188}Re decays by emitting high energy β^- particles (2.1 MeV) with a maximum penetration in tissue of 10–11mm making this radionuclide a suitable option for therapy of large tumour masses, as discussed before [66, 81]. Its gamma ray emission (0.155 MeV) can be exploited for dosimetry purposes and to monitor biological distribution during therapy [61, 66, 76, 82, 83]. It also has a relatively short physical half-life of 16.9 hours, which allows the use of high doses and reduces the problem of radioactive waste handling and storage [82, 84].

The element rhenium belongs to the third-row elements of the group VIIB of the periodic table. Rhenium can exist also in eight oxidation states, varying from (VII) to (-I). The highest oxidation state (VII) is occupied by a perrhenate anion (ReO_4^-) [75].

An important factor that adds value to ^{188}Re-labelled drugs is the fact that ^{99m}Tc is a chemical congener of Re, making the chemistry of both ^{99m}Tc and ^{188}Re the same or nearly identical in many cases. Therefore, when the chemistries of these radionuclides are similar, the ^{99m}Tc agents can be used as the “matched pair” for the corresponding ^{188}Re agent, making it feasible to obtain excellent diagnostic imaging in patients allowing for pre- and post-assessment of patients treated with therapeutic ^{188}Re analogues. Strategies for synthesizing ^{188}Re-labelled site-specific radiopharmaceuticals are based on, and parallel to, efforts being made to develop new ^{99m}Tc drugs [41].

2.2.4. ***Cold kits formulation for radionuclide labelling***

Radiopharmaceuticals are medical formulations containing radioisotopes which are safe for administration in humans for diagnosis or for therapy. Currently are

over 100 radiopharmaceuticals developed using either reactor or cyclotron produced radioisotopes [54].

The particularity of radiopharmaceuticals consist of their capability to retrieve information on a molecular level and to address systems with very low densities of receptor molecules *in vivo* and in a non-invasive way [41, 55].

The preparation of ^{99m}Tc pharmaceuticals is greatly facilitated by the availability of commercial cold kits containing the chemical ingredients as a lyophilized formulation ready for labelling with ^{99m}Tc-pertechnetate. The preparation of any ^{99m}Tc pharmaceutical is performed by using a commercial cold kit and adding the required ^{99m}Tc activity in a certain volume of sodium pertechnetate. The labelled product is a sterile, pyrogen-free solution suitable for intravenous injection. Any abnormality observed by visual inspection of the injected solution is a cause to reject the preparation [71].

Cold kits are prepared in such way as to have a long shelf life, ranging from several months to a few years, and may be transported at room temperature and then stored under refrigeration to ensure stability [54].

A kit contains the active ingredient (compound to be labelled with the radionuclide), a reducing agent, and may contain authorized excipients and additives, such as antimicrobial agents, antioxidants, buffer, a nitrogen atmosphere, etc. The reducing agent is responsible for the reduction of the radionuclide to a lower valency state. It's considered an essential material, because without reduction, there is no labelling reaction, considering that, for example pertechnetate anion that is in the oxidation state (VII) is not chemically reactive and therefore it must be reduced. The shelf-life of lyophilised kits is usually in excess of 1 year. Freeze-drying, or lyophilisation, is the drying of frozen materials by sublimation, this is the direct transition from the frozen state into vapour, without any intermediate liquid phase [71, 85].

The lyophilisation method is similar to ordinary vacuum distillation with one essential difference, that is the material to be dried is first frozen and then subjected to a very low absolute pressure (high vacuum) and controlled heat input. The heat drives the water from the solid to the vapour state. Under these

conditions, the water content, in the form of an ice matrix, is selectively removed via sublimation [85].

The same amount of heat that is required in the drying chamber for the sublimation of the water is subsequently liberated as the water vapour condenses at the ice condenser, and must be removed by means of refrigeration units. Therefore, three basic conditions have to be fulfilled in order to carry out the freeze-drying process: (i) the temperature of the material must be regulated so that thawing is avoided and vapour pressure above the material does not sink due to overcooling; (ii) the water vapour molecules escaping from the frozen material should be removed in such manner that saturation of vapour pressure above the substance to be dried is avoided; (iii) the process should take place in a vacuum so that removal of water molecules may not be impeded by the presence of residual gases [85].

In practice, the freeze-drying process should take place taking into account the following steps:

1. The solution is dispensed into the vial from 0.5 to 2.5 cm height for an efficient drying. The vials are loosely capped with rubber stoppers, and then are put into the vacuum chamber.
2. The vials with the product are gradually frozen below the eutectic point of the solution (typically to -40 °C).
3. The condenser is turned on and observed until it reaches its maximum value (typically -50 °C).
4. The vacuum pump is turned on until the lowest value of vacuum is obtained (typically 10 to 20 mHg).
5. Heat is then applied to the product through a controlled heating-cooling system, to facilitate the sublimation process.
6. A secondary drying cycle is usually applied so ensure the complete absence of humidity from the product.
7. After completion of the drying cycles, the product is closed with a rubber stopper in the vacuum chamber under a nitrogen atmosphere [85].

The ^{99m}Tc or ^{188}Re eluate used for radiolabelling must comply with the specifications stated in the pharmacopeia. Additionally, the specific activity and the activity concentration (activity/ml) should be known. Labelling with ^{99m}Tc or ^{188}Re can be performed directly or by exchange. Direct labelling is performed by adding ^{99m}Tc or ^{188}Re eluate in a suitable volume to a sterile kit. The labelling reaction requires reduction of pertechnetate/perrhenate, which is reacting with the ligand forming the labelled product in high yield (>90%). In a few exceptions, an intermediate ligand complex is formed that is stabilized by ligand exchange during heating [74].

After dissolving the lyophilisate in the added volume, incubation is an essential step to obtain the radiolabelled medicinal product, considering that is in this phase that the chemical reactions take place, resulting in ^{99m}Tc or ^{188}Re labelling. If incubation is inadequate, the labelling reaction may not be completed, and the radiopharmaceutical may not be suitable for administration. Each kit requires specific incubation conditions, but in general, this process is carried out at room temperature in a clean area. In certain cases, the incubation must be performed in a boiling water bath. Incubation is normally performed with occasional agitation of the shielded reaction vial [71].

Because there is no effective chemistry available to attach a pertechnetate or perrhenate ion to an organic moiety, reduction of ^{99m}Tc(VII) or ^{188}Re(VII) in TcO_4^- or $^{188}ReO_4^-$, to a lower oxidation state is a prerequisite for ^{99m}Tc and ^{188}Re complex formation in high yield and purity. Pertechnetate and Perrhenate are week oxidants, weaker than permanganate, being reduced by weak reductants in acid medium. Kits contain very low amounts of stannous ion for reduction of ^{99m}Tc-pertechnetate or ^{188}Re-perrhenate [74]. Nevertheless, $SnCl_2$ (stannous chloride)is usually in high excess, most of the time because stannous slats are spontaneously oxidized in air, and also to assure validity of kits beyond the expiration date [61, 74]. The amount of stannous chloride is empirically optimized for each individual kit formulation, being necessary to maintain the balance between two parameters, the first is that a large excess of stannous chloride should be used with respect to the added pertechnetate or perrhenate activity and the second is that the amount of stannous chloride should be kept as low as possible in order to avoid further reduction of pertechnetate or

perrhenate to a lower oxidation state. The amount of stannous chloride in the commercially available kits, ranges normally from 0.0076-0.5 mg, corresponding to a ratio of Sn to ^{99m}Tc in the range of 10^3 to 10^5 [61, 86].

Formation of colloidal TcO_2 or ReO_2 is avoided in the presence of ligand, which competes for the reduced technetium or rhenium species, producing the labelled ^{99m}Tc or ^{188}Re pharmaceutical. In the absence of ligand, a mixture of hydrolyzed, insoluble ^{99m}Tc or ^{188}Re species, $TcO_2.nH_2O$ and $ReO_2.nH_2O$, are formed. The kinetic mechanism of reduction-substitution is rather complicated, and sometimes it depends on the concentration of carrier $^{99m}TcO_4^-$ or $^{188}ReO_4^-$ [61, 86].

in conclusion, kit composition is optimized to ensure that the unique ^{99m}Tc- or ^{188}Re-labelled complex is obtained in high yield. Several factors influence the reduction/coordination process that is primarily the nature and the amounts of reductant and ligand, pH, and temperature. In order to provide suitable pH environment for the formation of a specific ^{99m}Tc or ^{188}Re complex, buffers are important components in kit formulations [61, 74].

2.2.5. ***Quality control of radiopharmaceuticals***

Since radiopharmaceuticals are intended for human administration, it is imperative that they undergo strict quality control measures. Quality control involves several specific tests and measurements that ensure the purity, potency, product identity, biological safety, and efficacy of radiopharmaceuticals. The quality control tests are divided in physicochemical tests and biological tests. The physicochemical tests indicate the level of radionuclidic and radiochemical impurities, determine the pH, ionic strength, osmolality, and physical state of the sample. The biological tests establish the sterility, apyrogenicity, and toxicity of the material [55, 61].

2.2.5.1. *Radiochemical purity*

The radiochemical purity of a radiopharmaceutical is the fraction of the total radioactivity in the desired chemical form in the radiopharmaceutical. Values above 90% are desirable, because a different label will yield a different biodistribution, and thus will result in a distortion of the image and/or lead to problems in therapy. Radiochemical impurities arise from decomposition due to the action of several factors like the solvent, change in temperature or pH, light, presence of oxidizing or reducing agents in inadequate concentrations, and radiolysis. Examples of radiochemical impurities are free pertechnetate or perrhenate ($^{99m}TcO_4^-$ or $^{188}ReO_4^-$) and reduced/hydrolysed ^{99m}Tc or ^{188}Re ($TcO_2.nH_2O$ or $ReO_2.nH_2O$) [55, 61].

A number of analytical methods are used to detect and determine the radiochemical impurities in a given radiopharmaceutical. One of the most important is the paper and thin-layer chromatography [55, 61].

Paper and thin-layer chromatography (TLC) is commonly used for the determination of radiochemical purity in nuclear medicine. The principle of this analytical method is that a mobile phase (solvent) moves along a layer of adsorbent (stationary phase) due to capillary forces. Depending on the distribution of components between the stationary and mobile phase, a radioactive sample spotted onto the stationary phase will migrate with different velocities, and consequently, impurities are separated. The distance each component of a sample migrates is expressed as the R_f value. The R_f is the relative distance of migration of a component in relation to the solvent front (SF), and can be calculated following the equation 2 [55]:

$$R_f = \frac{\text{Distance from origin of the component}}{\text{Distance of the SF}}$$

Equation 2. Equation for calculation of Rf. Rf is the distance of the migration of a certain component. SF is the solvent front (Cantone M. *et al.*, 2011).

The Rf values range from 0 to 1. If a component migrates with the solvent front, the R_f is 1, and if a component remains at the point of application (origin), the R_f

is 0. The main principles of separation are adsorption (electrostatic forces), partition (solubility), and ion exchange (charge). Depending on the movement of the mobile phase, TLC may be ascending or descending. In the nuclear medicine laboratory, ascending TLC is the method of choice [55, 87].

TLC offers reliable separation properties with easy and rapid performance. The applied sample remains quantitatively on the plate, and thus, no losses of radioactivity during analysis occur. A broad range of stationary phases is commercially available including silica gel, reversed-phase silica, aluminium oxide, synthetic resins (ion-exchange chromatography), and cellulose (partition chromatography). The length of plates (foils) may vary between 10 and 20 cm. The main limitation for standard TLC techniques is the time required for analysis. Due to the particle size (20 µm) of adsorbent materials, the developing time is usually > 30 minutes, this is to long considering additional time for measurements and quantification [88]. Instant TLC (ITLC) materials are the most frequently used stationary phases in nuclear medicine, because they fulfil the need for rapid and accurate analysis of the radiochemical purity of radiopharmaceuticals. ITLC plates are made of fibreglass sheets, impregnated with an adsorbent, usually silica gel. Due to the fine mesh material, the migration properties are increased many-fold comparing to TLC materials. The time for development in an ITLC plate may be reduced to < 5 minutes, without affecting the separation of radiochemical impurities. Although ITLC materials are more expensive than TLC materials, fibreglass sheets offer high economy, since the flexible material may be cut to any size [55, 87, 88].

The chemical properties of silica gel are based on siloxane (Si-O-Si) and silanol (Si-OH). Polar groups are responsible for the interaction of the adsorbent with water and with the sample to be analysed. Silica stationary phases (3-8 µm) have been produced for ITLC as silica gel (ITLC-SG) and silicic acid (ITLC-SA), being the ITLC-SG the most frequently used adsorbent for routine radiochemical purity determinations. Some separations of radiopharmaceuticals are based on adsorption chromatography with aluminium-coated plates. Also aluminium oxide (Al_2O_3) has polar properties it is also a weak anion exchange material.

Cellulose is an organic material that consists of polymerized glucose fibbers (400-500 molecules) in nature and also as a synthetic product (40-200 glucose molecules). Cellulose interacts with water and serves as stationary phase for the separation of polar substances by paper chromatography. As a powder, it is used as an adsorbent for TLC. Paper materials show low-resolution properties, however, since paper is robust and easy to cut, paper chromatography is still used for many applications. Like ITLC, paper chromatography is used "ascending" or "descending". Likewise, a developing distance of 8-10 cm is usually sufficient for the separation of free pertechnetate or perrhenate and colloidal impurities. The developing time might be slightly higher, but usually it takes only 10 minutes if small sized paper strips are used. Whatman 3MM is the material of choice for determination of the radiochemical purity by partition chromatography [55]. The migration properties of free pertechnetate or perrhenate may be influenced by the choice of different mobile phases. When silica gel or paper is used as stationary phase, the migration of free pertechnetate or perrhenate depends on the solubility of this anion in the solvent. In a polar solvent like saline, 80% of methanol, acetone or 2-butanone (methyl ethyl ketone, or MEK) pertechnetate or perrhenate migrates with the SF (R_f = 0.6 – 1.0). If a non-polar, lipophilic solvent (e.g., ethylacetate, chloroform) is used and the sample is dried, free pertechnetate or perrhenate remains at the origin. Colloids do not migrate in most paper chromatography or ITLC systems since insoluble material will stay at the origin, and hanging the mobile or the stationary phase will not affect the migration properties of colloidal ^{99m}Tc or ^{188}Re [87, 88]. In saline, free pertechnetate or perrhenate and ^{99m}Tc or ^{188}Re complex migrate with the SF, while reduced/hydrolysed ^{99m}Tc or ^{188}Re remains at the start [55].

Section II. Literature Review

Chapter 3.Primary Tumour and Metastases of Bone and the emerge of PEI-MP[2]

3.1. Introduction

Primary bone cancer means that the cancer originated from cells in the hard bone tissue [67]. Primary bone tumours are fairly rare (two in every 1000 cancers). Some conditions that may simulate primary bone tumours, such as metastasis and non-neoplastic conditions for instance inflammatory processes, bone cysts, fibrous dysplasia, non-ossifying fibroma, Paget's disease of bone, etc., by far outnumber the cases of true bone tumours. There are different types of primary bone cancer classified by the type of cell which occurs in the cancer. Types of benign bone tumours include osteoid osteoma, osteoblastoma, enchondroma, chondromyxoid fibroma. Types of malignant bone tumours include osteosarcoma, chondrosarcoma, Ewing's sarcoma, malignant fibrous histiocytoma, fibrosarcoma, giant cell tumour bone and chordoma [67, 89, 90]. A short characterization of each of these malignant bone tumours is presented in table 9 [90, 91].

Table 9. Characterization of malignant bone tumours (NCI, 2008; ACS, 2012).

Bone cancer	Tissue of origin	Affected bones
Osteosarcoma	Osteoide	Arms, legs and pelvis
Chondrosarcoma	Cartilage	Trachea, larynx and chest wall
Ewing's sarcoma	Bone, Soft tissue	Backbone, pelvis, legs and arms
Malignant fibrous histiocytoma	Soft tissue	Legs and arms
Fibrosarcoma	Soft tissue	Legs, arms and jaw
Giant cell tumour bone	Bone, Soft tissue	Legs and arms
Chordoma	Soft tissue	Skull and spine

Legend: Characterization of some malignant bone tumours, considering the tissue of origin and the most affected bones in the body by type of tumour.

[2] This Chapter is a modified version of the following publication: Ferreira S, Dormehl I, Botelho MF: Radiopharmaceuticals for bone metastasis therapy and beyond: a voyage from the past to the present and a look to the future. Cancer biotherapy & radiopharmaceuticals 2012, 27(9):535-551.

The three most common genuine primary bone malignancies are osteosarcoma, chondrosarcoma, and Ewing's sarcoma, accounting for only 0.2% of all malignancies in the United Kingdom and United States of America. However in children (< 15 years), malignant bone tumours account for approximately 5% of all malignancies [67, 89, 90]. The treatment and prognosis for bone cancers depend, to a large extent, on the patient's stage at diagnosis. One system that is used to stage all bone cancers is the American Joint Commission on Cancer (AJCC) system. It combines 4 factors to determine stage that go by the initials T, N, M, and G. The letter T stands for features of tumour (its size and if it is in more than one spot on the bone), N stands for spread of lymph nodes, M is for metastasis to distant organs, and G is for the tumour's grade. The grade of a tumour is based on how abnormal the cells look when seen under a microscope. The higher the number, the more abnormal the cells appeared. Higher grade cancers tend to grow and spread more quickly than lower grade tumours [90]. The TMNG stages for bone cancer are summarized in table 10 [90, 92].

Table 10.TMNG stages of bone cancer (ACS, 2012; CRUK, 2013).

Tumour (T)	Description
TX	Primary tumour can't be measured.
T0	No evidence of the tumour.
T1	Tumours that are 8 cm or less at their widest point.
T2	Tumours larger than 8 cm.
T3	High grade tumours where the tumour is in more than one place on the same bone.
Node (N)	**Description**
N0	There are no cancer cells in lymph nodes close to the tumour.
N1	There are cancer cells in nearby lymph nodes.
Metastasis (M)	**Description**
M0	The cancer has not spread to any other part of the body.
M1a	The cancer has spread to the lung.
M1b	The cancer has spread to other areas of the body apart from the lungs
Grade (G)	**Description**
G1-G2	Low grade.
G3-G4	High grade.

Legend: The TNMG stages of bone cancer is organized in four categories, namely the size of the primary tumour (T), the spread to lymph nodes (N), the presence of metastases (M) and the grade (G) of the tumour considering the number of abnormal cells, considering the origin. For

each of these categories, subdivisions may be made assigning a number to T, N, M or G, in a growing sequence, where the higher the number the lower is prognosis. For the category grade (G), two subdivisions are made, considering a low grade (G1-G2) and a high grade (G3-G4) tumour.

This information about the tumour, lymph nodes, metastasis, and grade is combined in a process called the stage grouping. The stage is then described in Roman numerals from I to IV. This information is summarized in table 11 [90].

Table 11. Bone cancer staging (ACS, 2012; CRUK, 2013).

Stage	Description
Stage I	
Stage IA	Low grade bone cancer that is still completely inside the bone in which is started. The tumour may press on the bone wall and cause swelling, but the cancer has not grown through the bone wall or spread to any other part of the body. This is called an intracompartmental bone cancer. T1, N0, M0, G1-G2. The tumour is 8 cm or less.
Stage IB	Low grade bone cancer but has grown through the bone wall. It is called an extracompartmental bone cancer (this means the cancer has grown out of the area of the bone in which it started). T2 or T3, N0, M0, G1-G2. The tumour is either larger than 8 cm or it is in more than one place on the same bone.
Stage II	
Stage IIA	High grade bone cancer but still completely within the bone in which it started. It has not spread to other areas of bone or any other part of the body. It is an intracompartmental cancer. T1, N0, M0, G3-G4. The tumour is 8 cm or less.
Stage IIB	High grade bone cancer that have grown through the wall of the bone into nearby tissues. They are extracompartmental cancers. T2, N0, M0, G3-G4. The tumour is larger than 8 cm.
Stage III	Tumours have not spread outside the bone but are in more than one place on the same bone. They are high grade. T3, N0, M0, G3-G4.
Stage IV	
Stage IVA	Any size or grade of tumour that has spread to the lung. Any T, N0, M1a, G1-G4.
Stage IVB	Any size or grade of tumour that has spread to the lymph nodes and/or a part of the body other than the lung. Any T, N1, any M, G1-G4 or any T, any N, M1b, G1-G4.

Legend: The combinations from the TNMG system can result in four stages of bone cancer, starting from stage I, representing a low grade bone cancer, where the tumour is still *in situ*, and then progressing to stages II, III and IV. The greater is the stage the higher the possibility of invasion to other bones, to lymph nodes and to other distant organs. These stages can also be subdivided in subcategories, representing an increase of severity within the group/stage.

The development of bone metastases is a common and often catastrophic event for the cancer patient. Overall, the skeleton is the third most common site of cancer metastases, surpassed only by lung and liver. Prostate, breast, and lung cancers are the most common malignancies in adults and are the most common tumours that metastasize to bone and about 70% of patients that had died from these cancers had evidence of metastatic bone disease [3, 67, 93]. Carcinomas of the thyroid, kidney, melanomas and bronchus also commonly give rise to bone metastasis, with an incidence at post mortem examination of 30% to 40%. Tumours of the gastrointestinal tract rarely (5%) produce bone metastasis [93, 94].

Bone metastasis is associated with increased morbidity and portends a poor outcome, with decreased survival, in cancer patients. Bone metastasis are classified as osteolytic, osteoblastic, or mixed, based on their radiographic appearance. Bone metastases from prostate cancer are predominantly osteoblastic, whereas metastatic lesions in bone from breast cancer can be osteoblastic, osteolytic, or mixed. Irrespective of the mechanisms involved in the generation of these radiographic phenotypes, the end result is a change in bone architecture, which predisposes the patient to a variety of skeletal complications [93, 95-97].

Bone metastases are usually multifocal and have a predilection for the hematopoietic marrow sites in the proximal long bones and axial skeleton (vertebrae, pelvis ribs, and cranium) [93, 98]. Continuous and dynamic turnover of the bone matrix and bone marrow provides a fertile ground for tumour cells to utilize the vast available resources (cells, growth factors, cytokines, and receptors) for their homing and subsequent proliferation. Evidence exists that blood from some anatomic sites may drain directly into the axial skeleton. The drainage of blood to the skeleton via the vertebral-venous plexus may, at least in part, explain the tendency of breast and prostate cancers, as well as those arising in kidney, thyroid, and lung, to produce metastasis in the axial skeleton and limb girdles [67, 93, 94]. Of course, the vertebral-venous plexus does not provide the entire explanation of why these cancers metastasize to the skeleton. Molecular and cellular biological characteristics of the tumour cells and the tissues to which they metastasize are of paramount importance and influence the pattern of metastatic spread [99]. Abundant sinusoids and

sluggish blood flow in the metaphysic facilitate an intimate interaction between endothelium and tumour cells, which is necessary for their initial colonization in the bone marrow. Moreover, it appears that a subset of bone marrow cells (vascular endothelial growth factor receptor-1 expressing hematopoietic progenitor cells and fibroblasts) may form a “pre-metastatic niche” in response to the humeral factors secreted by the primary neoplasm. The cells comprising the pre-metastatic niche express cell surface ligands and receptors (integrin and fibronectin), which provide a permissive environment for the migrating tumour cells. In addition, various growth factors and cytokines in the bone marrow such as endothelin-1, basic fibroblast growth factor, transforming growth factor TGFβ, IL-6, and IL-8 serve as paracrine regulators of the initial growth of metastatic tumour cells. The interaction of receptor molecules in the bone marrow stroma (urokinase receptor, vascular cell adhesion molecule-1, and fibronectin) with the ligands that are over expressed on the tumour cells (β_1, $\alpha_4\beta_1$ and $\alpha_5\beta_1$ integrins, cadherin-11, connective tissue growth factor, CXCR4 and CXCL12) promotes colonization of circulating malignant cells in the bone marrow. The extracellular matrix proteins (especially type I collagen, type IV collagen, vitronectin, fibronectin, osteopontin, osteocalcin, bone sialoprotein, osteonectin, and stromal cell derived factor-1) are chemotactic for tumour cells and promote colonization of circulating tumour cells in the bone marrow [93, 100].

Although bone metastasis are rarely the cause of cancer-related death, they lead to serious complications that limit the patient`s mobility: (1) 30-60% of patients develop pain symptoms of varying intensity, related with different causes, like an inflammatory event or a spinal cord and/or nerve root compression; (2) predominantly the osteolytic type has the tendency to develop fractures resulting in considerable morbidity; (3) a hypercalcemic syndrome due to increased bone resorption of osteolytic metastasis can occur, and this can also appear as a paraneoplastic syndrome; and (4) if there is extensive metastatic disease the bone marrow can be destroyed and clinically relevant alterations of the blood counts can be observed [97, 101, 102].

Different sites of bone metastasis are associated with distinct clinical pain syndromes. Common sites of metastatic involvement associated with pain are the base of skull (in association with cranial nerve palsies, neuralgias, and

headache), vertebral metastasis (producing neck and back pain with or without neurologic complications secondary to epidural extension), and pelvic and femoral lesions (producing pain in the back and lower limbs, often associated with mechanical instability and incident pain). The pathophysiologic mechanisms of pain in patients with bone metastasis are poorly understood but probably include tumour-induced osteolysis, tumour production of growth factors and cytokines, direct infiltration of nerves, stimulation of ion channels, and local tissue production of endothelins and nerve growth factors [69, 96, 97, 99].

It can be distinguish two types of pain, the nociceptive pain and the neurophatic or nerval pain. Pathophysiologicaly, it is difficult to differentiate these two types of pain. Nociceptive pain is mediated by free sensory nerve endings of the nociceptors that can be found throughout the body [69]. A large amount of nociceptors are located in the skin, the skeletal musculature, the tendons, the joints and the intestine [103]. Depending on their location, it's possible to differentiate between somatic and visceral or superficially and deeply located nociceptive pain. Visceral excitations are frequently projected to special skin regions, the so called dermatome. While the nociceptive pain is generally described by the patient as being of a stinging, gnawing or dull character, neuropathic pain is described as burning and appearing suddenly [95]. Therefore, anamnesis will lead to a differentiation between the two pain entities at an early stage. This is extremely important because radionuclide therapy is useful in nociceptive pain patients but not for neuropathy pain [95].

Physiologically, the nociceptor is not activated unless strong mechanical or thermal influences are present. However, the nociceptor can be sensitized by the production of endogenous pain mediators like those that occur in an arthritis patient that suffers from pain even if a small movement and/or a slight pressure is applied to an affected joint. In these cases, substances like prostaglandin E, bradykinin, histamine and interleukin act as pain mediators changing the microcirculation and permeability of vessels and leading to a decrease of excitation level [104]. Lymphocytes and macrophages assist in this process. The simultaneous excretion of different pain mediators can lead to an exponential increase in their effect. This principle is known in the field of pharmacology pain treatment, and therefore agents inhibiting the production of

prostaglandin E are successfully administered in pain patients. The nociceptor cell can also regulate its excitation level itself. By secretion of the so-called substance P, a vasodilatation and consequently an invasion of inflammatory cells and an enhanced secretion of pain mediators will occur. This process is often called a neurogenic inflammation. Bone metastasis can generate pain either by a strong mechanical impact to the nociceptor or by an osteoblastic excretion of pain mediators that result in the described sensitization of the nociceptors [69].

3.2. Demographics and epidemiology

Primary bone tumours are relatively uncommon and this has definitely limited the collection of data about their relative frequency, and as a consequence leads to the insufficient understanding of the risk factors. Although the incidence of benign bone tumours is higher than the incidence of primary malignant tumours, it is probable that benign lesions are underestimated considering that they often are asymptomatic and not clinically recognized. Therefore they remain undetected or are detected only incidentally at radiographic examinations for other reasons. In addition, primary bone tumours are outnumbered by metastases from carcinomas, melanoma, or hematologic malignancies [89, 105].

More than 75% of malignant bone tumours are osteosarcoma, chondrosarcoma, and Ewing's sarcoma [89]. The American Cancer Society's estimates for cancer of the bones and joints in 2013 the diagnosis of about 3,010 new cases and 1,440 deaths from these cancers. Primary cancers of bones account for less than 0.2% of all cancers. In adults, over 40% of primary bone cancers are chondrosarcomas. This followed by osteosarcomas (28%), chordomas (10%), Ewing's sarcoma (8%), and malignant fibrous histiocytomas/fibrosarcomas (4%). In children and teenagers (younger than 20 years), osteosarcoma (56%) and Ewing's sarcoma (34%) are much more common than chondrosarcoma (6%). Chondrosarcomas develop most often in adults, with average age at diagnosis of 51, and less than 5% of cases occur in patients younger than 20. Chordomas are also more common in adults, and

less than 5% of cases occur in patients younger than 20. Both osteosarcoma and Ewin's sarcoma occur most often in children and teens [90].

The incidence of malignant bone tumours shows a striking age-specific distribution, for example in the age group 0 to 40 years, there is an incidence peak between 10 and 20 years (primarily osteosarcoma and Ewing's sarcoma) and for the age group above 40 years there is steady increase in incidence up to 80 years (primarily chondrosarcoma and to a lesser degree Paget's related osteosarcoma) [89, 105].

In general, there is no significant gender predilection, although some tumours (e.g. Paget's sarcoma, chordoma) show a higher prevalence in males. According to SEER data, in the period of 2004 to 2008, the median age at diagnosis for cancer of the bones and joints was 40 years of age. Approximately 29.0% were diagnosed under age 20, 15.4% between 20 and 34, 10.5% between 35 and 44, 13.0% between 45 and 51, 11.4% between 55 and 64, 8.3% between 65 and 74, 9.1% between 75 and 84, and 3.5% over 85 years of age [105, 106].

Benign bone tumours and many bone stimulating, non-neoplastic conditions also show a striking age distribution, occurring in the vast majority in the first two decades of life [89, 105].

Several bone tumours may occur in the setting of inherited syndromes, nevertheless their histopathological features do not differ from those of sporadic cases. Additionally, although the majority of primary bone malignancies are *de novo*, there is increasing evidence that some develop in association with non-neoplastic precursors or in the setting of previous benign tumours. Paget's disease of bone, previous radiation therapy, and cartilaginous dysplasias are some of the most well known precancerous conditions for the development of bone sarcomas. High risk precursors are represented by Ollier's disease and Maffucci syndrome, familial retinoblastoma syndrome and Rothmund Thompson syndrome, while conditions representing a moderate risk include multiple osteochondromas, Paget's disease and radiation osteitis. A low risk for malignant transformation has been associated with fibrous dysplasia, bone

infarct, chronic osteomyelitis, prosthetic implants, osteogenesis imperfect, giant cell tumour, osteoblastoma and chondroblastoma [105].

The treatment of bone cancer is often very successful, particularly if the cancer has not spread to other parts of the body. Overall, more than 40 out of every 100 men (over 40%) and more than half of woman (over 50%) will live more than 5 years after their primary bone cancer is diagnosed and treated. Considering that, if bone cancer is low grade it is more likely to be cured, on the other hand if cancer has spread beyond the bone it is more difficult to cure. Therefore, almost everyone with stage 1A, more than 95% of people with stage 1B, more than 60% of people with stage 2A, over 40% of people with stage 2B bone cancer, lives more than 5 years [107].

Chemotherapy can work well at reducing the risk of the cancer coming back after surgery, particularly for Ewing's sarcoma. For Ewing's sarcoma that is localized and hasn't spread elsewhere in the body, about 70 out every 100 people (70%) live for at least 5 years after their diagnosis. If Ewing's sarcoma has spread to the lungs, around 30 out of every 100 people (30%) will live for at least 5 years after their diagnosis. If Ewing's sarcoma has spread to the brain then the 5 year survival is less than 10% [107].

Low grade osteosarcomas are not very common. However, over 90 out every 100 people (90%) with this type of tumour live for at least 5 years after their diagnosis. Regardless of grade, localised osteosarcomas have a 5 year survival rate of about 60%, meaning that 60 out every 100 people (60%) with this type of cancer live for at least 5 years. In people whose chemotherapy works very well, survival may be more than 70%. In people whose osteosarcoma has spread to the lungs at the time of diagnosis the survival is lower, 10 out of every 100 people (10%) live more than 5 years [107].

Chondrosarcoma is more likely to be curable if it is low grade, considering that at least 80 out every 100 people (80%) will live for more than 10 years after treatment. But if the cancer is high grade the outlook is poorer and about 30 out of every 100 people (30%) will live for at least 5 years [107].

3.2.1. ***Risk factors for primary bone cancer***

Most people with bone cancers do not have any apparent risk. The major risk factors for the development of bone cancers are the existence of genetic disorders, Paget disease, radiation, bone marrow transplantation and injuries [90].

A very small number of bone cancers, especially osteosarcomas, appear to be hereditary and are caused by mutations in certain genes, for example, children with certain rare inherited syndromes have an increased risk of developing osteosarcoma. The Li-Fraumeni syndrome makes people much more likely to develop several types of cancer, including breast cancer, brain cancer, osteosarcoma, and other types of sarcoma. Most of those cases are caused by a mutation of the *P53* tumour suppressor gene, but some are caused by mutations in the gene *CHEK2* (Checkpoint kinase 2 gene). Another syndrome that includes bone cancer is the Rothmund-Thomson syndrome. Children with this syndrome are short, have skeletal problems, and rashes, and are more likely to develop osteosarcoma. This syndrome is caused by abnormal changes in the gene *REQL4 (*ATP-dependent DNA helicase Q4 gene) [90]. Retinoblastoma is a rare eye cancer of children that can be hereditary. The inherited form of retinoblastoma is caused by a mutation of the *RB1* gene. Those with this mutation also have an inherited risk of developing bone or soft tissue sarcomas. Also, if radiation therapy is used to treat retinoblastoma, the risk of osteosarcoma in the bones around the eye is even higher. Finally there are several families with several members who have developed osteosarcoma without inherited changes in any of the known genes. Additionally, people with metal implants into bones, are more likely to develop osteosarcoma [90, 91]. Paget disease is a benign but pre-cancerous condition that affects one or more bones. It results in formation of abnormal bone tissue and is mostly a disease of people older than 50. Affected bones are heavy, thick, and brittle. They are weaker than normal bones and are more likely to fracture. Bone cancer (usually osteosarcoma) develops in about 1% of those with Paget disease, usually when many bones are affected [90].

Bone exposure to ionizing radiation may also increase the risk of developing bone cancer. A typical x-ray of a bone is not dangerous, but exposures to large doses of radiation pose a risk. Being treated at a younger age and/or being treated with higher doses of radiation (usually over 60 Gy) increases the risk of developing bone cancer. Exposure to radioactive materials such as radium and strontium can also cause bone cancer because these minerals build up in bones [90]. Osteosarcoma has been reported in a few patients who have undergone bone marrow transplantation. People have wondered whether injury to a bone can cause cancer, but this has never been proven [90].

Ewing sarcoma is not strongly associated with any hereditary cancer syndromes, congenital childhood diseases, or previous radiation exposure [90, 91]. Multiple exostoses (sometimes called multiple osteochondromas) syndrome is inherited conditions that cause many bumps on a person's bones. These bumps are made mostly of cartilage. They can be painful and cause bones to deform and/or fracture. This disorder is caused by a mutation in any of the 3 genes *EXT1*, *EXT2*, or *EXT3*. Patients with this condition have an inherited risk of chondrosarcoma. People who has multiple enchondromatosis (multiple enchondroma), have an increased risk of developing chondrosarcomas [90, 91].

Chordomas seem to run in some families. The genes responsible have not yet been found, but familial chordoma has been linked to changes on chromosome 7. Patients with inherited syndrome tuberous sclerosis, which can be caused by mutations in either of the genes *TSC1* and *TSC2*, seem to have a high risk of chordomas during childhood [90, 91].

Simply having cancer is a risk factor for bone metastases. Among people with the same kind of cancer, tumours that are larger and have already spread to lymph nodes are generally more likely to spread to bone. For some kinds of cancer, a high grade and certain genetic changes make the cancer more likely to spread to bones [98]. For patients with prostate, breast, or lung cancers, the risk of metastasis to bones is very high [67].

3.3. Diagnosis

A patient´s symptoms, physical exam, and results of imaging tests, and blood tests may suggest that bone cancer is present. The main signs and symptom of a bone cancer are pain, swelling, fractures, and other symptoms like height loss, fatigue, and symptoms associated with the organs affected by the spread of the cancer. Pain in the affected bone is the most common complain of patients with bone cancer. At first, the pain is not constant, and it may be worse at night or when the bone is used. As the cancer grows, the pain will be there constantly. The pain increases with activity and the person might limp if the leg is involved [90].

If cancer is diagnosed, bone metastases may sometimes be found before they have a chance to cause any symptoms. Since single bone metastasis can have the same sign and symptoms as a primary bone tumour, many doctors require a biopsy to diagnose a patient's first bone metastasis [90]. The biopsy is the only way to know that the tumour is cancer and not some other bone disease, or if it is a primary bone cancer or metastases. Several types of tissue and cell samples are used to diagnose bone cancer. The surgeon will choose a biopsy method based on whether the tumour looks benign or malignant and exactly what type of tumour is most likely. Some kinds of bone tumours can be recognized from needle biopsy samples, but larger samples are often needed to diagnose other types. [89, 90].

Several imaging techniques may be used for the diagnosis of primary bone cancer namely x-ray scans, bone scan, computed tomography (CT) scan, magnetic resonance imaging (MRI) procedure, positron emission tomography (PET) scan, and angiogram. Some of these imaging tests may be required to see how far the cancer has spread. This may be done before, during and after treatment [90, 91].

X-ray scans are often among the first tests ordered if a person with cancer is having bone pain or other symptoms. X-rays scans allow obtaining the information about location, size and shape of bone tumour. The bone at the site of the cancer may appear "ragged" instead of solid, and also appear as a hole in the bone. In osteolytic metastases, cancer cells will dissolve some of the

minerals in the bone, making an area of the bone less dense, therefore these changes will appear on x-ray as a darker hole in the gray-white bone image. In the case of osteblastic metastases, the area will appear denser and sclerotic. Also x-rays can show fractures in bones that have been weakened by metastases. CT and MRI allows obtaining more detailed morphologic images of the bones and tumours. The CT scans are also helpful in staging cancer helping to determine if the cancer has spread to other organs. CT scans can be useful especially if the bone metastases are likely to be osteolytic (hard to visualize in bone scans). A CT scan is sometimes used to guide a biopsy when a bone metastasis is deep in the body. CT scans are also good for judging the size and shape of a tumour in the bone and for assessing how stable a bone containing a tumour is. MRI scans are often best test to outlining a bone tumour, and are particularly helpful for looking at the brain and spinal cord. Bone scan and PET allows obtaining information, respectively, about the osteoblastic/osteoclastic activity and glucose metabolism (when administered ^{18}F-FDG). Bone scan allows determining if the cancer has spread to other bones. It can find metastasis earlier than regular x-rays, and also show how much damage the primary cancer has caused in the bone. Areas of active bone changes appear as hot spots on the skeleton. These areas may suggest the presence of cancer, but other bone diseases can also cause the same pattern. PET scan give useful information about the spread of the cancer to other organs, but this images lack on resolution, therefore newer machines combine PET and CT or PET and MRI [90, 91].

Some types of cancer release certain substances called tumour markers into the bloodstream. Patients with these types of cancer may have to do blood tests at regular intervals to see if levels of these markers are rising. An increase in tumour markers levels mean that the cancer has spread, but it doesn't show where the cancer has spread. Other tests will be needed to show if the metastases are in the bone or if they are somewhere else in the body. Prostate-specific antigen is an example of a tumour marker, more specifically from prostate cancer. Other examples of tumour markers are high blood calcium and alkaline phosphatase levels. These markers result from the presence of bone

metastases that can dissolve the bone. Also, several substances can be released into urine when bone is damaged, namely N-telopeptide [98].

3.4. Therapy

Treatment options depend on the type, size, location, and stage of the cancer, as well as the person´s age and general health [91]. Treatment options for primary bone cancer include surgery, chemotherapy, and radiation therapy [90, 91].

Surgery is the major treatment for most bone cancers, and it may be used to obtain a biopsy of the cancer. The type of surgery used will depend on the size of the cancer, the location in the body and whether it has grown into the tissues surrounding the bone. The main goal of the surgery is to remove all of the cancer, considering that if even a few cancer cells are left behind, they can grow and multiple to make a new tumour. Trying to be sure that this doesn't happen, surgeons remove the tumours plus some of the normal surrounding tissue. Various techniques can be used, namely the removal of the entire bone affected by the cancer, the limb sparing surgery, the amputation (when is a leg or arm) and the surgery to remove metastasis. Bone amputation may be performed if the tumour has spread into the tissues surrounding the bone, affecting the major nerves and blood vessels or muscles, or if the position of the tumour makes impossible the resource to limb sparing surgery. Sometimes, when a bone cancer has spread, the number and size of metastasis is small and the location is favourable, and can be removed surgically [90, 91].

Patients who have bone cancer usually receive a combination of anticancer drugs (chemotherapy). Chemotherapy works very well for some types of bone cancers, particularly Ewing's sarcomas and osteosarcomas, but not for all patients. Chemotherapy is often given before surgery to help shrink the tumour and make it easier to remove or after surgery to reduce the risk of the cancer coming back. Also, chemotherapy can be used to relieve the symptoms, by shrinkage of cancer. Chemotherapy is sometimes used for bone cancer that has spread through the bloodstream to the lungs and/or other organs. The drugs mainly used to treat bone cancer include the doxorubicin, cisplatin,

carboplatin, etoposide, ifosfamide, cyclophosphamide, methotrexate, and vincristine. Usually several drugs (two or three) are given together, for example, a very common combination is cisplastin and doxorubicin, ifosfamide and etoposide or ifosfamide and doxorubicin [90, 91].

Radiotherapy may also be used before surgery to shrink the tumour and make it easier to remove, or after surgery to help lower the risk of the cancer coming back. It is often used on tumours that do not respond well to chemotherapy, in patients who refuse surgery, or in unresectable bone tumours [90, 91].

For systemic treatment, and for most of the cases for palliative treatment, of bone metastasis, besides chemotherapy, also its possible to resort to hormone therapy (reducing osteoclast formation), immunotherapy, stimulation of bone formation (implanting biomaterials targeted with molecular signals designed to trigger the body's repair mechanism), growth factors, gene therapy, diphosphonates (inhibitors of bone resorption), and radiation therapy using radiopharmaceuticals [98, 108, 109].

Chronic pain syndrome is the most important complication of bone metastasis and has a negative impact on quality of life and at the social environment of the patient [101, 102]. Up to one-half of patients do not receive adequate pain treatment. About two-thirds of pain patients complain about break-through pain, meaning a simultaneous appearance of strong pain in spite of the intake of analgesics. It is therapeutically relevant that, in most of these patients with break-through pain, optimization of pain therapy is possible [69]. Nonsteroidal anti-inflammatory drugs are the first weapon to use in the treatment of such pain, followed up by opiates in a stepwise approach recommended by World Health Organization guidelines [110]. Some of the drugs have gastrointestinal side effects and lead to hepatic damage [111, 112]. Although narcotics are generally effective in relieving pain, the somnolence, nausea, and constipation that result from their use almost inevitably decrease the quality of life of the patient with advanced cancer [110].

Chemotherapy is used as the main treatment for many types of metastatic cancer that has spread, and is often able to shrink tumours reducing pain. Besides chemotherapy drugs kill cancer cells it also damage some normal cells, causing side effects (e.g. nausea, loss of appetite, loss of hair, mouth sores, diarrhoea, etc.) [98].

Hormones in the body drive the growth of some common cancers, for example estrogen (produced in the ovaries) promotes growth of some breast cancers, and androgens (testosterone produced in testicles) promote growth of most prostate cancers. One of the main ways to treat breast and prostate cancers is to surgically remove the organs that make the hormones. More often, drugs are given to keep the hormones from being made. Both for men and women, respectively with prostate or breast cancer, can be given drugs such as luteinizing hormone-releasing hormone agonists or antagonists, which block testosterone and estrogen production. Also, for women in menopause, the ovaries no longer make hormones, a small amount of estrogen is still made in fat tissue. Drugs called aromatase inhibitors stop this estrogen from being produced. Another approach is preventing the hormones from affecting the cancer cells, and in this case it can be given anti-androgens or anti-estrogens (e.g. tamoxifen). Side effects of hormone treatments depend on the type of treatment used, being the most common side effect hot flashes. Hormone therapy for prostate cancer can lead to anaemia, weight gain, loss of sex drive, etc. Tamoxifen use increases the risk of blood clots and uterine cancer [98].

Immunotherapy, sometimes called biologic therapy or biotherapy, is a systemic therapy that uses certain parts of the immune system to fight diseases such as cancer. This can be done by stimulating the immune system to work harder or smarter to attack cancer cells, or by giving man made versions of immune system proteins to kill cancer cells. It is used by itself to treat some cancers, but for many cancers it seems to work best when used along with other types of treatment. Several types of immunotherapy are used to treat patients with metastatic cancer, including monoclonal antibodies, tumours vaccines, and cytokines. Monoclonal antibodies (mAbs) are men-made versions of immune system proteins, and are very useful in treating cancer because they can be designed to attack a very specific part of a cancer cell, targeting specific antigens. A major advantage of these drugs is that they may have only mild side effects if the right antigen is identified. For cancer, this is not always easy, and so far mAbs have proven to be more useful against some cancers than others. Cancer vaccines are substances putt into the body to start an immune response against certain diseases, helping to prevent or treat cancer. Because some cancers are caused by viruses, like uterine cervix carcinoma caused by human

papilomas virus and liver cancer caused by hepatitis B virus, some vaccines may help to protect against infections and prevent some cancers resulting from these viruses. Cancer treatment vaccines are different from the vaccines that work against viruses, considering that these vaccines try to get the immune system to mount an attack against cancer cells in the body. Instead of preventing disease, they are meant to get the immune system to attack a disease that already exists. Sipuleucel-T is the only vaccine approved by the United States Food and Drug Administration (FDA) to help treat cancer, and is used to treat advanced prostate cancer that is no longer being helped by hormone therapy. Non-specific immunotherapies do not target a certain cell or antigen, they boost the immune system in a very general way, but may still result in more activity against cancer cells. Some examples of non-specific immunotherapy's are the ones that uses cytokines, interleukins, interferon's, and granulocyte-macrophage colony-stimulating factor [98, 113].

Diphosphonates or biphosphonates are analogues of pyrophosphate, a natural inhibitor of bone demineralization. They bind to hydroxyapatite crystals of the bone by adsorption, resulting in stabilization of bone mineral and inhibition of its dissolution. Moreover, it inhibits osteoclast function by various not fully understood mechanisms [98, 99, 114]. Recently, Yoneda *et al.* [115], in an experimental study with animal models of bone metastasis have shown that diphosphonates impaired the progression of bone metastasis primarily through enhancing apoptosis of osteoclasts and breast cancer cells colonised in bone [115]. However, the rate of bone resorption varies both between patients and within patients during periods of disease remission and progression, so it is somewhat simplistic to assume that all patients require the same dose of diphosphonates for treatment. Patients with normal or only minimally accelerated bone resorption probably do not need the intensity of treatment provided by current schedules of highly potent aminodiphosphonates. Additionally, clinical benefit from diphosphonates derivatives seems to be related to the effective suppression of accelerated bone resorption. There is growing evidence that treatment with diphosphonate in advanced cancer normalizes bone resorption, as in benign bone diseases [99]. Well known examples of diphosphonates include pamidronate (1-hydroxy-3-aminopropylidene-diphosphonic acid - APD) and etidronate (1-hydroxy-

ethylene-diphosphonic acid - HEDP), used to treat Paget´s disease, osteoporosis, and *osteogenesis imperfecta*, a hereditary bone disorder.

3.4.1. ***Targeted radionuclide therapy of bone metastases and PEI-MP***

The delivery of ionizing radiation to a bone containing a metastatic tumour can be achieved using either radiation from an external X-ray or gamma ray beam or injecting radioisotopes that localize in the bone [108]. Radiotherapy with external beams is a treatment of primary importance in bone metastasis pain palliation despite these patients being by definition incurable [111, 112, 116]. However, palliative radiotherapy can reduce or eliminate pain from bone metastasis in 80% of patients [117]. Although higher doses of radiation can better control the tumour, the dose that can be delivered is limited by the possibility of damaging normal tissue surrounding the tumour. Ulceration, fistulas, severe fibrosis, and strictures may develop months or years after treatment, severely affecting the quality of life. On the other hand, if a small portion of the cancer is excluded from the irradiated volume the treatment can fail. Recent advances in conformal radiotherapy allow better dose distribution to the target volume with better adjustment to the shape of the tumour. The value of conformal techniques has been demonstrated in the treatment of localized prostate cancer. Prospective dose escalation studies have shown that higher doses can be delivered with a marked improvement at 5-years, without any increase of latent toxicity [118, 119].

Treatment using tracer molecules to target radiation to tumour is well established [120, 121] and while local external beam irradiation is the first choice for palliative treatment for patients with a limited number of lesions [122], systemic radiotherapy with radiopharmaceuticals is preferable when widespread bone metastasis are present with multifocal sites of pain [84].

Interest in designing an effective radiopharmaceutical for palliative therapy and treatment of bone metastasis has increased in recent years [102]. This is primarily due to the emergence of new sophisticated molecular carriers that may provide vehicles for selective deposition of radioactivity in the vicinity of cancer cells. In order to develop effective radiopharmaceuticals for therapy, it is essential to carefully consider the choices of appropriate radionuclides in

conjunction with the *in vivo* localization and pharmacokinetic properties of the radiotracer [123]. The treatment with radionuclides is a safe and effective tool in medicine because it acts mostly in the peripheral nerve endings, where tumour, inflammatory and immune cells cumulate and release substances [116]. An ideal radiopharmaceutical for the treatment of neoplastic bone disease would be a radiolabelled compound that predominantly accumulates in bone lesions, with low toxicity to the bone marrow and limited uptake by normal bone and other organs [111, 112]. In order to get radiopharmaceuticals that predominantly accumulate in bone lesions they must have affinity for hydroxyapatite and its components, allowing a selective accumulation in bone, with special emphasis on the affected areas with high bone-turnover [108]. The therapeutic radiopharmaceuticals are commonly composed by two key components: a radionuclide and a targeting ligand with which it is complexed**.** The radionuclide produces a relief after selective uptake at the target, ideally with negligible damage to healthy tissue. The function of the ligand is prevent dissociation of the complex and facilitate the transfer of the radionuclide to the target, as in the case of secondary bone metastasis requiring that it should be bone-seeking. The ligand of choice should selectively accumulate in regions of high Ca^{2+} concentration which is characteristic of areas affected by secondary bone metastasis [59, 102, 124]. Although, the mechanisms by which pain is relieved remain poorly understood it is speculated that the radiopharmaceuticals used in pain palliation treatment work by adsorption or fixation on bone in the areas of increased osteoblastic activity. Radiation of the attached radionuclide will then cause death in a fraction of cells within the range of the particles emitted and depending on their energy. The resulting decrease in intra-osseous mass and pressure brings relief to the patient. However, it is found that the reduction of the pain intensity takes a few days as tumour mass shrinks. So, the mechanism by which radiotherapy achieves analgesia probably is a mixed response due both to tumour shrinkage and to inhibition of pain mediators, such as prostaglandins and neurogenic peptides [101].

In recent years there has been interest in the application of diphosphonates as potential radiopharmaceuticals for effective pain-palliation of metastatic bone cancer [112, 125, 126]. These versatile molecules are characterized by a P-C-P

structural element, and have a variety of important uses such as metal chelation ligands [127], therapeutic use in patients with two main types of disorders, ectopic calcification and ossification, and increased bone resorption [79] and in nuclear medicine as ligands for radiometals in bone-seeking diagnostic and therapeutic agents [128].

Phosphonates are known to have a particular affinity for calcium (Ca^{2+}), so they accumulate selectively in bone [102]. Some (di)phosphonic acid derivates include EDTMP (ethylene-diamine-tetramethylene-phosphonate), MDP (methylene-diphosphonic acid), HEDP (1-hydroxy-ethylene-diphosphonic acid), APD (1-hydroxy-3-aminopropylidene-diphosphonic acid), APDDMP (N,N,-dimethylene-phosphonate-1-hydroxy-4- aminopropylidene-diphosphonate) and recently, PEI-MP (polyethyleneiminomethyl phosphonic acid) [129]. The two last improve the properties of ^{153}Sm-EDTMP, widely used in the pain palliation therapy of patients suffering from bone cancer, not only providing pain relief but also suppressing and decreasing bone metastasis and even osteosarcomas [59, 102, 124]. APD had been applied in the inhibition of osteoclast activity by adsorption on the bone surface (hydroxyapatite). In addition to minimizing resorption, APD also regenerates bone tissue by mobilizing Ca^{2+} and Mg^{2+} from blood plasma and subsequent deposition onto bone [125]. Being such a versatile ligand, attempts were made to capitalize its capabilities by complexing it to a radioactive metal-ion, and use it as a bone-cancer diagnostic agent (e.g. ^{99m}Tc-APD for bone scintigraphy) [130]. However, in studies with trivalent lanthanides such as [131] $^{166}Ho^{3+}$ and $^{153}Sm^{3+}$ a neutral complex $(MLH)^0$ is obtained and, hence, a colloid is formed at pH 7.4, which results in excessive liver uptake. Furthermore, APD exhibited a high affinity for Ca^{2+} which inhibits the delivery of the radionuclide $^{166}Ho^{3+}$ to the bone. In an endeavour to avoid the formation of neutral species, APD was modified by adding two charged methylenephosphonate groups at the primary amine centre, resulting in the synthesis of APDDMP – with a net charge of 7. The radiolabelling of APDDMP with the same trivalent lanthanides resulted in complexes with a negative charge. Subsequent studies in animal models, using the complexes ^{166}Ho-APDDMP and ^{153}Sm-APDDMP demonstrated that the uptake by the liver was avoided to a large extent. However, only the complex ^{153}Sm-APDDMP showed

a good bone uptake, although was less than ^{153}Sm-EDTMP [132]. MDP is use as a radioactive bone imaging agent after labelling with ^{99m}Tc (^{99m}Tc-MDP). HMDP (hydroxymethylene diphosphonate) is sometimes used to replace MDP to target bone. Comparing both agents, studies showed that the cancerous/compact bone uptake is greater for HMDP than for MDP. Another ligand used is HEDP. Although the bone uptake of ^{99m}Tc-HEDP is lower and its blood clearance slower than of ^{99m}Tc-MDP, it gives a greater contrast between regions of higher and lower calcification rates. As the areas with higher rates of calcification should be the target of a possible palliative radiopharmaceutical, HEDP seems to be a promising candidate [133].

There are several beta-emitting radioisotopes currently being used for pain relief including phosphorus-32 (^{32}P), strontium-89 (^{89}Sr), yttrium-90 (^{90}Y), samarium-153 (^{153}Sm), holmium-166 (^{166}Ho), rhenium-186 (^{186}Re), rhenium-188 (^{188}Re) and Lutetium-177 (^{177}Lu). The individual nuclides differ in terms of efficacy, duration of pain relief, tumoricidal effects, repeatable treatments, toxicity and expense. Despite these differences all of the radionuclides or their attached ligands preferentially target osteoblastic surfaces, suggesting a greater benefit in metastasis associated with increased osteoblastic activity [59, 66].

The application of radionuclides for treatment of painful metastasis has been investigated for several decades. In 1960s, the first nuclide administered for pain therapy of multiple osseous metastases was ^{32}P [134]. Initially it was believed that its effect was mainly from incorporation into the tumour itself. However, the tumour to non-tumour ratio was not very favourable and the relief of pain is primarily because of its uptake by the bone mineral, and not by the tumour. In addition, uptake was high in a rapidly dividing tissue such as the bowel, but particularly in the red marrow itself [65]. Today, it's known that ^{32}P is incorporated into the DNA of rapidly proliferating cells of the bone marrow as well as in the trabecular and cortical structures of the bone. The ratio of normal bone to metastatic tissue was calculated as 1:2, and therefore is relatively low [120]. This unfavourable ratio and the frequently observed strong myelosuppression were the reasons for abandoning of the ^{32}P [69]. Also, the absence of any gamma radiation emitted during its decay complicated the study of its biodistribution and biokinetics in humans [65].

Many different beta-emitting radiopharmaceuticals like ^{89}Sr-chloride, ^{90}Y-citrate, ^{90}Y-DOTA-HBP, ^{153}Sm-EDTMP, ^{166}Ho-EDTMP, $^{186/188}$Re-HEDP, $^{186/188}$Re-MDP, have been investigated for use in therapy [134, 135].

Strontium-89 chloride was the nuclide most widely used in nuclear medicine for therapy. It has a long physical half-life, requiring a low administered activity, resulting in a rather low initial dose rate. In addition, it does not need repeated administrations for effect [134]. Laing *et al.* treated 119 prostate cancer patients with painful metastatic bone disease, who did not respond to conventional therapy, by application of ^{89}Sr. A total of 75% of the patients demonstrated a marked improvement of the pain status and 20% of these patients were almost completely pain free. The effect of ^{89}Sr treatment began 10-20 days post injection and reached a maximum after 6 weeks [135, 136]. The pain improvement lasted for 6 months on average with a variation between 4 and 15 months. The authors could not find a significant advantage of an activity of 3.0 MBq/kg body weight above that of 1.5 or 2.2 MBq/kg, resulting in a recommended activity of 150 MBq of ^{89}Sr. This activity has been considered the standard ever since [136]. Lewington *et al.* performed a randomized, placebo-controlled, double-blinded study in prostate cancer patients who were refractory to hormonal treatment and external radiation therapy. The patients treated with ^{89}Sr showed a significant pain reduction compared to the patients in the placebo group. Considering that these patients were end-stage patients who had failed all conventional therapy, the effect of ^{89}Sr treatment is impressive. Further studies confirmed the beneficial effect of ^{89}Sr for pain treatment in prostate cancer patients [137]. Quilty *et al.* demonstrated in 284 prostate cancer patients that one injection of ^{89}Sr was as efficient as a hemibody irradiation which often showed intolerable side effects [134, 138]. Depending on the extension of the metastatic disease, the tracer uptake in the skeletal system ranges between 12% and 90% of the administered activity. With extensive presence of bone metastasis the higher the uptake in to the skeleton is. The accumulation of ^{89}Sr-chloride in the metastatic lesions is 5-20 times as high as the accumulation in normal bone tissue. Ninety days after the administration, 10-88% of the injected ^{89}Sr activity was found in metastatic bone lesions [139]. The effective half-life was calculated to be over than 50 days, thus ^{89}Sr-chloride delivers a low dose

rate radiation [69]. Robinson RG reported a response rate of 81% in breast cancer patients with multiple bone metastases on investigating 500 patients with different tumours after injection of ^{89}Sr at a standard activity [140]. Baziotis *et al.* treated 64 breast cancer patients by a single injection with 2MBq/kg body weight of ^{89}Sr. They found an improvement of the pain situation in 80% of the cases including 35% of the patient demonstrating almost complete pain relief. The average time response was 3 months [141].

Like strontrium-89, the calcium analogue (it follows the biochemical pathways of calcium in the body) yttrium-90 (^{90}Y) is taken up by the bone depending on the intensity of the osseous metabolism [69, 138]. Yttrium-90 (^{90}Y) is a pure high energy beta emitter. Used as the citrate salt, it shows 80% uptake in the bones [142, 143]. In this form it has been used for pain palliation of metastatic disease. It has also the chemical properties suitable for chelation to several commonly used compounds or macrocyclic ligands such as DOTA (1,4,7,10-tetraazacyclododecane-1,4,7,10-tetraacetic acid) [143]. Although ^{90}Y-citrate indicates high accumulation in the bone, a part of the Y^{3+} released by the dissociation of the citrate complex binds to serum, which results in delayed blood clearance and accumulation in the liver. Ogawa K *et al.* hypothesized that a bone-specific ^{90}Y-labelled radiopharmaceutical could be developed. So, they chose DOTA as the chelating site, and DOTA was conjugated with 4-amino-1-hydroxybutylidene-1,1-bisphosphonate (HBP). They studied the biodistribution of ^{90}Y-DOTA-HBP and compared it with ^{90}Y-citrate. Their results showed that ^{90}Y-DOTA-HBP had superior biodistribution characteristics as a bone-seeking agent and led to a decrease in the level of unnecessary radiation exposure compared to ^{90}Y-citrate. Even so, the plasma stability of ^{90}Y-DOTA-HBP was not as high as expected. In addition, in the case of the absorbed dose to red marrow, which is the dose-limiting factor of radiopharmaceuticals for palliation of metastatic bone pain, the ratios of the absorbed dose in red marrow to that in osteogenic cells were almost the same for ^{90}Y-DOTA-HBP and ^{90}Y-citrate. Both compounds might show similar degrees of myelosuppression, which is the most important side effect. Because the radiation dose to bone marrow is highly influenced by the accumulation of radioactivity in the bone, improvement in the clearances from the blood and other tissues do not contribute much to the

radiation dose to red marrow. Meanwhile, although the ratios of the absorbed dose in soft tissues to that in osteogenic cells of ^{90}Y-DOTA-HBP were also lower than those of ^{153}Sm-EDTMP, ^{153}Sm-EDTMP has the advantage over ^{90}Y-DOTA-HBP in terms of the effective dose equivalent (0.387 mGy/MBq of ^{153}Sm-EDTMP compared with 0.840 mGy/MBq of ^{90}Y-DOTA-HBP) and effective dose (0.232 mGy/MBq of ^{153}Sm-EDTMP compared with 0.652 mGy/MBq of ^{90}Y-DOTA-HBP). It is attributed to the difference in the radiation of red marrow. Therefore ^{153}Sm could be preferred to ^{90}Y as a radionuclide used in palliation therapy because the energy of the ^{90}Y β particles could be too high [142].

Samarium-153 is one of the vital radionuclides amongst the lanthanide elements from the point of view of nuclear medicine. Due to its short half-life, ^{153}Sm replaced the comparatively long-lived ^{89}Sr isotope. The therapeutic activity is 30 times more economic than the ^{89}Sr-chloride. Clinical studies show that the toxicity is lower but the palliative effect is of shorter duration than desired [144, 145]. Samarium-153 chelated with EDTMP, is widely used in the clinic for the effective palliative treatment of widespread skeletal metastasis as it can be concentrated in bone metastasis having an osteoblastic component. Samarium-153 has a short physical half-life that can be advantageous because it can be administered repeatedly. However, because of its short physical half-life and its production by reactor, delivery is difficult. The range of its beta particles is short (average 0.55 mm), resulting in good bone to bone marrow ratios [65]. One hundred and eighteen patients with painful bone metastasis were randomly assigned to receive a single dose of 18.5MBq/kg of ^{153}Sm-EDTMP. The results of a patient-rated scale revealed a progressive decrease in pain during the first four weeks of the study in the treatment groups. ^{153}Sm-EDTMP is rapidly cleared from the blood into the urine and only 1% of injected activity remains in the blood four hours post-administration whereas it is retained in the bone for a long time [144-146]. Alberts *et al.* concluded from a trial with 35 patients that 0.04 MBq/kg activity is adequate for ^{153}Sm-EDTMP, often requiring multiple applications for safe palliation of pain associated with metastatic bone cancer [128, 147, 148]. Palliative and even curative effects have been demonstrated in dogs using ^{153}Sm-EDTMP to treat a variety of skeletal neoplasias, both primary and metastatic. In a double-blind placebo-

controlled study, Serafini *et al.* investigated the effect of ^{153}Sm-EDTMP in 80 prostate cancer patients. Four weeks after the injection of a single dose of 0.03 MBq/kg body weight, an improvement of the pain situation was observed in 72% of the patients. In 31% of the patients, an almost complete pain reduction could be found. Four months after the treatment, 43% of the patients showed a continuing improvement of pain symptoms. In this study, a visual analogue scale for different regions of the body, the consumption of analgesics and pain scoring performed by the physician served as criteria for treatment response. The response rate of ^{153}Sm-EDTMP group was significantly better than that of the placebo group, showing response rates of 40% and 2% after 4 weeks and 4 months, respectively [149]. However, Tian *et al.* were not able to confirm in their multicenter trial that the two different activity groups of ^{153}Sm experienced different quality on pain palliation [150]. Collins *et al* reported that the onset of pain relief can be expected after 7-14 days [151].

In an attempt to improve on the success of ^{153}Sm-EDTMP, two possible strategies may be deployed. The first alternative is to use higher-energy β^- emitting radionuclides, as was attempted with ^{166}Ho-EDTMP. Holmium-166 is a radionuclide that emits higher-energy β^--particles, which is thought to improve the therapeutic efficacy of bone-seeking radiopharmaceuticals due to the deeper soft tissue penetration. However, in the past few years others have argued that minimizing the dose to bone marrow by using low-energy particle emitters such as ^{117m}Sn, will spare the bone marrow and is, therefore, more likely to deliver a therapeutic dose to the cortical bone. However, the chemistry of a substitute radionuclide (which generally belongs to a different chemical element) will differ from that of ^{153}Sm. Even when the radionuclides are chemically similar and occur in the same oxidation state (3+ for Sm), there may still be a significant difference in their *in vivo* behaviour, as was proven for Ho(III). A different radionuclide normally requires a different ligand, so that the complex radiopharmaceutical shows a bone uptake which would resemble that of ^{153}Sm-EDTMP. The high natural abundance of ^{165}Ho, from which ^{166}Ho is easily produced by neutron activation, lowers the cost of production compared with that of ^{153}Sm. The attempts with the above-mentioned ligand together with ^{166}Ho proved to be unsuccessful, not because of the radiation characteristics of

^{166}Ho, but rather due to the chemical properties of Ho(III) in combination of the ligands investigated. With ^{166}Ho-EDTMP the *in vivo* stability of the complex proved to be inadequate (owing to changes in the Ho(III)-EDTMP formation constants, compared with Sm(III)-EDTMP), resulting in incomplete bone uptake [102].

^{186}Re and ^{188}Re are excellent examples of β^--emitting radionuclides that could be used for pain palliation of bone metastasis [76, 77]. ^{186}Re-HEDP is the diphosphonate complex most frequently studied [152-154]. This radiopharmaceutical can also be prepared using ^{188}Re to form ^{188}Re-HEDP, requiring both the carrier Re to ensure a good yield of the bone seeking agent [148, 155]. The physical half-life of ^{186}Re allows frequent repeat administrations in a short period of time. However, the average beta energy is considerably higher than of the ^{153}Sm and, consequently, the range is higher what is undesirable for the bone marrow [65]. Reaction conditions for the synthesis of ^{186}Re-MDP must be acidic (pH 1.4 –1.6) in order to facilitate reduction of the perrhenate with stannous ion and to keep the reduced species from being oxidized [156]. The synthesis and stabilization of ^{186}Re-HEDP is different and can be accomplished at pH 5–8 [65]. It has also been reported that the comparative instability of the ^{186}Re-HEDP radiopharmaceutical to *in vivo* oxidation in to perrhenate is a possible advantage [123]. The radiopharmaceutical ^{186}Re-HEDP washes off from normal bone faster than it does from cancerous bone and, consequently, the abnormal/normal bone uptake ratio increases with time [128, 148]. ^{188}Re-HEDP has shown therapeutic efficacy in the treatment of metastatic bone pain associated with cancer of the breast, prostate, lung and others [77, 84, 157]. Both ^{186}Re-HEDP and ^{188}Re-HEDP have been used quite successfully in alleviating pain and for treatment of multiple metastatic foci of bone in bone cancer patients [65]. Hsieh B-T *et al.* compared various rhenium-188-labelled diphosphonates for the treatment of bone metastasis. In this study, they labelled MDP, HEDP, and HDP with ^{188}Re and they analysed the biodistribution and bone uptakes following an intravenous injection in rabbits. Their results showed that ^{188}Re-MDP and ^{188}Re-HDP tended to accumulate in the soft tissue and the liver. They believe that reactions between rhenium and diphosphonates are not the same as those

between technetium and diphosphonates, irrespective of being in the same group on the periodic table. In fact, technetium is inherently a better oxidant than rhenium. More $SnCl_2$ needs to be added in the labelling of the rhenium-diphosphonate complex. In this study, they concluded that the presence of carrier significantly affects the biodistribution of ^{188}Re-HEDP in rabbits. The bone to soft tissue ratio of ^{188}Re-HEDP significantly increased after adding the carrier to the preparation. However, carrier did not affect the biodistribution of ^{188}Re-MDP or ^{188}Re-HDP. The mechanism of the carrier effect is still not clear, requiring further study. Thus the authors concluded that the HEDP was better than MDP and HDP as a bone-seeking tracer together with ^{188}Re [148].

^{177}Lu can be produced at adequate specific activities by irradiation of the natural lutetium target in moderate-flux reactors, and its long half-life allows for shipment over long distances. Additionally, its 208-keV gamma-emission (11% abundance) allows imaging of its distribution to facilitate dose calculations. Recently, the usefulness of ^{177}Lu-1,4,7,10-tetraazacyclododecane-1,4,7,10-tetramethylene phosphonate (^{177}Lu-DOTMP) was demonstrated in a study performed in a mouse model [158]. The polyazamacrocyclic ligand framework may offer a complex which is kinetically more inert than ^{153}Sm-EDTMP [159]. Dogs with osteosarcomas were previously demonstrated to be important models of naturally occurring disease in humans [160]. The results showed that the dogs receiving ^{177}Lu-DOTMP tolerated the administration and the effects of the compound without apparent clinical toxicity, supporting the further evaluation in tumour-bearing dogs of ^{177}Lu-DOTMP as a potential therapy for metastatic bone cancer and primary bone tumours in humans and dogs [143].

In contrast to the beta-emitters, the alpha-particle emitters deliver a much more energetic and localized radiation, defined as high-linear energy-transfer (LET) radiation [1, 160]. Despite the fact that alpha-emitters are more toxic and mutagenic than beta emitters, these adverse properties can be compensated in the targeted therapy due to irradiation of smaller volumes of normal cells when alpha emitters are targeting tumour cell clusters. Also the spatial distribution of the hydroxyapatite target within an osteoblastic tumour would facilitate a volume distribution of the radionuclide where the tumour cells would be easier reached by alpha-particles despite the limited track lengths [120].

The progress in the biomedical application of alpha emitters have been delayed by the low availability of radionuclides with proper physical and chemical characteristics, supply limitations, as well as the costs for the most popular alpha emitters, ^{211}At (astatine-211; t½ = 7.2 h), ^{213}Bi (bismuth 213; t½ = 45.6 min) and ^{225}Ac (actinium-225; t½ = 10 days) [59, 120]. Recent research on alpha emitters led to the development of long term operating generators that can provide them in large quantities. Examples of such alpha-emitters are ^{223}Ra (radium-223; t½ = 11.4 days), ^{224}Ra (radium-224; t½ = 3.7 days), ^{227}Th (thorium-227; t½ = 18.7 days) and the alpha-emitter ^{212}Pb (lead-212; t½ = 10.6 h). In the absence of suitable complexing agents for radium isotopes investigation of ^{223}Ra in radioimmunotherapy could not occur, but methods have recently been developed to encapsulate ^{223}Ra and ^{225}Ac into liposomes, ensuring adequate stability [120].

Like strontium, radium is a natural bone seeker that has previously been used for targeting non-malignant skeletal diseases, such as in the use of ^{224}Ra (Radium-224) for treating ankylosing spondylitis, characterized by elevated bone synthesis [137]. Radium-223 (^{123}Ra) is the most promising radium isotope, with favourable properties for use in targeted radiotherapy. ^{223}Ra decays via a chain of daughter radionuclides with shorter half-life into stable lead, producing four alpha-particles. Radium-223 can be effectively produced in large amounts from sources of the precursor ^{227}Ac (t½ = 21.7 years) in a long-term operating generator. Moreover, ^{223}Ra half-life provides enough time for its preparation, distribution (including long distance shipment), and administration to patients. Its low gamma-irradiation facilitates handling, radiation protection, and treatment on an outpatient basis [120]. Based on the excellent physical characteristics of ^{223}Ra, were performed a series of studies, aiming to analyse the potential of this radioisotope in the treatment of bone metastases. In a study with ^{223}Ra in mice, biodistribution was measured at 1h, 6h, 24h, 3 days, and 14 days after injection. A rapid uptake and prolonged retention was demonstrated in the skeleton, whereas soft tissue radioactivity cleared relatively rapidly [161, 162]. Animal data and dosimetric studies have indicated that bone-targeting alpha-emitters can deliver therapeutically useful radiation doses to bone surfaces and skeletal metastases, at activity levels that are acceptable for

sparing bone marrow [163]. In a comparative study of ^{223}Ra and the beta-emitter ^{89}Sr it was found out that ^{223}Ra and ^{89}Sr had similar bone uptake, and estimates of dose deposition in bone marrow demonstrated a clear advantage of alpha-particle emitters being bone marrow sparing [164].

The therapeutic efficacy of ^{223}Ra was studied in a nude mice model. In this study the animals were injected with 10 million MT-1 human breast cancer cells into the left ventricle. Seven days later they were treated with ^{223}Ra dosage, ranging 6 to 30 kBq per animal. All untreated control animals had to be sacrified due to tumour induced paralysis 20 to 30 days following injection of tumour cells, whereas the mice treated with an activity superior to 10 kBq of ^{223}Ra showed a significantly increased symptom-free survival. Based on the encouraging preclinical results, a phase I study has been conducted. This study involved 25 patients with bone metastases (10 females and 15 males). Each of the patients received a single injection of ^{223}Ra and were monitored closely at the injection day, days 1, 2 and 7, and thereafter weekly to 8 week after the injection of ^{223}Ra. Five patients were enrolled at each dosage level; starting at 46 kBq/kg and then increasing to 93, 163, 213 and 250 kBq/kg of body weight. ^{223}Ra was well tolerated at therapeutically relevant dosages. The mild myelotoxicity, the generally weak side effects, and the encouraging pain scores found in this study encouraged the authors to conduct a phase II study [161].

In a randomised, double-blind, placebo-controlled, multicentre phase II study, the aim was to investigate the effect of repeated ^{223}Ra doses in men with symptomatic, hormone-refractory prostate cancer. Sixty four patients due to receive local-field, external-beam radiotherapy to relieve pain from bone metastases were assigned to receive either four repeated monthly injections of 50 kBq/kg ^{223}Ra (33 patients) or repeated injections of saline (31 patients). Treatment lasted for 12 weeks, during which four injections were given at 4-week intervals, with the first injection given at the time of external-beam radiotherapy and no later than 7 days afterwards. The results showed that ^{223}Ra was well tolerated with little or no myelotoxic effect, and showed promising evidence of efficacy [165].

A phase III, randomized, placebo-controlled, double-blind international human study had been conducted, comparing Alpharadin against placebo in men with symptomatic castration-resistant prostate cancer that has metastasized to the bone (ALSYMPCA – Alpharadin in Symptomatic Prostate Cancer). It involved 921 patients, in over 100 centres in 19 different nations. They were all either ineligible for docetaxel, could not tolerate it, or had not responded to the therapy with docexatel. Patients were given either Alpharadin or a placebo intravenously up to six times, four weeks apart. In this study 809 patients of the 921 patients were included in a planned interim analysis. In June 3, 2011 the Independent Data Monitoring Committee recommended stopping the trial early due to evidence of a significant treatment benefit. The more recent data of the 921 patients showed that Alpharadin improved overall survival by 44%, resulting in a 30.5% reduction in the risk of death compared to placebo. The median overall survival benefit with Alpharadin was 3.6 months (14.9 months in patients given Alpharadin vs. 11.3 months with placebo). In addition to improving overall survival, ^{223}Ra dichloride led to a statistically significant delay in the time to skeletal-related events. Alpharadin has been granted Fast Track designation by the FDA. Bayer plans to file Alpharadin seeking marketing approval for castration-resistant prostate cancer with regulatory authorities in the United States and Europe based on the ALSYMPCA data in the second half of 2012 [166, 167].

A radionuclide that could prove promising is radioactive ^{177m}Sn. It emits mono-energetic conversion electrons (energies of 126-158 keV) with a discrete range (0.2-0.3 mm) in bone tissue, which allows for larger bone radiation doses without excessive radiation to the bone marrow. Being an Auger emitting radionuclide, ^{117m}Sn will introduce a highly localized distribution of the electrons once inside or close to the cell. Furthermore, ^{117m}Sn possesses a favourable half-life of 13.6 days that, depending on *in vivo* pharmacokinetics, is long enough to deliver more auger electrons for the treatment. In addition to these favourable radiation characteristics, tin-ions exhibit an inherent affinity for bone as is observed in biodistribution experiments with rats and adsorption studies of hydroxyapatite [112]. Although difficult to produce with the required specific activity, the interest in ^{117m}Sn arises from its favourable half-life and discrete

range in bone tissue, as compared with ^{153}Sm, ^{32}P and ^{166}Ho [148]. In a study of Atkins HL, a bone to marrow ratio of 11 has been recorded for ^{117m}Sn-DTPA, which is far better than its closest rival, ^{153}Sm-EDTMP. Considering ^{166}Ho, its short half-life (26.7 h), might prove to be inadequate, while ^{117m}Sn (13.6 days half-life) would be ideal with a long half-life which is not too long to require radiation safety precautions. The oxidation state of the Sn is also important [102]. Zeevaart JR *et al.* sought an improved bone-seeking radiopharmaceutical, so they used ^{117m}Sn (II)–APDDMP. The results, using ECCLES (blood plasma model based on thermodynamic equilibrium), clearly showed that the target organs were the kidneys and bladder. ECCLES could in this case accurately predict that ^{117m}Sn (II)–APDDMP would have some bone as well as liver uptake. It furthermore, could explain the reasons for the high kidney uptake, namely ^{117m}Sn (II) radiopharmaceuticals are also dependant on the weakness of the complex between Sn (II) and the ligand carrier. This was verified by animal experiments with ^{117m}Sn (II)–APDDMP [94, 168].

A recent approach to develop an effective radiopharmaceutical for therapy of bone cancer, ensuring the selective uptake of the radiopharmaceutical, was to design a water-soluble polymer which is bone-seeking, and which would exploit the disrupted vasculature in tumours according to “Enhanced Permeability and Retention” (EPR) effect, as discussed by Maeda *et al.* [169] and Seymour [170] – the process in which macromolecules accumulate within tumour tissue due to leaky blood vessels and poor lymphatic clearance. The principal behind this scenario is that water-soluble macromolecules accumulate passively in solid tumours [171, 172].

The EPR effect is commonly observed in most solid tumours, either primary or metastatic in nature. In tumour biology, little is known about selective or tumour-specific characteristics compared with those of normal tissues or organs. The concept of the EPR effect in solid tumours is one of the few tumour-specific characteristics that are becoming a gold standard in antitumor drug delivery [169].

Lyer A *et al.* explained this phenomenon by analysing the anatomy of the tumour vasculature [173]. The blood vessels in the tumour are irregular in

shape, dilated, leaky or defective, and the endothelial cells are poorly aligned or disorganized with large fenestration. Also the perivascular cells and the basement membrane, or the smooth-muscle layer, are frequently absent or abnormal in the vascular wall. The tumour vessel has a wide lumen, whereas tumour tissues have poor lymphatic drainage. This anatomical defect, along with functional abnormalities, results in extensive leakage of blood plasma components, such as macromolecules, nanoparticles and lipid particles, into the tumour tissue. Moreover, the slow venous return to tumour tissue and the poor lymphatic clearance mean that macromolecules are retained in the tumour, whereas extravasation into the tumour interstitium continues. The EPR effect is also modulated or mediated by various factors produced by tumour cells, infiltrating leukocytes or even tumour-surrounding normal cells. Blood vessels near tumour tissue are affected by vascular mediators, such as vascular permeability factor, bradykinin and prostaglandins, nitric oxide, peroxynitrite and matrix metalloproteinases, which increase the vascular permeability of the tumour tissue [171, 173, 174].

Through this phenomenon very high local concentrations of polymeric drugs at the tumour site can be achieved, for instance 10-50-fold higher than in normal tissue within 1-2 days. Interestingly, the EPR effect does not apply to low-molecular-weight drugs because of their rapid diffusion into the circulating blood followed by renal clearance [173]. The polymer must, therefore, be large enough not to be taken up by healthy tissue, but not so large as to trapped in organs such as the liver or kidneys [111].

Because accumulation of macromolecules by the EPR effect is a progressive phenomenon, it is essential that the drugs are stable in the plasma for long periods. In addition to prolonging the half-life in plasma of low-molecular-weight drugs or proteins, polymer conjugation also guides the drugs or radionuclides to their target by the EPR effect. The alteration in conformation of some proteins or molecules constituting a drug gave a stealth character and the ability to suppress the antigenicity, as well as diminishes uptake by the reticuloendothelial system or macrophages. For example, succinylation of proteins or conjugation of poly(D-Glu-D-Ala-D-Lys) or poly(D-Glu-D-Lys) were all found to decrease substantially the immunogenicity of albumin, lactoglobulin,

myoglobin, γ-globulin and lysozyme. Therefore, the half-life of polymeric drugs in the blood circulation can be extended greatly [173].

Owing to the prolonged retention of the polymeric complexes by the EPR effect and the enhanced plasma half-life, polymer-conjugated drugs or radionuclides require less frequent administration compared with free drugs, which is a great benefit to patients [173, 175]. So, tumour-selective properties combined with a radionuclide with a short tissue penetration (with the resulting higher possible administered dose) could enable a very effective way of producing a radiopharmaceutical that would have not only palliative, but also therapeutic properties [102].

Dormehl IC *et al.*, aiming for a molecule for use in palliative therapy for bone metastases after suitable radiolabelling and considering the EPR effect, developed PEI-MP (polyethyleneiminomethyl phosphonic acid), a water-soluble polymer polyethyleneimine, functionalised with methyl phosphonate groups, synthesized by condensation of polyethyleneimine, phosphonic acid and formaldehyde [111]. In addition to being bone-seeking, PEI-MP would accumulate in solid tumours due to the EPR effect. Studies followed to establish the biodistribution and pharmacokinetic properties of different complexes PEI-MP/metal (^{99m}Tc, ^{117m}Sn and ^{186}Re) [129, 168].

They used various molecular sized PEI-MP radiolabelled with ^{99m}Tc, taking into account the EPR effect, choosing three different sizes of the PEI-MP, namely 30-300 kDa, 100-300 kDa and 10-30 kDa, to compare differences in their biodistribution and pharmacokinetics, using a normal primate model and scintigraphy. From the results, macromolecules with sizes ranging between 30-300 kDa were characterized by excessive liver (21-57%) and kidney (40%) uptake and accompanying long residence times ($t_{1/2}$ up to 24 hours). The percentage bone uptake averaged at 8% for these particles excluding sizes 100-300 kDa, where very little bone uptake was seen (<1%). In this case the blood clearance was also slow ($t_{1/2}$ approximately 2 hours). The fraction size 10-30 kDa had comparatively low accumulation and short residence times in the liver (20%; 22 minutes) and kidneys (17.5%; 20 minutes) and although the bone uptake of 18% in this case was high, it is still low for a bone-seeking agent.

These particles cleared from the blood with $t_{1/2}$ of 25 minutes, and seemed suitable for labelling with a therapeutic radioisotopic agent. Anionic species in the fraction of 10 to 30 kDa achieve good tumour uptake with minimum uptake in healthy bone, kidneys or liver. The polymer clearly demonstrates the potential to deliver a therapeutic radionuclide selectively to tumours [111].

Zeevaart *et al.* proposed that PEI-MP could be combined with radioactive ^{117m}Sn. For the EPR effect to apply, the macromolecules of ^{117m}Sn-PEI-MP should be larger than 40 kDa, i.e. large enough to avoid renal clearance [102]. Choosing two different sizes of the PEI-MP, namely 30-50 kDa and 10-30 kDa, Jansen D *et al.* compared differences in their absorption characteristics when radiolabelled with ^{117m}Sn in two different oxidation states (Sn^{2+} and Sn^{4+}). In addition to the size of the polymer, the oxidation state of the tin had a significant effect on the adsorption behaviour. The affinity of the tin in both valence forms was governed by the size of the PEI-MP ligand, with a four-fold increase in the affinity constants, accompanied by a slight improvement in the maximum absorption capacities when in presence of the smaller fraction, namely PEI-MP (10-30 kDa). In general, the optimum results were with Sn^{2+} in the presence of PEI-MP (10-30 kDa), where the metal-ion exhibited a higher affinity than the ligand whilst the adsorption capacity of the two were essentially equivalent. However this may not necessarily be an optimal combination when considering the EPR effect, in which the larger PEI-MP fraction could predominate, whilst the adsorption characteristics serve merely to complement the EPR accumulation. Furthermore, the Tin-PEI-MP complexes were not effectively desorbed and became immobilized on the hydroxyapatite surface, which may be advantageous for therapy, thereby facilitating passive accumulation of the radiopharmaceutical [176].

Section II. Literature Review

Chapter 4.Bladder Cancer

4.1. Introduction

Bladder cancer is the most common malignancy of the urinary tract. The three main types of cancers that affect the bladder are urothelial carcinoma (transitional cell carcinoma), squamous cell carcinoma, and adenocarcinoma. Transitional cell carcinoma originate from the epithelial cells of the inner lining of the bladder wall, squamous cell carcinoma originate in thin, and flat squamous cells and adenocarcinoma originate in glandular cells that make and release mucus and other fluids. The cells that form squamous cell carcinoma and adenocarcinoma develop in the inner lining of the bladder as a result of metaplasia and chronic irritation and inflammation [177, 178].

Transitional cell carcinoma is by far the most common form of bladder cancer accounting for more than 90% of these cancers, and is the second most common malignancy of genitourinary tract and the third most common cause of death among genitourinary tumours. Squamous cell carcinoma account for only 6% to 8%, and adenocarcinoma account for 3% of all bladder cancers [177, 178]. Transitional cell carcinoma is the 7^{th} most common cancer in men and the 17^{th} most common in women worldwide [179].

Transitional cell carcinoma can be subdivided by grade, stage and subtype [180]. Pathologic staging of bladder cancer is clinically the most powerful determinant in regard to patient prognosis and treatment decision in addition to grading [181-183]. Pathologic staging is based on the presence or absence of invasion and, in the case of invasive tumours, on the extent of invasion into the bladder wall, with the layers of the bladder wall and adjacent organs serving as staging landmarks [181].

Transitional cell carcinoma has been traditionally characterized as either superficial or invasive. The clinical staging of bladder carcinoma is determined by the depth of invasion of the bladder wall by the tumour. This determination

requires a cytoscopy examination that includes biopsy, and examination under anaesthesia to assess the size and mobility of palpable masses, the degree of invasion of the bladder wall, and the presence of extravesical extension or invasion of adjacent organs. Bladder cancer tends to spread progressively from its origin in the mucosa to the lamina propria, muscularis, perivesical fat, and subsequently to contiguous pelvic structures, with an increasing incidence of pelvic lymph node metastases at each stage. Obviously, distant metastasis occurs via haematogenous dissemination, with increasing incidence of distant metastasis with higher stage of disease. The most affected organs by distant metastases of a bladder cancer are liver, lungs and bones [184]. It is important to note that even at the earliest stages of invasive bladder cancer, distant metastases can develop [177]. Most cases of transitional cell carcinoma (70%) present as superficial, limited to the mucosa, submucosa, or lamina propria [185, 186]. In general, progressive invasion into the bladder wall by microscopic level increases stage, including papillary urothelial carcinoma confined to the mucosa (pTa), papillary or nodular tumours with involvement of the lamina propria (pT1), nonexophytic or “flat” carcinoma in situ (CIS) confined to the urethelium (pTis), superficial or deep muscularis propria (pT2a and pT2b, respectively), perivesical fat either microscopically (pT3a) or macroscopically (pT3b), and adjacent organs (pT4a) or the pelvic/abdominal wall (pT4b). A schematic representation of transitional cell carcinoma staging is represented in fig. 5 [181, 185, 187].

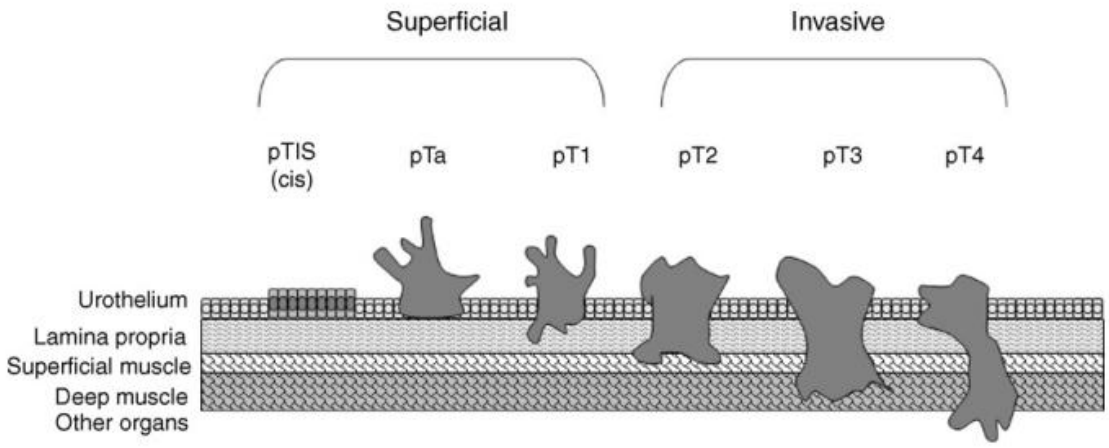

Figure 5. Transitional cell carcinoma staging. Carcinoma in situ, Tis or cis, are flat lesions showing dysplasia and are believed to be precursors to invasive urothelial cell carcinomas. Ta tumours represent the mildest form and show exophytic growth but do not engage the lamina propria. T1 tumours have transverse the basal membrane and engage the lamina propria. These tumours may also show a more solid growth pattern. Invasive tumours engage the underlying muscles and the surrounding organs in the most severe forms. Ta and T1 tumours are occasionally grouped together and characterized as superficial (Hoglund M., 2007).

The National Cancer Institute organizes and describes the stages for bladder carcinoma, as shown in the table 12, from stage 0 to IV [188].

Table 12. The National Cancer Institute staging for Bladder Carcinoma (NCI, 2014).

Stage	Description
Stage 0a	Called papillary carcinoma, may look like tiny mushrooms growing from the lining of the bladder.
Stage 0is	Called carcinoma in situ, is a flat tumour on the tissue lining the inside of the bladder.
Stage I	Cancer has spread to the layer below the inner lining of the bladder.
Stage II	Cancer has spread to either the inner half or outer half of the muscle wall of the bladder.
Stage III	Cancer has spread from the bladder to the fatty layer of tissue surrounding it, and may have spread to the reproductive organs (prostate, uterus, and vagina).
Stage IV	Cancer has spread from the bladder to the wall of the abdomen or pelvis. Cancer may have spread to one or more lymph nodes or to other parts of the body.

Legend: According to the National Cancer Institute, bladder carcinoma can be grouped in six stages. It starts by stages 0a and 0is that correspond to initial stages of the cancer where the cancer is still very superficial and contained. As it progresses to stages I, II, III and IV, the invasion to adjacent tissues or distant organs is increasingly likely.

The 2002 revision of the American Joint Committee on Cancer/International Union Against Cancer/Union International Contre le Cancer (AJCC/UICC) TNM system is the most widely used staging system at this time, and is summarized in table 13. This version was updated in 2009, but it has no changes for bladder tumours [189, 190].

Table 13. The 2009 TMN Staging System for Bladder Cancer (Edge S.B. *et al.*, 2010).

Primary tumour (T)	
TX	Primary tumour cannot be assessed.
T0	No evidence of primary tumour.
Ta	Non-invasive papillary carcinoma.
Tis	Carcinoma *in situ*: "flat tumour".
T1	Tumour invades subepithelial connective tissue (lamina propria).
T2	Tumour invades muscle (muscularis propria) of bladder wall.
T2a	Tumour invades superficial muscle (inner half).
T2b	Tumour invades deep muscle (outer half).
T3	Tumour invades perivesical tissue.
T3a	Microscopically.
T3b	Macroscopically (extravesical mass).
T4	Tumour invades any of the following: prostate, uterus, vagina, pelvic wall, and abdominal wall.
T4a	Tumour invades prostate, uterus or vagina.
T4b	Tumour invades pelvic or abdominal wall.
Regional lymph nodes (N)	
NX	Regional lymph nodes cannot be assessed.
N0	No regional lymph node metastasis.
N1	Metastases in a single lymph node in the true pelvis (hypogastric, obturator, external iliac, or presacral), 2 cm or less in greatest dimension.
N2	Metastases in a single lymph node in the true pelvis (hypogastric, obturator, external iliac, or presacral), more than 2 cm but not more than 5 cm in greatest dimension.
N3	Metastasis in iliac lymph node(s), more than 5 cm in greatest dimension.
Distant Metastasis (M)	
MX	Distant metastasis cannot be assessed.
M0	No distant metastasis.
M1	Distant metastasis.

Legend: The TNM staging system for bladder cancer stages is organized in three categories, namely the size of the primary tumour (T), the spread to lymph nodes (N), and the presence of metastases (M). For each of these categories, subdivisions may be made assigning a number to T, N or M, in a growing sequence, where the higher the number the lower is prognosis. TX, NX or MX means that the tumour, invasion to regional lymph nodes and the presence of metastases cannot be assessed.

In addition to the TNM system, the cancer may also be evaluated and assigned a grade (G). Physicians use the term “grade” to describe how much the tumour tissue looks like normal bladder tissue under a microscope. Pathologic grade, which is based on cellular atypia, nuclear abnormalities, and the number of mitotic figures, is of great prognostic importance. Many urologic surgeons classify grading based on the chance that the cancer will recur or progress, and plan their treatment based on the grade. In 2004 the World Health Organization (WHO) developed a new grading system for early bladder cancer, which is increasingly being used. This system divides bladder cancers into the following groups, summarized in table 14 [188, 191]:

Table 14. The 2004 WHO Grading System for Bladder Cancer (Miyamoto H. *et al.*, 2010).

Grading	**Description**
Urothelial papilloma	Non cancerous (benign) tumour.
Papillary urothelial neoplasm of low malignant potential (PUNLMP)	Very slow growing and unlikely to spread. These types of cancer may recur but have a low risk of progressing.
Low grade papillary urothelial carcinoma	Slow growing and unlikely to spread. These types of cancer are more likely to recur and progress compared with PUNLMP.
High grade papillary urothelial carcinoma	More quickly growing and more likely to spread. These types of cancer are the most likely to recur and progress.

Legend: The 2004 WHO grading system for bladder cancer, is divided in four groups, starting with the urothelial papilloma that is a benign tumour, followed by groups with a increasingly higher malignancy, the papillary urothelial neoplasm, the low grade papillary urothelial carcinoma, ending with the high grade papillary urothelial carcinoma. The higher the grade, the greater is the ability of invasion and growth.

Ta lesions account for approximately 70% of superficial transitional cell carcinoma. Histologically, these papillary tumours are composed of a branching fibrovascular core and mucosa greater than 8 cells layers with features of anaplasia [192, 193]. Most Ta tumours are low grade, rarely progress, and are associated with a favourable prognosis, whereas high-grade Ta and T1 tumours represent a significant risk of tumour progression and recurrence. Carcinoma *in situ*, Tis, is a flat lesion commonly found in association with malignant tumours

and is generally believed to be precursor of invasive cancer, being considered of high grade [187, 194].

Transitional cell carcinoma is characterized by a number of chromosomal and genetic alterations. Cytogenetic loss and loss of heterozygosity of chromosome 9 is particularly frequent occurring in 40-50% of the cases [187]. The most commonly lost region in 9p includes *CDKN2A* (Cyclin-dependent kinase inhibitor 2A gene) that frequently also shows homozygous losses. Several regions of chromosome arm 9q have been suggested to harbour tumour suppressor genes but no definite gene has so far been identified [195]. The receptor gene *FGFR3* (Fibroblast growth factor receptor 3 gene) is activated by mutations in up to 70% of the Ta tumours but less frequently in invasive tumours [196]. The reverse pattern is seen for *P53*. This has led to the suggestion that transitional cell carcinoma may constitute two entities of tumours developing through two different genetic pathways [197].

4.2. Demographics and epidemiology

Bladder cancer is the fifth most common tumour world-wide and is responsible for about 2% of all cancer deaths [183, 198]. More than 110.000 new cases were diagnosed in Europe in 2008 [199], and the estimated incidence of bladder cancer in the United States is approximately 70.000 new cases a year [183]. It is less common in women than men, ranking as the eight most common cancer and tenth leading cause of cancer-related death in women. A genetic susceptibility to bladder cancer is suggested by the marked differences in the gender and ethnic-related incidences of this cancer [194]. Although most patients are older than 60 years of age, bladder cancer may affect younger patients [180].

In most countries of the Western world, bladder cancer is predominantly of transitional cell type; and the great majority of cases are thought to be induced by inhaled carcinogens in cigarette smoke, whereas in countries in which bilharziasis is endemic, most bladder cancers are squamous cell carcinomas. There are significant variations in incidence, morbidity, and mortality rates of

bladder cancer in different countries and ethnic groups [200]. African American men have a much lower incidence of bladder cancer, but their mortality rates are similar to whites [201].

The incidence of transitional cell carcinoma ranks it as the sixth most common cancer and as the fourth most common if transitional cell carcinoma stage Ta is included. The variations noted can partly be attributed to different methodology, mainly the inclusion of transitional cell carcinoma stage Ta or carcinoma in situ in different national registries, thus even among countries with comparable intensity of care and similar transitional cell carcinoma risks, epidemiologic data vary [179].

Non-muscle-invasive tumours have a high prevalence because their low progression rates allow many patients to survive a long time, while patients with muscle-invasive disease are at significantly higher risk of dying from their disease. The prevalence of transitional cell carcinoma is among the highest for all urologic malignancies [179].

4.2.1. Risk factors for urothelial bladder cancer

Risk factors are best differentiated into inherited genetic predispositions and external exposures [179].

The risk of bladder cancer is two-fold higher in first-degree relatives of bladder cancer patients. Inherited genetic factors, such as the genetic slow acetylator N-acetyltransferase 2 variants and glutathione S-transferase mu 1 null genotypes, have been established as risk factors for bladder cancer. Factors such as slow acetylation may not intrinsically lead to bladder cancer but may confer additional risk to exposure of carcinogens such as tobacco products [179].

Smoking is recognized as the most important risk factor for urothelial bladder cancer and is estimated to account for 50% of tumours [202]. In 1956 Lillienfield *et al* [203] first documented an association between cigarette smoking and bladder cancer, and this relationship has since been confirmed in multiple epidemiologic studies. Smokers have a 4-times higher increased incidence of

cancer versus non-smokers, and this risk correlates with number of cigarettes, duration of smoking, and degree of inhalation [182, 204]. Tobacco smoke contains aromatic amines, such as β-naphthylamine, and polycyclic aromatic hydrocarbons known to cause urothelial bladder cancer. These are renally excreted and exert a carcinogenic effect on the entire urinary system. Tobacco consumption is common, and thus its epidemiologic impact is massive [202].

Following smoking, occupational exposures to carcinogens – namely, aromatic amines (benzidine, 4-aminobiphenyl, 2-naphthylamine, 4-chloro-o-toluidine), polycyclic aromatic hydrocarbons, and chlorinated hydrocarbons – is viewed as the second most important risk factor for urothelial bladder cancer. Roughly 20% of all urothelial bladder cancers have been suggested to be related to such exposure, mainly in industrial areas processing paint, dye, metal, and petroleum products [179, 180, 194, 205]. Detoxification of these carcinogens by the rapid acetylation of aromatic amines may prevent their carcinogenic action [206]. Higher bladder cancers rates are also seen in those with defects in the P450 cytochrome oxidase system, suggesting a role for this system in carcinogen detoxification [207]. The number of bladder cancers resulting from exposure to aromatic amines is at this time very small, given to the banning of many of these carcinogens and their derivates from the workplace. [194].

As for other cancers, nutritional aspects have been attributed to urothelial bladder cancer risk. Fluid intake is commonly evaluated because of its impact on voiding, but the association with bladder cancer is controversial. On one hand, the amount of fluid ingested may reduce exposure of urothelial tissue to carcinogens by diluting urine and increasing the frequency of micturition, but on the other hand, the type of fluid is related to urothelial bladder cancer risk if it contains relevant carcinogens such as arsenic and disinfection by-products [179, 208].

Michaud *et al* performed a case-control study finding water intake to be inversely associated with urothelial bladder cancer risk, as they observed urothelial bladder cancer risk halved in subjects consuming greater compared with smaller amounts of fluids per day. Chlorination of drinking water and subsequent levels of trihalomethanes have been viewed as one source of

relevant carcinogens [209]. While coffee, a complex mixture of chemicals, has been suggested as a possible urothelial bladder cancer relevant carcinogen, such an effect remains controversial. Villanueva *et al* recently evaluated the relation of coffee consumption to urothelial bladder cancer incidence in a case-control study and found only a modest increase in risk among coffee drinkers, which was confounded by smoking [210]. In a recent meta-analysis of 16 case-control and 3 cohort studies, Pelucchi *et al* found no association between amount of alcohol consumption and urothelial bladder cancer risk [211].

Besides fluid intake, dietary habits have been considered relevant in urothelial bladder cancer tumorigenesis, as many carcinogens ingested via food are excreted into the urine, resulting in direct exposure of the urothelium. In other cancers, consumption of meat has been suggested to increase risk while consumption of vegetables and fruits has been suggested to be beneficial. In urothelial bladder cancer, however, neither effect is evident [179].

With regard to gender, women have a lower urothelial bladder cancer incidence and a higher mortality rate than men. Palou *et al* found female gender to be an adverse prognosticator of time of recurrence, progression, and cancer-specific survival in patients with pT1 urothelial bladder cancer undergoing bacillus Calmette-Guérin therapy [212]. While there is no uniform theory to explain these phenomena, unequal access to health care, delays in diagnosis and treatment, environmental exposure to carcinogens, anatomic and hormonal factors have been suggested [179].

Few data on the impact of race in urothelial bladder cancer incidence exist. However, African Americans show a lower age-standardized incidence rate per 100 000 of 13, compared with 22 in white individuals in the United States, and black race has been reported to be associated with adverse stage at initial presentation and reduced survival in a recent Surveillance Epidemiology and End Results (SEER) analysis [213].

In a further SEER analysis, marital status has been reported to affect urothelial bladder cancer survival, as married men had better survival than unmarried men independent of other factors such as race, socioeconomic status, comorbidities, or aggressive treatment [214]. Low socioeconomic status has

been related to unfavourable urothelial bladder cancer-specific survival in an analysis of patients receiving social welfare medical aid in a recent analysis, while previous reports did not find such an effect [215]. While no stringent explanations have been established for these phenomena, reduced access to health care and increased exposure to the main urothelial bladder cancer-related carcinogen – that is, smoking – have been postulated [179].

Medical conditions may predispose individuals to bladder tumorigenesis through direct causation or as a side effect of treatment. Examples of direct causative roles include chronic urinary retention and upper tract dilation increasing urothelial exposure to carcinogens and carcinogenesis associated with chronic inflammation or schistosomiasis [179].

Chemotherapeutic agents and pelvic radiotherapy have also been implicated in the development of bladder cancer. Cyclophosphamide induces bladder cancer in human beings in a dose-response relationship that may be related to the development of drug-induced hemorrhagic cystitis. Overall, patients treated with cyclophosphmide have up to a 9-fold increased risk of bladder cancer [216].

Pelvic radiotherapy results in a 4-fold increase in the risk of bladder cancer in women receiving between 30 and 60 Gy for the treatment of cervical cancer [217]

The risk factors for the development of superficial transitional cell carcinoma are summarized in table 15.

Table 15. Major risk factors for development of superficial transitional cell carcinoma (Amling C.L., 2001; Burger M. *et al.*, 2013).

Cigarette smoking
4-Aminobiphenyl
O-toluidine
Occupational arylamine exposure
2-Naphthylamine
Benzidine
4-Aminobiphenyl
Chemotherapy
Cyclophosphamide
Pelvic radiotherapy

Legend: The major risk factors for the development of superficial transitional cell carcinoma are mainly the exposition to aromatic amines, polycyclic aromatic hydrocarbons, and chlorinated hydrocarbons resulted from cigarette smoking and occupational exposure. Also the exposure to chemotherapeutic agents and pelvic radiation resulted from pelvic radiotherapy, are risk factors for the development of superficial transitional cell carcinoma.

4.3. Diagnosis

Physical examination should include rectal and vaginal bimanual palpation. A palpable pelvic mass can be found in patients with locally advanced tumours. In addition, bimanual examination under anaesthesia should be carried out before and after transurethral resection to assess whether there is a palpable mass or if the tumour is fixed to the pelvic wall. However, considering the discrepancy between bimanual examination and pT stage after cystectomy (11% clinical overstaging and 31% clinical understaging) some caution is suggested with the interpretation of bimanual examination [188].

The most common sign of bladder cancer is haematuria. Approximately 80% of all patients with transitional cell carcinoma will be diagnosed with either gross or microscopic haematuria [218]. The distinction between gross and microscopic haematuria is not a useful guideline to distinguish between patients who need evaluation and those who do not [183]. Cystoscopy must usually be included for an adequate evaluation of haematuria and remains the cornerstone for the diagnosis of bladder cancer. Urine cytologic study is an important non-invasive tool used in the diagnosis and follow-up of patients with transitional cell carcinoma. It can be obtained from both voided and bladder barbotage urine specimens [219]. The disadvantage of urine cytologic study is its poor sensitivity

for detection of low-grade cancers. Because the cells of such tumours closely resemble normal urothelium, it is much more difficult to identify them as abnormal [220].

However, although bladder cancer is usually asymptomatic, some patients (particularly those with carcinoma in situ) will initially be seen with significant symptoms of bladder irritability, including urinary frequency, urgency, and dysuria [194].

Various imaging modalities are used not only for detection but also for staging of infiltrating urothelial carcinoma. They include ultrasound, intravenous urography (IVU), CT and MRI [180].

Transabdominal ultrasonography of the bladder is quick, non-invasive, inexpensive and available in most institutions. However, staging accuracy is less than 70% for infiltrating bladder tumours. Sensitivity reaches only 63%, yet with a specificity of 99% [180]. Ultrasonography may be useful in detecting the presence of a renal mass and in determining whether it is solid or cystic in nature. However, is inadequate to evaluate the urothelium for filling defects that would be most consistent with transitional cell carcinoma [183].

While IVU is reliable in diagnosing intraluminal processes in ureter, pelvis and – with lesser accuracy – in bladder, it fails to detect the extent of extramural tumour [180]. Although it has obvious limitations, IVU is still the preferred initial imaging modality. The upper urinary tract collecting system is usually well visualized by IVU with or without concomitant retrograde pyelography. However, IVU is significantly more sensitive in detecting filling defects in the upper urinary tract than in the bladder [183].

Recent studies have begun to explore the utility of CT scanning in the initial evaluation of microscopic haematuria. The advantage of this modality is a more sensitive evaluation of the renal parenchyma for small renal masses, improved detection of non-urologic disease processes that otherwise would have been missed on IVU [194]. In most institutions CT is used as a primary staging tool as it is more accessible and more cost effective than MRI. However, both CT and MRI scanning often fail to differentiate between edema post-transurethral

resection and tumour [180]. The urothelium is not well evaluated by CT, particularly for identification of smaller urothelial lesions. In the bladder, CT scanning is unable to detect tumours smaller than 1 cm and cannot differentiate between superficial and intramural tumour invasion [194]. Staging accuracy of CT has been described in the range of 55% for urothelial carcinoma in the urinary bladder. Understaging of lymph node metastases in up to 40% and overstaging 6% of the cases are the major causes of error [180]. However, CT scanning can detect extravesical tumour extension (stages T3 and T4) with 80% accuracy and is useful in ruling out lymph node involvement and distant metastases [221]. MRI appears to be somewhat better to assess the depth of intramural invasion and extravesical tumour growth but does not exceed 83% [180].

Unlike in other tumours diagnostic accuracy of positron emission tomography (PET) in patients with invasive carcinoma of the bladder is poor [180].

If a bladder tumour has been visualised unequivocally in earlier imaging studies, such as CT, MRI, or US, a diagnostic cytoscopy may be omitted and the patient can proceed directly to TUR for a histological diagnosis. The goal of TUR is to enable histopathological diagnosis and staging, which requires the inclusion of bladder muscle in the resection biopsies. The strategy of resection depends on the size of the lesion. Small tumours (less than 1 cm) can be resected en bloc, where the specimen contains the complete tumour plus a part of the underlying bladder wall including bladder muscle. Larger tumours have to be resected separately in fractions, which include the exophytic part of the tumour, the underlying bladder wall with the detrusor muscle and the edges of the resection area [188, 222].

4.4. Therapy

Systemic treatment options for bladder cancer include surgery, chemotherapy, radiation, and immunotherapy. Treatment modalities are often combined. In early bladder cancer, transurethral resection is a common mode while partial or

radical cystectomy is performed for muscle-invasive and locally advanced bladder cancer [177].

The standard initial treatment of superficial bladder cancer is transurethral resection of all visible bladder lesions. This establishes the diagnosis and allows pathologic analysis of the resected tumour specimen for tumour grade and depth of bladder invasion [177, 194]. A significant number of patients with superficial bladder cancer who are treated with transurethral resection alone will have development of tumour recurrence or progression at some point in their follow-up. Sixty to seventy percent of superficial bladder cancers recur, and 20% to 30% of these recurrent tumours will eventually progress to higher stage or grade disease. The high recurrence rate and the probability of disease progression have led to widespread use of intravesical therapy after initial tumour resection. The main goal of intravesical therapy in the treatment of superficial bladder cancer is to prevent tumour recurrence and progression [223].

In patients with low-risk tumours, that is, tumours that are small, solitary, well-differentiated, and pathologic stage Ta, adjuvant treatment after surgical resection may be unnecessary. These patients have a relatively benign type of superficial cancer that is unlikely to recur after transurethral resection. A much larger group of patient consists of those who will have development of a superficial recurrence of their cancer without progression. In these patients, intravesical chemotherapies may be given to decrease the recurrence rate [224].

Some chemotherapeutic agents used for intravesical therapy are thiopeta, doxorubicin, mitomycin-C, epirubicin and ethoglucid.

Thiopeta is an alkylating agent that inhibits the synthesis of nucleic acid, therefore interfering with protein synthesis. Because its molecular weight is relatively low at 189, systemic absorption and toxicity can occur [194].

Doxorubicin is an anthracycline antibiotic that exerts its antineoplastic effect by binding to pairs of DNA, interrupting DNA replication and transcription and inhibits protein synthesis. Although it is classified as a non-cell cycle-specific

agent, its most toxic effect is seen in the S-phase of the cell cycle. Doxorubicin has a relatively high molecular weight of 580, and thus absorption and systemic toxicity is extremely rare [225].

Mitomycin-C is an alkylating agent with a mechanism of action that is poorly understood. Some evidence suggests that it acts by binding to DNA resulting in synthesis intubation and strand breakage. Although it is classified as a non-cell cycle-specific agent, mitomycin-C is most sensitive in late G1 and the early S-phase. With a molecular weight of 334 kDa, mitomycin-C is minimally absorbed [194].

Epirubicin is an anthracycline derivative of doxorubicin. The mechanism of action of this agent is similar to that of doxorubicin. The toxicity profile, however, appears to be more favourable [226].

Ethoglucid is a podophyllin derivative with molecular weight of 262 kD. Its mechanism of action is similar to that of an alkylating agent [227].

In a review of the long-term results of intravesical therapy in superficial bladder cancer, Lamm [228] found that in a group of 3899 patients the percentage of patients with short-term recurrences decreased 14% with the use of intravesical chemotherapeutic agents. The results among various chemotherapeutic agents were comparable. However, the modest 14% short-term advantage to intravesical chemotherapy disappears within a period of 5 years with no apparent advantage to the use of maintenance therapy [229]. The use of chemotherapy should be restricted to patients with tumours of intermediate or low-risk.

Photodynamic therapy is another option that allows effective ablation of most superficial tumours. The advantages of laser treatment are minimal bleeding, ability to use with flexible cytoscopes, and the potential for less postoperative irritative symptoms [230]. Photodynamic therapy relies on the photosensitization of cancerous cells with subsequent administration of light therapy.

Treatment of superficial bladder cancer with photodynamic therapy was first described in 1975 [231]. A hemoporphyrin photosensitizer was given intravenously with subsequent activation by mercury light illumination of the

bladder [232]. Effective photosensization and cell death requires oxygen in addition to the sensitizer and the light source. After excitation by light exposure, the photosensitizer reacts with oxygen to form cytotoxic free radicals [233]. Photodynamic therapy is less effective in larger bladder cancers, likely because of the relative lack of oxygen in portions of these tumours.

Photofrin (porfimer sodium), a porphyrin mixture of dihematoporphrin ethers and esters, is the most commonly used sensitizer in bladder cancer [232]. Although photodynamic therapy appears to be effective, its widespread use has been limited by its toxicity. Most patients have significant irritative bladder symptoms associated with microscopic haematuria that usually peaks on the second post-treatment day. Dermal sensitivity resulting in sunburn has been reported in 19% of patients. Decreased bladder volume (at least 50%) occurs in 16% of patients and debilitating bladder fibrosis can also occur, leading to cystectomy [232].

Intravesical immunotherapy is used successfully in patients in whom other forms of intravesical therapy failed [194]. Immunotherapy can be used to enhance the host immune functions against tumour cells. Intravesical immunotherapy in bladder cancer has been attempted with agents such as bacilli Calmette-Guerin (BCG), interferon, bropirimine, keyhole limpet hemocyanin, etc.

BCG is commonly used and is the most effective immunotherapeutic agent against superficial transitional cell carcinoma [234, 235] and is known to decrease the rate of progression [236, 237]. However, only two thirds of patient respond to BCG and one third of the responses will have recurrent disease [238-241]. The exact mechanism of action of BCG remains uncertain, however it is known that BCG organisms bind to the urothelium, facilitated by fibronectin, and initiate an immune response [242, 243]. It is uncertain whether the antitumor effect of BCG is due to a tumour antigen-specific humoral or cell mediated response or whether it is due to local release of cytokines. However, although an intact T-cell immune system appears to be necessary for antitumor effect of BCG, tumour-specific T cells have not been shown to be induced by BCG treatment [244]. Also care should be taken to avoid the toxicity associated with this agent [245].

Keyhole-limpet hemocyanin (KLH) is a high-molecular weight protein antigen derived from the hemolymph of the giant keyhole limpet (sea mollusk). It is a nonspecific immunostimulant inducing both a cell-mediated (delayed type) and humoral (antibody) response in human beings. Olsson *et al* [246] reported the first use of KLH for superficial bladder cancer in 1974. A randomized control study demonstrated that KLH was as effective as mitomycin-C in the prophylaxis of recurrent tumours [247]. KHL appears to be less effective than BCG with regard to tumour prophylaxis [247].

Interferon-α has been the most extensively studied interferon for the treatment of bladder cancer. Interferon's are produced by several cell types in response to antigenic stimuli and have multiple antitumor activities. It is effective with either papillary disease or carcinoma in situ and can be useful in patients whose conditions have failed to respond to BCG previously [248].

For muscle invasive bladder cancer the standard treatment is radical cystectomy. Although 70% muscle invasive bladder cancer recur or progress to metastatic disease despite radical treatment, radical cystectomy with bilateral pelvic lymph node dissection remains the gold standard for patient management and is associated with 5 and 10 year relapse-free survival rates of respectively 68% and 66% [249].

Conservative management with organ preservation is now the standard of care in numerous malignancies, including carcinomas of the breast, the anus, and the head and neck region, where radical surgery can be avoided in most patients without compromising survival [250].

Radical cystectomy may cause important changes in the lives of patients, not only in urinary and sexual function, but also in social function, daily living activities and satisfaction with body image [186, 251]. Bladder preservation to the patient means less surgery, no need for a urinary diversion, and the possibility of a normal sexual life. Modern sophisticated techniques for urinary diversion have not altered the fact that cystectomy is still associated with physical and psychological limitations [252].

The non-surgical treatment of invasive bladder cancer has been traditionally reserved for patients who are unfit for, or refuse radical cystectomy, but there is growing evidence that the evolution of radiotherapy techniques and the availability of new chemotherapeutic protocols have made bladder-saving treatment a competitive alternative to radical cystectomy in selected patients [198]. However, although bladder preservation may be attained by means of transurethral resection, chemotherapy or radiotherapy as single treatments, historical series show that local disease in controlled in only about 20% of patient treated with transurethral resection alone [253, 254] and 40% treated with radiotherapy alone [255, 256].

Some studies have shown that combined transurethral resection and chemotherapy [230, 257] or radiotherapy and chemotherapy [258, 259] can improve the disease, but the best results are obtained using a trimodality strategy in which radiochemotherapy follows transurethral resection.

Current therapy options may be summarized and organized according to the stage of the tumour, as can be seen in table 16.

Table 16. Current treatment options for bladder carcinoma, according with the stage of tumour (Witjes J.A. *et al.*, 2013).

Stage	Treatment options
Stage 0	TUR with fulguration alone, followed by intravesical BCG or intravesical chemotherapy. Segmental cystectomy (rarely indicated) or radical cystectomy in selected patients with extensive or refractory superficial tumour.
Stage I	TUR with fulguration alone, followed by intravesical BCG or intravesical chemotherapy. Segmental cystectomy (rarely indicated) or radical cystectomy in selected patients with extensive or refractory superficial tumour. Interstitial implantation of radioisotopes with or without external-beam radiation therapy.
Stage II	Radical cystectomy with or without pelvic lymph node dissection. Neoadjuvant platinum-based combination chemotherapy followed by radical cystectomy. External-beam radiation therapy (EBRT) with or without concurrent chemotherapy. Interstitial implantation of radioisotopes before or after EBRT. TUR with fulguration (in selected patients). Segmental cystectomy (in selected patients).
Stage III	Radical cystectomy with or without pelvic lymph node dissection. Neoadjuvant platinum-based combination chemotherapy followed by radical cystectomy. EBRT with or without concurrent chemotherapy or with interstitial implantation of radioisotopes Segmental cystectomy (in highly selected cases).
Stage IV	Radical cystectomy with pelvic lymph node dissection. External-beam radiation therapy. Urinary diversion or cystectomy for palliation. Chemotherapy as an adjunct to local treatment.

Legend: The current treatment options for bladder cancer according with the stage of the tumour are TUR and segmental cystectomy for initial stages, resorting to more aggressive therapies in the more advanced stages of the tumour, like radical cystectomy, chemotherapy and radiotherapy. As can be seen, the therapy is not achieved by applying only one technique, but rather by combining several therapeutic techniques.

Over the last decade, the growing use of targeted therapies in everyday clinical practice has led to dramatic changes in the medical treatment of all but a few tumours. Unfortunately, bladder cancer is not one of these: a number of trials of epidermal growth factor receptor and/or vascular endothelial growth factor-targeting tyrosine-kinase inhibitors have led to discouraging results when

administered alone to patients with advanced disease [260-264], and the role of monoclonal antibodies combined with chemotherapy in unclear [265, 266].

Also there is no reference to the use of radionuclides/radiopharmaceuticals for systemic radiotherapy, it is important to notice that some molecules with specific properties, properly radiolabelled could have an important potential to be used as agents for directed therapy, or even diagnosis, of bladder cancer and its metastasis. As described in Chapter 3, from the various studies performed with PEI-MP labelled with several radionuclides, the dosimetric calculations demonstrated that the critical organ was consistently the bladder [111, 129, 174, 267]. The high value of accumulation and retention by the bladder wall by different radiolabelled PEI-MP complexes seems something that deserves to be further and better studied. If these complexes are highly uptake by normal bladder cells, could it be that the uptake by bladder tumour cells is also high? And also taking in consideration the EPR effect associated with PEI-MP [169, 170], thus this polymer has a potential for therapy or diagnosis after convenient radiolabelling? These are some questions that led to the development of this work.

Section III. Experimental Studies

Chapter 5.*In vitro*

5.1. Introduction

As described in Chapter III, polyethyleneiminomethyl phosphonic acid (PEI-MP) was developed by Dormehl IC *et al* [111], is a water-soluble polymer for use in palliative therapy of bone metastases after suitable radiolabelling [67, 111]. After preliminary experiments to achieve biodistribution of and pharmacokinetic properties of different complexes PEI-MP/metal radionuclides [129, 174, 267], it was clear that the bladder wall was the critical organ [111, 267]. The high uptake and retention by the bladder wall cells of different PEI-MP/metal radionuclides seems something that deserves to be further and better studied. As referred in Chapter 4, the possibility of a high uptake of PEI-MP complexes by bladder tumour cells, associated with the EPR effect [169, 170], assigns a high potential to the PEI-MP, if appropriately radiolabelled, for diagnosis and therapy of bladder cancer. More specifically, through the use of ^{99m}Tc-PEI-MP for nuclear medicine imaging or of ^{188}Re-PEI-MP for radionuclide therapy. This second complex could be used as a theranostic agent.

Thus, the aim in this chapter is to explore *in vitro*, the potential of PEI-MP radiolabelled with ^{99m}Tc or ^{188}Re, for the early diagnosis and therapy of bladder cancer, through the evaluation of the chemical properties of PEI-MP, the radiotoxicity of ^{99m}Tc and the kinetics of ^{99m}Tc-PEI-MP and ^{188}Re-PEI-MP in a human bladder transitional cell carcinoma cell line. It is also an objective to compare the potential of those complexes in a human osteosarcoma cell line, taking into account the original intent of the synthesis of PEI-MP.

To perform this work, it is reported the synthesis, the radiolabelling procedures, the quality control protocol, the partition coefficient determination of ^{99m}Tc-PEI-MP, the evaluation of cytotoxicity of PEI-MP by MTT assay and flow cytometry, the evaluation of radiotoxicity of ^{99m}Tc by clonogenic assay and flow cytometry and the cellular uptake and retention studies of the ^{99m}Tc-PEI-MP and of the ^{188}Re-PEI-MP.

5.2. Material and methods

5.2.1. *Synthesis of PEI-MP*

Synthesis of the polymer PEI-MP was achieved by condensation of polyethyleneimine (PEI), phosphorous acid and formaldehyde by a modified Mannich-type reaction in the presence of hydrochloric acid, as described by Moedritzer and Irani [111, 132, 268], and prepared in the Radiochemistry Department of the Nuclear Energy Corporation of South Africa (NECSA) laboratories by doctors Werner Louw and Jan Zeevaart. The reaction was performed under an inert atmosphere by continuous purging with argon. Phosphorous acid (18.4 g) (Riedel-de Haën AG) was dissolved in 51.3 ml of concentrated hydrochloric acid (32%, pro analysis, E Merck, Darmstadt) and then was added to a reaction vessel equipped with a thermometer, a magnetic stirrer bar, a dropping funnel and a condenser. Dissolution of the phosphorous acid was achieved by stirring and heating to 80ºC. The dropping funnel was charged with 32% formaldehyde solution (23.3 ml) (pro analysis, E Merk, Darmstsdt) which was added drop wise to the reaction mixture. On completion the temperature was raised to 90ºC (refluxing temperature) and a solution of polyethyleneimine (8.33 g in 40 ml of water, Polymin^{TM} Water-Free, a BASF product in which the ratio of primary, secondary and tertiary amine groups is 1:1:1) was slowly added to the reaction mixture at a rate of 0.3 ml/min with the aid of a peristaltic pump. On completion of the addition of polyethyleneimine, the mixture was stirred under reflux for an additional hour, then allowed to cool slowly during which the product separated as viscous oil. After decanting the mother liquor, 50 ml of water was added to oil which formed a doughy mass upon stirring. The liquid phase was decanted and the process repeated twice. The doughy material was dissolved in 37 ml molar sodium carbonate solution to form the water-soluble sodium salt of the PEI-MP. After lyophilisation, 12 g of product were obtained.

To obtain 10 to 30 kDa fraction, the macromolecule PEI-MP was further purified into different macromolecular sized MW-fractions using membrane ultrafiltration (polyether sulfone membranes). An aqueous solution of sodium PEI-MP was subjected to a sequential filtration process through a sequence of 300, 100, 50, 30, 10 and 3 kDa ultrafiltration membranes (Filtron Technology Corporation.

Mass., USA). The membrane was washed with distilled water to a theoretically calculated purity of 99%, to yield 3-10, 10-30, 30-50, 50-100 and 100-300 kDa macromolecular sized MW-fractions. Typical elemental analysis gave a C:N molar ratio of 2.97:1, which on the basis of an empirical formula of a PEI-MP monomer of $C_9H_{18}N_3O_9P_3$, indicates a high level of methylphosphonation, in contrast to PEI with a monomer empirical formula of $C_6H_5N_3$ and a ratio C:N of 2:1 [111, 269]. The chemical structure of PEI-MP is represented in fig. 6 [270].

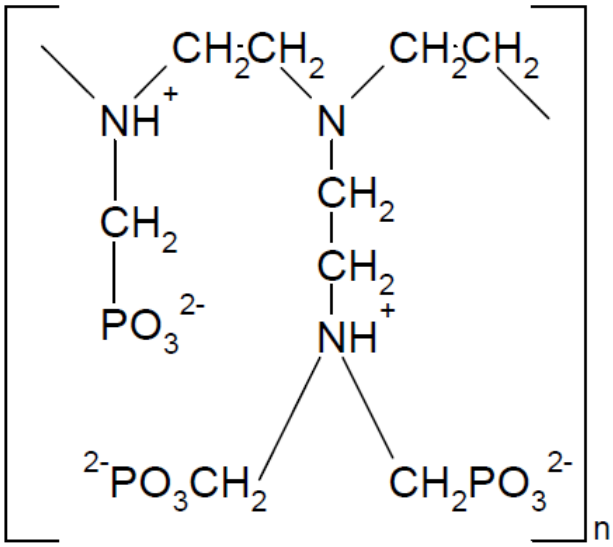

Figure 6. Chemical structure of PEI-MP (Milner R.J., 2013).

5.2.2. ***Preparation of PEI-MP labelling kits***

The reconstitution of the PEI-MP labelling kits were performed by adding 500 mg of PEI-MP (10 to 30 kDa) in 25 ml of water (pH = 6.0). The solution was purged with argon during 15 minutes and subsequently was filtrated through a 0.22 µm filter (Frilabo 1520012). To this solution was added 0.05 ml of a solution previously prepared, comprising 0.5 mg of $SnCl_2.2H_2O$ (Merck 1116845) dissolved in 1.0 ml 10M hydrochloric acid (Sigma H1758), pH = 5.0 to 6.0. The volume of this solution was adjusted with water and 1ml was dispensed into sterile vials. This solution was lyophilized and the vials flushed and filled with sterile argon.

5.2.3. ***Preparation of ^{99m}Tc- PEI-MP and ^{188}Re-PEI-MP***

For the preparation of ^{99m}Tc-PEI-MP, it was added directly to the PEI-MP kit, 1739 to 1850 MBq (47 to 50 mCi) of sodium pertechnetate ($Na^{99m}TcO_4$) in a volume of 2 ml, without introducing air. The kit was inverted a few times to dissolve the freeze-dried contents. It was left to stabilize at room temperature for 15 minutes before use. The labelling was possible given to the reduction of ^{99m}Tc from the oxidation state +7 to +5, making ^{99m}Tc reactive and able to form chemical bonds with the nitrogen of the amine groups in PEI, and/or make chemical bonds with phosphorus in the methyl-phosphonate groups [74, 269]. All ^{99m}Tc-pertechnetate was given by the Departments of Nuclear Medicine of the Hospitais da Universidade de Coimbra, Centro Hospitalar e Universitário de Coimbra, and Instituto Português de Oncologia de Coimbra Francisco Gentil, E.P.E.

For the preparation of ^{188}Re-PEI-MP, it was necessary to acquire an ^{188}W/^{188}Re generator (itm AG Rhenium-188 Generator), to obtain sodium perrhenate ($Na^{188}ReO_4$). For the preparation of ^{188}Re-PEI-MP, a more complex labelling process was needed. The range of ^{188}Re activities obtained by the elution of ^{188}W/^{188}Re to perform the labelling of PEI-MP at this time were about 370-740 MBq (10-20 mCi), and the specific activity of ^{188}Re was 982 Ci/mg, meaning that for 10 mCi there was 10 ng of ^{188}Re. For the amount of PEI-MP present in the labelling kits, the introduction of 10 mCi of ^{188}Re would result in poor radiochemical purity. To this reason it was needed to add cold rhenium in the form of sodium perrhenate ($NaReO_4$).

For the preparation of cold $NaReO_4$ it was dissolved 5 mg of Re-metal were dissolved in 2 ml of 10% hydrogen peroxide (H_2O_2). The solution was left to react during 2 hours at room temperature to form perrhenic acid ($HReO_4$). The $HReO_4$ was neutralized with a stoichiometric amount of 0.1M of sodium hydroxide (NaOH) to form $NaReO_4$. The solution was then evaporated to dryness (80-90 ºC) overnight.

To the labelling it was used only deoxygenated solvents and solutions, and performed all operations under an inert atmosphere of argon. The labelling kit was dissolved in 1.0 ml of ultrapure and deoxygenated water, and was added

an appropriate volume of NaReO4 (3.83 mg/ml) and 370-740 MBq (10-20 mCi) of $Na^{188}ReO_4$. The pH of the solution was adjusted to 1 with 1M hydrochloric acid (HCl). The kit was heated in boiling water bath during 30 minutes and after left to cool to room temperature. After, citrate buffer 1.0M was added and the pH was adjusted to 5.0-7.0 with NaOH 1M. The solution was then, 3 times submitted to ultrasound during 7 minutes and left to stabilize overnight, and filtered before use.

The labelling was possible given to the reduction of ^{188}Re from the oxidation state +7 to +5, making ^{188}Re reactive and able to form chemical bonds with the nitrogen of the amine groups in PEI, and/or make chemical bonds with phosphorus in the methyl-phosphonate groups [74, 269], in the same way as it happens with the labelling of PEI-MP with ^{99m}Tc.

5.2.4. ***Radiochemical quality control***

The radiochemical purity of ^{99m}Tc-PEI-MP and ^{188}Re-PEI-MP was evaluated using ascendant thin-layer chromatography, at 1, at 2, at 3, at 4 and at 5 hours after the radiolabelling. To accomplish this goal two chromatographic systems were used: the first one to isolate free pertechenetate/perrhenate and the second one to isolate colloidal forms. The first consisted of instant thin layer of silica gel impregnated glass-fibre sheets (ITLC-SG, Varian, US) as stationary phase and acetone ($CH_3(CO)CH_3$; Sigma-Aldrich 34850) as mobile phase. The second system was Whatman® 3MM cellulose paper (3MM, Maidstone, UK) as stationary phase and a solution of citrate buffer (pH = 7.0, 1.0 M) as mobile phase. These two systems were chosen to determine the percentage of free ^{99m}Tc or ^{188}Re and the percentage of hydrolysed/reduced ^{99m}Tc or ^{188}Re species, respectively for the first and second system [87, 271]. The strips of the stationary phases were prepared by marking the final length that corresponds to the solvent front with a colour pen and the start (origin) with a pencil. When the solvent gets in contact with the marker, the colour also migrates with the solvent, indicating that the solvent reach the end of the development. The strip should be marked in such a way that the colour does not interfere with the sample track to avoid artificial results [87]. A sample of 5 µl of ^{99m}Tc-PEI-

MP/^{188}Re-PEI-MP was spotted in the middle of origin of the stationary phase, which was placed vertically in a chromatographic chamber previously prepared with a saturated atmosphere. After applying the sample, the strip must be placed into the chromatographic chamber and developed immediately, without drying the spot. Dried samples may lead to artificial results due to oxidation of ^{99m}Tc/^{188}Re complexes and formation of free pertechnetate/perrhenate. The strip was placed into the chamber vertically and carefully avoiding any damage of the surface. These solid phases, have limited mechanical resistance, whereby should be supported (e.g., clipped to the lid of the chamber), otherwise they will slip into the solution or touch the chamber wall during the development. The solvent should cover the bottom no more than 5 mm high, to be below the level of the origin line of the stationary phase [87]. The strips were prepared as demonstrated in fig. 7.

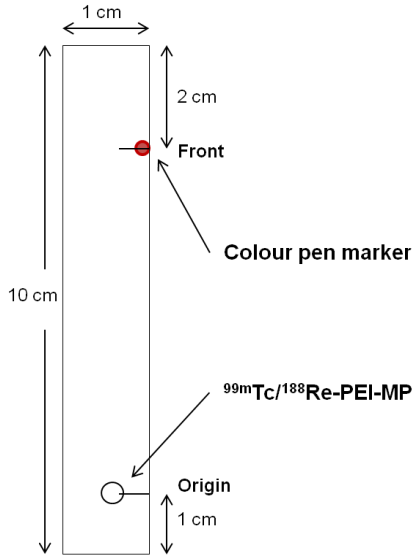

Figure 7. Schematic representation of a stationary phase for radiochemical quality control.

When the solvent reached the final mark, the strips were removed from their respective chromatographic chambers and allowed to dry at room temperature. Subsequently each strip was cut in half, and each half after being cut in small pieces, was placed into radioimmunoassay (RIA) tubes, and the radioactivity present in each portion was measured separately in a well-type gamma counter (Gamma-C 12 DPC, Berthold, Germany), to quantify radioactivity on each half

strip. The results of measurements are used to calculate the radiochemical purity as the ratio between the radioactivity corresponding to the half-strip of interest, divided by the total recovered radioactivity of the chromatogram. The final results are shown as a percentage. The background radioactivity is subtracted from each count leading to a more accurate analysis. Each experiment was performed in 3 different sets of tests.

There are several methods for the quantification of radiochromatograms. Depending on the available instrumentation, the resolution will vary, and the amount of the radioactivity used for analysis will differ considerably. The quantification with a well-type gamma counter has as an advantage the sensitivity. The resolution is dependent on the sample geometry which should be maintained at the counting tube bottom. For this reason each half-strip is cut in small pieces kept together at the bottom of the RIA tube. The main limitations of this method are that the saturation of the counter due to the activities of the half-strip of interest, and the time consumption once the procedure has many sequential steps such as cut the samples and fill the RIA tubes, time of measurements, and posterior percentage calculations. Also a gamma-camera could be used to perform this quantification. The dried strip can be placed over the head of the gamma camera, and images are acquired. Using the region of interest (ROI) technique, for each ROI drawn the total counts are obtained and the radiochemical purity is expressed as a fraction of the total strip activity. As advantage of this methodology is the use of undiluted sample for chromatography allowing measurement with high count rates. The main disadvantage is related with the time-consuming procedure (measurement and analysis), and consequently, the time of machine [87].

In order to investigate the effect of temperature and cell culture medium (Dulbecco´s Modified Eagle´s Medium, Sigma D-5648) in radiochemical purity of ^{99m}Tc-PEI-MP, and using the same chromatographic systems and methods of quantification, the radiochemical purity was assessed over time (30 minutes, 1h, 3h and 5h). The solution of ^{99m}Tc-PEI-MP and in saline with and without cell culture medium was exposed to temperatures of 22°C, 37°C and 45°C. The temperatures were regulated by a digital thermoblock (FALC Instruments, Treviglio, Italy). Each experiment was performed in 4 independent sets of tests.

5.2.5. ***Determination of partition coefficient of ^{99m}Tc-PEI-MP***

Partition coefficient (log $P_{o/w}$) of ^{99m}Tc-PEI-MP was calculated after the determination of $P_{o/w}$, that is the ratio of specific activities of the organic and aqueous phases [272, 273], 1h, 2h, 3h and 4 h after radiolabelling. A mixture of 1 ml of 1-octanol (Sigma O4500) and 1 ml of 0.9% sodium chloride (0.9% NaCl, Braun) containing 3.7 MBq (0.1 mCi) of ^{99m}Tc-PEI-MP at 37 °C was vortexed for 2 minutes and left 5 minutes to rest. Following centrifugation at 1872 g (3000 rpm) (Multifuge 1L-R, Germany) for 5 minutes, equal aliquots (100 µl) of sample were taken from each phase and counted for radioactivity in a well-type counter (Gamma-C 12 DPC, Berthold, Germany). Each experiment was performed in duplicate and repeated in 4 independent sets of tests.

5.2.6. ***Cell culture***

Human bladder transitional carcinoma cell line (HT-1376 - ATCC® CRL1472™) and human osteosarcoma cell line (MNNG/HOS – ATCC®CRL-1547™) (fig. 8), acquired from American Type Culture Collection (ATCC), were cultured in Dulbecco´s Modified Eagle´s Medium (Sigma D-5648) supplemented with 100 mM sodium pyruvate (Gibco 11360), 5% heat-inactivated foetal bovine serum (Sigma F7524), and 1% antibiotic/antimycotic (100 U/ml penicillin, 10 µg/ml streptomycin and 25 µg/ml amphotericin B, Sigma A5955) (fig. 9).

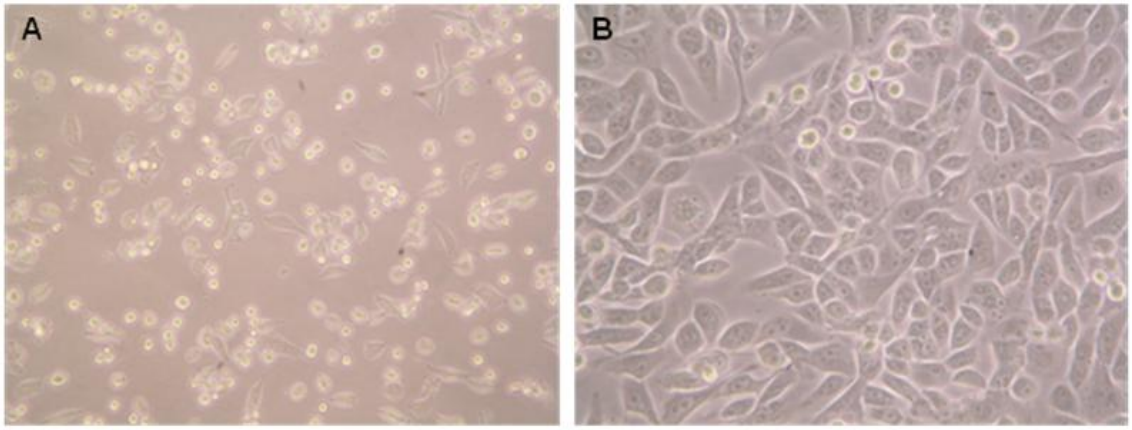

Figure 8.HT-1376 (A) and MNNG/HOS (B) cell lines in culture, visualized in a optical microscope (Nikon Eclipse TS100, Japan) with a magnification of 10x.

Figure 9. Culture medium Dulbecco´s Modified Eagle´s Medium supplemented with 100 mM sodium pyruvate, 5% heat-inactivated foetal bovine serum, and 1% antibiotic/antimycotic.

Cells were maintained at 37 °C with 95% air and 5% CO_2 (fig. 10) in a cell incubator (BINDER, CO^2 incubator C 150, 150 litres, 230 V, 1 N, 50/60 Hz).

Figure 10. Cells in adherent culture flasks maintained at 37 ºC with 95% air and 5% CO_2 in the incubator.

In order to obtain cell suspensions for use in the *in vitro* studies, cells were washed with PBS, than harvested with a solution of 0.25% trypsin/EDTA (Sigma T4049), centrifuged at 209 G (1000 rpm) (Multifuge 1L-R, Germany) during 5 minutes and finally resuspended in medium. To count the number of viable cells in each cell suspension, it was used the trypan blue exclusion method. The trypan blue exclusion method is based on the principle that viable cells had intact membranes that prevent entry of the dye, while the disrupted membranes of the non-viable cells can't prevent that penetration of the dye into the cell. Upon entry into the cell, the dye crosses the nuclear membrane, and the nuclei are stained in blue. Thus, the blue cells correspond to dead cells while the viable cells have a shiny appearance (not stained of blue) [274]. To perform this procedure, an aliquot of 20µl of cell suspension is added to 20µl of trypan blue (Sigma T0776) in an eppendorf tube, and after homogenization, cell suspension was placed in a haemocytometer using a micropipette, to be viewed under an optical microscope (Nikon Eclipse TS100, Japan). The cell count was performed in the four quadrants of the haemocytometer.

5.2.7. Evaluation of the cytotoxicity of PEI-MP

5.2.7.1. Metabolic activity

To evaluate the effect of PEI-MP in the metabolism of cells, it was used the colorimetric test MTT (3-(4,5-dimethylthiazolyl-2)2,5-diphenyltetrazolium bromide; Sigma M2128). The dehydrogenase enzymes, present in metabolically active cells, have the ability to cleave the tetrazolium ring of MTT and form dark blue formazan crystals (fig. 11) that can subsequently be solubilised and the colour of the resulting solution quantified by spectrophotometry [275-277].

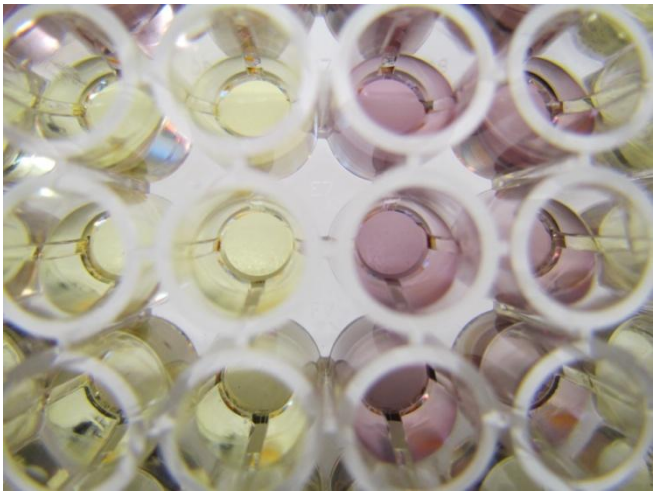

Figure 11. Representation of coloured solutions obtained after MTT test showing the blue coulour as a result of formazan crystals formation.

For each experiment, cells were plated in 48 multiwells plates (Corning Costar, USA) in a concentration of 25 000 cells/ml and kept in the incubator overnight to allow the cells attachment. Cells were incubated with different concentrations of PEI-MP (1, 5, 15, 25, 50, 100, 250, 500 and 1000 µM), obtained by dissolving the PEI-MP with 0.9% sodium chloride (0.9% NaCl, Braun), during 24, 48, 72 and 96 hours. After these periods of time, cell metabolism was evaluated. For this purpose, culture medium was removed, 500 µl of phosphate buffered saline (PBS) was added and then discarded, and finally a 100 µl of MTT solution (5 mg/ml, Sigma M2128) was added. After 3 hours, 100 µl of a solution of isopropanol (Sigma 279544) in 0.04M hydrochloric acid (Sigma H1758) was added and cells were re-suspended. The content of each well was transferred

to a plate with 96 wells (Sarstedt, USA) and the absorbance was quantified at 570 nm with a reference filter of 620 nm in an ELISA spectrophotometer (SLT-Spectra). Each experiment was performed in duplicate and repeated in 5 independent sets of tests. These tests were performed in the two cell lines referred above.

5.2.7.2. Flow cytometry

To characterize the redox intracellular environment after incubation of PEI-MP, it was chosen the maximum concentration of 1000 µM to determine by flow cytometry the cell viability, the reactive oxygen species (ROS) production, the expression of reduced glutathione (GSH) and the changes of mitochondrial membrane potential. The analysis was performed using a six-parameter four-color FACSCalibur flow cytometer (Becton Dickinson, San Jose, CA) equipped with a 15 nW argon laser. For each assay, at least 10^4 events were collected using Cell Quest software (Becton Dickinson, San Jose, CA, USA), and analysed using Paint-a-Gate software (Becton Dickinson, San Jose, CA). For flow cytometry analysis, 400 000 cells were seeded in 75 cm^2 adherent culture flasks (Corning, USA) and after 5 days were incubated with 1000 µM of PEI-MP. After 24 hours, cells were washed with PBS, harvested with a solution of 0.25% trypsin/EDTA (Sigma T4049), centrifuged at 1300 G (2500 rpm) (Multifuge 1L-R, Germany) during 5 minutes and finally in phosphate buffered saline (PBS) for examination by flow cytometry. Each experiment was performed in duplicate and repeated in 4 independent sets of tests. These tests were performed in the two cell lines referred above.

a) Cell viability and death

The first cell death to be defined was necrosis, and then the apoptosis [278]. Apoptosis is a regulated process, carried out in a controlled manner to ensure the safety of surrounding cells and tissues. Apoptosis is strictly defined by morphological criteria including changes of the nucleus (chromatin condensation and margination, condensation and reduction in the size of the

cell nucleus associated with its fragmentation) cellular shrinkage and ruffling of the plasma membrane, called budding [279]. The DNA is furthermore fragmented in several steps to form mono- and/or oligomers of 200 base pairs [280]. Eventually the cell becomes divided in apoptotic bodies, which consist of cell organelles and/or nuclear material surrounded by an intact plasma membrane. Apoptotic bodies expose phosphatidylserine residues, that normally exist in the inner leaflet of plasma membranes [281]. This allows for the recognition of apoptotic bodies, which are generally phagocyted and destroyed by neighbouring cells without damage to adjacent tissue. The execution of apoptosis is closely linked to serial activation of a family of proteases called caspases [282, 283], even though caspase-independent apoptosis pathways also exist through apoptosis inducing factor, Endonuclease G, and/or serine protease HTRA2 (HtrA serine peptidase 2) [284, 285]. Necrosis is generally considered to be an accidental and unregulated cell death [279] even though programmed necrosis also has been described [286]. When necrosis is induced, a rapid plasma membrane permeabilization occurs, which leads to leakage of cell content and induction of inflammation. Necrosis is usually defined in a negative fashion, as a type of cell demise that involves rupture of the plasma membrane without the hallmarks of and without massive autophagic vacuolization [287]. The main features of necrosis include an improvement of cell volume that finally culminates in rupture of the plasma membrane, and the unorganized dismantling of swollen organelles.

To evaluate cell viability, a double labelling with annexin-V and propidium iodide (AV/PI) was used. One of the main features of cell death by apoptosis is the redistribution of plasma membrane phosphatidylserine, a phospholipid that, in apoptotic cells, is translocated from the inner to the outer leaflet of the plasmatic membrane and binds to annexin-V. Complementarily, PI, which does not permeate viable cells, in cells with membrane lesions like cells on late apoptotic and/or necrosis, can reach the nucleus and binds to deoxyribonucleic acid (DNA) intercalating between the bases [288]. In this assay, 10^6 cells were incubated during 15 minutes, at room temperature in the dark, with a binding buffer with 2.5 µl of Annexin V (Immunostep, Salamanca, Spain) and 1 µl of PI (Immunostep, Salamanca, Spain), subsequently cell suspension was vortexed

to homogenize. In the cytometer cells were excited with a light of a wavelength of 525 nm for AV and with 640 nm for PI, collecting 10^4 events to assess the percentage of viable, early apoptotic, late apoptotic/necrotic, and necrotic cells [289].

b) Detection of intracellular peroxides and superoxide

There are many types of radicals, but those of most important in biological systems are derived from oxygen, and known collectively as reactive oxygen species. Oxygen has two unpaired electrons in separate orbitals in its outer shell. This electronic structure makes oxygen especially susceptible to radical formation. Sequential reduction of molecular oxygen leads to formation of a group of reactive oxygen species like superoxide anion (O_2^-), peroxide (O_2^{2-}) and hydroxyl radical (OH•). Oxygen-derived radicals are generated constantly as part of normal aerobic life, being formed in mitochondria as oxygen is reduced along the electron transport chain. Mitochondria are unique organelles, as they are the main site of oxygen metabolism, accounting for approximately 85–90% of the oxygen consumed by the cell. Incomplete processing of oxygen and/or release of free electrons results in the production of oxygen radicals. Mitochondria constantly metabolize oxygen thereby producing reactive oxygen species (ROS) as a by-product. This organelle has its own ROS scavenging mechanisms that are required for cell survival. Under normal conditions, the effects of ROS are counteracted by a variety of antioxidants, by both enzymatic and non-enzymatic mechanisms. Oxidative stress is considered to be the result of an imbalance of two opposing and antagonistic forces, ROS and antioxidants, in which the effects of ROS are more potent than the compensatory capacity of antioxidants [290]. Reactive oxygen species are also formed as necessary intermediates in a variety of enzyme reactions. Other situations may lead to the formation of reactive oxygen species, like drugs with oxidizing effects or ionizing radiation. The production of ROS is associated with many forms of apoptosis. Excessive ROS can induce apoptosis through both the extrinsic and intrinsic pathways. In the extrinsic pathway of apoptosis, ROS are generated by FAS ligand as an upstream event for FAS activation via

phosphorylation, which is necessary for subsequent recruitment of Fas-associated protein with death domain and caspase 8 as well as apoptosis induction. In the intrinsic pathway, ROS function to facilitate cytochrome c release by activating pore-stabilizing proteins (BCL-2 and BCL-XL) as well as inhibiting pore-destabilizing proteins (BCL-2-associated X protein, BCL-2 homologous antagonist/killer). Even higher ROS levels can result in both apoptosis and necrosis in cancer cells. ROS can also induce cell death through autophagy, which is a self-catabolic process involving sequestration of cytoplasmic contents (exhausted organelles and protein aggregates) for degradation in liposomes [291-293].

2,7-dichlorodihydrofluorescein diacetate ($DCFH_2$-DA) a lipid permeable and non-fluorescent compound, is cleaved by intracellular esterase by entering cells and leads to 2,7-dichlorodihydrofluorescein ($DCFH_2$). In the presence of peroxides, $DCFH_2$ is oxidised with formation of dichlorofluorescein (DCF), a highly green fluorescent compound, upon excitation at 488 nm, proportional to the concentration of intracellular peroxides [294]. Peroxides, along with superoxide are responsible to activate the intrinsic apoptotic pathway, and therefore an increase in the amount of free radicals will signify an increase in apoptosis [295]. A cell suspension of 10^6 cells was incubated with 5 µM of $DCFH_2$-DA (Sigma D6883) (1 µl) for 45 minutes at 37 °C in the dark. Subsequently, the cells were centrifuged at 1300 G (2500 rpm) (Multifuge 1L-R, Germany) during 5 minutes, then the supernatant was discarded and the cells were washed with PBS and analysed by flow cytometry. The analysis was performed with an excitation light with a wavelength of 504 nm, being the emission wavelength 529 nm. The results were obtained as mean fluorescence intensity (MFI) values, and then were normalized in relation to the control to which was assigned the value of 1.

Dihydroethidium (DHE) easily crosses cell membranes and is converted by superoxide radical to ethidium, a red fluorescent compound that merges the DNA remaining inside the cell [296]. A cell suspension of 10^6 cells was resuspended in PBS and incubated with 5 µM of DHE (Sigma 37291) dissolved in DMSO (Sigma D8418) (2.5 µl) for 15 minutes at 37 °C in the dark. Subsequently, the cells were centrifuged at 1300 G (2500 rpm) (Multifuge 1L-R,

Germany) during 5 minutes, then the supernatant was discarded and the cells were washed with PBS and analysed by flow cytometry. The analysis was performed with an excitation light with a wavelength of 620 nm. The results were obtained as mean fluorescence intensity (MFI) values, and then were normalized in relation to the control to which was assigned the value of 1.

c) GSH expression

L-glutamyl-L-cysteinyl-glycine (GSH) in its reduced form is a tripeptide enzymatically formed by glycine, cysteine and glutamate, and is the most abundant non-protein thiol in mammalian cells. GSH acts as a reducing agent and as a major antioxidant within cells by maintaining a tight control of the redox status. GSH is also involved in many distinct physiological reactions including cellular signalling, metabolism of xenobiotics, thiol disulfide exchange reactions, and as an important reservoir of cysteine. Intracellular GSH depletion is an early hallmark of progression of cell death in response to different apoptotic stimuli. Has been reported that GSH depletion during apoptosis induced by cytotoxic agents, such as xenobiotics, chemotherapeutics, and metals, may induce oxidative stress mediated by GSH oxidation to glutathione disulphide (GSSG) by reactive species of oxygen (ROS) and nitrogen (RNS), or by its conjugation to highly reactive compounds. GSH depletion has been shown to regulate both extrinsic and intrinsic apoptotic signalling cascades at distinct checkpoints. GSH depletion may predispose cells to apoptosis or, alternatively, directly trigger cell death which can result from, by modulation of the permeability transition pore formation or by activation of execution caspases [295, 297].

The expression of GSH, was performed by flow cytometry using the fluorescent compound mercury orange [295]. This compound binds stoichiometrically to mercurial sulphydryl groups with the formation of fluorescent ducts. However, this compound faster reacts with GSH than with the sulphydryl groups of proteins and the reaction product emits an intense red fluorescence when excited with an argon laser at a wavelength of 488 nm [298]. A cell suspension of 10^6 cells was incubated with 1 µl of mercury orange (Sigma 83377) in acetone (Sigma 650501) for 15 minutes at room temperature in the dark.

Subsequently, the cells were centrifuged at 1300 G (2500 rpm) (Multifuge 1L-R, Germany) during 5 minutes, the supernatant discarded and the cells washed with PBS and analysed by flow cytometry. The analysis was performed with an excitation light with a wavelength of 620 nm. The results were obtained as mean fluorescence intensity (MFI) values, and then were normalized in relation to the control to which was assigned the value of 1.

d) Mitochondrial membrane potential measurement

The intrinsic pathways of apoptosis involve the mitochondria, the endoplasmatic reticulum, and the DNA damaging pathways. These pathways are activated by a wide variety of stimuli including chemotherapeutic and cytotoxic agents (environmental pollutants, xenobiotics, drugs), stress (radiation, hyperglycaemia, hypoxia, oxidative and osmotic stress), and cytokine withdrawal. Activation of the mitochondria pathway mediates the release of cytochrome c that is associated with the opening of the mitochondrial permeability transition pore and loss of the mitochondrial membrane potential. Also mitochondria use substrates able to be oxidized to produce a membrane potential in the form of a proton gradient across the mitochondrial inner membrane. It was shown recently that the supply of these substrates to mitochondria depends on the concentration of external growth factors. Withdrawal of growth factors or loss of the extracellular glucose supply will lead to a decline of mitochondrial membrane potential. If growth factor or glucose deprivation persists, cells ultimately undergo apoptosis that is initiated by cytochrome c release from mitochondria [295, 299]. The lipophilic cationic 5,5´,6,6´-tetrachloro-1,1´,3,3´-tetraethylbenzimidazol-carbocyanine iodide (JC-1) is a molecule able to selectively enter the cell and which exists in two forms, monomers (M) and aggregates (A), depending on the state of polarization/depolarization of the mitochondrial membrane, that will be reduced when the cell is apoptotic [295]. When the membrane potential is high, the JC-1 forms aggregates that emit red fluorescence (590 nm). On the other hand, as the mitochondrial membrane potential decreases or in cases where the membrane is depolarized, JC-1 is excluded from mitochondria and remains in

the cytoplasm in the form of monomers that emits green fluorescence (529 nm). Thereby the ratio between the intensities of green and red fluorescence's (M/A), determined by flow cytometry, provides an estimate of mitochondrial membrane potential [300]. To perform JC-1 (Invitrogen, T-3168) assay the cells were incubated at a final concentration of 5 mg/ml, in DMSO (1 µl) during 15 minutes at 37 °C in the dark. Subsequently, the cells were centrifuged at 1300 G (2500 rpm) (Multifuge 1L-R, Germany) during 5 minutes, the supernatant discarded and the cells washed with PBS and analysed by flow cytometry. The results were obtained as aggregate/monomer ratio, and then were normalized in relation to the control to which was assigned the value of 1.

5.2.8. Evaluation of the radiocytotoxicity of ^{99m}Tc

5.2.8.1. Clonogenic activity

The clonogenic cell survival assay determines the ability of a cell to proliferate, thereby retaining its reproductive ability to form a large colony or a clone. Although clonogenic cell survival assays were initially described for studying the effects of radiation on cells and have played an essential role in radiobiology, they are now widely used to examine the effects of agents with potential applications in the clinic. Several mechanisms have been described for cell death; however, loss of reproductive integrity and the inability to proliferate are the most common features. Therefore, a cell that keeps its ability to synthesize proteins and DNA and go through one or two mitoses, but is unable to divide and produce a large number of progeny is considered dead. This is very commonly referred to as loss of reproductive integrity or reproductive death and is the end point measured with cells in culture. On the other hand, a cell that is not reproductively dead and has retained the capacity to divide and proliferate can produce a large clone or a large colony of cells and is referred as "clonogenic." The ability of a single cell to grow into a large colony that can be visualized with the naked eye is proof that it has retained its capacity to reproduce. The loss of this ability as a function of dose of radiation or chemotherapy agent is described by the dose-survival curve. A cell survival curve is therefore defined as the relationship between the dose of the agent

used to produce an insult and the fraction of cells that retain their ability to reproduce [301]. Technetium-99m, besides emitting gamma rays also emits less than 1% of auger electrons per decay. These electrons have been recognized as potentially useful for targeted tumour radiotherapy, specially do to the auger electron range (which is of manometer range) and the high ionization density of electrons [302]. However, to this study, the aim of using this radioisotope is for diagnostic imaging, and therefore in the range of diagnostic radiation doses, the ^{99m}Tc shouldn't be radiotoxic to cells. The effective doses for most nuclear medicine diagnostic procedures varies between 0.3 and 20 mSv (equivalent to 0.3 and 20 mGy) [303]. With the clonogenic assay the aim was to determine cell survival based on the ability of a single cell to grow and form a colony after the cells being subjected to doses of radiation, either being irradiated externally (determining gamma radiation effects) or internally (determining gamma radiation and auger electrons effects). For this study, 2 million cells were seeded in 75 cm^2 adherent culture flasks (Corning, USA). After 24 hours the cells where irradiated externally or internally with 2, 5, 10 and 20 mGy of ^{99m}Tc. For external irradiation the flaks containing cells were placed on top of a 75 cm^2 adherent culture flasks filled with water, were it was added the correct amount of $Na^{99m}TcO_4$. For internal irradiation it was added the correct activity of $Na^{99m}TcO_4$ to the flaks containing the cells. The time of exposure was calculated for the doses taking in consideration the distance, added activity and decay. After irradiation the cells where washed with PBS, harvested with a solution of 0.25% trypsin/EDTA (Sigma T4049) and finally medium was added. After, for HT-1376 cells, 300 and 600 cells were seeded in triplicate in a six well plate (Corning Costar 3516, USA), and for MNNG/HOS 100 and 200 cells were seeded also in triplicate in a six well plate (Corning Costar 3516, USA). After 5 days, the medium was changed and at twelfth day the colonies were prepared for visualization. For that, culture medium was aspirated, cells were washed with PBS, and methanol (Sigma 34860) was added to fix the colonies, a procedure that was repeated twice. After, the plates have been dried, and the crystal violet dye (Sigma M2128; 0.5% diluted in methanol) was added. Subsequently, the plates were washed with warm water and allowed to dry, after which the number of colonies were

counted and the plate efficiency (equation 3) and survival factor (equation 4) determined following the formulas below [276].

$$\text{Plate efficiency } \% = \frac{\text{Number of counted colonies}}{\text{Number of seeded colonies}} \times 100$$

Equation 3. Percentage of plate efficiency, that is determined by the ratio of the number of counted colonies and the number of seeded colonies.

$$\text{Survival factor } \% = \frac{\text{Plate efficency of treated samples}}{\text{Plate efficiency of control samples}} \times 100$$

Equation 4. Percentage of survival factor, which is determined by the ratio of the plate efficiency of treated samples and the plate efficiency of control samples.

Each experiment was performed in triplicate and repeated in 4 independent sets of tests for internal irradiation and 5 independent sets of tests for external irradiation. These tests were performed in the two cell lines referred above.

5.2.8.2. Flow cytometry

To characterize the redox intracellular environment after internal or external irradiation with ^{99m}Tc, it was chosen the dose of 20 mGy, to determine by flow cytometry the cell viability, the reactive oxygen species (ROS) production, the expression of reduced glutathione (GSH), changes of mitochondrial membrane potential and distribution of cells in cell cycle. The analysis and process was performed using the equipment and procedures described before.

For flow cytometry analysis, 2 million cells were seeded in 75 cm^2 adherent culture flasks (Corning, USA). After 24 hours the cells where irradiated externally or internally with 20 mGy with ^{99m}Tc following the procedures described in clonogenic assays. After 24 hours, cells were washed with PBS, than harvested with a solution of 0.25% trypsin/EDTA (Sigma T4049) and finally resuspended in phosphate buffered saline (PBS) for examination by flow cytometry. Each experiment was performed in duplicate and repeated in 4

independent sets of tests. These tests were performed in the two cell lines referred above.

Procedures of flow cytometry to evaluate cell viability, detection of intracellular peroxides and superoxide radical, GSH expression and mitochondrial membrane potential was the same as described before. Although the procedure is similar, is necessary to understand some concepts, namely the induction of apoptosis and necrosis by ionizing radiation. Radiation induced apoptosis can be subdivided into early apoptosis, or interphase apoptosis which occurs within hours following the apoptotic stimuli, and delayed apoptosis, or post-mitotic apoptosis which occurs days after exposure to the stimuli, during or following mitosis [304-306]. Radiation induced early apoptosis occurs only a few hours after exposure in interphase and as premitotic event without requirement for cell division. This mode of radiation induced apoptosis has been characterized and demonstrated to include pyknosis, cell shrinkage and internucleosomal breakdown of chromatin, all of which are hallmarks of apoptotic death [306]. This apoptotic process is highly radiosensitive and most often activated in a P53-dependent way. However, the relatively low levels of radiation induced apoptosis that take place in solid tumours are generally observed much later following mitotic catastrophe. This delayed type of apoptosis, has been reported that occurs in association to the G2/M arrest or as post-mitotic event [306-309]. The morphology of this delayed type of radiation induced apoptosis can differ from that of classical apoptosis as it often occurs in cells that are “giant” instead of cells with shrunken volume [310, 311]. Radiation induced necrosis can be subdivided into early necrosis and delayed necrosis. Early necrosis is an ultra-fast cell death that is induced following particularly strong stimuli, such as high doses of irradiation (i.e. bigger than 100 Gy) [312]. Delayed necrosis is a slow cell death and one of the mechanisms by which mitotic catastrophe is executed [313].

a) Cell cycle

The cell cycle is divided into the tour fundamental parts: 1) mitosis, during which one cell divides into two identical progeny cells; 2) G1 phase; 3) S phase, in which occurs DNA synthesis; and 4) G2 phase [1, 59, 314]. The length of cell cycle varies from hundreds of hours for some stem cells to 24 hours for quick dividing mammalian cells. DNA damage delays normal cell cycle progression. A complex network of responses is activated as soon as the damage is registered in the genome, and these are rapidly manifested at cell cycle checkpoints. Massive insults to DNA, such as double-strand DNA breaks after cellular exposure to ionizing radiation, may induce changes in any cell cycle checkpoint, ultimately leading to the outcome of cell survival if DNA is properly repaired or, if not, to cell death. The checkpoint protein P53 has been established as one of the most important and it plays a major role in the complex cellular responses to radiation. The most important function for P53 after irradiation exposure is its acting as transcription factor with action in target genes that influences cell cycle arrest, DNA repair, apoptosis, senescence and autophagy. In general, cells are most radiosensitive in M and G2 phases and most radioresistant in latter part of S phase, while for cells with long cycle time, it's possible to see another peak of resistance in early G1 [1, 59, 314]. After irradiation, DNA damage can cause a progression delay in G1, S and G2 phases, to give cells time to repair the damages. In each checkpoint there are a series of cyclin-dependent kinases (CDK), which regulate cell progression from one phase to another. If DNA damage happened in G1 phase, the G1/S arrest will give to cell time to repair the damage before entry into S phase avoiding replication of the damaged DNA damaged. There is a very close relationship between the functional status of P53 and G1 arrest. The DNA damage can cause the accumulation of P53, which in turn up-regulate the CIP1 protein. CIP1 binds to cyclin/CDK complex and inhibit its activity resulting in the delay of cell cycle. Similarly, the G2/M arrest can enable the cell to repair DNA damage before cell division. G2 phase arrest is a prominent checkpoint of DNA damage and the mechanisms of DNA damage-induced G2 arrest have been intensively studied. Currently, two main mechanisms are proposed for G2 phase arrest, one related

to the cyclin B1/p34cdc2 complex and another involves the oncogene *RAS*. The S phase arrest occurs only after relatively high dose radiation [1, 59, 314].

Propidium Iodide (PI) is the most commonly used dye for DNA and cell cycle analysis for flow cytometry. The PI binds to DNA by intercalating into the double stranded macromolecule. PI also binds to RNA, and is necessary to remove the RNA with a nucleases treatment (RNase) for optimal DNA resolution. The quantification of the DNA, allows the knowledge about distribution of a cell population along the different phases of the cell cycle. The principle with these dyes is that they are stoichiometric, this is they bind in proportion to the amount of DNA present in the cell. In this way cells that are in S phase will have more DNA than cells in G1. They will take up proportionally more dye and will fluoresce more brightly until they have doubled their DNA content. The cells in G2 will be approximately twice more bright then G1 cells [315]. In this assay, 10^6 cells were vortex with 200 µl of 70% ethanol and incubated during 30 minutes in the dark at a refrigerator. Since PI is membrane impermeable, ethanol is used to both fix and permeabilize cells. After the cells were washed with PBS and centrifuged at 1300 G (2500 rpm) (Multifuge 1L-R, Germany) during 5 minutes. Supernatant was discarded and 500 µl of PI/RNase solution was added, with a gently stir in the vortex. The cells were incubated during 15 minutes, at room temperature in the dark, in binding buffer with 500 µl of PI/RNase (Immunostep, Salamanca, Spain). Subsequently, cells were excited with a light of a wavelength of 640 nm and 10^4 events to assess the percentage of cells in Pre-G1, G0/G1, S, and G2/M were collecting.

5.2.9. ***Cellular uptake and retention studies***

To evaluate the *in vitro* cellular kinetics of ^{99m}Tc-PEI-MP and ^{188}Re-PEI-MP it was proceeded to the evaluation of the cellular uptake (what enters to the cell) and retention (what stays in the cell) over time. These studies were performed in both cell lines HT-1376 and MNNG/HOS.

Cells were washed with PBS, than harvested with a solution of 0.25% trypsin/EDTA (Sigma T4049) and finally resuspended in medium to obtain a concentration of 2×10^6 cells/ml in 25 cm^2 flasks. After 1 hour of incubation at

37°C ^{99m}Tc-PEI-MP or ^{188}Re-PEI-MP was added to the cell suspension with an activity of 0.925MBq/ml (25µCi/ml), following methodologies described elsewhere [316]. Duplicate samples of 200 µl were collected to eppendorf tubes containing ice-cold PBS for determination of tracer uptake at 1 (only for ^{99m}Tc-PEI-MP), 5, 15, 30, 45, 60, 90, 120, 150, 210 and 240 minutes. These samples are then centrifuged at 5585 G (10000 rpm) (Costar Mini Centrifuge, USA), during 60 seconds to separate pellet from the supernatant, twice. Radioactivity of cell pellets and supernatants was measured separately in a well-type gamma counter (Gamma-C 12 DPC, Berthold, Germany) to determine tracer's uptake percentage, and then draw the influx curves. The obtained experimental values of cellular uptake were fitted to an exponential model (equation 5) using the software OriginPro (OriginLab Corporation, Northampton, EUA), version 8.0:

$$Uptake\ (\%) = A \cdot \left(1 - e^{-\ln(2) \cdot t / T_{50\%}}\right)$$

Equation 5. Percentage of cellular uptake, where A is the maximum uptake obtained (steady state) and T50% is the time needed to reach half of the maximum uptake.

To determine the percentage of retention over time, the procedure was very similar to the protocol of the uptake studies. The preparation of the cell suspension to the studies was the same, obtaining a cell suspension of 2×10^6/ml in a 50 ml falcon. ^{99m}Tc-PEI-MP or ^{188}Re-PEI-MP was added to the cell suspension with an activity of 0.925MBq/ml (25µCi/ml), and incubated at 37°C during 150 minutes. After this time the cell suspension was centrifuged at 3512 G (4000 rpm) (Multifuge 1L-R, Germany) during 1 minute at 4°C and then it was substituted the culture medium. The cell suspension was transferred to 25 cm^2 flasks and duplicate samples of 200 µl were collected to eppendorf tubes containing ice-cold PBS to determination of tracer retention at 1, 3 (times 1 and 3 only for ^{99m}Tc-PEI-MP), 5, 7, 15, 30, 45, 60, 90, 120, 150, 210 and 240 minutes. During tracer retention studies, for every sample taken, the cells were resuspended in order to ensure uniformity. These samples are then centrifuged at 5585 G (10000 rpm) (Costar Mini Centrifuge, USA) during 60 seconds to separate *pellet* from the supernatant. This procedure was repeated twice. Radioactivity of cell pellets and supernatants was measured separately in a

well-type gamma counter (Gamma-C 12 DPC, Berthold, Germany) to determine tracer's retention percentage in the cells. The obtained experimental values for the cellular retention were fitted to an exponential model (equation 6) using the software OriginPro (OriginLab Corporation, Northampton, EUA), version 8.0:

$$Retention\ (\%) = 100 - A \cdot \left(1 - e^{-\ln(2) \cdot t / T_m}\right)$$

Equation 6. Percentage of cellular retention, where A is the minimum retention obtained (steady state) and T_m is the time delay to reach 50% of the retention plus A/2, this is, the midpoint between 100% and the minimal retention.

As a control, the uptake and retention percentages were determined after the addition of ^{99m}Tc-Pertechnetate or ^{188}Re-Perrhenate, following the same protocols for each complex. For the retention studies, cell suspensions were incubated with ^{99m}Tc-Pertechnetate or ^{188}Re-Perrhenate during 60 minutes before starting the studies. Each experiment was performed in duplicate and repeated in 4 independent sets of tests. These tests were performed in the two cell lines referred above.

5.2.10. ***Statistical analysis***

The obtained results were analysed using the software IBM® SPSS® (IBM Corporation, Armonk, New York, EUA), version 20, at a significance level of 5% ($p < 0.05$). The descriptive analysis of quantitative variables under study, was performed by calculating estimators of central tendency, dispersion and location. In inferential analysis, the normal distribution of quantitative variables was assessed using the Shapiro-Wilk test.

The comparison of values from the radiochemical purity of ^{99m}Tc/^{188}Re-PEI-MP, and the partition coefficient of ^{99m}Tc-PEI-MP over time, were made according to the Friedman test with multiple comparisons according to Bonferroni correction. The comparison of values from the radiochemical purity of ^{99m}Tc-PEI-MP over time, at several temperatures and incubation with culture medium, were made according to the Friedman test with multiple comparisons according to

Bonferroni correction, and between conditions according to Kruskal-Wallis. The results of the MTT assay obtained after the incubation with various concentrations of PEI-MP by MTT assay were compared for each cell line and time of incubation. The comparison of values between concentrations was made according to the ANOVA test in case they check a normal distribution and homogeneity of variance or according to the Kruskal-Wallis otherwise. The multiple comparisons were performed according to the Bonferroni correction. The comparison of the results of cell death, peroxides and superoxide radical production, GSH expression, mitochondrial membrane potential and cell cycle, between groups and cell lines, in both studies cytotoxicity of PEI-MP and radiotoxicity of ^{99m}Tc by flow cytometry, were made according to the t Student test for independent samples in case they check a normal distribution or according to the Mann-Whitney otherwise. The comparison of peroxides and superoxide radical production, GSH expression and mitochondrial membrane potential values after exposure to PEI-MP, with the control, was performed according to the t Student test for a mean, comparing the sample values to 1. The comparison of peroxides and superoxide radical production and mitochondrial membrane potential values after exposure to doses of ^{99m}Tc, with the control, was performed according to the t Student test for a mean, comparing the sample values to 1. For the cell viability and cell cycle the comparison was performed according to the t Student test for independent samples or Mann-Whitney, according to the previously explained.

The comparison of values from the clonogenic activity after external and internal irradiation for each cell line and with the control were made according to the t Student test for a mean in comparison with the control (reference value 1), and using the test ANOVA of a factor (in the case of normal distribution and homogeneity of variances) or according to the Kruskal-Wallis test (otherwise) with multiple comparisons, with Bonferroni correction for the comparison between the remaining doses.

The parameters obtained in uptake and retention studies were compared using the ANOVA test of a factor, with multiple comparisons according to the Bonferroni correction. It was considered a type I error of 0.05 for all the comparisons.

5.3. Results

5.3.1. Radiochemical quality control

The radiochemical purity was evaluated over time, using two chromatographic systems described before. When the acetone migrates through the ITLC-SG strip, ^{99m}Tc-Pertechnetate or ^{188}Re-Perrhenate migrates with the solvent front (Rf = 1.0), allowing the determination of the percentage of these impurities. On the other hand, when citrate migrates through the W3MM strip, ^{99m}Tc/^{188}Re-Hydrolyzed/Reduced remains at the origin (Rf = 0.0), and the rest of the ^{99m}Tc/^{188}Re species migrates with the solvent front, allowing the determination of the percentage of these radiochemical impurities [87, 271]. By analysing the radiochemical purity of ^{99m}Tc-PEI-MP kit over time (during 5 hours after radiolabelling), it's possible to verify that the labelling efficiency remained high, varying from 89.46% in the first hour to 92.72% five hours after the radiolabelling (table 17), revealing the high stability of the labelling kit formulation and the high labelling efficiency just one hour after the radiolabelling. The variation of the labelling efficiency over time was not statistically significant.

Table 17. ^{99m}Tc-PEI-MP radiochemical purity control over time. The results express the average of 3 independent experiments ± standard deviation.

Time (hours)	%^{99m}Tc-PEI-MP	% ^{99m}Tc-Reduced/ Hydrolyzed	%^{99m}Tc-Pertechnetate
1	89.46±0.47	10.48±0.44	0.08±0.02
2	90.02±1.55	9.89±1.46	0.03±0.02
3	91.14±0.96	8.74±0.86	0.09±0.07
4	90.23±1.32	9.66±1.25	0.11±0.07
5	92.72±1.11	7.27±1.12	0.02±0.01

Legend: Percentage of ^{99m}Tc species over time (1, 2, 3, 4 and 5 hours after radiolabelling), for radiochemical purity control. The percentage of the desired ^{99m}Tc-PEI-MP was always superior to 89% over time.

By analysing the radiochemical purity of ^{188}Re-PEI-MP kit over time (during 5 hours after radiolabelling), it's possible to verify that the labelling efficiency remained relatively high, varying from 85.00% in the first hour to 81.73% five hours after the radiolabelling (table 18), revealing the high stability of the labelling kit formulation and the high labelling efficiency just one hour after the radiolabelling, even though less than that obtained with ^{99m}Tc-PEI-MP. The variation of the labelling efficiency over time was only statistically significant between 4 and 5 hours after radiolabelling ($p = 0.019$), decreasing from 90.50% at 4h to 81.73% at 5h. The decrease of the radiochemical purity seems to be associated with the increase of the percentage of the reduced/hydrolyzed ^{188}Re species between 4h (4.80%) and 5h (17.00%), with statistical significant differences ($p = 0.019$).

Table 18. ^{188}Re-PEI-MP radiochemical purity control over time. The results express the average of 3 independent experiments ± standard deviation.

Time (hours)	%^{188}Re-PEI-MP	% ^{188}Re-Reduced/ Hydrolyzed	%^{188}Re-Perrhenate
1	85.00±2.46	13.10±3.15	2.47±0.40
2	87.97±1.81	8.50±1.42	2.43±0.93
3	86.80±2.65	7.30±1.21	2.40±0.35
4	90.50±0.92	4.80±1.06	2.47±0.45
5	81.73±3.15	17.00±1.39	3.70±0.60

Legend: Percentage of ^{188}Re species over time (1, 2, 3, 4 and 5 hours after radiolabelling), for radiochemical purity control. The percentage of the desired ^{188}Re-PEI-MP was always superior to 81% over time.

Also it was investigated the effect of temperature (22, 37 and 45°C) and of cell culture medium (DMEM) in radiochemical purity of ^{99m}Tc-PEI-MP over time (30 minutes, 1h, 3h and 5h). The changes in temperatures are important because the human body temperature is 37°C as well as the cell culture propagation. As room temperature is normally around 22°C, we also choose this value. The higher temperature (45°C) was chosen in order to have a high value. By analysing the table 19, we can observe that the variation of the labelling efficiency over time, among temperatures and among temperatures plus DMEM was not statistically significant, and the values remained relatively constant, showing that both the variation of temperature and exposure to DMEM has no influence on the radiochemical purity.

Table 19. Radiochemical purity of ^{99m}Tc-PEI-MP, at 22 ºC, 37 ºC and ºC 45 ºC, and for the same temperatures and the exposure to DMEM. The results express the average of 4 independent experiments ± standard deviation.

Conditions	Time	%^{99m}Tc-PEI-MP	% ^{99m}Tc-Reduced/ Hydrolyzed	%^{99m}Tc-Pertechnetate
22ºC	30 min	87.40 ± 0.37	12.59 ± 0.37	0.00 ± 0.00
	1h	85.80 ± 1.01	14.13 ± 0.95	0.05 ± 0.01
	3h	85.05 ± 0.34	14.81 ± 0.32	0.10 ± 0.01
	5h	81.38 ± 1.51	17.86 ± 1.94	1.89 ± 0.31
22ºC + DMEM	30 min	83.34 ± 1.89	16.47 ± 1.93	0.17 ± 0.05
	1h	88.52 ± 0.55	10.40 ± 0.71	1.84 ± 0.50
	3h	87.91 ± 1.18	11.65 ± 1.06	0.43 ± 0.03
	5h	88.92 ± 2.33	11.02 ± 2.32	0.06 ± 0.02
37ºC	30 min	85.70 ± 3.48	14.30 ± 3.48	0.01 ± 0.00
	1h	85.09 ± 3.70	14.86 ± 3.70	0.05 ± 0.01
	3h	79.10 ± 1.80	20.73 ± 1.78	0.04 ± 0.01
	5h	82.02 ± 3.24	16.05 ± 3.52	2.30 ± 0.48
37ºC + DMEM	30 min	84.29 ± 3.27	15.55 ± 3.26	0.17 ± 0.01
	1h	90.13 ± 0.71	8.77 ± 0.78	1.14 ± 0.05
	3h	86.70 ± 1.06	12.74 ± 1.30	0.42 ± 0.06
	5h	88.05 ± 2.09	11.85 ± 2.07	0.10 ± 0.04
45ºC	30 min	85.81 ± 2.06	14.19 ± 2.05	0.00 ± 0.00
	1h	86.88 ± 2.38	13.05 ± 2.39	0.07 ± 0.02
	3h	79.09 ± 4.76	19.87 ± 4.87	0.15 ± 0.08
	5h	80.95 ±3.15	17.08 ± 3.90	3.68 ± 2.89
45ºC + DMEM	30 min	83.94 ± 4.95	20.58 ± 3.50	0.25 ± 0.04
	1h	88.66 ± 1.61	8.85 ± 0.46	1.65 ± 0.41
	3h	85.77 ± 1.72	13.68 ± 1.78	0.55 ± 0.10
	5h	88.68 ±1.95	11.22 ± 1.97	0.11 ± 0.03

Legend: Percentage of ^{99m}Tc species over time (30 min, 1h, 3h and 5h after radiolabelling), when exposed to temperatures of 22 ºC, 37 ºC and 45 ºC, and for the same temperatures when exposed to DMEM.

5.3.2. Determination of the partition coefficient of ^{99m}Tc-PEI-MP

In order to determine the hydrophilicity or lipophilicity of ^{99m}Tc-PEI-MP, it was determined the partition coefficient over time. After obtained the counts of each phase (1-octanol/water), and calculated the partition coefficient of the ^{99m}Tc-PEI-MP with the formula presented before, it was verified that the 1-octanol/water partition coefficient was always negative during time (4 hours) and the values were relatively constant, ranging from -3.28±0.08 at 1 hour and -3.82±0.01 at 4 hours (table 20). These results demonstrate that ^{99m}Tc-PEI-MP is a hydrophilic complex.

Table 20. Partition coefficient of ^{99m}Tc-PEI-MP over time. The results express the average of 4 independent experiments ± standard deviation.

Time (hours)	$P_{O/W}$ ^{99m}Tc-PEI-MP
1	-3.28±0.08
2	-3.64±0.05
3	-3.62±0.06
4	-3.82±0.01

Legend: Partition coefficient ($P_{O/W}$) of ^{99m}Tc-PEI-MP over time (1h, 2h, 3h and 4h after radiolabelling). The partition coefficient was always negative revealing the hydrophilicity of the complex.

5.3.3. Evaluation of the cytotoxicity of PEI-MP

5.3.3.1. Metabolic activity

It was intended to verify if the PEI-MP was cytotoxic to cells, and whether it could function as a carrier and not as a drug. To this, the effects of PEI-MP in the metabolic activity of the HT-1376 and MNNG/HOS cells were examined for different concentrations of PEI-MP and periods of incubation, using MTT assay. With the values obtained, it wasn't possible to estimate the IC_{50} for each cell line and time of incubation, therefore it was compared the various concentration used for each cell line and time of incubation. The fig. 12 represents the percentage of metabolic activity of HT-1376 and MNNG/HOS cells 24, 48, 72 and 96 hours after incubation. We can see in the fig. 12, that for each concentration of PEI-MP, the percentage of cellular metabolic activity for each cell line and incubation time was always equal or superior to 100%, demonstrating that PEI-MP doesn't have a significantly inhibitory influence on

cell metabolic activity. There are no significant statistical differences between the two cell lines, or within each cell line, for every concentration of PEI-MP and incubation time.

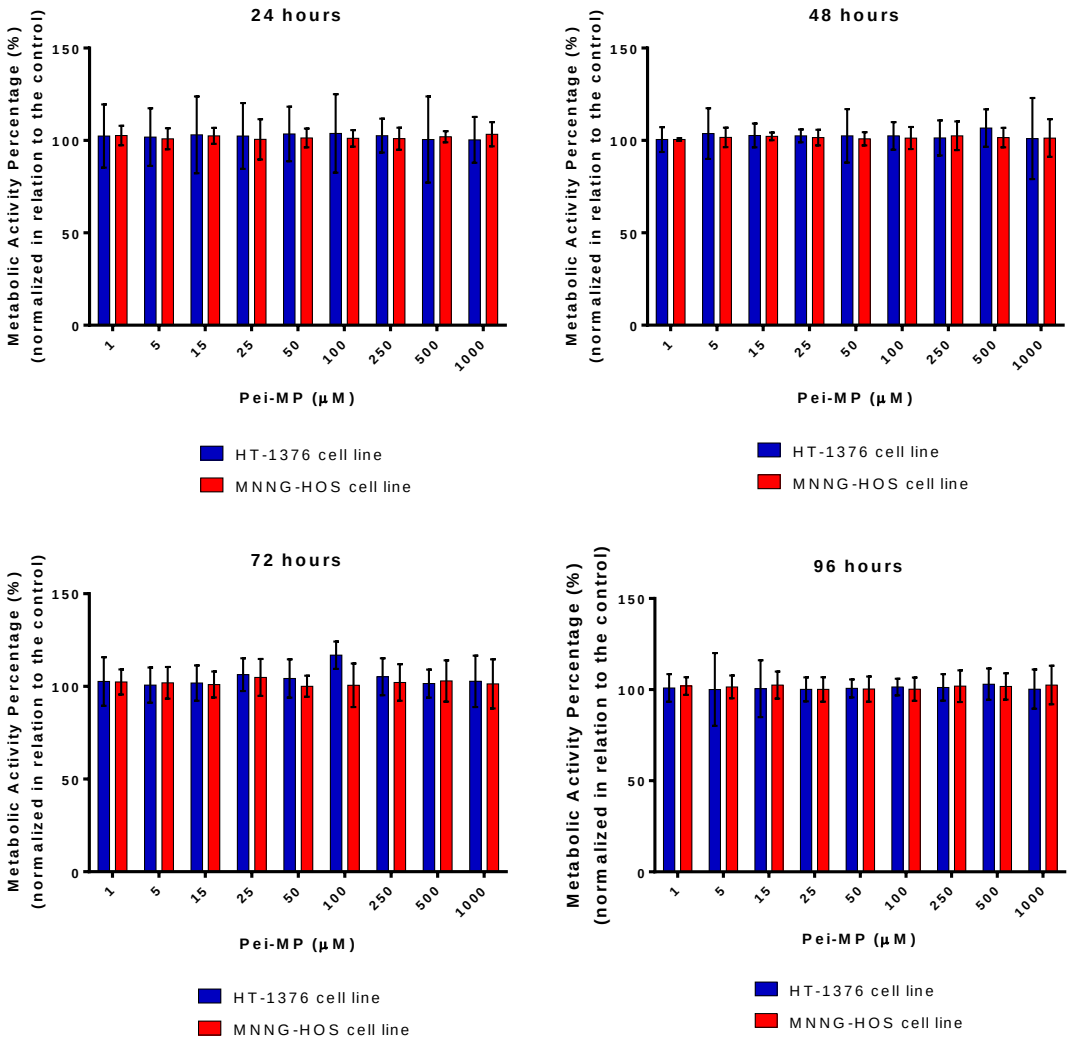

Figure 12. Percentage of metabolic cell activity 24, 48, 72 and 96 hours after exposure to concentrations of PEI-MP in HT-1376 and MNNG/HOS cell lines. The results express the average of 5 independent experiments ± standard deviation.

5.3.3.2. Flow cytometry

In order to support the results obtained by the MTT assay, the effects of PEI-MP, with the maximum concentration of 1000 µM, in HT-1376 and MNNG/HOS cells, was evaluated by flow cytometry, studying the cell viability, the ROS

production, the expression of GSH and changes in mitochondrial membrane potential.

The assessment of cell viability was performed by flow cytometry using the AV/PI incorporation assay. This technique allows distinguishing different cell populations: viable cells, cells in early apoptosis, cells in late apoptosis/necrosis and necrosis. Cytometry studies demonstrated that after 24 hours of incubation with PEI-MP, there are no statistical significant differences in cell viability between the control and the exposed cells, remaining above 82% in both cell lines, as shown in fig. 13. Despite cell viability didn't decrease, apoptosis increased in both cell lines after the incubation with PEI-MP, with a reduction of necrosis. Besides the small values, statistically significant differences were found for apoptosis in HT-1376 cells ($p = 0.006$) and MNNG/HOS cells ($p = 0.029$). Also necrosis has reduced significantly for MNNG/HOS ($p = 0.004$).

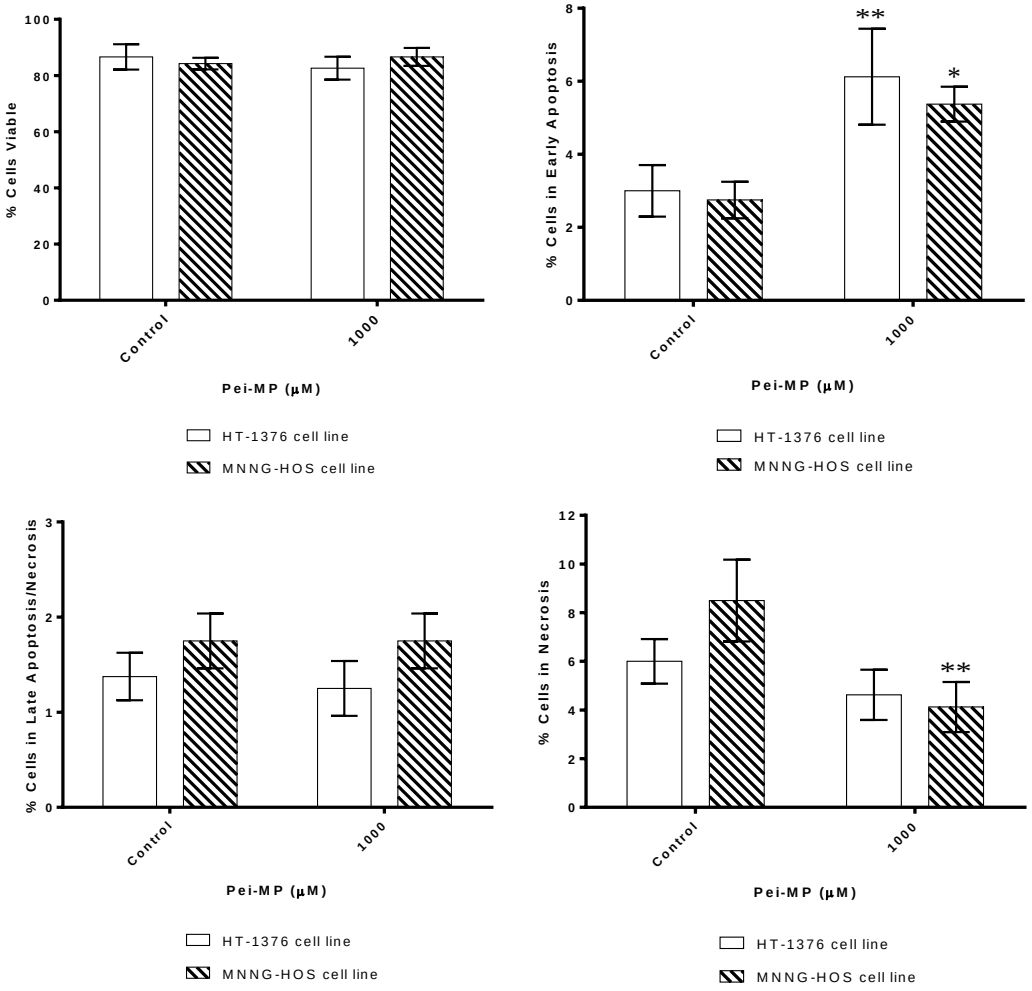

Figure 13. Cell viability by flow cytometry using dual staining with AV and PI. Figure represents the percentage of viable cells, in early apoptosis, in late apoptosis/necrosis, and necrosis after 24 hours of incubation with 1000 µM of PEI-MP in HT-1376 and MNNG/HOS cells. The results express the average of 4 independent experiments ± standard deviation.

The production of ROS was also evaluated by the quantification of the expression of peroxides and superoxide radicals. To evaluate the production of peroxide and superoxide radicals, it was used DCFH2-DA and DHE, respectively, for the analysis of the fluorescence intensities by flow cytometry. As can be seen in the fig. 14, there is an increase in the intracellular production of peroxides in both cell lines, particularly for HT-1376 cells, after 24 hours of incubation with 1000 µM of PEI-MP. However, it wasn't found any statistically significant differences in the production of peroxides in relation to the control and between cells lines. Also is possible to see that the production of

superoxide seems not to alter with the exposure to PEI-MP, and comparing the values it wasn't found any statically significant differences.

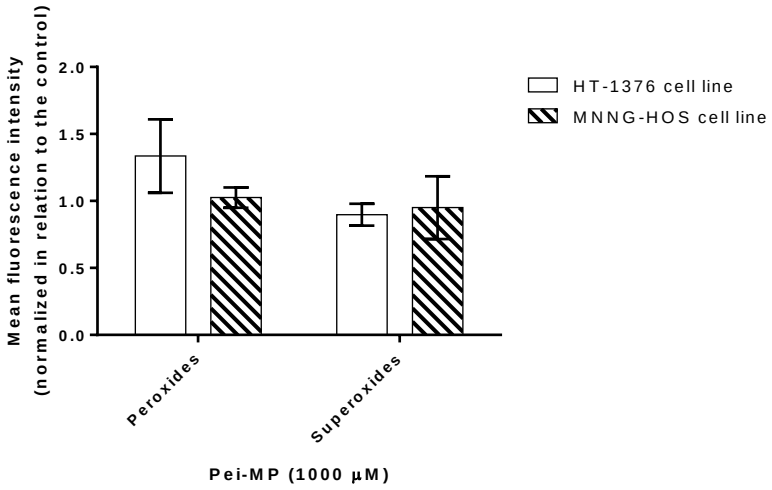

Figure 14. Production of peroxides and superoxide by flow cytometry using DCFH2-DA and DHE, respectively. HT-1376 and MNNG/HOS cells were incubated during 24 hours with 1000 µM of PEI-MP and subsequently the production of peroxides and superoxide was detected. The results are expressed as mean intensity normalized in relation to the control, comparing the results with the value of 1. The results express the average of 4 independent experiments ± standard deviation.

To evaluate the expression of intracellular GSH, it was used the orange mercury probe and the fluorescence intensities was analysed by flow cytometry. Through the analysis of fig. 15, there is a decrease in the expression of GSH in both cell lines, particularly for HT-1376 cells, after 24 hours of incubation with 1000 µM of PEI-MP. However, it wasn't found statistically significant differences, between the control and the cell lines.

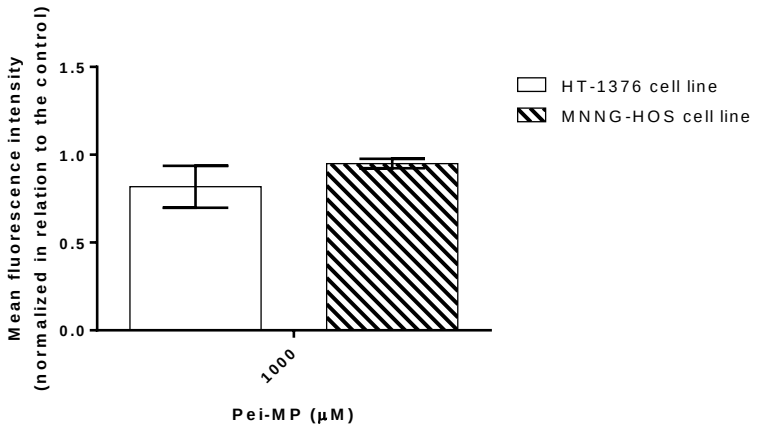

Figure 15. Expression of GSH by flow cytometry using orange mercury. HT-1376 and MNNG/HOS cells were incubated during 24 hours with 1000 µM of PEI-MP and subsequently the expression of intracellular GSH was detected. The results are expressed as mean intensity normalized in relation to the control, comparing the results with the value of 1. The results express the average of 4 independent experiments ± standard deviation.

To evaluate the mitochondrial membrane potential, it was used the JC-1 probe, a molecule able to selectively enter the cell and which exists in two forms, monomers (M) and aggregates (A), depending on the state of polarization/depolarization of the mitochondrial membrane. As can be seen in fig. 16, there is a slightly decrease in mitochondrial membrane potential in both cell lines after 24 hours of incubation with PEI-MP, in the concentration of 1000 µM. It wasn't found statistically significant differences between the two cell lines or in relation to the control.

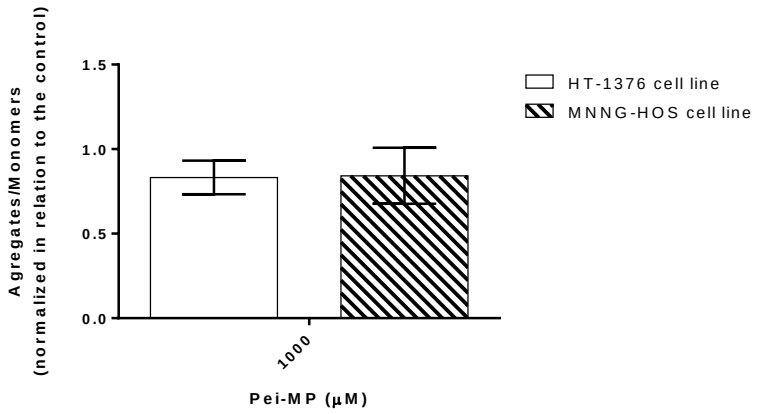

Figure 16. Analysis of mitochondrial membrane potential by flow cytometry using the fluorescent probe JC-1. HT-1376 and MNNG/HOS cells were incubated during 24 hours with 1000 µM of PEI-MP and subsequently mitochondrial membrane potential was detected. The results are expressed as mean intensity normalized in relation to the control, comparing the results with the value of 1. The results express the average of 4 independent experiments ± standard deviation.

5.3.4. Evaluation of the radiocytoxicity of ^{99m}Tc

5.3.4.1. Clonogenic activity

It was intended to verify if doses of ^{99m}Tc-Pertechnetate activities in the range of diagnostics had influence in cell survival based on the ability of a single cell to grow and form a colony, either being irradiated externally (evaluation of gamma rays effects) or internally (evaluation of gamma rays and auger electrons effects). To this, it was examined the clonogenic activity of HT-1376 and MNNG/HOS cells after external and internal irradiation with 2, 5, 10 and 20 mGy of ^{99m}Tc.

The fig. 17 and fig. 18 represents the medium survival factor of HT-1376 and MNNG/HOS cells after external and internal irradiation, respectively, with 2, 5, 10 and 20 mGy of ^{99m}Tc.It can be seen in fig. 17 and fig. 18 that for each dose of ^{99m}Tc, independently of the irradiation be internal or external, the cell survival didn't decrease, demonstrating that for diagnostic effective doses, the gamma rays and auger electrons, has no apparent effect on cell survival. In the comparison of all the conditions, it wasn't found statistically significant differences.

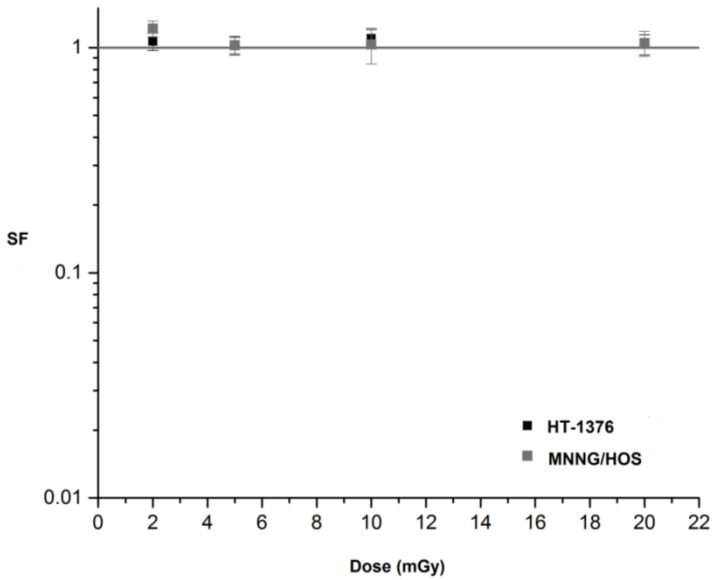

Figure 17. Cell survival after external irradiation with doses of ^{99m}Tc in HT-1376 and MNNG/HOS cell lines. The results express the average of 5 independent experiments ± standard deviation.

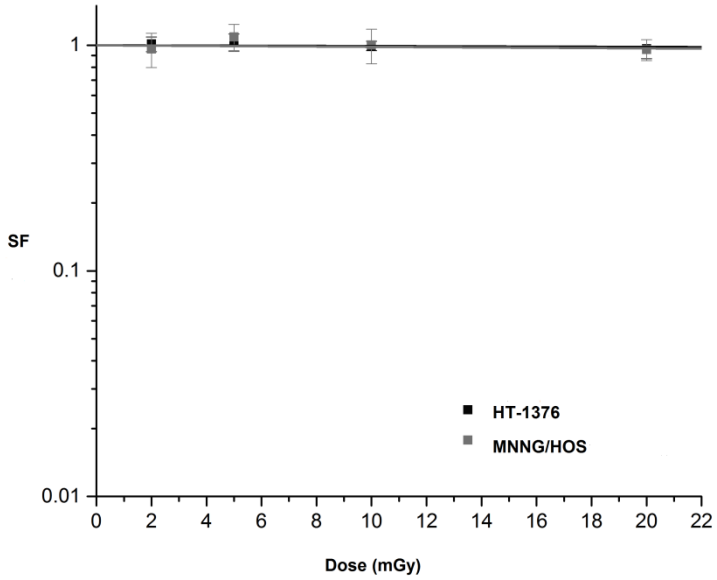

Figure 18. Cell survival after internal irradiation with doses of ^{99m}Tc in HT-1376 and MNNG/HOS cell lines. The results express the average of 4 independent experiments ± standard deviation.

5.3.4.2. Flow cytometry

In order to support the results obtained with clonogenic test, the effects of 20 mGy of ^{99m}Tc, after external and internal irradiation of HT-1376 and MNNG/HOS cells, was evaluated by flow cytometry, studying the cell viability,

the ROS production, the expression of GSH, changes in mitochondrial membrane potential and distribution of cells in cell cycle.

The assessment of cell viability was performed by flow cytometry using the AV/PI incorporation assay. This technique allows distinguishing different cell populations: viable cells, cells in early apoptosis, cells in late apoptosis/necrosis and necrosis. Cytometry studies show that after external irradiation with 20 mGy of ^{99m}Tc, cell viability didn't decrease, remaining above 82% in both cell lines, as shown in fig. 19. To these values of cell viability it wasn't found any statistical significant differences between the control and the irradiated cells, in both cell lines. Early apoptosis, late apoptosis/necrosis seems to increase for both cell lines after the external irradiation, especially for HT-1376 cells. However, statistical significant differences were not found. Necrosis seems to increase for HT-1376 and decrease for MNNG/HOS cells, however these differences were not statistically significant.

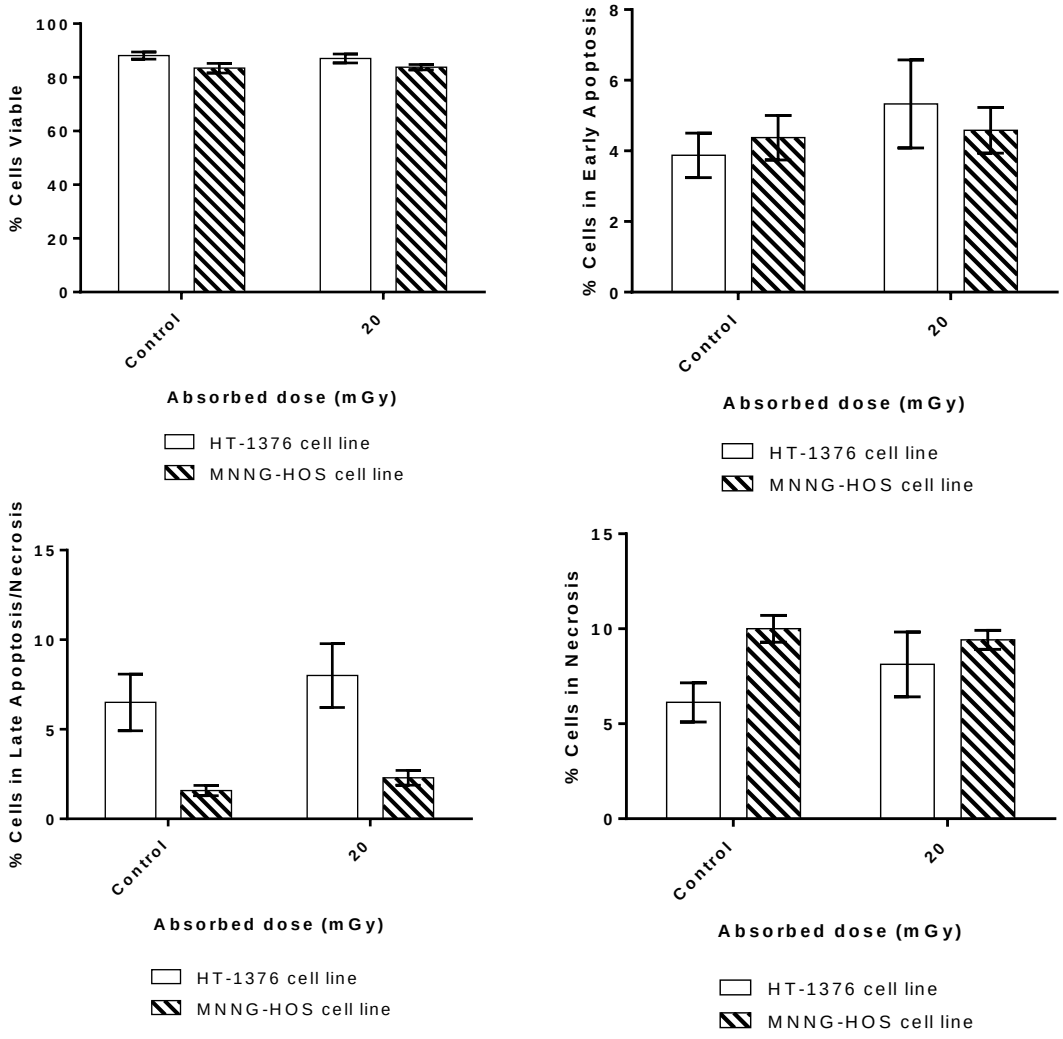

Figure 19. Cell viability by flow cytometry using dual staining with AV and PI. Figure represents the percentage of viable cells, in early apoptosis, in late apoptosis/necrosis, and necrosis after external irradiation with 20 mGy of ^{99m}Tc in HT-1376 and MNNG/HOS cells. The results express the average of 4 independent experiments ± standard deviation.

For internal irradiation, cytometry studies show that after irradiation with 20 mGy of ^{99m}Tc, cell viability didn't decrease, remaining above 84% in both cell lines, as shown in fig. 20. To these values of cell viability it wasn't found any statistical significant differences between the control and the irradiated cells, in both cell lines. Late apoptosis/necrosis seems to increase for both cell lines after the internal irradiation, especially for HT-1376 cells. However, statistical significant differences were not found. Necrosis seems to decrease for HT-1376 and increase for MNNG/HOS cells, however these differences were not statistically

significant. Also, it was not found statistically significant differences for apoptosis in both cell lines.

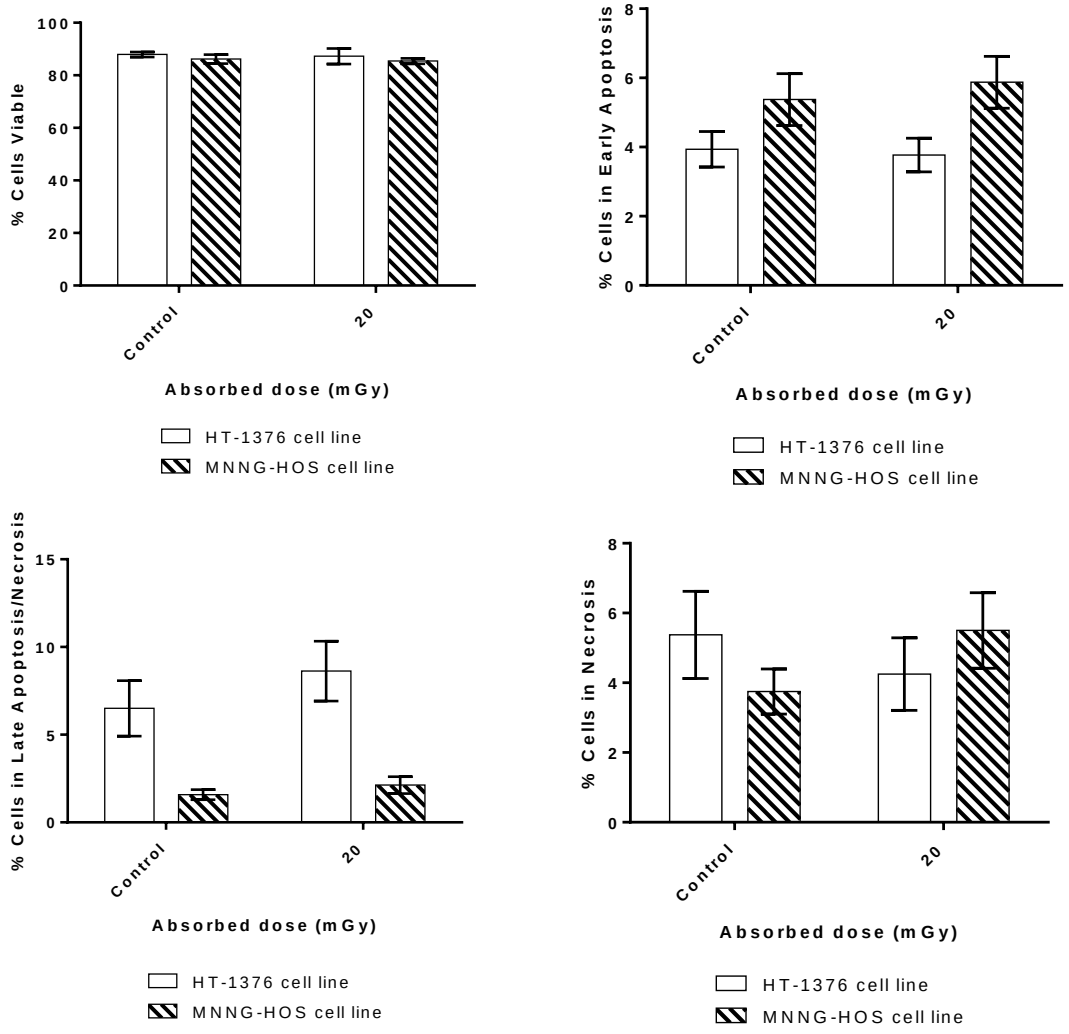

Figure 20. Cell viability by flow cytometry using dual staining with AV and PI. Figure represents the percentage of viable cells, in early apoptosis, in late apoptosis/necrosis, and necrosis after internal irradiation with 20 mGy of ^{99m}Tc in HT-1376 and MNNG/HOS cells. The results express the average of 4 independent experiments ± standard deviation.

The production of ROS was also evaluated by the quantification of the expression of peroxides and superoxide radicals. To evaluate the production of peroxide and superoxide radicals, it was used DCFH2-DA and DHE, respectively, for the analysis of the fluorescence intensities by flow cytometry. As can be seen in the fig. 21, there is slight increase in the intracellular production of peroxides for MNNG/HOS and superoxide in both cell lines, after external irradiation with 20 mGy of ^{99m}Tc. However, it wasn't found any

statistically significant differences in the production of peroxides and superoxide in relation to the control and between cells lines. Also is possible to see that the production of peroxides in HT-1376 cells seems not to alter after the external irradiation with 20 mGy of ^{99m}Tc, and comparing the values it wasn't found any statically significant differences.

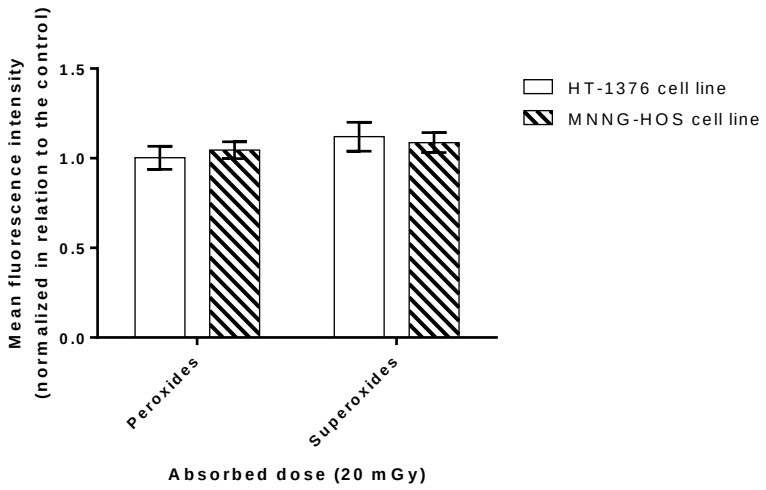

Figure 21. Production of peroxides and superoxide by flow cytometry using DCFH2-DA and DHE, respectively. HT-1376 and MNNG/HOS cells were irradiated externally with 20 mGy of ^{99m}Tc and subsequently the production of peroxides and superoxide was detected. The results are expressed as mean intensity normalized in relation to the control, comparing the results with the value of 1. The results express the average of 4 independent experiments ± standard deviation.

For internal irradiation, as can be seen in the fig. 22, the production of peroxides in both cell lines and the production of superoxide for HT-1376 cells seem not to change after the internal irradiation with 20mGy of ^{99m}Tc, and comparing the values it wasn't found any statically significant differences. Also, it was possible to visualize a slight increase in the intracellular production of superoxide in MNNG/HOS cells, after internal irradiation with 20 mGy of ^{99m}Tc. However, it wasn't found any statistically significant differences in the production of superoxide in relation to the control and between cells lines.

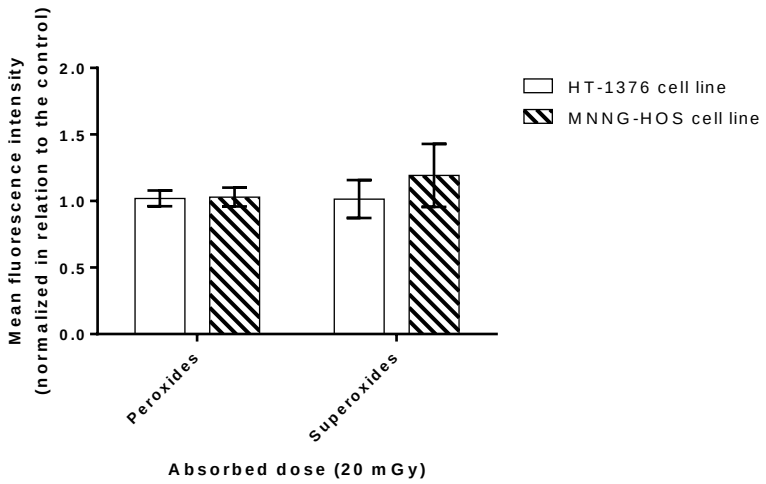

Figure 22. Production of peroxides and superoxide by flow cytometry using DCFH2-DA and DHE, respectively. HT-1376 and MNNG/HOS cells were irradiated internally with 20 mGy of ^{99m}Tc and subsequently the production of peroxides and superoxide was detected. The results are expressed as mean intensity normalized in relation to the control, comparing the results with the value of 1. The results express the average of 4 independent experiments ± standard deviation.

To evaluate the expression of intracellular GSH, it was used the orange mercury probe and the analysis of the fluorescence intensities by flow cytometry. As can be seen in fig. 23, the expression of intracellular GSH seems to decrease slightly for HT-1376 cells and not having alterations for MNNG/HOS cells. However, it wasn't found any statistically significant differences in the expression of intracellular GSH in relation to the control and between cells lines.

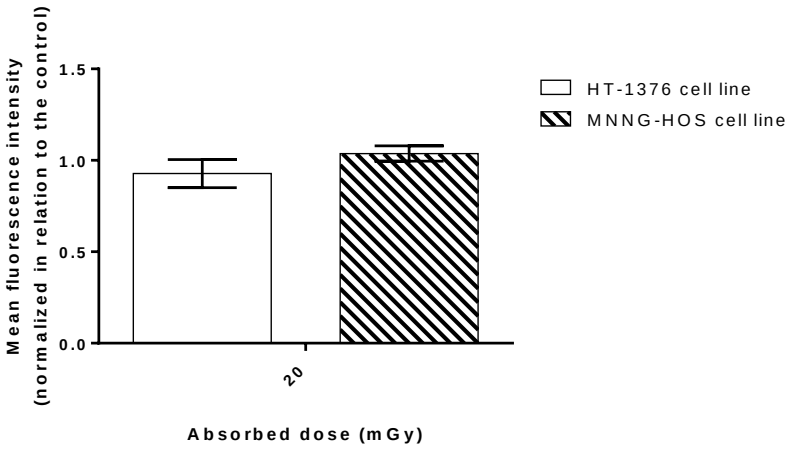

Figure 23. Expression of GSH by flow cytometry using orange mercury. HT-1376 and MNNG/HOS cells irradiated externally with 20 mGy of ^{99m}Tc and subsequently the expression of intracellular GSH was detected. The results are expressed as mean intensity normalized in relation to the control, comparing the results with the value of 1. The results express the average of 4 independent experiments ± standard deviation.

For internal irradiation, as can be seen in fig. 24, the expression of intracellular GSH seems to increase slightly for both cell lines. However, it wasn't found any statistically significant differences in the expression of intracellular GSH in relation to the control and between cells lines.

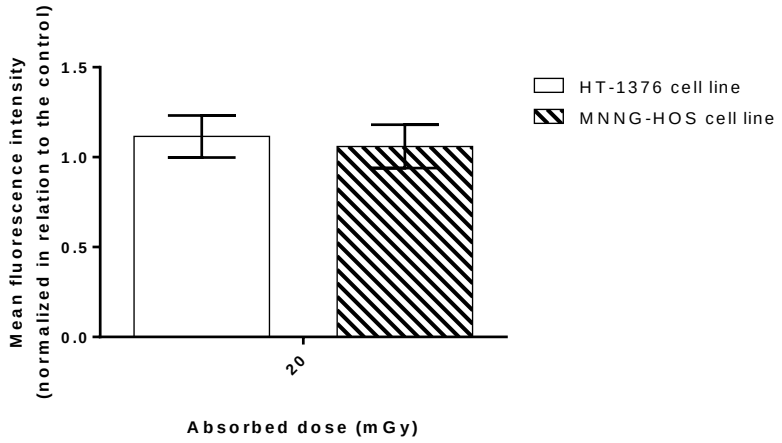

Figure 24. Expression of GSH by flow cytometry using orange mercury. HT-1376 and MNNG/HOS cells irradiated internally with 20 mGy of ^{99m}Tc and subsequently the expression of intracellular GSH was detected. The results are expressed as mean intensity normalized in relation to the control, comparing the results with the value of 1. The results express the average of 4 independent experiments ± standard deviation.

To evaluate the mitochondrial membrane potential, it was used the JC-1, a molecule able to selectively enter the cell and which exists in two forms,

monomers (M) and aggregates (A), depending on the state of polarization/depolarization of the mitochondrial membrane. For external irradiation, as can be seen in the fig. 25, the mitochondrial membrane potential seems not to alter in both cell lines after the external irradiation with 20mGy of ^{99m}Tc, and comparing the values it wasn't found any statically significant differences.

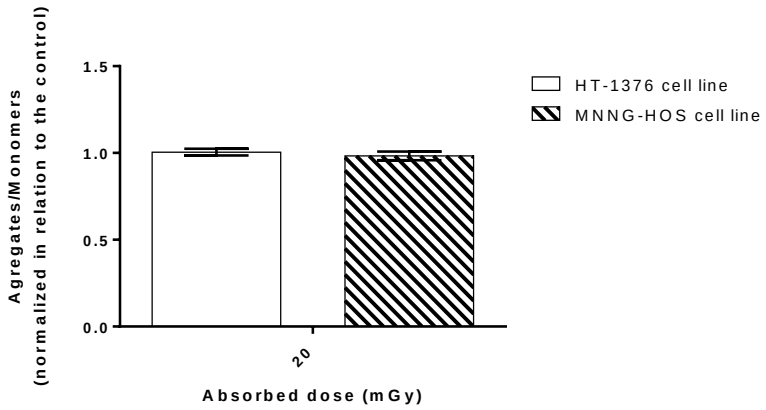

Figure 25. Analysis of mitochondrial membrane potential by flow cytometry using the fluorescent probe JC-1. HT-1376 and MNNG/HOS cells irradiated externally with 20 mGy of ^{99m}Tc and subsequently mitochondrial membrane potential was detected. The results are expressed as mean intensity normalized in relation to the control, comparing the results with the value of 1. The results express the average of 4 independent experiments ± standard deviation.

For internal irradiation, as can be seen in the fig. 26, the mitochondrial membrane potential seems not to alter in both cell lines after the internal irradiation with 20mGy of ^{99m}Tc, and comparing the values it wasn't found any statically significant differences.

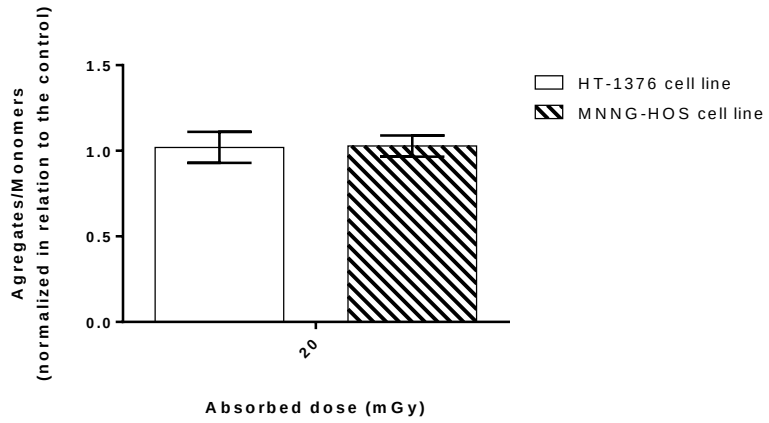

Figure 26. Analysis of mitochondrial membrane potential by flow cytometry using the fluorescent probe JC-1. HT-1376 and MNNG/HOS cells irradiated internally with 20 mGy of ^{99m}Tc and subsequently mitochondrial membrane potential was detected. The results are expressed as mean intensity normalized in relation to the control, comparing the results with the value of 1. The results express the average of 4 independent experiments ± standard deviation.

The assessment of cell cycle was performed by flow cytometry using the PI/RNase incorporation assay. This technique allows distinguishing the distribution of cells in cell cycle: pre G1, G0/G1, S and G2/M phases. Cytometry studies show that after external irradiation with 20 mGy of ^{99m}Tc, the distribution of cells in cell cycle didn't alter for both type of cells, as shown in fig. 27, and comparing the values it wasn't found any statically significant differences.

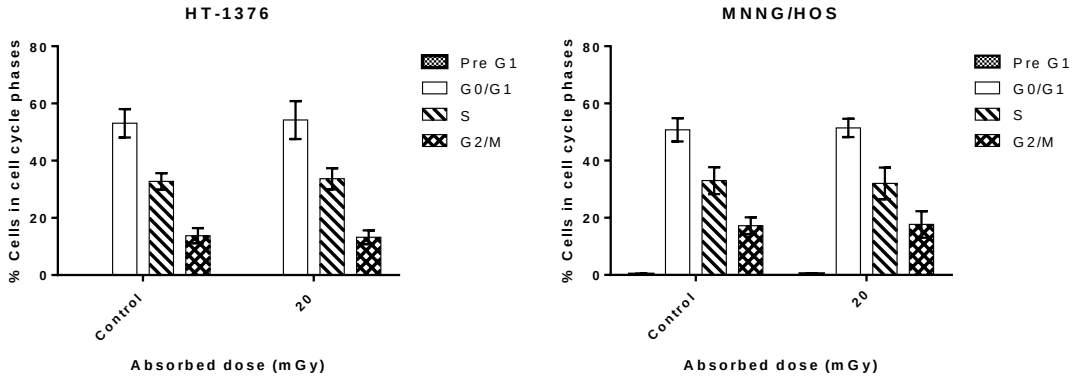

Figure 27. Cell cycle distribution by flow cytometry using PI/RNase. Figure represents the percentage of cells in pre G1, G0/G1, S and G2/M phases, after external irradiation with 20 mGy of ^{99m}Tc in HT-1376 and MNNG/HOS cells. The results express the average of 4 independent experiments ± standard deviation.

For internal irradiation, cytometry studies show that after irradiation with 20 mGy of ^{99m}Tc, the distribution of cells in cell cycle didn't alter for both type of cells, as shown in fig. 28, and comparing the values it wasn't found any statically significant differences.

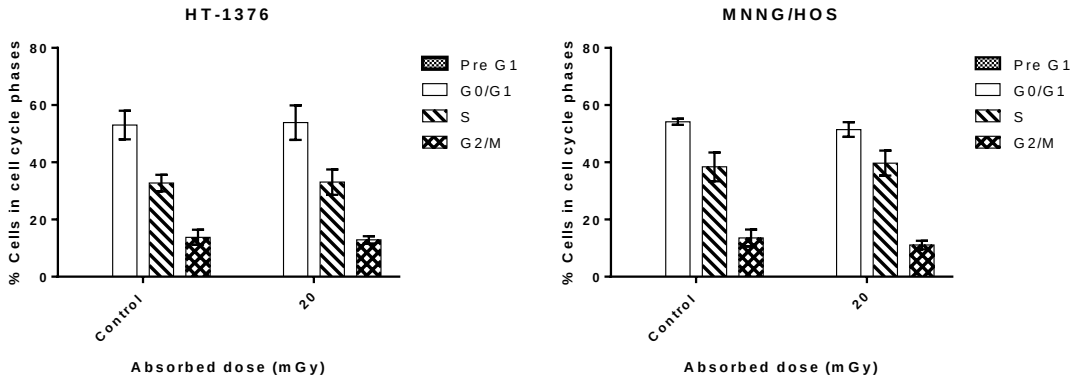

Figure 28. Cell cycle distribution by flow cytometry using PI/RNase. Figure represents the percentage of cells in pre G1, G0/G1, S and G2/M phases, after internal irradiation with 20 mGy of ^{99m}Tc in HT-1376 and MNNG/HOS cells. The results express the average of 4 independent experiments ± standard deviation.

5.3.5. Cellular uptake and retention studies

To evaluate the *in vitro* cellular kinetics of ^{99m}Tc-PEI-MP and ^{188}Re-PEI-MP it was proceeded to the evaluation of the cellular uptake and retention over time.

From the results showed in fig. 29, fig. 30 and table 21, the maximum uptake for ^{99m}Tc-PEI-MP in both cell lines was higher than for ^{99m}Tc-Pertechnetate. In cell line HT-1376 the maximum uptake of ^{99m}Tc-PEI-MP obtained was in the order of 1.16 instead of the lower value 0.27 of maximum uptake for ^{99m}Tc-Pertechnetate, being the differences statistically significant ($p = 0.001$). Also it was verified that the maximum uptake was higher for ^{99m}Tc-PEI-MP, the time spend to reach half of the maximum uptake was higher for ^{99m}Tc-PEI-MP (55.46 minutes) than for ^{99m}Tc-Pertechnetate (3.88 minutes), however it wasn't found statistically significant differences. In cell line MNNG/HOS the maximum uptake of ^{99m}Tc-PEI-MP obtained was in the order of 1.00, a higher value than the 0.19 of maximum uptake for ^{99m}Tc-Pertechnetate, being found statistically significance differences ($p < 0.001$). Similarly as for the HT-1376 cell line, the time spend to reach half of the maximum uptake was higher for ^{99m}Tc-PEI-MP

(10.12 minutes) than for ^{99m}Tc-Pertechnetate (0.89 minutes), however it wasn't found statistically significant differences.

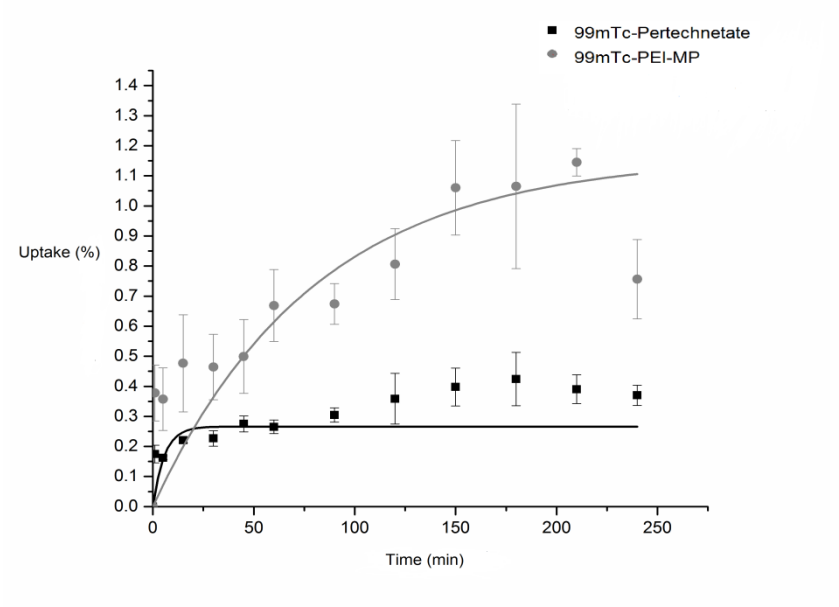

Figure 29. Uptake of ^{99m}Tc-PEI-MP and ^{99m}Tc-Pertechnetate by HT-1376 cells over time. The cells were incubated with 0.925MBq/ml (25 µCi/ml), and after the percentage of uptake of the radiotracer formulation by influx studies was determined. The results express the mean of 4 independent experiments ± standard deviation.

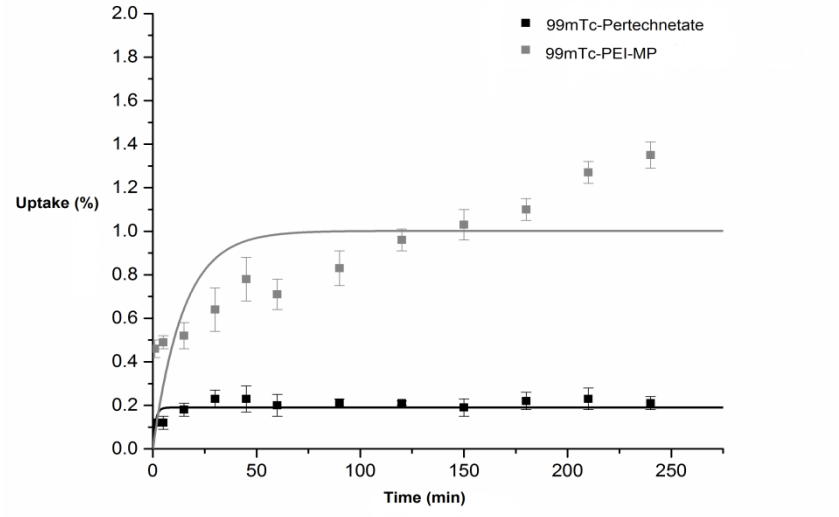

Figure 30. Uptake of ^{99m}Tc-PEI-MP and ^{99m}Tc-Pertechnetate by MNNG/HOS cells over time. The cells were incubated with 0.925MBq/ml (25 µCi/ml), and after the percentage of uptake of the radiotracer formulation by influx studies was determined. The results express the mean of 4 independent experiments ± standard deviation.

From the results demonstrated in fig. 31, fig. 32 and table 22, the minimum retention for ^{99m}Tc-PEI-MP in both cell lines was higher than for ^{99m}Tc-Pertechnetate. In cell line HT-1376 the minimum retention of ^{99m}Tc-PEI-MP obtained was in the order of 3.89 instead of the lower value 1.03 for ^{99m}Tc-Pertechnetate, being the differences statistically significant ($p < 0.001$). In cell line MNNG/HOS the minimum retention of ^{99m}Tc-PEI-MP obtained was in the order of 3.78, a higher value than the 0.54 for ^{99m}Tc-Pertechnetate, being found statistically significance differences ($p < 0.001$). There were no statistically significant differences between the Tm (min) of ^{99m}Tc-Pertechnetate and ^{99m}Tc-PEI-MP in both cell lines.

Table 21.Mean values of A (%) and T50% (min) for the uptake of ^{99m}Tc-Pertechnetate and ^{99m}Tc-PEI-MP in the cell lines HT-1376 and MNNG/HOS. The results analysed were obtained from 4 independent experiments.

Cell Line	Radiopharmaceutical	A (%)	T50% (min)
HT-1376	^{99m}Tc-Pertechnetate	0.27±0.02	3.88±0.90
	^{99m}Tc-PEI-MP	1.16±0.16	55.46±21.60
MNNG/HOS	^{99m}Tc-Pertechnetate	0.19±0.01	0.89±3.02
	^{99m}Tc-PEI-MP	1.00±0.11	10.12±7.7

Legend: Mean values of A ± standard deviation and T50% ± standard deviation, for the uptake of ^{99m}Tc-Pertechnetate and ^{99m}Tc-PEI-MP in the cell lines HT-1376 and MNNG/HOS. The A is the maximum uptake and T50% is the time needed to reach half of the maximum uptake.

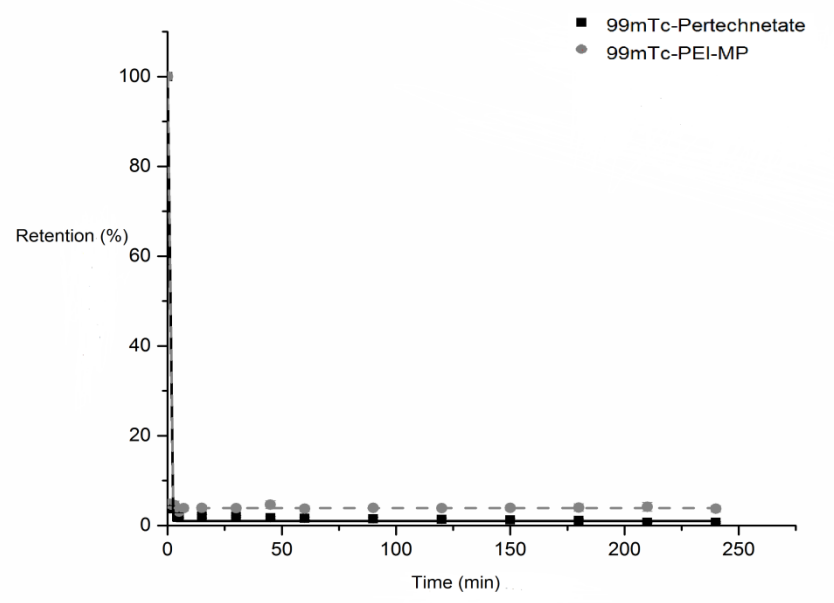

Figure 31. Retention of ^{99m}Tc-PEI-MP and ^{99m}Tc-Pertechnetate by HT-1376 cells over time. The cells were incubated with 0.925MBq/ml (25 µCi/ml) during 150 minutes and then culture medium was substituted, and the percentage of retention of the radiotracer formulation by efflux studies was determined. The results express the mean of 4 independent experiments ± standard deviation.

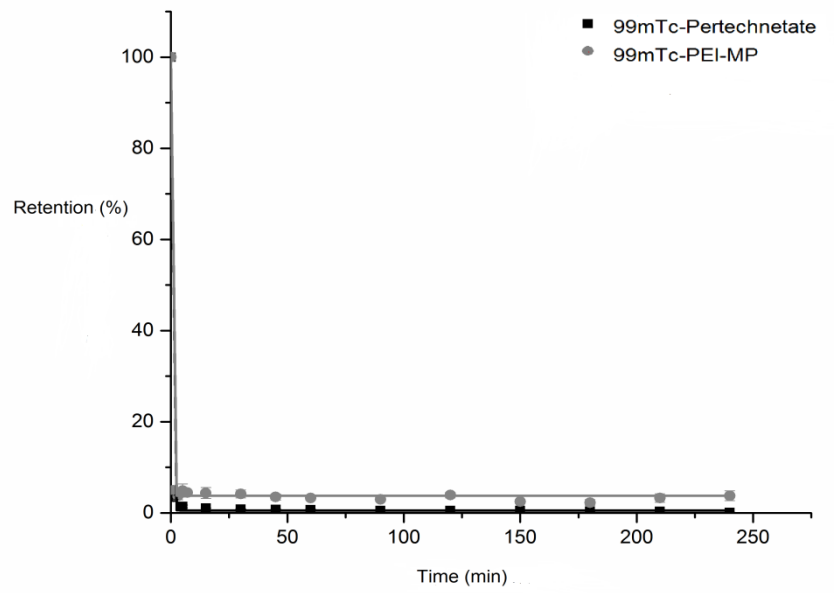

Figure 32. Retention of ^{99m}Tc-PEI-MP and ^{99m}Tc-Pertechnetate by MNNG/HOS cells over time. The cells were incubated with 0.925MBq/ml (25 µCi/ml) during 150 minutes and then culture medium was substituted, and the percentage of retention of the radiotracer formulation by efflux studies was determined. The results express the mean of 4 independent experiments ± standard deviation.

Table 22. Mean values of A (%) and Tm (min) for the retention of ^{99m}Tc-Pertechnetate and ^{99m}Tc-PEI-MP, in the cell lines HT-1376 and MNNG/HOS. The results analysed were obtained from 4 independent experiments.

Cell Line	Radiopharmaceutical	A (%)	T_m (min)
HT-1376	^{99m}Tc-Pertechnetate	1.03±0.16	0.19±0.04
	^{99m}Tc-PEI-MP	3.89±0.06	0.15±0.02
MNNG/HOS	^{99m}Tc-Pertechnetate	0.54±0.13	0.20±0.09
	^{99m}Tc-PEI-MP	3.78±0.24	0.16±0.04

Legend: Mean values of A ± standard deviation and Tm ± standard deviation, for the retention of ^{99m}Tc-Pertechnetate and ^{99m}Tc-PEI-MP in both the cell lines HT-1376 and MNNG/HOS. The A is the minimum retention and Tm is the time delay to reach 50% of the retention plus A/2, or the midpoint between 100% and the minimal retention.

From the results showed in fig. 33, fig. 34 and table 23, the maximum uptake for ^{188}Re-PEI-MP in both cell lines was higher than for ^{188}Re-Perrhenate. In cell line HT-1376 the maximum uptake of ^{188}Re-PEI-MP obtained was in the order of 9.88 instead of the lower value 0.16 of maximum uptake for ^{188}Re-Perrhenate, being the differences statistically significant ($p = 0.001$). Also it was verified that the maximum uptake was higher for ^{188}Re-PEI-MP, the time spend to reach half of the maximum uptake was lower for ^{188}Re-PEI-MP (0.06 minutes) than for ^{188}Re-Perrhenate (26.07 minutes), however it wasn't found statistically significant differences. In cell line MNNG/HOS the maximum uptake of ^{188}Re-PEI-MP obtained was in the order of 13.09, a higher value than the 0.20 of maximum uptake for ^{188}Re-Perrhenate, being found statistically significance differences ($p < 0.001$). The time spend to reach half of the maximum uptake was higher for ^{188}Re-PEI-MP (0.09 minutes) than for ^{188}Re-Perrhenate (0.06 minutes), however it wasn't found statistically significant differences.

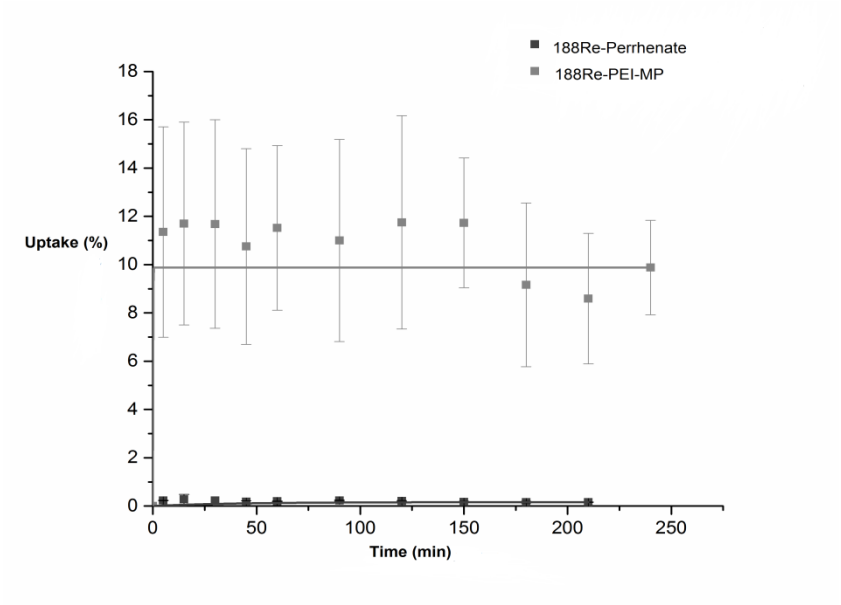

Figure 33. Uptake of ^{188}Re-PEI-MP and ^{188}Re-Perrhenate by HT-1376 cells over time. The cells were incubated with 0.925MBq/ml (25 µCi/ml), and after the percentage of uptake of the radiotracer formulation by influx studies was determined. The results express the mean of 4 independent experiments ± standard deviation.

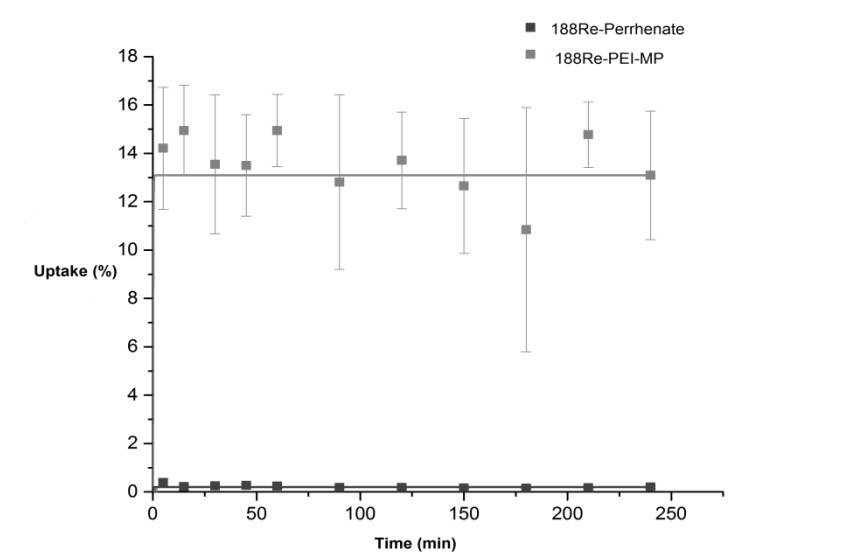

Figure 34. Uptake of ^{188}Re-PEI-MP and ^{188}Re-Perrhenate by MNNG/HOS cells over time. The cells were incubated with 0.925MBq/ml (25 µCi/ml), and after the percentage of uptake of the radiotracer formulation by influx studies was determined. The results express the mean of 4 independent experiments ± standard deviation.

Table 23. Mean values of A (%) and T50% (min), for the uptake of ^{188}Re-Perrhenate and ^{188}Re-PEI-MP in both the cell lines HT-1376 and MNNG/HOS. The results analysed were obtained from 4 independent experiments.

Cell Line	Radiopharmaceutical	A (%)	T50% (min)
HT-1376	^{188}Re-Perrhenate	0.16±0.00	26.07±0.00
	^{188}Re-PEI-MP	9.88±0.44	0.06±0.00
MNNG/HOS	^{188}Re-Perrhenate	0.20±0.01	0.06±0.01
	^{188}Re-PEI-MP	13.09±0.48	0.09±0.00

Legend: Mean values of A ± standard deviation and T50% ± standard deviation, for the uptake of ^{188}Re-Perrhenate and ^{188}Re-PEI-MP in the cell lines HT-1376 and MNNG/HOS. The A is the maximum uptake and T50% is the time needed to reach half of the maximum uptake.

From the results demonstrated in fig. 35, fig.36 and table 24, the minimum retention for ^{188}Re-PEI-MP in both cell lines was higher than for ^{188}Re-Perrhenate. In cell line HT-1376 the minimum retention of ^{188}Re-PEI-MP obtained was in the order of 45.67 instead of the lower value 0.24 for ^{188}Re-Perehenate, being the differences statistically significant ($p < 0.001$). In cell line MNNG/HOS the minimum retention of ^{188}Re-PEI-MP obtained was in the order of 68.94, a higher value than the 0.21 for ^{188}Re-Perrhenate, being found statistically significance differences ($p < 0.001$). There are no statistically significant differences between the Tm (min) of ^{188}Re-Perrhenate and ^{188}Re-PEI-MP in both cell lines.

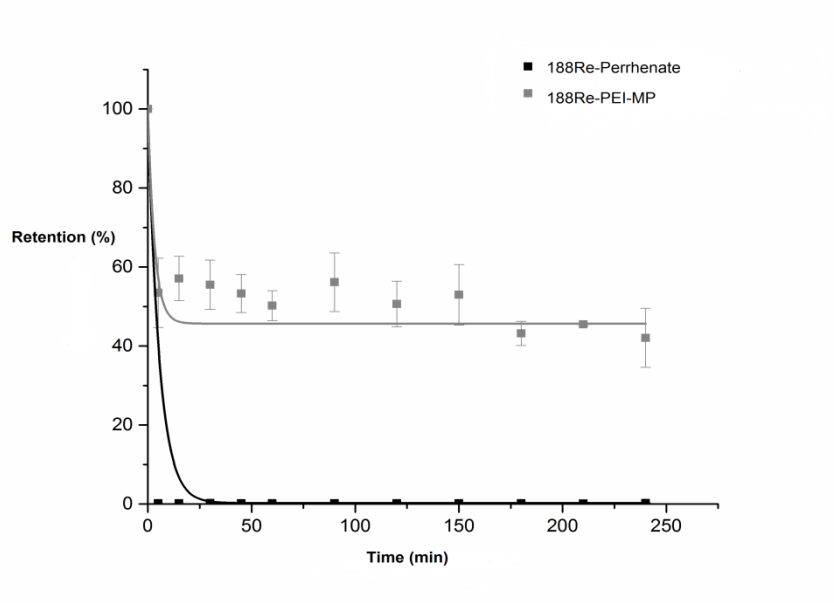

Figure 35. Retention of ^{188}Re-PEI-MP and ^{188}Re-Perrhenate by HT-1376 cells over time. The cells were incubated with 0.925MBq/ml (25 µCi/ml) during 150 minutes and then culture medium was substituted, and the percentage of retention of the radiotracer formulation by efflux studies was determined. The results express the mean of 4 independent experiments ± standard deviation.

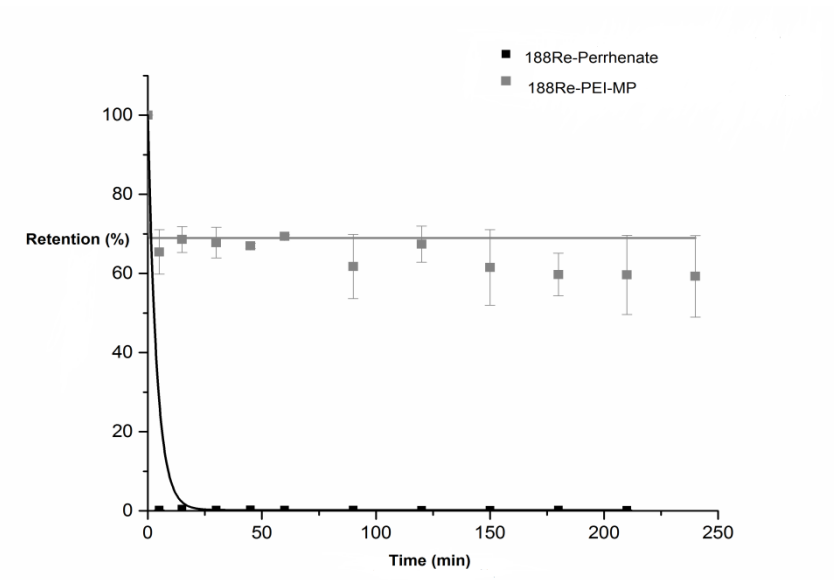

Figure 36. Retention of ^{188}Re-PEI-MP and ^{188}Re-Perrhenate by MNNG/HOS cells over time. The cells were incubated with 0.925MBq/ml (25 µCi/ml) during 150 minutes and then culture medium was substituted, and the percentage of retention of the radiotracer formulation by efflux studies was determined. The results express the mean of 4 independent experiments ± standard deviation.

Table 24. Mean values of A (%) and Tm (min), for the retention of ^{188}Re-Perrhenate and ^{188}Re-PEI-MP in both the cell lines HT-1376 and MNNG/HOS. The results analysed were obtained from 4 independent experiments.

Cell Line	Radiopharmaceutical	A (%)	T_m (min)
HT-1376	^{188}Re-Perrhenate	0.24±0.00	3.82±0.00
	^{188}Re-PEI-MP	45.67±0.47	2.21±1.39
MNNG/HOS	^{188}Re-Perrhenate	0.21±0.00	2.67±0.00
	^{188}Re-PEI-MP	68.94±0.44	0.08±0.00

Legend: Mean values of A ± standard deviation and Tm ± standard deviation, for the retention of ^{188}Re-Perrhenate and ^{188}Re-PEI-MP in both the cell lines HT-1376 and MNNG/HOS. The A is the minimum retention and Tm is the time delay to reach 50% of the retention plus A/2, or the midpoint between 100% and the minimal retention.

5.4. Section discussion

With the intention of analysing *in vitro* the potential of PEI-MP radiolabelled with ^{99m}Tc for diagnosis and with ^{188}Re for therapy of bladder cancer, in this chapter it was evaluated the chemical properties of PEI-MP, the radiotoxicity of ^{99m}Tc and the cellular uptake and retention of ^{99m}Tc-PEI-MP and ^{188}Re-PEI-MP, using for this cell lines of human bladder transitional cell carcinoma and osteosarcoma (considering the first propose of using PEI-MP) [111, 317].

Following the success in the synthesis of the polymer PEI-MP and the preparation of the labelling kits, it was proceeded with the radiolabelling with ^{99m}Tc-Pertechnetate and ^{188}Re-Perrhenate. Thus, once the aim was to use ^{99m}Tc-PEI-MP for imaging and ^{188}Re-PEI-MP for therapy, it was necessary to determine the radiochemical purity by ascendant microchromatography. The results demonstrated that the radiochemical purity for ^{99m}Tc-PEI-MP and ^{188}Re-PEI-MP, during 5 hours after radiolabelling, was always high and superior to 89% and 85%, respectively for ^{99m}Tc-PEI-MP and ^{188}Re-PEI-MP, just in the first hour. These results reveal the stability of the kit formulation, and thus ensure its use for a long period of time. After several experiments with different chromatographic systems, it was perceived that the two systems chosen were appropriated. ^{99m}Tc/^{188}Re-PEI-MP are polar and water-soluble molecules, therefore by using a stationary phase that is strongly polar, like ITLC-SG, ^{99m}Tc/^{188}Re-PEI-MP will have a strong interaction with the stationary phase, and will not move with the solvent, in this case the acetone. On the other hand,

^{99m}Tc-Pertechnetate and ^{188}Re-Perrhenate that are non-polar molecules will have no affinity for the stationary phase and will be dragged by the polar solvent. The ^{99m}Tc/^{188}Re-Reduced-Hydrolyzed being non-soluble molecules will remain in the origin, presenting an R_f equal to zero. This way it is possible to calculate the percentage of ^{99m}Tc-Pertechnetate and ^{188}Re-Perrhenate that present an R_f equal to one. Upon use the stationary phase W3MM and the citrate as mobile phase the aim was to separate the ^{99m}Tc/^{188}Re-Reduced-Hydrolyzed from ^{99m}Tc/^{188}Re-PEI-MP, ^{99m}Tc-Pertechnetate/^{188}Re-Perrhenate. To this W3MM demonstrated to be an adequate stationary phase. Because W3MM is non-polar, using a polar solvent like citrate, ^{99m}Tc/^{188}Re-PEI-MP will be drag by the solvent, as well as ^{99m}Tc-Pertechnetate or ^{188}Re-Perrhenate, and ^{99m}Tc/^{188}Re-Reduced-Hydrolyzed being non-soluble molecules will remain in the origin [87, 271]. Therefore, knowing the percentage of ^{99m}Tc-Pertechnetate or ^{188}Re-Perrhenate and the percentage of ^{99m}Tc/^{188}Re-Reduced-Hydrolyzed it was possible to calculate the percentage of ^{99m}Tc-PEI-MP or ^{188}Re-PEI-MP.

Also it was investigated the effect of temperature and presence of cell culture medium (DMEM) in radiochemical purity of ^{99m}Tc-PEI-MP over time, once to perform the *in vitro* studies, the complex is exposed to cellular culture medium and environmental temperatures that may vary from 22 to 45 ºC. The results demonstrated that the radiochemical purity was not affected significantly, being equal or superior to 85% in the first hour for all conditions, at least during 5 hours after radiolabelling, when in contact with culture medium and exposed to different temperatures. Therefore the *in vitro* studies could be performed with ^{99m}Tc-PEI-MP, ensuring that the results were not altered by the loss of radiochemical purity. Considering the similarities of ^{188}Re-PEI-MP with ^{99m}Tc-PEI-MP, the results discussed before were also expected for ^{188}Re-PEI-MP.

The hydrophilicity or lipophilicity of a labelled compound is crucial for the biodistribution *in vivo*, therefore the determination of the partition coefficient (log $P_{o/w}$) of ^{99m}Tc-PEI-MP was crucial. The results demonstrated that ^{99m}Tc-PEI-MP is a hydrophilic complex, with an increased hydrophilicity over time (at least 4 hours after radiolabelling), but with no statistical significant differences. Also, it wasn't possible to calculate the hydrophilicity of the ^{188}Re-PEI-MP, however due to the similarity of the complexes, it is expected similar values of hydrophilicity.

This water solubility could be an advantage in terms of unnecessary liver and fat tissue uptake, and also a faster kidney-uptake, if administered *in vivo* [273]. These results may represent a theoretical advantage either for imaging and therapy however, *in vivo* studies must be performed for a final conclusion on this topic.

To understand if PEI-MP would act as a carrier without any secondary effects to cells, it was verified the effects on cell metabolic activity after the incubation with several concentrations of PEI-MP, in different periods of time. To this it was used the human cell lines of bladder carcinoma and osteosarcoma. The results obtained by MTT assay demonstrated that, for any of the cell lines used for the experiment, and any of the concentrations in each period of time, PEI-MP didn't had significantly inhibitory influence on metabolic activity, remaining equal or superior to 100%. To confirm and reinforce these last results, it was study other possible responses of cells when incubated with 1000 µM of PEI-MP during 24 hours. To this it was resorted to flow cytometry, and it was studied the types of cell death and viability, the production of free radicals, the expression of reduced GSH, and changes in the mitochondrial membrane potential. The results demonstrated that cell viability didn't decrease significantly, remaining superior to 82% in both cell lines, despite the increase of apoptosis and a slight decrease of the mitochondrial membrane potential, especially in the HT-1376 cells. The intrinsic pathway of apoptosis involves the mitochondria, and mediates the release of cytochrome c that is associated with the opening of the mitochondrial permeability transition pore and loss of the mitochondrial membrane potential. Therefore it is expected that with the increase of apoptosis the mitochondrial membrane potential may also be decreased [299], as it was expressed in the previous results. However there are reasons to believe that this increase in apoptosis is not relevant, and does not preclude its use, considering the results obtained in the MTT tests and the other results of flow cytometry, where cell viability didn't decrease and that weren't found significant changes in the production of free radicals and in the expression of GSH. Therefore, the idea that PEI-MP can act as a carrier without significant side effects and that can be labelled with ^{99m}Tc for functional imaging or labelled with

^{188}Re for therapy still remains, considering the consistent results obtained by the MTT assay and flow cytometry.

Because it was intended to use ^{99m}Tc-PEI-MP for diagnosis, it's important that the doses of radiation used don't represent a risk. As described before ^{99m}Tc not also emits gamma rays of low energy (140 keV), but also highly energetic auger electrons, that could represent a risk [59]. Therefore it was proceeded with the analysis of the radiotoxicity of ^{99m}Tc with several doses in the range of diagnostics, for both bladder cancer and osteosarcoma cells. The effective doses for most nuclear medicine diagnostic procedures varies between 0.3 and 20 mSv (equivalent to 0.3 and 20 mGy) [303], therefore it was performed clonogenic tests to evaluate cell survival based on the ability of a single cell to grow and form a colony after external and internal irradiation of cells with several doses, namely 2, 5, 10 and 20 mGy. After external irradiation it's possible to evaluate the effects of gamma rays and not of auger electrons. Only with internal irradiation it's possible to evaluate the effects of gamma rays plus auger electrons, considering the low range of these electrons, therefore it needs to be in close contact with cells to produce effects [302]. The results demonstrated, as expected, that for doses of ^{99m}Tc in the range of diagnosis, and independently of the irradiation being external or internal, there are no significant influence in cell survival for both bladder carcinoma and osteosarcoma cells. The cell survival didn't decrease, at least in terms of capacity to grow and form a colony, demonstrating that for diagnostic effective doses, the gamma rays and auger electrons, has no apparent effect on cell survival. To support the results obtained with clonogenic assay, it was study other possible responses of cells when irradiated with 20 mGy of ^{99m}Tc. For this purpose, flow cytometry was used to study the types of cell death and viability, the production of free radicals and the expression of reduced GSH, the changes in the mitochondrial membrane potential and the cell cycle. The results demonstrated that cell viability didn't decrease significantly, remaining superior to 82% for external irradiation and above 84% for internal irradiation in both cell lines, with no significant differences for apoptosis or necrosis. The absence of significant alterations in the production of peroxides and superoxide, expression of GSH, changes in the mitochondrial membrane and changes in the

distribution throughout the cell cycle, after external an internal irradiation support the results of flow cytometry for cell death and viability and the results obtained in clonogenic studies, demonstrating that doses of ^{99m}Tc in diagnostic range is considered harmless and ^{99m}Tc-PEI-MP may be used for nuclear medicine imaging. Unfortunately, given the impossibility of getting a new generator of ^{188}W/^{188}Re, it was not possible to evaluate the radiotoxicity ^{188}Re. However taking into consideration that this radionuclide emits high-energy β^- particles, we can predict a decrease of cell survival and all the consequences of the effects of ionizing radiation on human tissues [290, 291, 293, 295, 297, 306, 309, 310]. And because ^{188}Re is harmful for cancer cells, it is also for healthy cells, therefore there is a great need of specificity that may be given by PEI-MP for bladder cancer.

To be used for imaging, ^{99m}Tc-PEI-MP should have a significant cellular uptake and retention over time. Thus it was evaluated the cell uptake and retention of ^{99m}Tc-PEI-MP in both bladder carcinoma and osteosarcoma cells. From the results, it was possible to verify that in both cell lines the maximum percentage of uptake of ^{99m}Tc-PEI-MP (1.16% in HT-1376 cells; 1.00% in MNNG/HOS cells), was significantly higher than the maximum uptake of ^{99m}Tc-Pertechnetate (0.27% in HT-1376 cells; 0.19% in MNNG/HOS cells). Also the percentage of uptake of both ^{99m}Tc-PEI-MP and ^{99m}Tc-Pertechnetate in HT-1376 cells was higher than in MNNG/HOS cells, is not statistically significant. Relatively to the percentage of retention, it was possible to verify that in both cell lines the minimum percentage of retention of ^{99m}Tc-PEI-MP was relatively high (3.89% in HT-1376 cells; 3.78% in MNNG/HOS cells), and superior to ^{99m}Tc-Pertechnetate (1.03% in HT-1376 cells; 0.54% in MNNG/HOS cells). Also it's important to refer that the retention over time seems to be more stable for both cell lines, particularly for HT-1376 cells.

These values of uptake and retention, demonstrate that PEI-MP is possible an excellent carrier for ^{99m}Tc to cancer cells, namely to bladder carcinoma and osteosarcoma cells. Therefore ^{99m}Tc-PEI-MP could be an excellent agent for imaging *in vivo*.

To be used for therapy, ^{188}Re-PEI-MP should also have a significant cellular uptake and retention over time. Thus it was evaluated the cell uptake and

retention of ^{188}Re-PEI-MP in both cell lines, HT-1376 and MNNG/HOS, using the same procedures as for ^{99m}Tc-PEI-MP. From the results, it was possible to verify that in both cell lines the percentage of uptake of ^{188}Re-PEI-MP (9.88% in HT-1376 cells; 13.09% in MNNG/HOS cells), over time, was significantly higher than the uptake of ^{188}Re-Perrhenate (0.16% in HT-1376 cells; 0.20% in MNNG/HOS cells). Relatively to the percentage of retention, it was possible to verify that in both cell lines the minimum percentage of retention of ^{188}Re-PEI-MP was relatively high (45.67% in HT-1376 cells; 68.94% in MNNG/HOS cells), and superior to ^{188}Re-Perrhenate (0.24% in HT-1376 cells; 0.21% in MNNG/HOS cells). Also it's important to refer that the retention over time seems to be more stable for both cell lines, particularly for HT-1376 cells. Therefore, these results could be an indication that ^{188}Re-PEI-MP could be used for therapy *in vivo* of both bladder and bone cancer. The results of uptake and retention obtained for ^{188}Re-PEI-MP in proportion are a bit different to those obtained with ^{99m}Tc-PEI-MP, demonstrating that changing the radionuclide used for radiolabelling PEI-MP, the uptake and retention besides being always high is also superior when radiolabelled with ^{188}Re. Given that ^{188}Re has an atomic mass number superior to ^{99m}Tc [61], the complex ^{188}Re-PEI-MP is possibly a larger molecule than ^{99m}Tc-PEI-MP and, as it is known, the cellular tumour uptake of large molecules is dominated by the EPR effect, and possibly for this reason the uptake and retention of ^{188}Re-PEI-MP is higher. However, comparing the results of uptake and retention of ^{99m}Tc-PEI-MP or ^{188}Re-PEI-MP with the ones of control (^{99m}Tc-Pertechnetate or ^{188}Re-Perrhenate), the uptake and retention of the radiolabelled PEI-MP were always significantly higher, independently of the radionuclide used for labelling, being an indication of the possible specificity of PEI-MP to bladder carcinoma and osteosarcoma cells.

Since *in vitro* studies are conducted in a controlled environment, the results may not correspond to those obtained in a living organism. Therefore it was important to conduct *in vivo* studies.

Section III. Experimental Studies

Chapter 6.*In vivo* and *Ex vivo*

6.1. Introduction

Considering the *in vitro* results, and knowing that these studies are not enough to answer to all questions, including if the dynamic behaviour of the ^{99m}Tc-PEI-MP or the ^{188}Re-PEI-MP in tumour mass in terms of uptake and retention is maintained, what are the target organs, what are the routes of excretion, or if will they be good agents for imaging or therapy *in vivo*? Trying to answer these questions, *in vivo* and *ex vivo* studies were performed.

Thus, the aim of this chapter was to explore through *in vivo* and *ex vivo* evaluations, the potential of PEI-MP radiolabelled with ^{99m}Tc or ^{188}Re for the early diagnosis and/or therapy of bladder cancer, based on the results obtained *in vitro*. These *in vivo* and *ex vivo* studies include the biodistribution and biokinetics of ^{99m}Tc-PEI-MP and ^{188}Re-PEI-MP, in controls and in animal models of bladder cancer and osteosarcoma, using imaging to control the administration of the complexes, and to see the biodistribution, which was complemented with the uptake quantification for each organ after animal sacrifice.

Taking into consideration the results of the partition coefficients it was expected that the complexes would be mainly excreted by renal system what was confirmed by the image visualization and by *ex vivo* studies. These showed a high count rate in kidneys, bladder and urine after the intravenous administration of the ^{99m}Tc-PEI-MP or ^{188}Re-PEI-MP.

For this work it was necessary the development of animal models of bladder cancer and osteosarcoma, which could be used not only for nuclear medicine imaging but also for *ex vivo*, evaluations, to achieve the biodistribution studies after administration of ^{99m}Tc-PEI-MP and ^{188}Re-PEI-MP complexes. All procedures described in this chapter were performed after approval by the Ethics Committee for Health of the Faculty of Medicine of the University of Coimbra.

6.2. Material and methods

6.2.1. *Animal tumour models*

Experimental models of cancer have played an important role in cancer drug discovery for more than 60 years. *In vivo* cancer models can be considered to fall within two broad classes, transplantable models, and *in situ* models, each with some subtypes. Additionally, with recent advances in preclinical imaging technologies, these models proved to be useful in the development and testing of new imaging techniques and contrast agents. There are several types of tumour models such as the transplantable syngeneic models, spontaneous and autochthonous models, orthotopic models, human tumour xenografts, models of metastasis and transgenic tumour models [318].

Transplantable syngeneic leukaemia and solid tumour models were developed from spontaneous or induced tumours, subsequently adapted to a serial *in vivo* passage in the same animal strain. Disadvantages of these models are related with the different genetic background of murine cancer, not always identical to human counterparts, decreasing the expectation of a clinical correlation [319]. Spontaneous and autochthonous models may be relevant to understand the development of human disease because the tumours reside in the tissue appropriate for the histotype. However, these kind of studies are difficult because of low tumour incidence, characteristic variations, and delayed onset of tumour growth, as well as the deep location of the tumour tissues [318]. An orthotopic model involves the implantation of a tumour into the organ from which it arose [320-322]. Orthotopic models have additional advantages over subcutaneous besides the cellular microenvironment context. These advantages may include retention of differentiated structures within the tumour, vascular growth differences, more realistic tissue pharmacokinetics at the tumour site, and metastatic spread. However, tumour implantation for orthotopic models requires potentially complex surgery procedures. Observation of tumour growth in internal organs typically requires serial sacrifice of cohorts of animals, the acceptance and the growth tumour rates can be highly variable, and may be difficult and costly the pharmacodynamic and pathological analyses of the tumours. These factors increase costs and decrease the yield [318].

The application of xenotransplantation (transplantation of tissues or organs from one species into different species) techniques to the growth of human tumours in experimental animals was a major breakthrough in cancer biology and drug discovery research [318]. One of the first of these models was to take advantage of the immunologically privileged status of the subrenal capsule (SRC) [323, 324], where human tumour fragments were implanted under this capsule. Unfortunately, the SRC xenograft assay is labour intensive and both tumour growth and response to therapy are often highly variable [318]. A major breakthrough in the *in vivo* evaluation of novel agents against human tumours was the development and the characterization of immunodeficient mice and rats. These animals have genetic immune deficiencies that minimize or prevent the rejection of the grafted tissues from other species. The difficulty in using immune compromised animals is that they are highly susceptible to viral, bacterial, and fungal infections. These infections can change the outcome and the reproducibility of experiments. Therefore, immunodeficient animals are maintained in specific pathogen-free environments, dramatically increasing research costs [318]. Nude, scid, xid and beige mice are the four primary types of immunodeficient mice. Each type of immunodeficient mouse has one or more mutations that diminish the animal´s capacity to reject transplantable allografts and xenografts. None of the mutations completely eliminates the immune system function [325-327]. Nude and scid mice are predominantly used for cancer drug evaluation. Xenografted tumours often exhibit a more neoplastic phenotype in scid mice than in nudes, presumably because of the more severe immunodeficiency of scid mice. The availability of these animals, has introduced new paradigms on the drug discovery. There are different approaches for xenograft studies in immunocompromised mice such as the subcutaneous xenografts and the hollow fibber assay. Subcutaneous xenografts are human tumour xenografts (cells, brei, or fragments) that are injected underneath the skin of immunodeficient animals and not into the underlying tissue or cavities. These models are cost effective, and provide a direct assessment of tumour size through simple, non-invasive calliper measurement of tumour axes. The accessibility of the tumour is also an advantage for harvesting of tumour tissue [328-330]. Although the use of human tumour xenografts has many advantages, there are also a number of disadvantages. Human cells are placed in a murine

environment generating interactions that may not faithfully reflect the human disease process (e.g., differences in the local cellular environment, cytokines, chemokines, growth factors or immunologic state, among others) [318]. The hollow fibber assay [331] uses polyvinylidene fluoride hollow fibbers inoculated with human tumour cell lines [332]. The fibbers are then sealed and implanted into the intraperitoneal cavity or subcutaneously of immunodeficient mice for 3-10 days. After a treatment, the fibbers are removed and live cells are counted. Advantages of this method are that multiple cell lines can be tested simultaneously in one animal, contributing to low cost and high throughput. Disadvantages are that the technique requires surgery, the tumour cells are unable to interact with the normal animal stroma, and the cells have no opportunity to develop a blood supply. Hence, this assay does not reflect treatment-induced changes in stroma-tumour interactions nor vascular effects [318]. The general stability of the tumour tissue in the models discussed above are an advantage, however often they lack some key features of human cancer, such as dissemination to secondary organ. Several models of metastatic dissemination employ direct or systemic injection techniques. The choice of the site or route of administration is generally based on vascular proximity to the injection place. Spontaneous models of metastatic dissemination, including subcutaneous, transgenic, orthotopic, and autochthonous models provide a better representation of the entire process than direct injection models, and are especially suited for testing therapeutics for prevention of metastasis [318]. The massive shift of drug discovery efforts toward inhibition of specific oncogene or suppressor gene related targets has led to increased interest in the use of transgenic models for target validation and the evaluation of drug candidates [333-335]. Transgenic tumour models are created by the introduction of heritable (germ line) or somatic mutations that are implicated in neoplastic transformation. Target genes can be replaced by new alleles, conditionally expressed, conditionally turned off, or mutated. A key advantage of transgenic models is that the aetiology of the tumour development closely mimics that in humans. The animals can be treated with therapeutic agents at any stage of tumour development to further elucidate therapeutic efficacy and the mechanism of action [335]. Transgenic models driven by germ line mutations can be problematic. Mutations of interest are often embryonically lethal.

Additionally, adverse physiological or toxic effects during the development may occur that render the model unusable. Organ specificity can also be difficult to control and the study of multiple gene defects can require complex breeding efforts. Lastly, these animal models are often characterized by long tumour latency periods [318].

For the development of *in vivo* and *ex vivo* studies, and considering the animal models discussed before and the resources available, it was chosen as animal tumour model the balb/c nu/nu mice, 6 to 8 weeks old with a body weight ranging 20 to 31 g, for the development of subcutaneous xenografts of bladder carcinoma and osteosarcoma. *In vivo* studies allowed obtain information on the routes of metabolism and excretion, as well as the target organs of the ^{99m}Tc-PEI-MP and ^{188}Re-PEI-MP. This strain was chosen because of the advantages referred before and because these animals have gallbladder, allowing to obtain important information about biodistribution of ^{99m}Tc-PEI-MP and ^{188}Re-PEI-MP.

To obtain the xenografts of the tumours under study it was injected subcutaneously in the right axilla dug of blab/c nu/nu mice a suspension of 5 million HT-1376 or MNNG/HOS cells, respectively for bladder carcinoma and osteosarcoma, in 0.1 ml of saline. This injection zone was chosen because it has several advantages with respect to the development of xenograft, emphasizing the fact that is contra lateral to the heart, is away from the liver, bladder and kidneys, avoiding the overlapping of structures in images. On the other hand, is a good area for expansion, and has good vascularisation, which allows the quick development of xenograft.

The volume of tumours was controlled every week by simple calliper measurement. The determination of the tumour's volume was calculated following the equation 7.

$$V = \frac{L_T \times S^2}{2}$$

Equation 7. Tumour volume determination. LT corresponds to the largest tumour diameter and S the smallest diameter (Dagrosa M.A. *et al.*, 2003)

Studies with xenograft of bladder carcinoma and xenograft of osteosarcoma started when the tumour volumes reached 500-1000 mm^3.

6.2.2. ***Nuclear medicine imaging***

Molecular imaging is a growing research tool in preclinical area that allows testing novel drugs, reagents, and methods, giving fundamental information through image that mapping a specific step of a molecular pathways *in vivo*, some of them key-targets in disease processes [39, 55]. The current assessment of disease is based on anatomic or physiologic changes that are a late manifestation of molecular alterations which truly underlie disease. Functional information of these molecular changes will affect the patient care because they allow earlier detection of disease. In addition, with these functional images is possible to observe the effects of therapy shortly after its beginning, allowing to quickly determining the effectiveness of treatment. Oppositely, in the morphological imaging methods, many months are often required to determine whether pharmacologic or biological intervention has been beneficial [39, 55]. Widely used, molecular imaging agents are radiopharmaceuticals, paramagnetic materials, fluorescent/luminescent materials, and microbubbles, among others [55].

Nuclear medicine imaging involves the image formation through the detection of gamma rays with energies preferably ranging 100-200 keV, or annihilation photons with energy of 511 keV, emitted during the decay of a radioisotope, which may be attached or not to a molecule. The gamma-camera, also known as Anger camera, emerged as the standard device for single photon nuclear imaging. The key element for image formation is a scintillation crystal with a high atomic number. In this crystal, radiation interactions occur, and gamma photons are converted into a multiple visible light photons. Sodium iodide doped with thallium (Na(Tl)) crystals meets the requirement for single photon nuclear imaging. A mechanical collimator is placed in front of the crystal, and is useful to define the direction of the gamma photons emitted by the radioactive source. The collimator will enable the selection of gamma-rays nearly perpendicularly to the crystal surface, while obliquely incident gamma-rays are absorbed in the

collimator septa. Each light photon generated in the scintillation crystal will undergo to low-noise amplification in a photomultiplier dynode system and further amplification and shaping in the preamplifier. The electrical output signals from these photomultipliers are used for localization (position (x,y) absorbed within the crystal) and for pulse height analysis following summation. The integrator smoothes the signal, while the pulse height analyser, performs a rough pre-selection of signal amplitude. The signal then undergoes analogue-to-digital conversion and is passed on to a multichannel analyser, in which individual signals are binned according to their pulse amplitudes. Given that this pulse height is proportional to the energy of the absorbed gamma-ray photon, the accumulated spectrum of pulse heights will represent the energy spectrum of the gamma-radiation incident on the detector [336].

Therefore, for the *in vivo* evaluation of the biodistribution and biokinetics of ^{99m}Tc-PEI-MP and ^{188}Re-PEI-MP, nuclear medicine imaging after the administration of ^{99m}Tc-PEI-MP or ^{188}Re-PEI-MP in mice, were performed. To obtain these images a gamma-camera (GE 400 AC) coupled with a low energy, parallel hole and high resolution collimator, as represented in fig. 37, was used.

Figure 37. Gamma-camera (GE 400 AC) coupled with a low energy, parallel hole and high resolution collimator.

Before starting with the image acquisition, mice were anesthetized with a solution of ketamine 77% (Ketalar®, Parke-Davis) and chlorpromazine 23% (Largactil®, Vitoria Laboratories) injected subcutaneously in the back of the mice, with an adequate dosage considering weight.

Taking into account that, one of the adverse effects of anaesthesia is the decrease on body temperature, it is necessary to maintain the body temperature of the mice during all the image acquisition. For this purpose the mice were kept in a box airy, spacious and heated with an electric blanket, as represented in fig. 38. The temperature was adjusted continuously in order to maintain the animal comfort condition.

Figure 38. Balb/c nu/nu mice with xenografts, anesthetized for holding images after administration of the radiopharmaceutical.

During image acquisition a warm light was projected over mice, to maintain body temperature, taking care to cover the eyes once they are photosensitive. For image acquisition, mice were placed in prone on top of the gamma-camera collimator, previously shield with a plastic to avoid direct contamination of the collimator, as can be seen in fig.39.

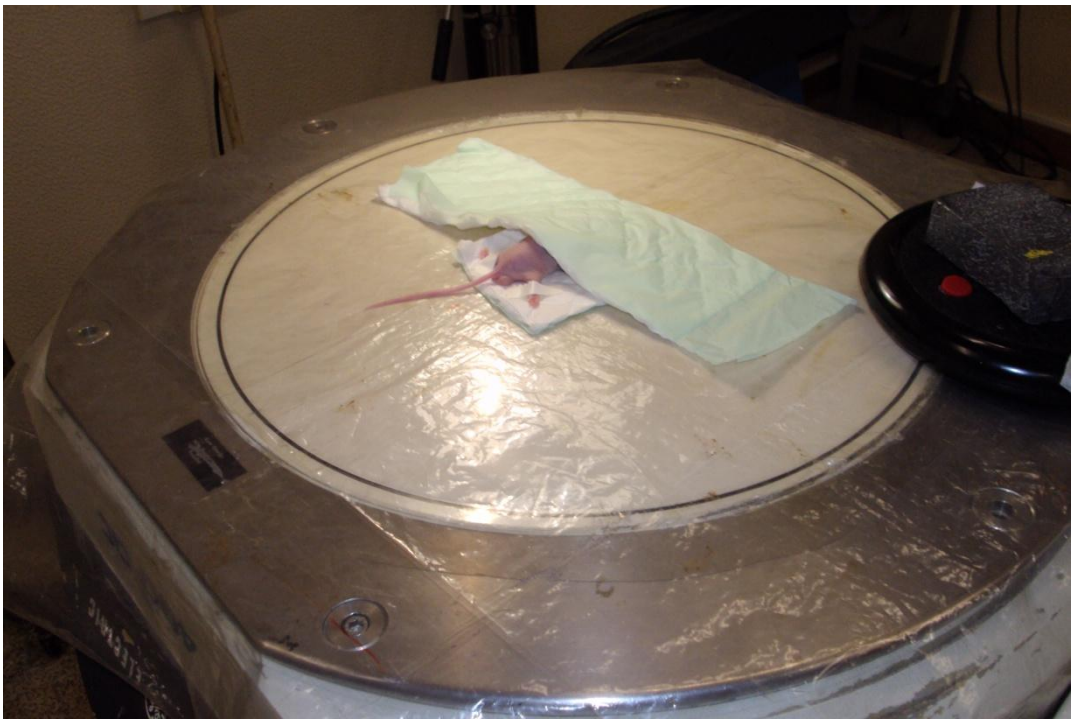

Figure 39. Positioning of balb/c nu/nu mouse in the detector of the gamma-camera (GE 400 AC).

Images started with the intravenous administration in the animal tail vein, of the radiopharmaceuticals ^{99m}Tc-Pertechnetate, ^{99m}Tc-PEI-MP, ^{188}Re-Perrhenate or ^{188}Re-PEI-MP. As control animal model balb/c mice 6 to 8 weeks old with a body weight ranging 20 to 31 g were used. As tumour animal models it was used the ones referred before.

6.2.2.1. Imaging with ^{99m}Tc-Pertechnetate and ^{99m}Tc-PEI-MP

Images were acquired in control mice, and in mice with xenograft of bladder carcinoma and osteosarcoma. For each type of mice it was administered ^{99m}Tc-Pertechnetate or ^{99m}Tc-PEI-MP. For each group, taking in consideration the type of mice and the radiopharmaceutical administered, images were acquired up to 120 minutes and up to 240 minutes. The organization of these groups is summarized in the table 25.

Table 25. Number and organization of mice by type, administered radiopharmaceutical (^{99m}Tc-Pertechnetate or ^{99m}Tc-PEI-MP) and time of the final images.

Mice	Images	Radiopharmaceuticals	
		^{99m}Tc-Pertechnetate	^{99m}Tc-PEI-MP
Normal	Up to 120 min	4 mice	4 mice
	Up to 240 min	4 mice	4 mice
Xenograft of bladder carcinoma	Up to 120 min	4 mice	4 mice
	Up to 240 min	4 mice	4 mice
Xenograft of osteosarcoma	Up to 120 min	4 mice	4 mice
	Up to 240 min	4 mice	4 mice

Legend: Number of mice used for imaging studies, according to the radiopharmaceutical administered (^{99m}Tc-Pertechnetate or ^{99m}Tc-PEI-MP) and the type of animal model, that is, normal mice, mice with xenograft of bladder carcinoma and mice with xenograft of osteosarcoma. Each of these groups were divided in two, where depending if the images were performed until 120 minutes or 240 minutes hours after the intravenous administration of ^{99m}Tc-Pertechnetate or ^{99m}Tc-PEI-MP.

The images obtained with the ^{99m}Tc-Pertechnetate are controls for the biodistribution of the radiopharmaceutical under evaluation, since it can be a radiochemical impurity produced during the normal process of labelling of PEI-MP kit with ^{99m}Tc-Pertechnetate. The normal ^{99m}Tc-Pertechnetate biodistribution show a high uptake in thyroid, stomach, and choroid plexus. In turn, if there was the presence of reduced/hydrolysed technetium species, as radiochemical impurities, is expected to see a high uptake in the liver and spleen. In fact, the biodistribution verified in the images will be a mirror of the radiochemical purity of the complex ^{99m}Tc-PEI-MP, which makes very important the quality control of the radiochemical purity after radiolabelling.

After the administration of 18-37 MBq (0.5-1.0 mCi) of ^{99m}Tc-Pertechnetate or ^{99m}Tc-PEI-MP in a small volume (0.1 ml) into the tail vein of the mice, a dynamic acquisition was carried out through the gamma-camera controlled by the Genie Acq computer to a workstation Xeleris for further visualization and data processing. The dynamic imaging sequence besides the distribution of the radiopharmaceuticals in the bloodstream of mice, gave us also information about the quality of the injection. The dynamic images acquisition was followed by the acquisition of static images until the predefined times in order to achieve information about the biodistribution of the radiopharmaceuticals. For that, the static images were performed every 30 minutes until 120 or 240 minutes, after

the administration of the radiopharmaceuticals. The image parameters used for the acquisition of dynamic and static images are summarised in table 26.

Table 26. Gamma-camera image parameters for dynamic and static acquisition after the administration of ^{99m}Tc-Pertechnetate or ^{99m}Tc-PEI-MP.

Image parameters	Dynamic acquisition	Static acquisition
Number of images	60 images	8 images
Time per image	10 seconds	2 minutes
Total time for imaging	10 min	Images at 30, 60, 90, 120, 150, 180, 210 and 240 minutes after administration
Matrix	128x128 pixels	256x256 pixels
Zoom	2	2
Photopeak	140 keV	140 keV
Energy window, centred at photopeak	20%	20%

Legend: Gamma-camera image parameters for the acquisition of dynamic and static images after the administration of ^{99m}Tc-Pertechnetate or ^{99m}Tc-PEI-MP, namely the number and time per image, the matrix, the zoom given to the image (considering the small size of mice), the photopeak that corresponds to the energy of the gamma rays emitted by ^{99m}Tc, and the energy acceptance window that must be centred in the photopeak, accepting only gamma rays with energies ranging from 130 to 150 keV.

After the end of the last image, the mice were euthanized to the achievement of ex-vivo studies.

After mice with xenograft of bladder carcinoma or osteosarcoma, in which was administered ^{99m}Tc-PEI-MP were sacrificed, the tumour and a muscle of the thigh of the hind paw were collected and imaged. The tumour and muscle were positioned in an absorbent pad over the gamma-camera detector and in the centre of the collimator. The tumour was positioned in the right lower quadrant, and the muscle was positioned in the left higher quadrant. The image of the tumour and the muscle was acquired during 5 minutes, for a matrix of 256x256 pixels, zoom of 2, a photopeak of 140 keV and an energy window of 20%, centred in the photopeak.

6.2.2.2. Imaging with ^{188}Re-Perrhenate and ^{188}Re-PEI-MP

Images were also performed after the administration of ^{188}Re-Perrhenate or ^{188}Re-PEI-MP. As described in the topic 6.2.2.1., these images were also acquired in control mice, and in mice with xenograft of bladder carcinoma and osteosarcoma. Equally, for each group, and taking into account the type of mice and the radiopharmaceutical administered, images were acquired up to 120 minutes and up to 240 minutes. The organization of these groups is summarized in the table 27.

The images obtained with the ^{188}Re-Perrhenate are controls for the biodistribution of the radiopharmaceutical under evaluation, since it can be a radiochemical impurity produced during the normal process of labelling of PEI-MP kit with ^{188}Re-Perrhenate. As with the ^{99m}Tc-Pertechnetate, the normal ^{188}Re-Perrhenate biodistribution show a high uptake in thyroid, stomach, and choroid plexus. In turn, if there was the presence of reduced/hydrolysed rhenium species, as radiochemical impurities is expected to see a high uptake in the liver and spleen. In fact, the biodistribution verified in the images will be a mirror of the radiochemical purity of the complex ^{188}Re-PEI-MP.

Table 27. Number and organization of mice by type, administered radiopharmaceutical (^{188}Re-Perrhenate or ^{188}Re-PEI-MP) and time of the final images.

Mice	Images	Radiopharmaceuticals	
		^{188}Re-Perrhenate	**^{188}Re-PEI-MP**
Normal	Up to 120 min	4 mice	4 mice
	Up to 240 min	4 mice	4 mice
Xenograft of bladder carcinoma	Up to 120 min	4 mice	4 mice
	Up to 240 min	4 mice	4 mice
Xenograft of osteosarcoma	Up to 120 min	4 mice	4 mice
	Up to 240 min	4 mice	4 mice

Legend: Number of mice used for imaging studies, according to the radiopharmaceutical administered (^{188}Re-Perrhenate or ^{188}Re-PEI-MP) and the type of animal model, that is, normal mice, mice with xenograft of bladder carcinoma and mice with xenograft of osteosarcoma. Each of these groups were divided in two, where depending if the images were performed until 120 minutes or 240 minutes after the intravenous administration of ^{188}Re-Perrhenate or ^{188}Re-PEI-MP.

After the administration of 18-37 MBq (0.5-1 mCi) of ^{188}Re-Perrhenate or ^{188}Re-PEI-MP in a small volume (0.1 ml) into the tail vein of the mice, a dynamic and

static acquisition was carried out through the gamma-camera controlled by the Genie Acq computer to a workstation Xeleris for further visualization and data processing. The dynamic and static imaging had the same proposes as described in the topic 6.2.2.1. Image parameters were similar to those chosen for the acquisition of images after the administration of ^{99m}Tc-Pertechnetate or ^{99m}Tc-PEI-MP, with only changes in the parameters dependent of the physical characteristics of radionuclide used. The image parameters chosen for the acquisition of dynamic and static images after the administration of ^{188}Re-Perrhenate or ^{188}Re-PEI-MP are summarised in table 28.

Table 28. Gamma-camera image parameters for dynamic and static acquisition after the administration of ^{188}Re-Perrhenate or ^{188}Re-PEI-MP.

Image parameters	Dynamic acquisition	Static acquisition
Number of images	20 images	8 images
Time per image	30 seconds	2 minutes
Total time for imaging	10 min	Images at 30, 60, 90, 120, 150, 180, 210 and 240 minutes after administration
Matrix	128x128 pixels	256x256 pixels
Zoom	2	2
Photopeak	159 keV (I-123 photopeak)	159 keV (I-123 photopeak)
Energy window, centred at photopeak	20%	20%

Legend: Gamma-camera image parameters for the acquisition of dynamic and static images after the administration of ^{188}Re-Perrhenate or ^{188}Re-PEI-MP, namely the number and time per image, the matrix, the zoom given to the image (considering the small size of mice), the photopeak that should correspond to the energy of the gamma rays emitted by ^{188}Re, that is 155 keV. Considering the options for photopeak selection in the computer acquisition, and that the energy of gamma rays emitted by ^{188}Re during its decay is 155 keV, the choice of iodine-123 photopeak (159 keV) seems to be the most suitable. Also the energy window selected will allow accepting gamma-rays with energies ranging between 149-169 keV, being contained in this interval the gamma-rays emitted by ^{188}Re.

Tumour and muscle images were also acquired for mice with xenograft of bladder carcinoma or osteosarcoma, in which was administered ^{188}Re-PEI-MP, in the same way as described in topic 6.2.2.1. These images were only performed after the sacrifice of mice, and after the excision of the tumour and muscle of the thigh of the hind paw. The tumour and the muscle were

positioned in an absorbent pad over the gamma-camera detector and in the centre of the collimator. The tumour was positioned in the right lower quadrant, and the muscle was positioned in the left higher quadrant of the absorbent pad. The image of the tumour and the muscle was acquired during 5 minutes, for a matrix of 256x256 pixels, zoom of 2, a photopeak of 159 keV and an energy window of 20%, centred in the photopeak.

6.2.3. ***Ex-vivo biodistribution studies***

For the evaluation of the biodistribution and biokinetics of ^{99m}Tc-PEI-MP and ^{188}Re-PEI-MP, *in vivo* imaging may not be enough to respond to all questions. These limitations result from the image characteristics once they are projections and the organs can be superimposed each other which makes the ROI's drawing difficult. Also, the images resolution may not be adequate to obtain quantitative data, having into account the animal size Thereby, it was necessary to sacrifice the animals to collect the organs, tissues and tumours to quantify the percentage of ^{99m}Tc-PEI-MP or ^{188}Re-PEI-MP administered activity per gram of organ/tissue/fluid. The ex-vivo studies performed in mice after the administration of ^{99m}Tc-Pertechnetate or ^{188}Re-Perrhenate are controls of ^{99m}Tc-PEI-MP and ^{188}Re-PEI-MP, respectively.

6.2.3.1. Ex-vivo biodistribution studies with ^{99m}Tc-Pertechnetate and ^{99m}Tc-PEI-MP

As referred before, each group of mice (controls, xenograft of bladder carcinoma and xenograft of osteosarcoma) who were administered ^{99m}Tc-Pertechnetate or ^{99m}Tc-PEI-MP, was split in two, one in which the images were acquired up to 120 minutes and another in which images were acquired up to 240 minutes. After last image acquisition, the mice were euthanized by cervical dislocation in accordance with the legislation. Subsequently several organs were collected (heart, lung, thyroid, gallbladder, liver, spleen, stomach, small intestine, large intestine, genital, urinary bladder, brain and cerebellum) as well

as some tissues (cartilage, muscle, bone, blood) and fluids (urine and bile). The preparation of mice for organ and tissue collection is presented in fig. 40.

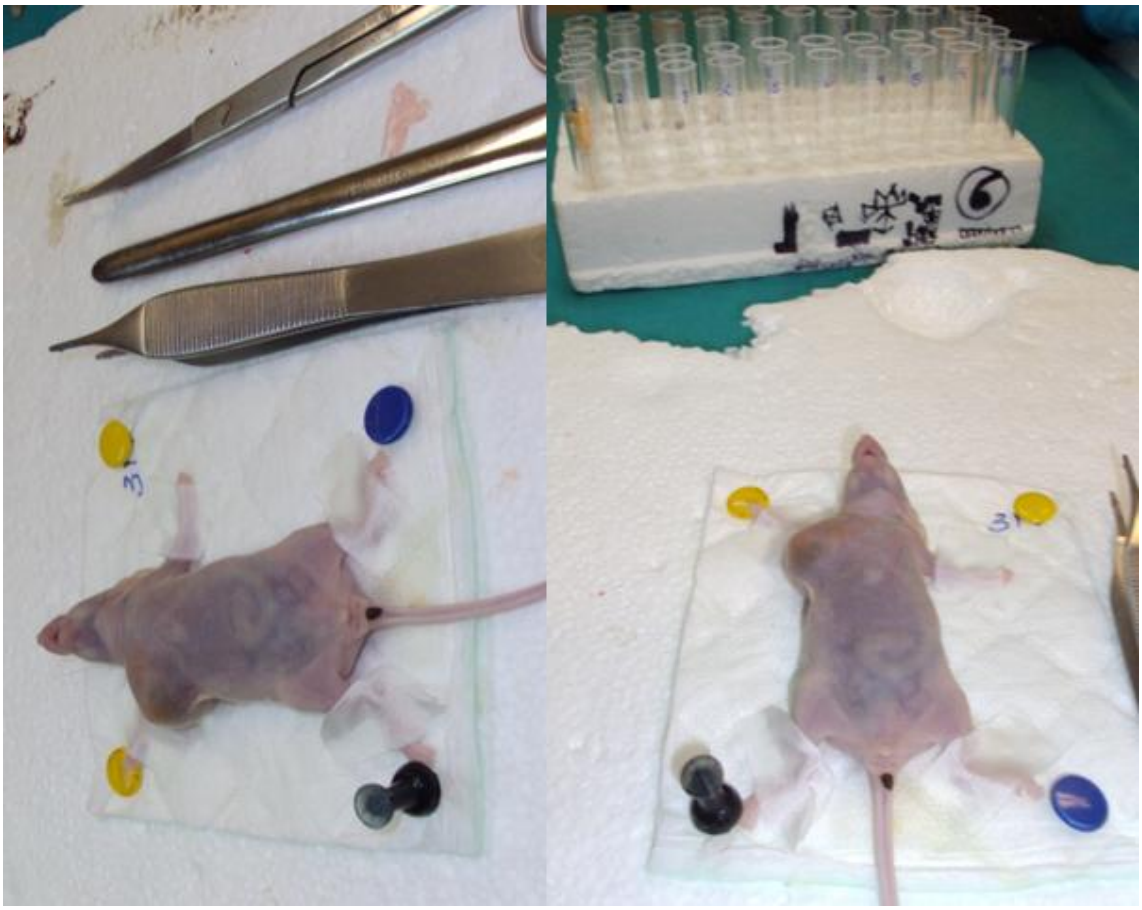

Figure 40. Euthanized mouse ready for collection of organs and tissues.

Each organ, tissue or fluid was weighted (in grams) and placed in a radioimmunoassay (RIA) tube. Each tube was counted in a well-type gamma counter (Gamma-C 12 DPC, Berthold, Germany) to obtain counts per minute (CPM). For xenograft of bladder carcinoma or osteosarcoma, also the tumour was collected, weighted and counted in a well counter to obtain CPM. With the values of CPM obtained, and converted into activity, we calculated the percentage of activity (^{99m}Tc-Pertechnetate or ^{99m}Tc-PEI-MP) administered per gram of organ/tissue/fluid (% injected activity/gram), according to equation 8.

$$\%\, Injected\ activity/g = \frac{cpm\ organ/mass\ organ\ (g)}{cpm\ (administered\ activity)}$$

Equation 8. Percentage of injected activity per gram of organ/tissue/fluid. It's determined by dividing the ratio of counts per minute and mass of each organ/tissue /fluid with the total administered activity.

Beyond the calculation of the percentage of activity injected per gram of organ/tissue/fluid, it was also determined the values of the ratios tumour/muscle, tumour/bladder, tumour/liver, tumour/lung and tumour/bone, for all groups. The bladder cancer has its origin in the bladder wall and can invade surrounding organs even in an early stage [184]. In case of metastization the major target organs are the liver, the lungs and the bone. This dissemination justifies the choice of the organs to calculate the specific uptake and to determine the tumour ratios. These calculations allow to determine whether the tumour uptake of a administered radiopharmaceutical is higher or lower than those organs, which is important for nuclear medicine be able to distinguish the lesions, and consequently to make a clear diagnosis. If the uptake of the radiopharmaceutical by the tumour or its metastases is equal to the uptake of the other organs, it's not possible to identify them, and therefore the diagnosis could be inconclusive or negative to metastases or tumour.

6.2.3.2. Ex-vivo biodistribution studies with ^{188}Re-Perrhenate and ^{188}Re-PEI-MP

As referred before, for each group of mice (controls, xenograft of bladder carcinoma and xenograft of osteosarcoma) who were administered ^{188}Re-Perrhenate or ^{188}Re-PEI-MP, was split in two, one in which the images were acquired up to 120 minutes and another in which images were acquired up to 240 minutes. After last image acquisition, the mice were euthanized by cervical dislocation in accordance with the legislation. Subsequently several organs, some tissues, and fluids were collected following the procedures referred in the topic 6.2.3.1. Each organ, tissue or fluid was weighted (in grams) and placed in a radioimmunoassay (RIA) tube. Each tube was counted in a well-type gamma

counter (Gamma-C 12 DPC, Berthold, Germany) to obtain CPM. For xenograft of bladder carcinoma or osteosarcoma, also the tumour was collected, weighted and counted in a well counter to obtain CPM. With the values of CPM obtained, and converted into activity, it was calculated the percentage of radiopharmaceutical ^{188}Re-Perrhenate or ^{188}Re-PEI-MP administered per gram of organ/tissue/fluid (% injected activity/gram), according to equation 8 referred before.

Beyond the calculation of the percentage of activity injected per gram of organ/tissue/fluid, it was also determined the values of the ratios tumour/muscle, tumour/bladder, tumour/liver, tumour/lung and tumour/bone for all groups. Considering the evolution of a bladder carcinoma, explained in before, to determine whether the tumour uptake of an administered radiopharmaceutical is higher than these organs, is crucial to determine these tumour ratios, so that when performing radionuclide therapy the main target is the tumour and its metastasis, and the non-target organs are spared of the effects of high doses of ionizing radiation. If the uptake of the radiopharmaceutical by the tumour or its metastases is equal or lower to the uptake of the other organs, it's not possible to perform the therapy, since it would be the non-target organs the most affected by ionizing radiation and the therapy would not be effective, and possibly it would result in serious side effects.

6.2.4. ***Statistical analysis***

Results were analysed using the software IBM® SPSS® (IBM Corporation, Armonk, New York, EUA), version 20, at a significance level of 5% ($p < 0.05$). The comparison of the ratios tumour/muscle, tumour/bladder, tumour/liver, tumour/lung and tumour/bone, for mice with xenograft of bladder carcinoma and xenograft of osteosarcoma, both injected with ^{99m}Tc-PEI-MP or ^{188}Re-PEI-MP, were made according to the t Student test for a mean, comparing the sample values to 1, that represents the equality of uptake for both tissues, and with the Bonferroni correction for multiple comparisons.

6.3. Results

6.3.1. *Animal tumour models and nuclear medicine imaging*

As animal tumour model it was chosen balb/c nu/nu mice with xenograft of bladder carcinoma and xenograft of osteosarcoma. To obtain the xenograft of bladder cancer and osteosarcoma it was injected subcutaneously in the right axilla dug of blab/c nu/nu mice a suspension of 5 million cells. The volume of tumours was controlled by calliper measurement and determined following the equation 7. For the development of xenografts of bladder carcinoma and osteosarcoma it was needed 4 and 3 weeks, respectively. Studies *in vivo* and *ex-vivo* using these animal models started when the tumour volumes reached 500-1000 mm^3.

Images were performed after the development of the xenograft. For image acquisition, mice were anesthetized and placed in prone on top and in the middle of the gamma-camera detector. Images started immediately after the administration, in the tail vein of the mice, of ^{99m}Tc-Pertechnetate, ^{99m}Tc-PEI-MP, ^{188}Re-Perrhenate or ^{188}Re-PEI-MP, with activities ranging 18-37 MBq (0.5-1 mCi). Immediately after the administration and during 10 minutes dynamic images were acquired and posterior static images were performed every 30 minutes after the administration of the radiopharmaceutical until 120 or 240 minutes. The mice were always sacrificed after the last image.

As a control of these animal models, mice with no tumour, namely balb/c mice, were used. To these mice it was also performed images after the administration of ^{99m}Tc-Pertechnetate, ^{99m}Tc-PEI-MP, ^{188}Re-Perrhenate or ^{188}Re-PEI-MP, following the same procedures explained before.

6.3.1.1. Imaging with ^{99m}Tc-Pertechnetate and ^{99m}Tc-PEI-MP

By analysing the image, presented in fig.41, obtained after the intravenous administration of ^{99m}Tc-Pertechnetate in the tail vein of balb/c without any tumour (normal mice), it is possible to visualize a high uptake by the thyroid gland, stomach and bladder. This biodistribution is considered normal as explained before. The activity present in bladder is explained by the fact that

^{99m}Tc-Pertechnetate is excreted by the renal system and therefore eliminated through urine.

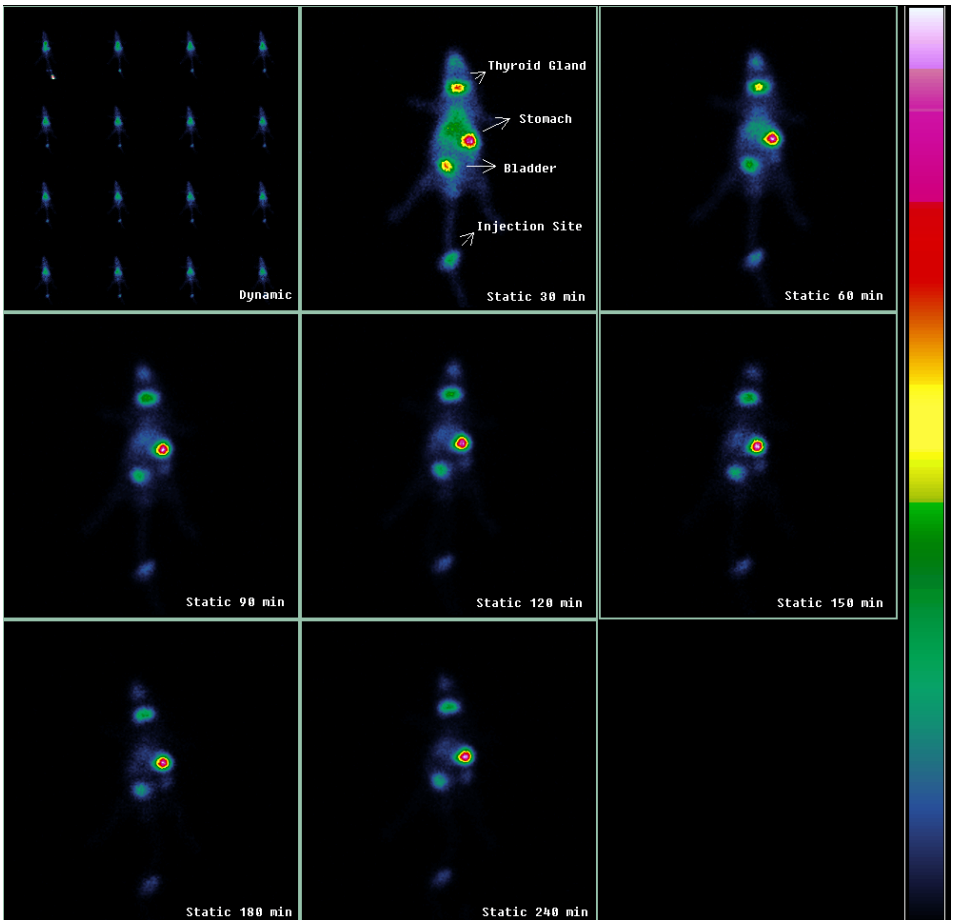

Figure 41. Images obtained after the administration of ^{99m}Tc-Pertechnetate in the dorsal vein of the tail of balb/c mouse. The first images are dynamic and obtained immediately after the administration of the radiopharmaceutical. After static images were acquired every 30 minutes after the administration until 240 minutes.

By analysing the images obtained after the intravenous administration of ^{99m}Tc-Pertechnetate in the tail of balb/c nu/nu mice with xenograft of bladder carcinoma (fig. 42) and xenograft of osteosarcoma (fig.43), it was also possible to visualize a high uptake by the thyroid gland, stomach and bladder, corresponding to the same biodistribution verified in normal balb/c mice. The uptake of tumour, in both bladder carcinoma and osteosarcoma xenograft, is faintly visible and possible dependent on the blood flow.

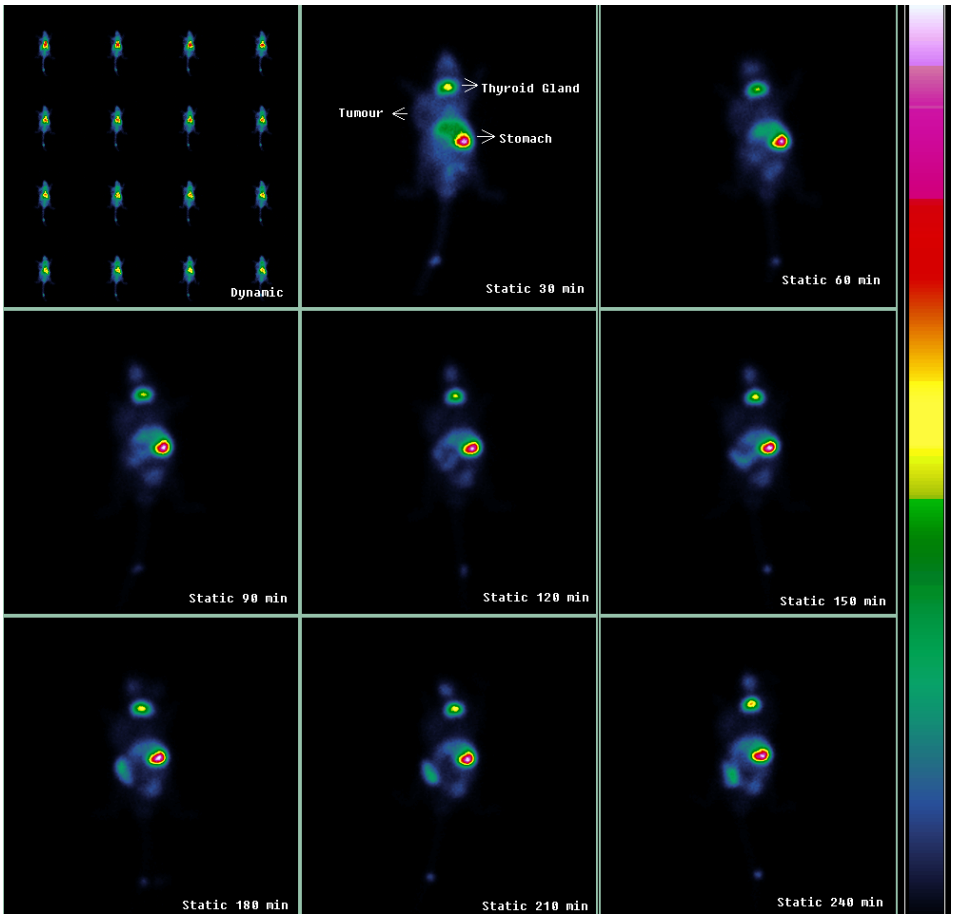

Figure 42. Images obtained after the administration of ^{99m}Tc-Pertechnetate in the dorsal vein of the tail of balb/c nu/nu mouse with a xenograft of bladder carcinoma. The first images are dynamic and obtained immediately after the administration of the radiopharmaceutical. After static images were acquired every 30 minutes after the administration until 240 minutes.

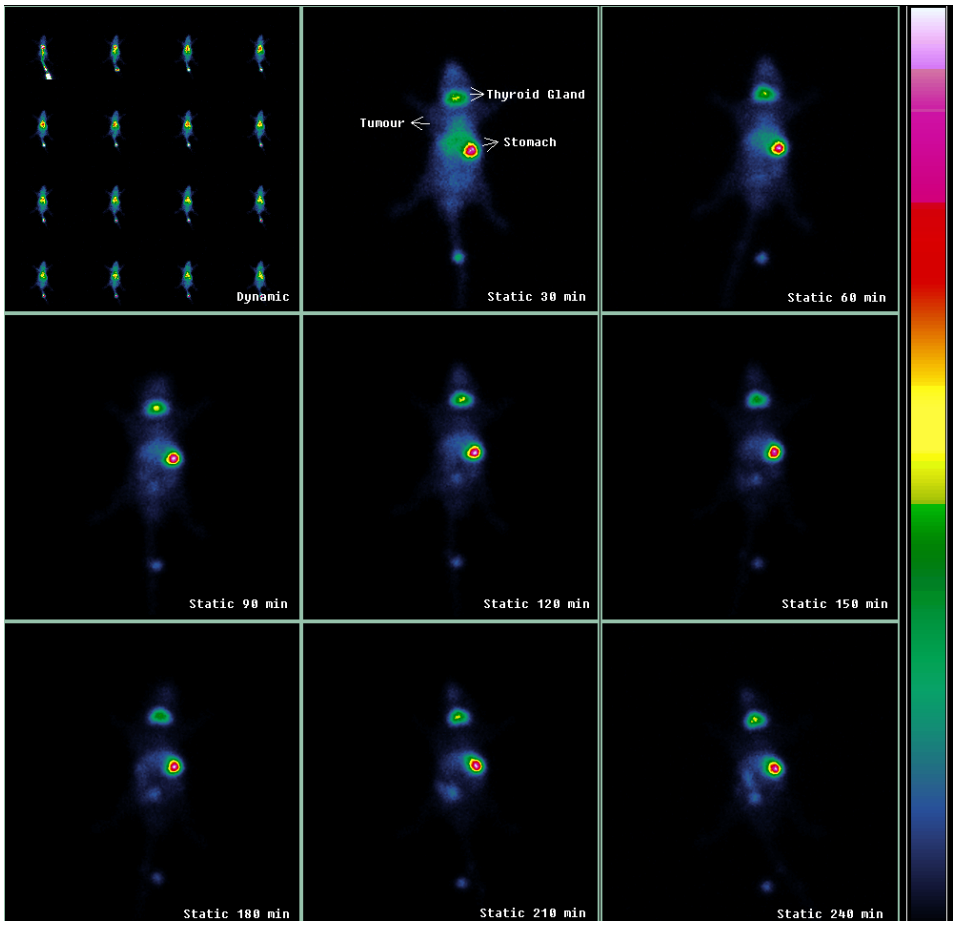

Figure 43. Images obtained after the administration of ^{99m}Tc-Pertechnetate in the dorsal vein of the tail of balb/c nu/nu mouse with a xenograft of osteosarcoma. The first images are dynamic and obtained immediately after the administration of the radiopharmaceutical. After static images were acquired every 30 minutes after the administration until 240 minutes.

After obtaining the images of ^{99m}Tc-Pertechnetate in normal balb/c mice, and in mice with xenografts of bladder carcinoma and osteosarcoma, the same animal models were evaluated after administration of ^{99m}Tc-PEI-MP. By analysing the images obtained after the intravenous administration of ^{99m}Tc-PEI-MP in the tail of controls balb/c mice, presented in fig. 44, it is possible to visualize a high uptake in kidneys and bladder. This biodistribution may indicate that the ^{99m}Tc-PEI-MP is mainly excreted through the renal system and therefore eliminated through urine. Also it's visible a faint uptake by the lungs, demonstrating some retention on this organ.

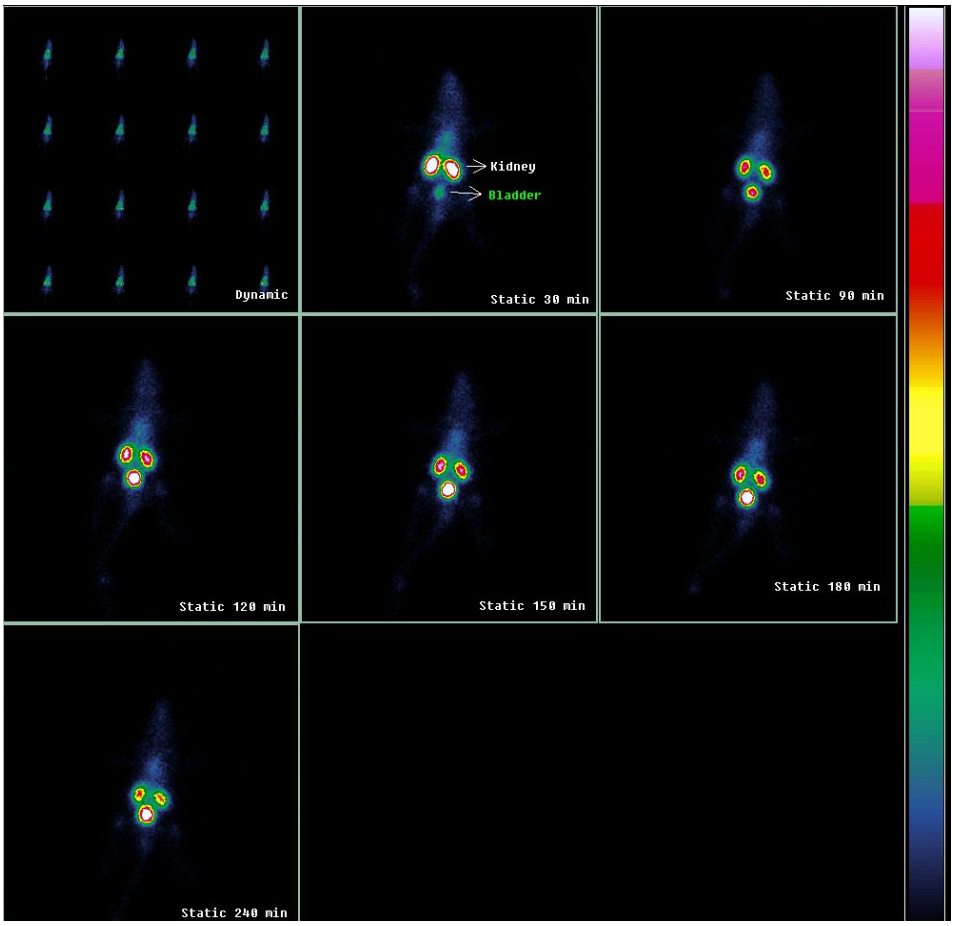

Figure 44. Images obtained after the administration of ^{99m}Tc-PEI-MP in the dorsal vein of the tail of balb/c mouse. The first images are dynamic and obtained immediately after the administration of the radiopharmaceutical. After static images were acquired every 30 minutes after the administration until 240 minutes.

By analysing the images obtained after the intravenous administration of ^{99m}Tc-PEI-MP in the tail vein of balb/c nu/nu mice with a xenograft of bladder carcinoma (fig. 45) and xenograft of osteosarcoma (fig. 46), it is also possible to visualize a high uptake in kidneys and bladder. It is also possible to visualize a faint uptake by the lungs in both xenografts (bladder carcinoma and osteosarcoma), which seems to diminish over time. Moreover the tumour is small in both xenografts, and despite low resolution of the gamma camera, is possible to visualize a faint uptake of the ^{99m}Tc-PEI-MP by both type of tumours.

The quantification of ^{99m}Tc-PEI-MP uptake by the tumour will be only possible with *ex vivo* studies.

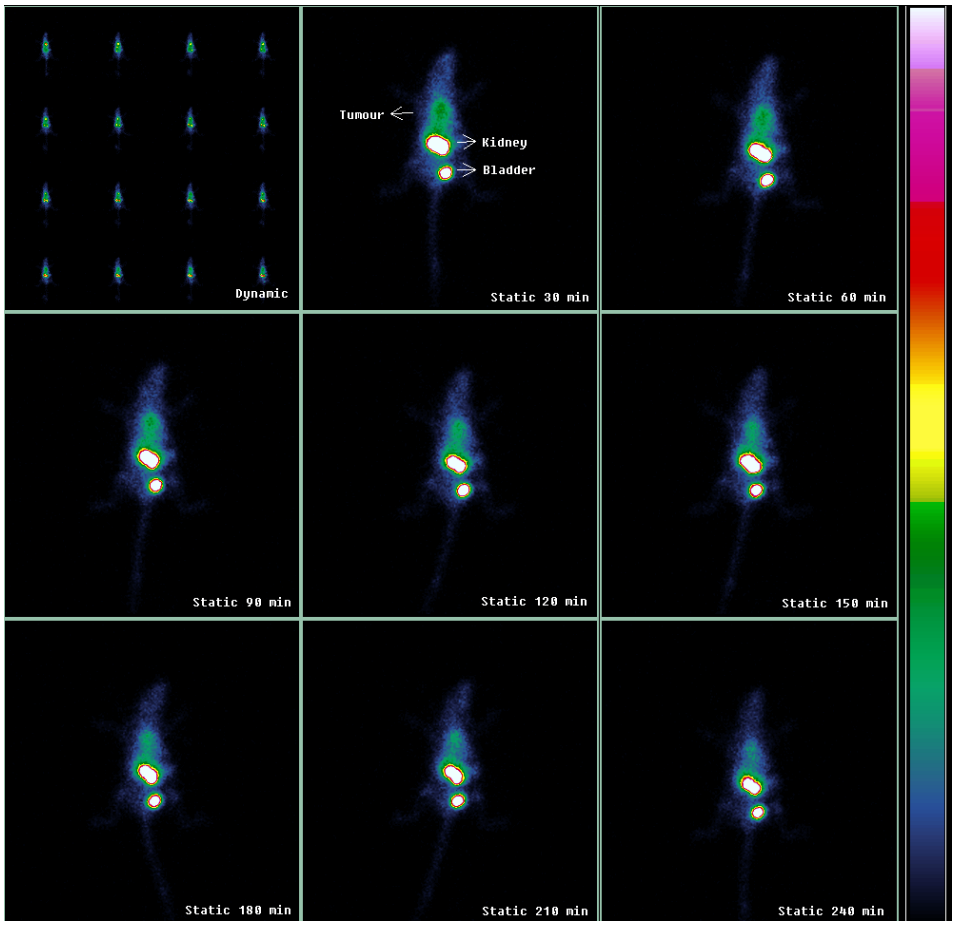

Figure 45. Images obtained after the administration of ^{99m}Tc-PEI-MP in the dorsal vein of the tail of balb/c nu/nu mouse with a xenograft of bladder carcinoma. The first images are dynamic and obtained immediately after the administration of the radiopharmaceutical. After static images were acquired every 30 minutes after the administration until 240 minutes.

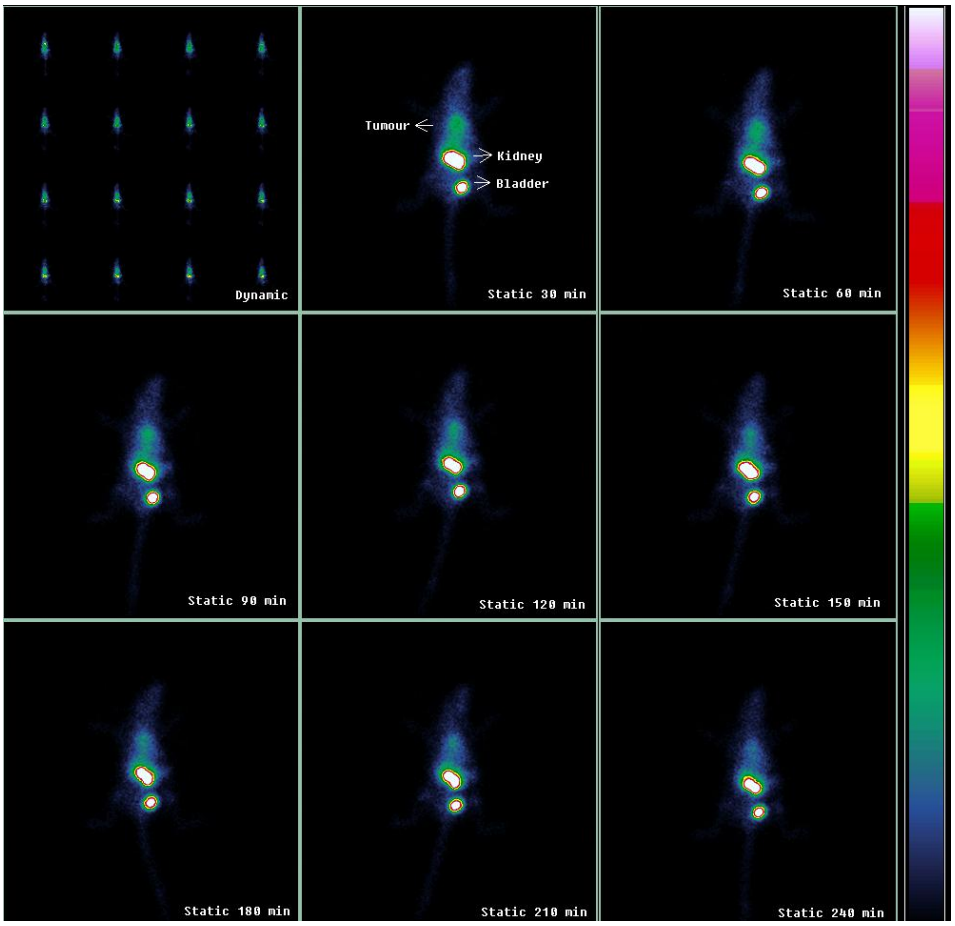

Figure 46. Images obtained after the administration of ^{99m}Tc-PEI-MP in the dorsal vein of the tail of balb/c nu/nu mouse with a xenograft of osteosarcoma. The first images are dynamic and obtained immediately after the administration of the radiopharmaceutical. After static images were acquired every 30 minutes after the administration until 240 minutes.

6.3.1.2. Imaging with ^{188}Re-Perrhenate and ^{188}Re-PEI-MP

By analysing the images obtained after the intravenous administration of ^{188}Re-Perrhenate in the tail of balb/c mice, presented in fig. 47, it is possible to visualize a high uptake by the thyroid gland and stomach. This biodistribution is considered normal as explained before.

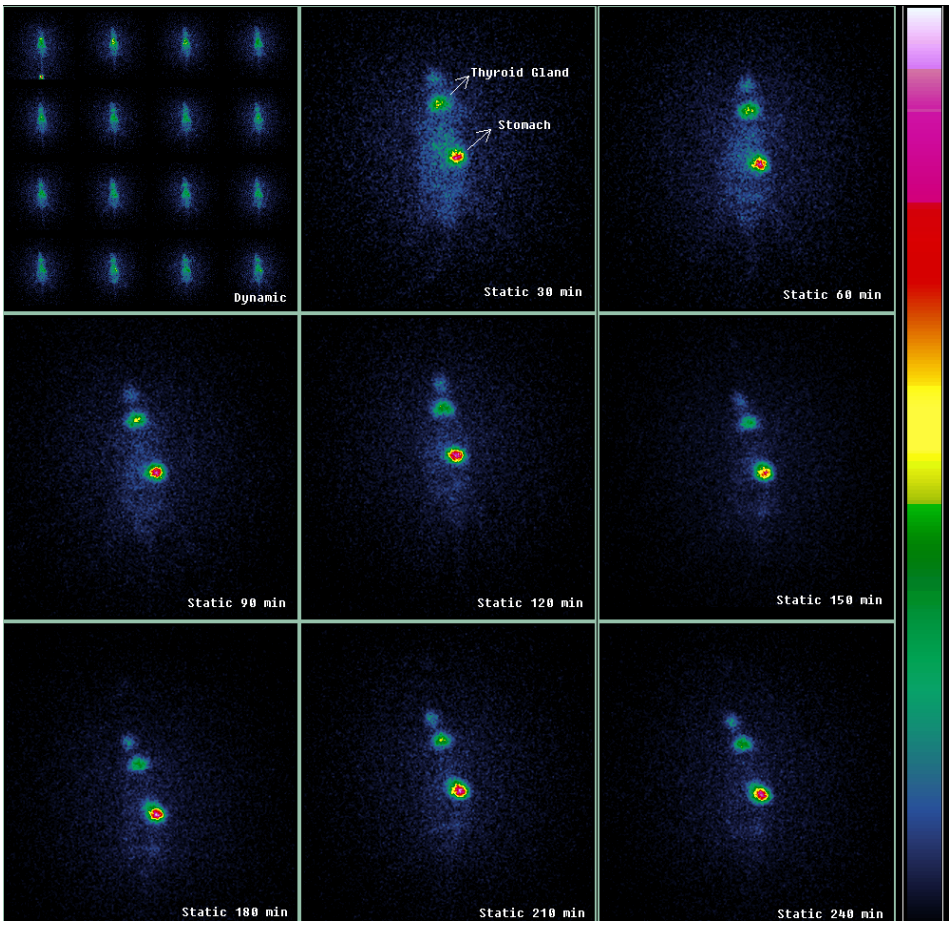

Figure 47. Images obtained after the administration of ^{188}Re-Perrhenate in the dorsal vein of the tail of balb/c mouse. The first images are dynamic and obtained immediately after the administration of the radiopharmaceutical. After static images were acquired every 30 minutes after the administration until 240 minutes.

By analysing the images obtained after the intravenous administration of ^{188}Re-Perrhenate in the tail vein of balb/c nu/nu mice with xenograft of bladder carcinoma (fig.48) and xenograft of osteosarcoma (fig 49), presented in fig.48 and fig 49, it was is also possible to visualize a high uptake by the thyroid gland and stomach, corresponding to the same biodistribution verified in normal balb/c mice. The uptake of tumour is not visible in the mouse of the fig.48, and faintly visible on the mouse of the fig. 49, and possibly dependent on the blood flow. The fact that the photonic flow of gamma rays of 155 keV from ^{188}Re is low, and in association with a low resolution of the gamma camera detector, considering the size of the animal and its organs, its normal that the resolution of the images with ^{188}Re-Perrhenate or ^{188}Re-PEI-MP will be lower comparing with the ones

obtained with ^{99m}Tc-Pertechnetate or ^{99m}Tc-PEI-MP, considering the higher photonic flow of the 140 keV from ^{99m}Tc.

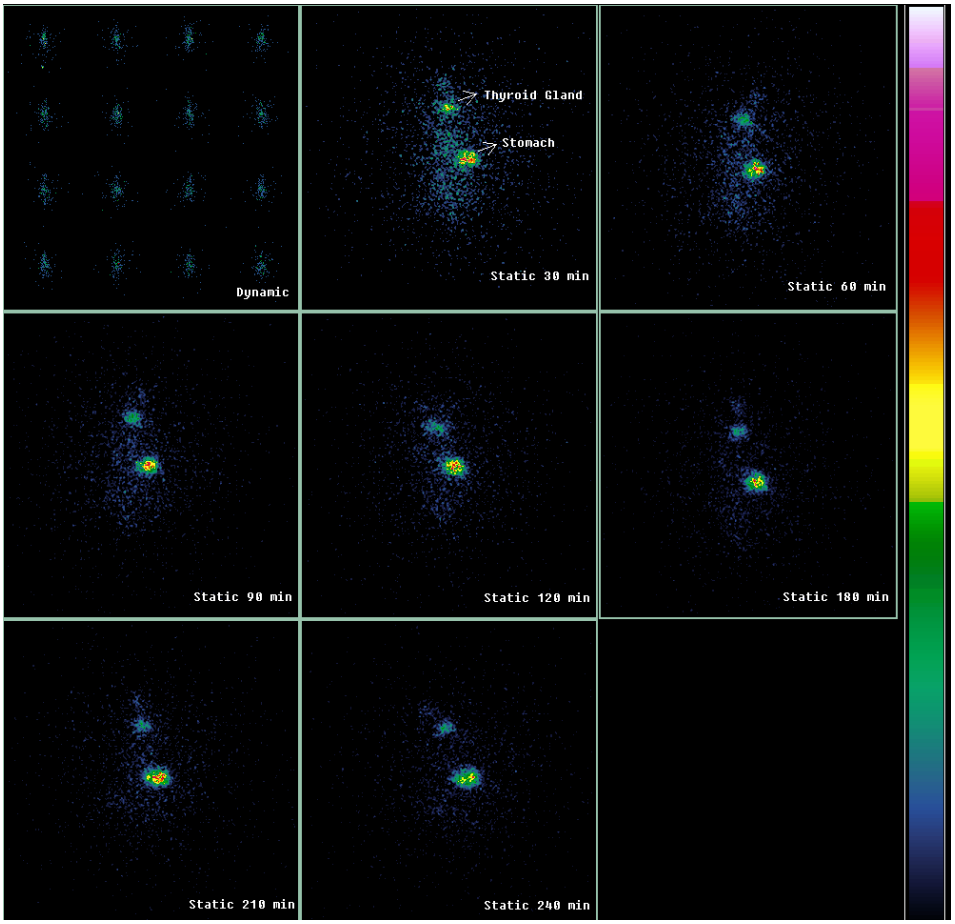

Figure 48. Images obtained after the administration of ^{188}Re-Perrhenate in the dorsal vein of the tail of balb/c nu/nu mouse with a xenograft of bladder carcinoma. The first images are dynamic and obtained immediately after the administration of the radiopharmaceutical. After static images were acquired every 30 minutes after the

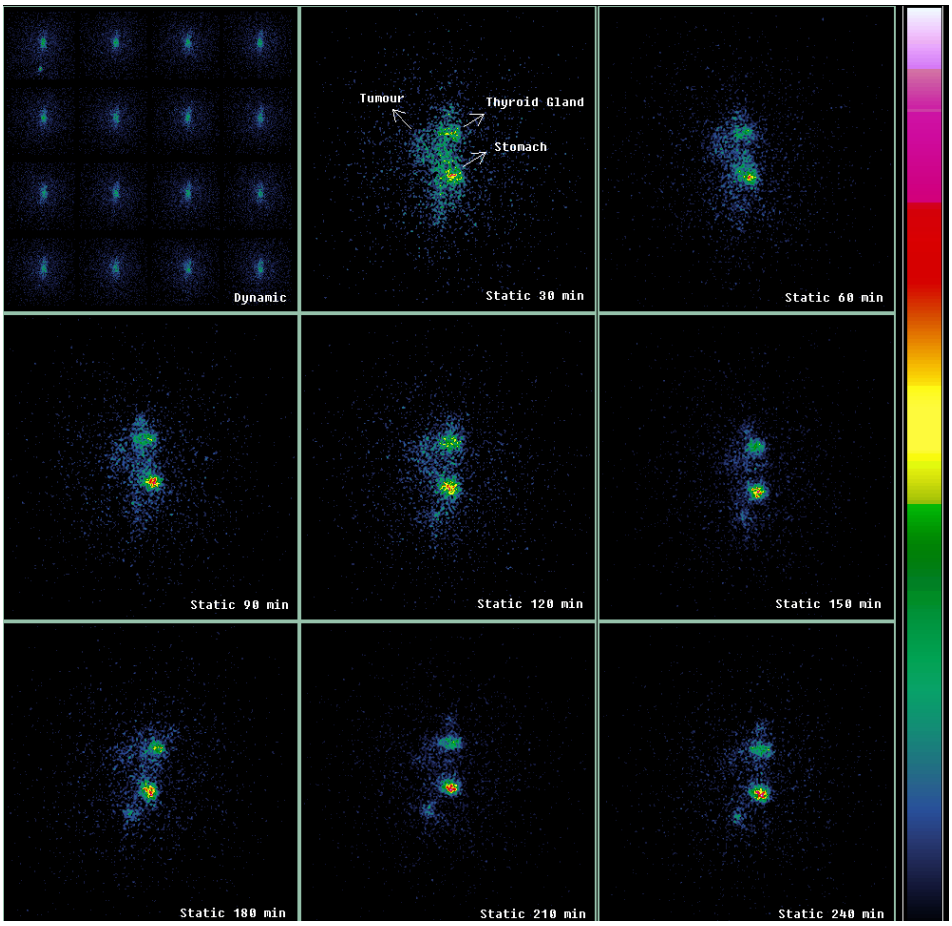

Figure 49. Images obtained after the administration of ^{188}Re-Perrhenate in the dorsal vein of the tail of balb/c nu/nu mouse with a xenograft of osteosarcoma. The first images are dynamic and obtained immediately after the administration of the radiopharmaceutical. After static images were acquired every 30 minutes after the administration until 240 minutes.

After obtaining the images of ^{188}Re-Perrhenate in normal balb/c mice, and in mice with xenografts of bladder carcinoma and osteosarcoma, the same animal models were evaluated after administration of ^{188}Re-PEI-MP. By analysing the images obtained after the intravenous administration of ^{188}Re-PEI-MP in the tail of controls balb/c mice, presented in fig. 50, it is possible to visualize a high uptake by the bladder. This biodistribution may also indicate that the ^{188}Re-PEI-MP is mainly excreted through the renal system and therefore eliminated through urine. Also it's possible to visualize a faint uptake by lungs that seem to diminish over time, but also the uptake seems more intense than the one verified in images of mice where ^{99m}Tc-PEI-MP was administered. For a more reasonable and quantitative conclusions it should be consider the results obtained in ex-vivo studies.

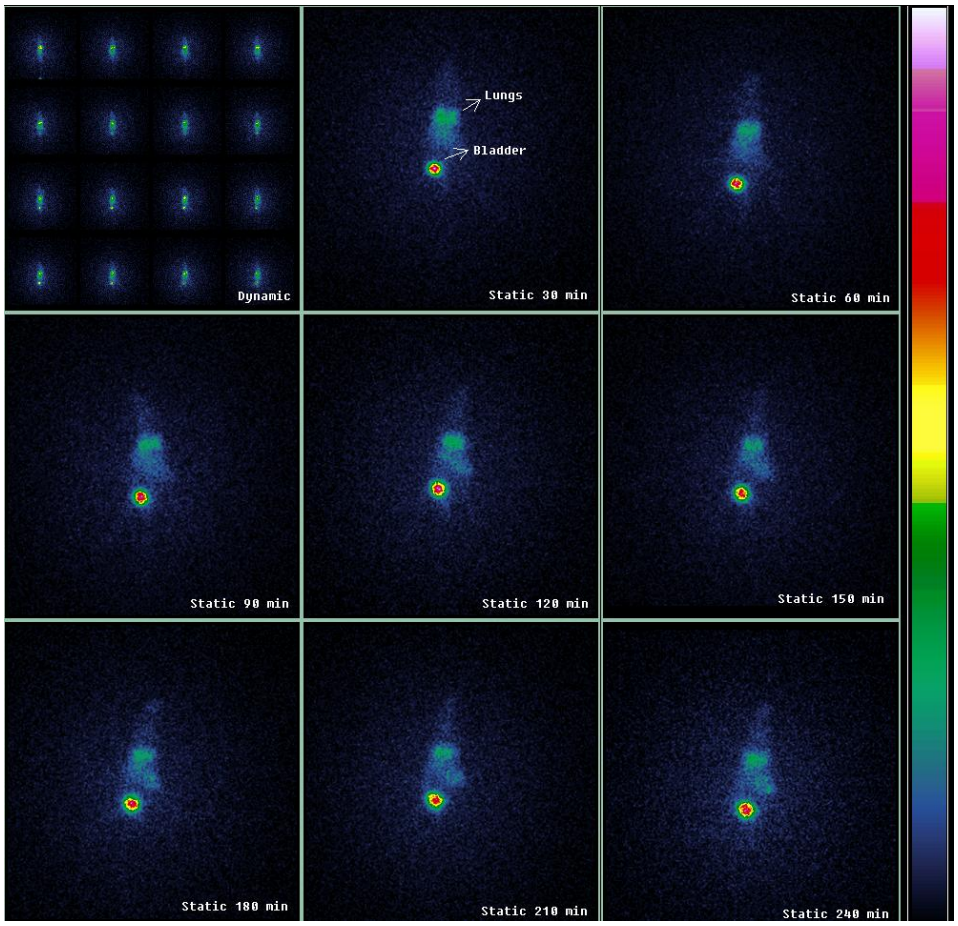

Figure 50. Images obtained after the administration of ^{188}Re-PEI-MP in the dorsal vein of the tail of balb/c mouse. The first images are dynamic and obtained immediately after the administration of the radiopharmaceutical. After static images were acquired every 30 minutes after the administration until 240 minutes.

By analysing the images obtained after the intravenous administration of ^{188}Re-PEI-MP in the tail of balb/c nu/nu mice with a xenograft of bladder carcinoma (fig. 51) and xenograft of osteosarcoma (fig. 52), it is also possible to visualize a high uptake by the bladder, as in the case of control balb/c mice were ^{188}Re-PEI-MP was administered. For both xenografts it's possible to visualize the uptake of ^{188}Re-PEI-MP by lungs, which seem to diminish over time. Moreover the tumour is small in both xenografts, and because the low resolution of the gamma camera, the tumours are almost not visible in the images.

The quantification of ^{188}Re-PEI-MP uptake by the tumour will be only possible with *ex vivo* studies.

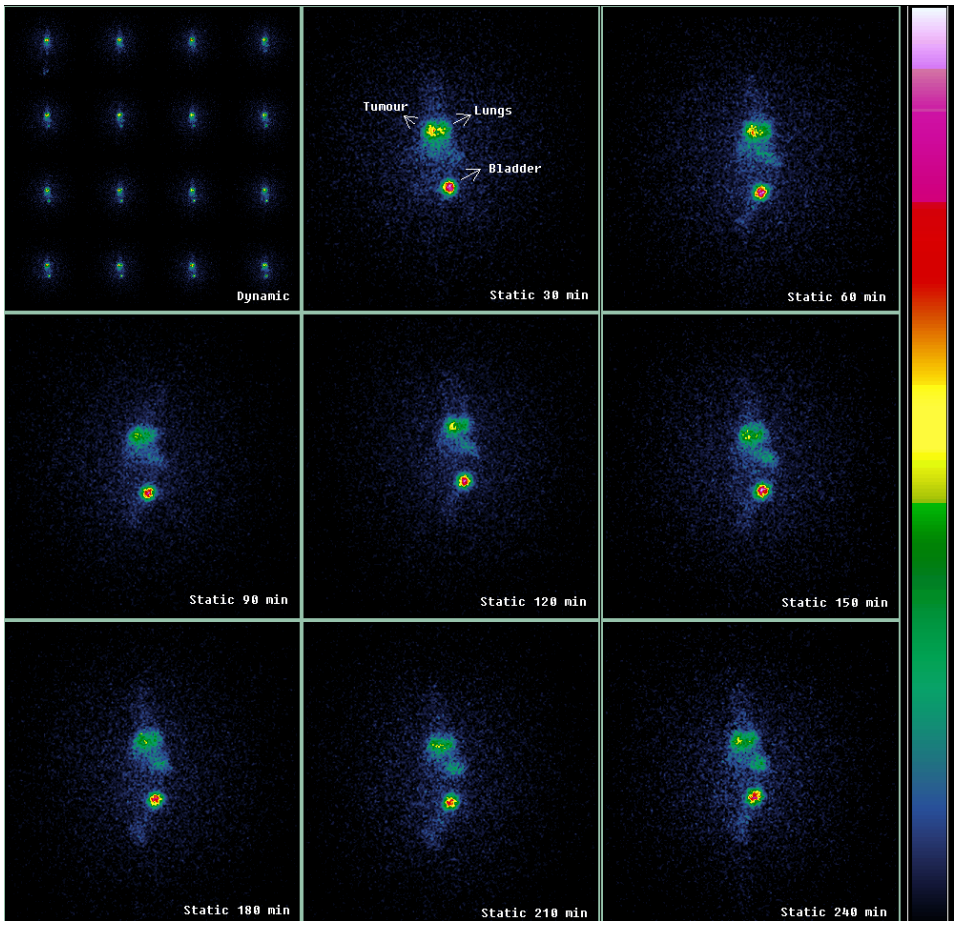

Figure 51. Images obtained after the administration of ^{188}Re-PEI-MP in the dorsal vein of the tail of balb/c nu/nu mouse with a xenograft of bladder carcinoma. The first images are dynamic and obtained immediately after the administration of the radiopharmaceutical. After static images were acquired every 30 minutes after the administration until 240 minutes.

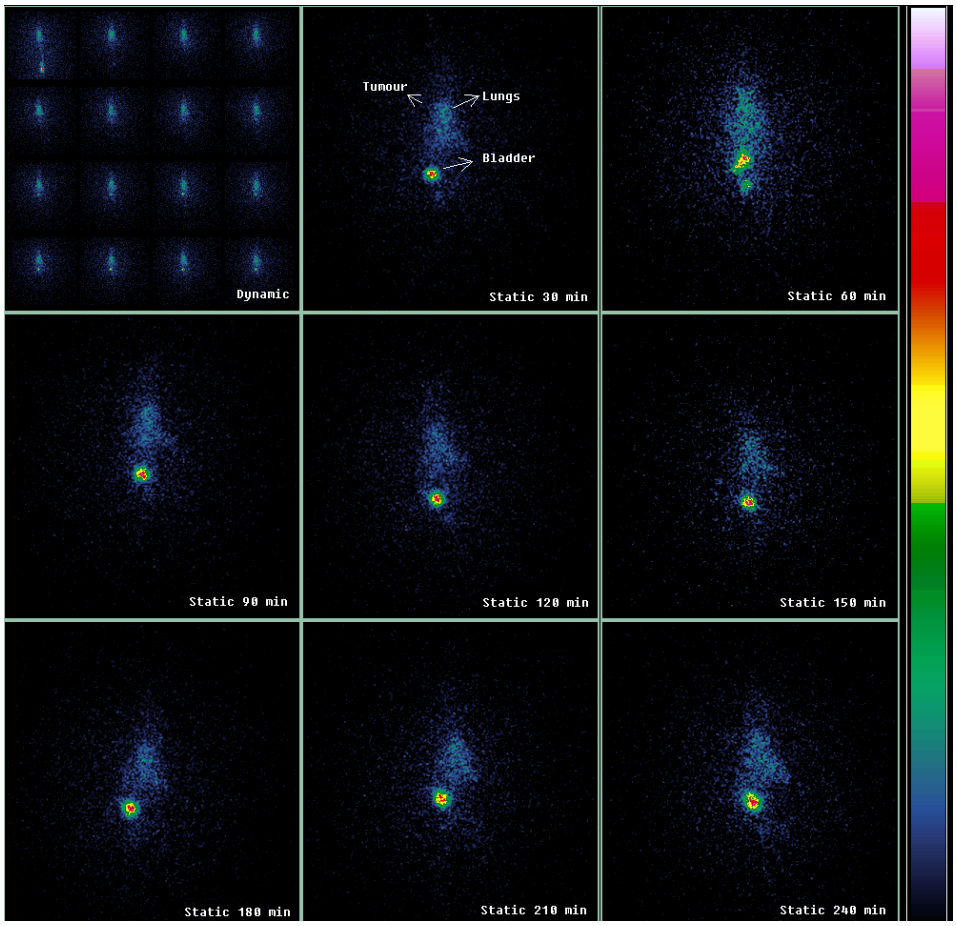

Figure 52. Images obtained after the administration of ^{188}Re-PEI-MP in the dorsal vein of the tail of balb/c nu/nu mouse with xenograft of osteosarcoma. The first images are dynamic and obtained immediately after the administration of the radiopharmaceutical. After static images were acquired every 30 minutes after the administration until 240 minutes.

6.3.2. ***Biodistribution studies ex vivo***

As explained before the images were performed until 120 or 240 after the administration of ^{99m}Tc-Pertechnetate, ^{99m}Tc-PEI-MP, ^{188}Re-Perrhenate or ^{188}Re-PEI-MP, and then normal mice, mice with xenograft of bladder cancer and xenograft of osteosarcoma were euthanized by cervical dislocation.

Several organs (heart, lung, thyroid, gallbladder, liver, spleen, stomach, small intestine, large intestine, genital, urinary bladder, brain and cerebellum), tissues (cartilage, muscle, bone, blood), fluids (urine and bile) and tumour (if applicable) were collected and placed in RIA tubes for gamma counting and weighing to obtain the percentage of radiopharmaceutical administered per gram of

organ/tissue/fluid. Also the ratios tumour/muscle, tumour/bladder, tumour/liver, tumour/lung and tumour/bone were determined for all groups of mice with xenografts.

6.3.2.1. *Ex-vivo biodistribution studies with ^{99m}Tc-Pertechnetate and ^{99m}Tc-PEI-MP*

By analysing the fig. 53 that correspond to the normal mice sacrificed 120 and 240 minutes after the administration of ^{99m}Tc-Pertechnetate, it's possible to visualize a high uptake in the thyroid gland and stomach. This biodistribution is considered normal as explained before and supports the results observed in the images of the biodistribution *in vivo* of ^{99m}Tc-Pertechnetate in normal mice.

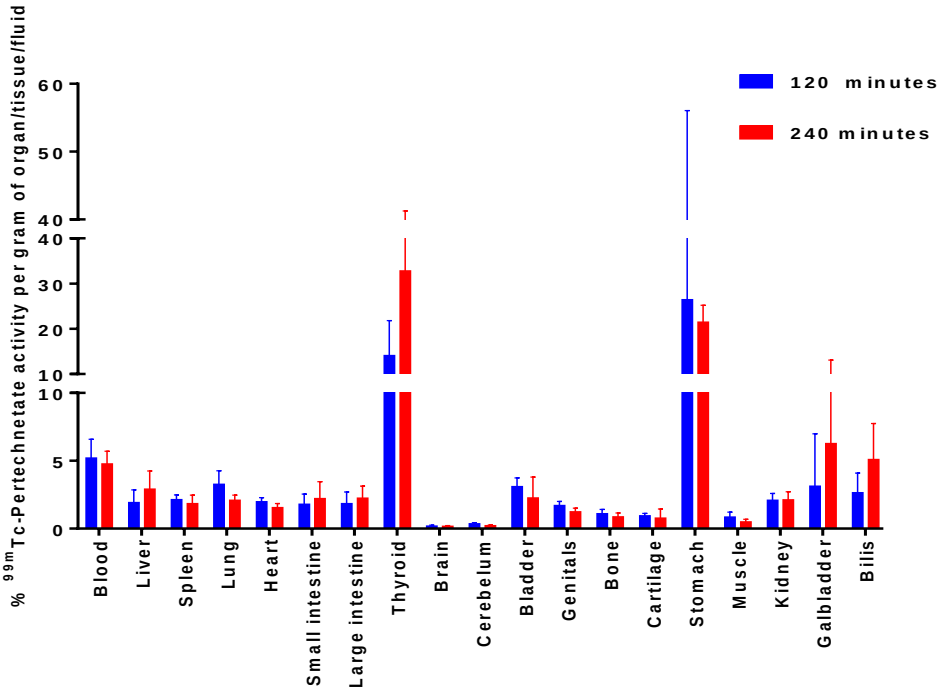

Figure 53. Biodistribution represented in percentage of activity per gram of organ/tissue/fluid, 120 and 240 minutes after the administration of ^{99m}Tc-Pertechnetate and determined ex-vivo in normal mice.

The results that correspond to mice with xenograft of bladder cancer (fig. 54) and xenograft of osteosarcoma (fig. 55), sacrificed 120 and 240 minutes after

the administration of ^{99m}Tc-Pertechnetate, showed a high uptake in the thyroid gland and stomach, supporting the results obtained in the images of the biodistribution *in vivo* of ^{99m}Tc-Pertechnetate in mice with xenografts of bladder cancer and osteosarcoma. Also it's possible to visualize a small uptake by the tumours, which is possibly related with the blood flow to the xenograft. This uptake by the tumours was also verified in the *in vivo* biodistribution images, however faintly visible, but now confirmed by the *ex vivo* studies.

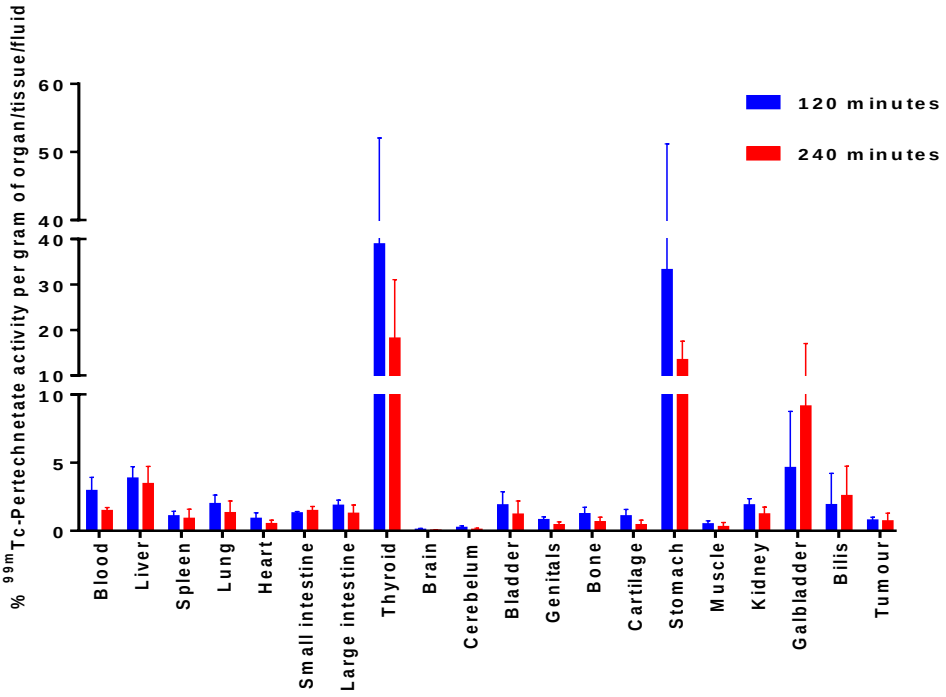

Figure 54. Biodistribution represented in percentage of activity per gram of organ/tissue/fluid, 120 and 240 minutes after the administration of ^{99m}Tc-Pertechnetate and determined ex-vivo in mice with xenografts of bladder cancer.

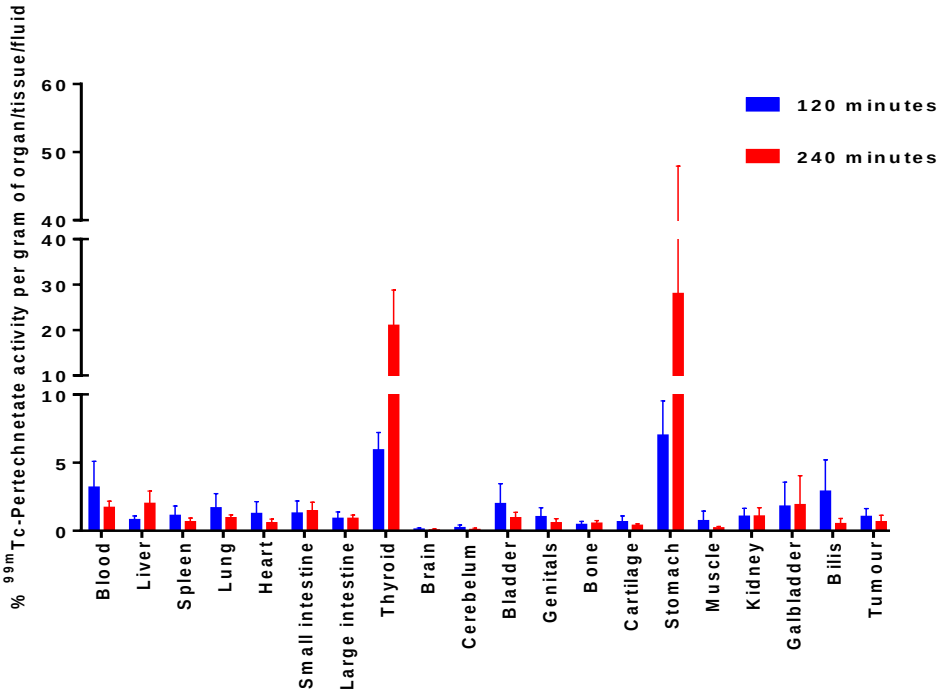

Figure 55. Biodistribution represented in percentage of activity per gram of organ/tissue/fluid, 120 and 240 minutes after the administration of ^{99m}Tc-Pertechnetate and determined ex-vivo in mice with xenografts of osteosarcoma.

Additionally, tumour/muscle, tumour/bladder, tumour/liver, tumour/lung and tumour/bone ratios were determined for both types of animal models, with xenograft of bladder cancer and with xenograft of osteosarcoma. Analysing the fig. 56, that represents the tumour ratios of mice with xenograft of bladder carcinoma injected with ^{99m}Tc-Pertechnetate, it is possible to visualize that tumour/muscle ratio is high comparing with the other tumour ratios, especially 240 minutes after the administration of ^{99m}Tc-Pertcehnetate. For 120 and 240 minutes after the administration, the tumour/muscle ratio was 1.67±0.72 and 2.54±0.56, respectively, demonstrating that the uptake by the tumour is higher than of the muscle. However, comparing these values with 1, that represents the equality of the numerator and the denominator, the tumour/muscle ratio was statistically significantly higher than the unit ($p=0.048$) only at 240 minutes. Tumour/bladder (0.48±0.20 at 120 min; 0.69±0.45 at 240 min), tumour/liver (0.22±0.09 at 120 min; 0.25±0.26 at 240 min), tumour/lung (0.41±0.11 at 120 min; 0.58±0.22 at 240 min) and tumour/bone (0.66±0.15 at 120 min; 1.02±0.30

at 240 min) ratios were always inferior or equal to one, demonstrating that the uptake by the tumour was inferior or equal comparing to these organs. However these tumour ratios were only statistically significant lower than one for tumour/liver at 120 minutes ($p<0.001$) and 240 minutes ($p=0.040$), and for tumour/lung at 120 minutes ($p=0.008$). Considering these results, metastasis from a bladder carcinoma in liver, lung and bones would appear as cold lesions in nuclear medicine images, after the administration of ^{99m}Tc-Pertechenetate. However, the probability of detecting metastases in the liver at 120 and 240 minutes and in the lungs at 120 minutes after the administration of ^{99m}Tc-Pertechnetate will be greater, considering that the values of these tumour ratios were significantly lower than one.

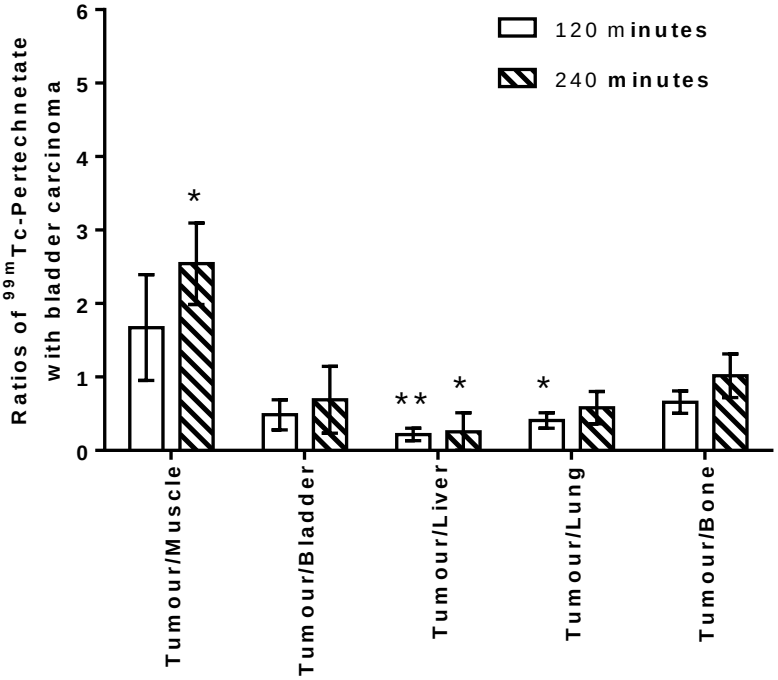

Figure 56. Tumour/muscle, tumour/bladder, tumour/liver, tumour/lung and tumour/bone ratios obtained for balb/c nu/nu mice with xenografts of bladder carcinoma after administration of ^{99m}Tc-Pertechnetate.

Analysing the fig. 57, that represents the tumour ratios of mice with xenograft of osteosarcoma and injected with ^{99m}Tc-Pertechnetate, it's possible to visualize that tumour/muscle ratio is high comparing with the other tumour ratios,

especially 240 minutes after the administration of ^{99m}Tc-Pertcehnetate. For 120 and 240 minutes after the administration, the tumour/muscle ratio was 2.93±1.12 and 3.51±0.55, respectively, demonstrating that the uptake by the tumour is higher than of the muscle. However comparing these values with 1, the tumour/muscle ratio was not statistically significantly higher than the unit. Tumour/bladder (0.72±0.38 at 120 min; 0.66±0.46 at 240 min) and tumour/lung (0.65±0.10 at 120 min; 0.66±0.47 at 240 min) ratios were always inferior to one, demonstrating that the uptake by the tumour was inferior comparing to these organs. However these tumour ratios were only statistically significant lower than one for tumour/lungs at 120 minutes (p=0.028). Tumour/liver ratio was higher than one at 120 minutes (1.23±0.65) and lower than one at 240 minutes (0.35±0.31), demonstrating that at 120 minutes the uptake by the tumour is higher than the liver and at 240 minutes occurs the inverse situation. However these differences are not statistically significant. Tumour/bone ratios at 120 minutes (2.02±0.69) and 240 minutes (1.19±0.96) were always superior to one, even at 240 minutes were the tumour/bone ratio decreases. However these differences are not statistically significant. Considering these results, metastasis from an osteosarcoma in lung would appear as cold lesions, in liver would appear at 120 minutes as hot lesions and at 240 minutes as cold lesions, and in bone it would appear as hot lesions in nuclear medicine images, after the administration of ^{99m}Tc-Pertechenetate. However, the probability of detecting metastases in the lungs at 120 after the administration of ^{99m}Tc-Pertechnetate will be greater, considering that the value of this tumour ratio was significantly lower than one.

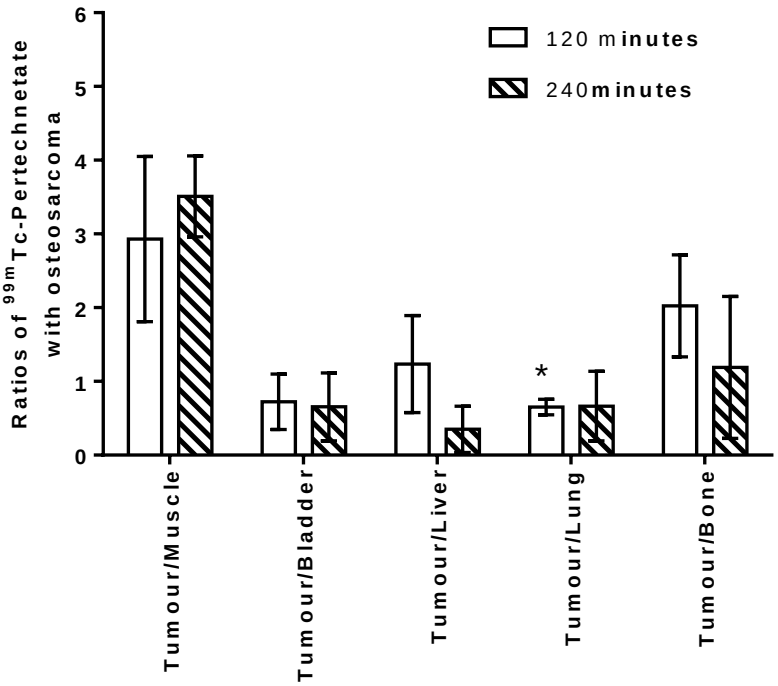

Figure 57. Tumour/muscle, tumour/bladder, tumour/liver, tumour/lung and tumour/bone ratios obtained for balb/c nu/nu mice with xenografts of osteosarcoma after administration of ^{99m}Tc-Pertechnetate.

By analysing the fig. 58 that correspond to the normal mice sacrificed 120 and 240 minutes after the administration of ^{99m}Tc-PEI-MP, it's possible to visualize a high uptake by the bladder wall and kidneys. These results support those obtained in the images of the biodistribution *in vivo* of ^{99m}Tc-PEI-MP in normal mice. As explained before this may indicate that ^{99m}Tc-PEI-MP is mainly excreted through the renal system. However, considering that the bladder is carefully washed to remove any traces of urine, this uptake by the bladder wall demonstrates once again that ^{99m}Tc-PEI-MP as affinity for bladder cells, being this the primary reason to suspect that PEI-MP had some affinity to bladder carcinoma cells. The activity in the kidneys and bladder diminished at 240 minutes. The high uptake by the gallbladder indicates that ^{99m}Tc-PEI-MP is also excreted through the hepatobiliary route. Being PEI-MP a polymer and a large molecule it is possible that ^{99m}Tc-PEI-MP is trapped by the Kupffer cells in the liver, that make part of the reticuloendothelial system. The activity in the liver and gallbladder diminished at 240 minutes. Also it is possible to verify some

uptake by the lungs, supporting the results obtained in the *in vivo* images of normal mice, however is diminished at 240 minutes. Considering the first propose of PEI-MP, that was for palliative therapy of bone metastases and also the results obtained in previous biodistribution studies [111], it's not surprising the uptake at bones. Also it's possible to visualize some retention of ^{99m}Tc-PEI-MP in the spleen, demonstrating that some percentage of this complex is trapped by the reticuloendothelial system. The percentage of ^{99m}Tc-PEI-MP in blood is also high and seems to diminish over time.

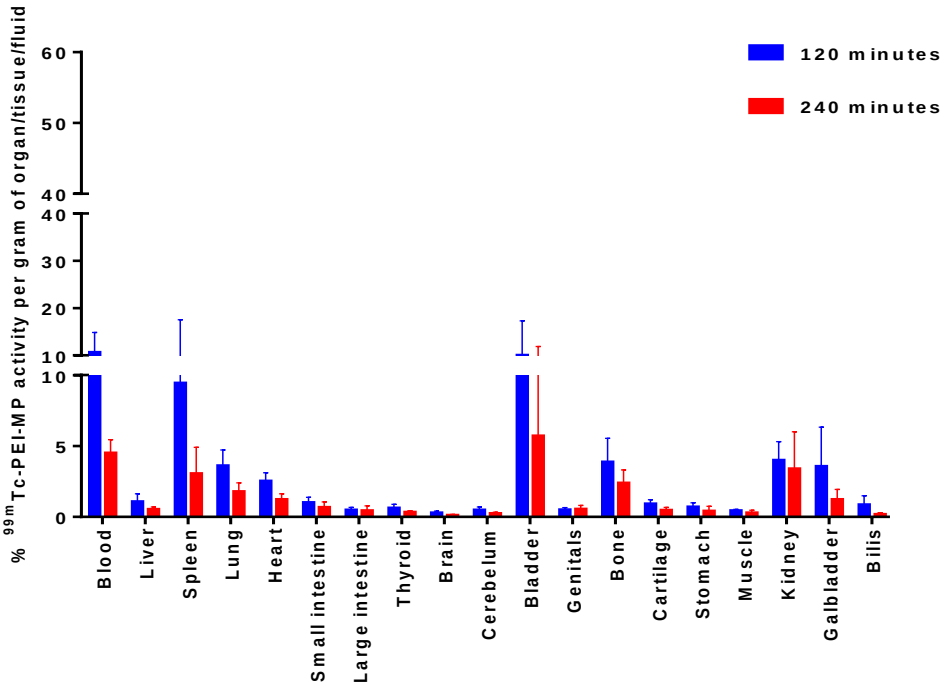

Figure 58. Biodistribution represented in percentage of activity per gram of organ/tissue/fluid, 120 and 240 minutes after the administration of ^{99m}Tc-PEI-MP and determined ex-vivo in normal mice.

By analysing the fig. 59 and fig. 60, which correspond to the mice with xenograft of bladder carcinoma and osteosarcoma, respectively, sacrificed 120 and 240 minutes after the administration of ^{99m}Tc-PEI-MP, it is possible to visualize a high uptake by the bladder wall and kidneys. These results support those obtained in the *in vivo* images of mice with xenograft of bladder carcinoma and xenograft of osteosarcoma after the administration of ^{99m}Tc-PEI-MP, and are supported by the results of the biodistribution *ex vivo* for normal mice after the

administration of ^{99m}Tc-PEI-MP. As explained before this may indicate that ^{99m}Tc-PEI-MP is mainly excreted through the renal system and that has an affinity for bladder cells. The high uptake by the gallbladder indicates once again that ^{99m}Tc-PEI-MP is also excreted through the hepatobiliary route. The activity in the liver and gallbladder diminished at 240 minutes. Also it is possible to verify some uptake by the lungs, supporting the results obtained in the *in vivo* images. In the same way as for *ex vivo* biodistribution studies in normal mice after the administration of ^{99m}Tc-PEI-MP, in fig.59 and fig.60 it is possible to visualize some uptake by spleen and bone, possibly explained by the reasons presented before. The percentage of ^{99m}Tc-PEI-MP in blood is also high and seems to diminish over time.

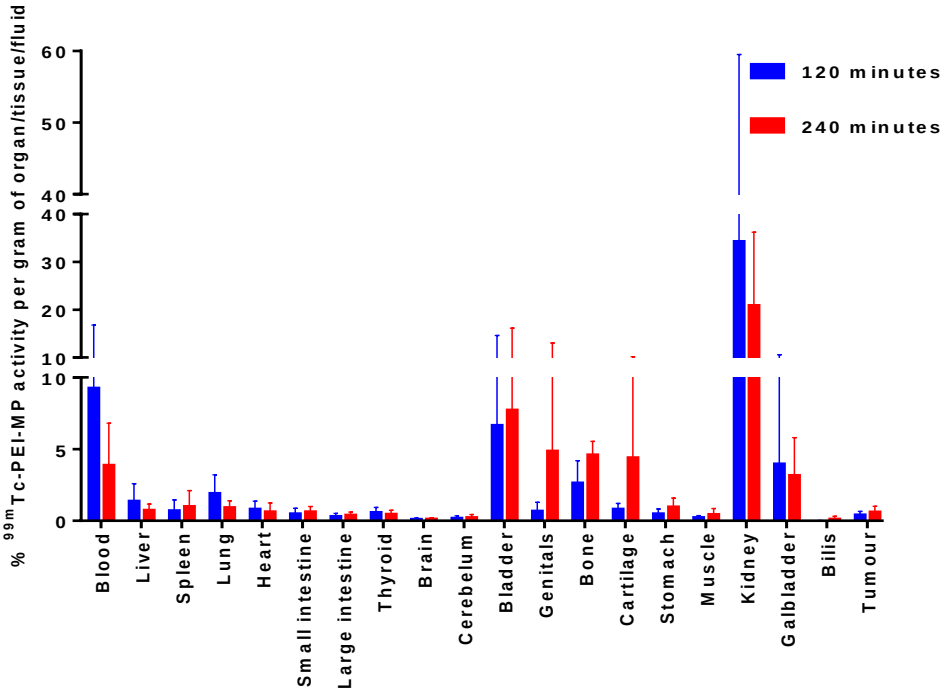

Figure 59. Biodistribution represented in percentage of activity per gram of organ/tissue/fluid, 120 and 240 minutes after the administration of ^{99m}Tc-PEI-MP and determined ex-vivo in mice with xenografts of bladder cancer.

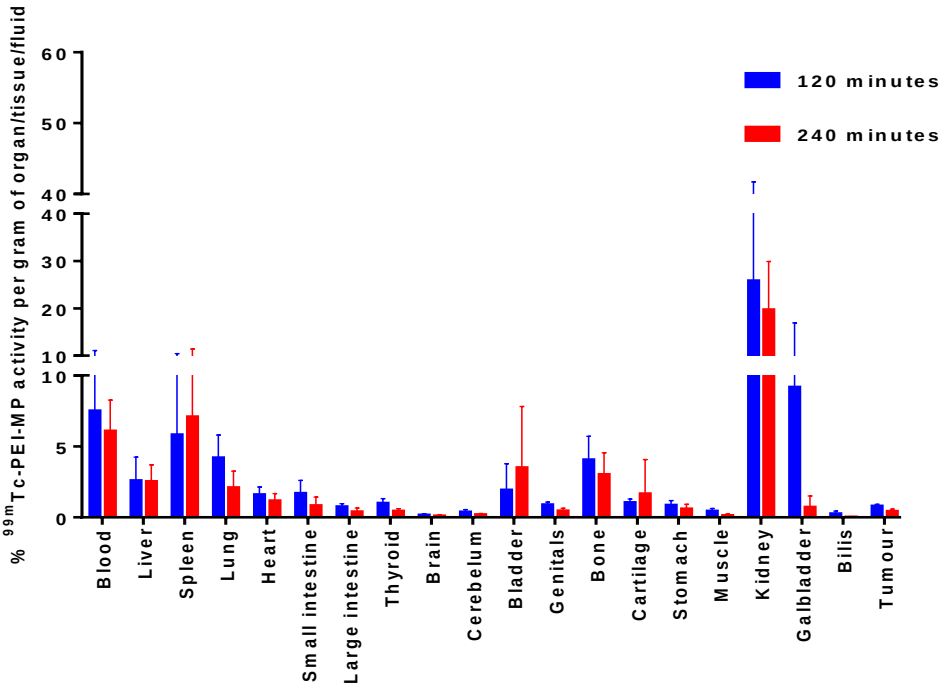

Figure 60. Biodistribution represented in percentage of activity per gram of organ/tissue/fluid, 120 and 240 minutes after the administration of ^{99m}Tc-PEI-MP and determined ex-vivo in mice with xenografts of osteosarcoma.

Analysing the fig. 61, that represents the tumour ratios of mice with xenograft of bladder carcinoma and injected with ^{99m}Tc-PEI-MP, it's possible to visualize that tumour/muscle ratio is high comparing with the other tumour ratios. For 120 and 240 minutes after the administration, the tumour/muscle ratio was 1.81±0.34 and 1.88±0.38, respectively, demonstrating that the uptake by the tumour is higher than of the muscle. However comparing these values with 1, the tumour/muscle ratio was not statistically significantly higher than 1 at 120 or 240 minutes. Tumour/bladder (0.23±0.27 at 120 min; 0.12±0.09 at 240 min), tumour/liver (0.50±0.38 at 120 min; 0.92±0.62 at 240 min), tumour/lung (0.29±0.16 at 120 min; 0.64±0.17 at 240 min) and tumour/bone (0.22±0.16 at 120 min; 0.13±0.07 at 240 min) ratios were always inferior to 1, demonstrating that the uptake by the tumour was inferior comparing to these organs. However these tumour ratios were only statistically significant lower than 1 for tumour/bladder at 120 minutes ($p=0.044$) and 240 minutes ($p<0.001$), for tumour/lung at 120 minutes ($p=0.012$) and for tumour/bone at 120 minutes

(p=0.008) and 240 minutes (p<0.001). Considering these results, metastasis from a bladder carcinoma in liver, lung and bones would appear as cold lesions in nuclear medicine images, after the administration of ^{99m}Tc-PEI-MP. However, the probability of detecting metastases in the lungs at 120 and 240 minutes and in the bones at 120 and 240 minutes after the administration of ^{99m}Tc-PEI-MP will be greater, considering that the values of these tumour ratios were significantly lower than one.

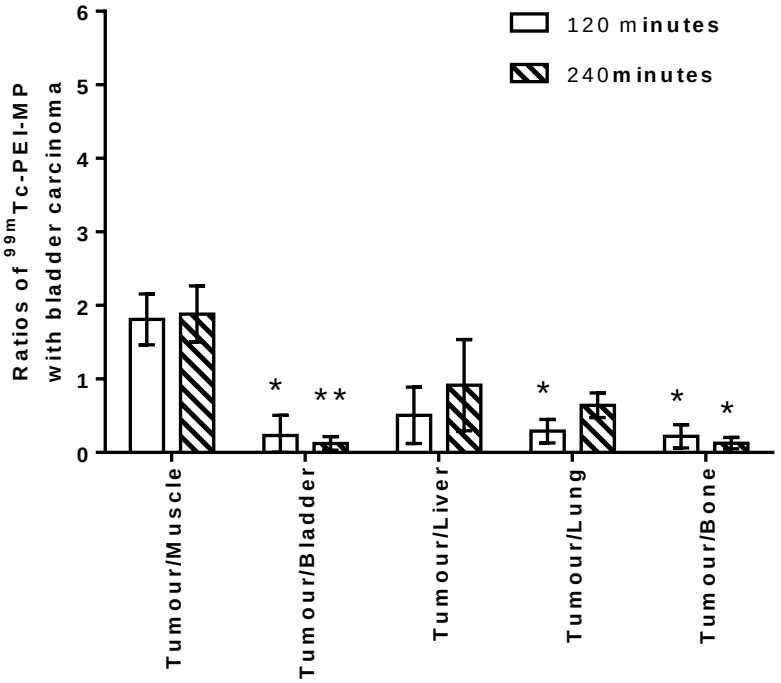

Figure 61. Tumour/muscle, tumour/bladder, tumour/liver, tumour/lung and tumour/bone ratios obtained for balb/c nu/nu mice with xenografts of bladder carcinoma after administration of ^{99m}Tc-PEI-MP.

Analysing the fig. 62, that represents the tumour ratios of mice with xenograft of osteosarcoma and injected with ^{99m}Tc-PEI-MP, it's possible to visualize that tumour/muscle ratio is high comparing with the other tumour ratios. For 120 and 240 minutes after the administration, the tumour/muscle ratio was 1.90±0.53 and 3.72±1.60, respectively, demonstrating that the uptake by the tumour is higher than of the muscle. However comparing these values with 1, the tumour/muscle ratio was not statistically significantly higher than 1 at 120 or 240 minutes. Tumour/bladder (0.70±0.47 at 120 min; 0.33±0.26 at 240 min),

tumour/liver (0.42±0.25 at 120 min; 0.21±0.11 at 240 min), tumour/lung (0.21±0.06 at 120 min; 0.24±0.10 at 240 min) and tumour/bone (0.25±0.16 at 120 min; 0.17±0.08 at 240 min) ratios were always less than 1, demonstrating that the uptake by the tumour was inferior comparing to these organs. However these tumour ratios were only statistically significant lower than one for tumour/liver at 240 minutes ($p=0.004$), for tumour/lung at 120 minutes ($p<0.001$) and at 240 minutes ($p=0.04$), and for tumour/bone at 120 minutes ($p=0.008$) and 240 minutes ($p<0.001$). Considering these results, metastasis from an osteosarcoma in liver, lung and bones would appear as cold lesions in nuclear medicine images, after the administration of ^{99m}Tc-PEI-MP. However, the probability of detecting metastases in the liver at 240 minutes, in the lungs at 120 and 240 minutes and in bones at 120 and 240 minutes after the administration of ^{99m}Tc-PEI-MP will be greater, considering that the values of these tumour ratios were significantly lower than 1.

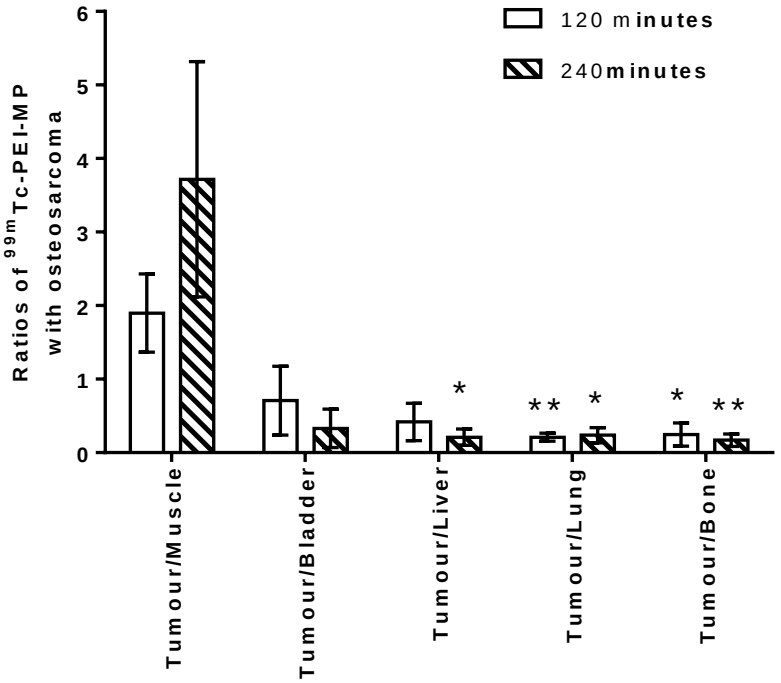

Figure 62. Tumour/muscle, tumour/bladder, tumour/liver, tumour/lung and tumour/bone ratios obtained for balb/c nu/nu mice with xenografts of osteosarcoma after administration of ^{99m}Tc-PEI-MP.

6.3.2.2. *Ex-vivo biodistribution studies with ^{188}Re-Perrhenate and ^{188}Re-PEI-MP*

By analysing the fig. 63 that correspond to the normal mice sacrificed 120 and 240 minutes after the administration of ^{188}Re-Perrhenate, it is possible to visualize a high uptake by the thyroid gland and stomach. This biodistribution is considered normal as explained before and supports the results observed in the images of the biodistribution *in vivo* of ^{188}Re-Perrhenate in normal mice.

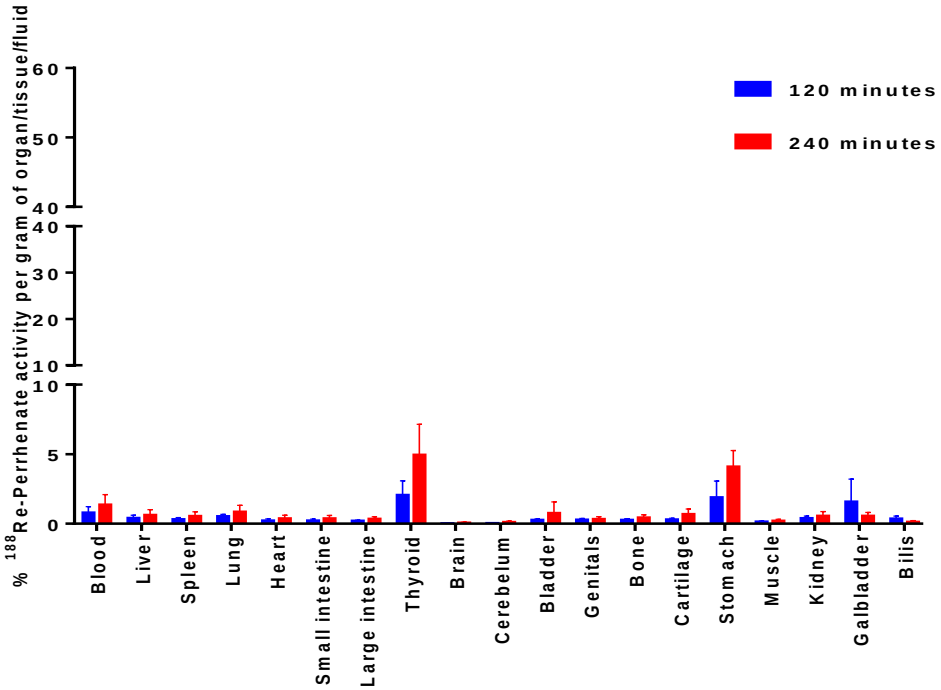

Figure 63. Biodistribution represented in percentage of activity per gram of organ/tissue/fluid, 120 and 240 minutes after the administration of ^{188}Re-Perrhenate and determined ex-vivo in normal mice.

By analysing the fig. 64 and fig. 65, that correspond to mice with xenografts of bladder cancer and osteosarcoma, respectively, sacrificed 120 and 240 minutes after the administration of ^{188}Re-Perrhenate, it's also possible to visualize a high uptake by the thyroid gland and stomach, supporting the results obtained in the images of the biodistribution *in vivo* of ^{188}Re-Perrhenate in mice with xenografts of bladder cancer and osteosarcoma, respectively. Also it is possible to visualize a small uptake by the tumours that can be related with the blood flow to the xenograft. This uptake by the tumours was verified in the *in vivo*

biodistribution images, however faintly visible, but now confirmed by the *ex vivo* studies.

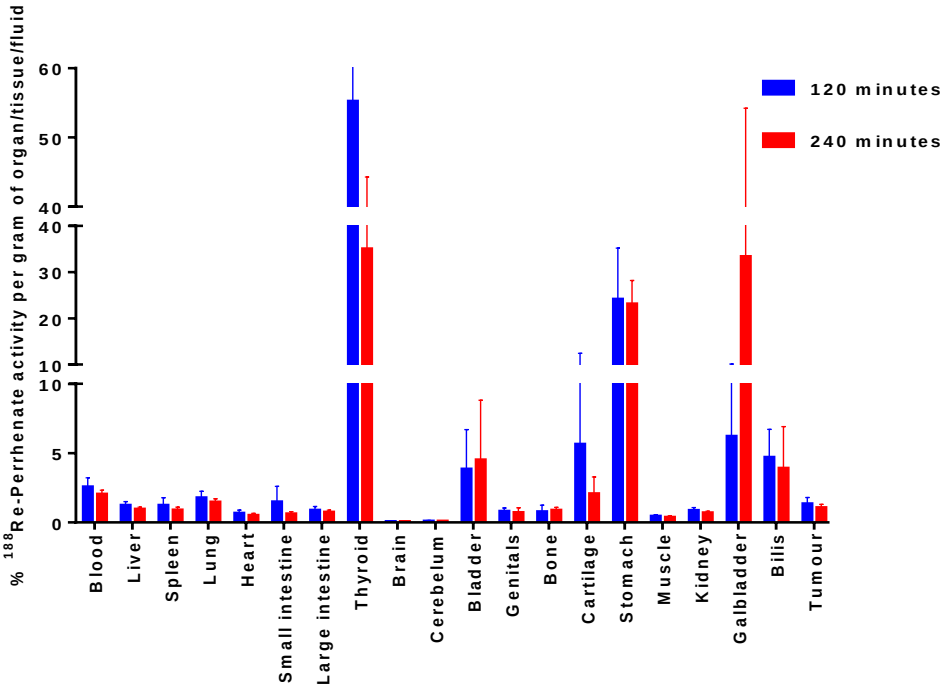

Figure 64. Biodistribution represented in percentage of activity per gram of organ/tissue/fluid, 120 and 240 minutes after the administration of ^{188}Re-Perrhenate and determined ex-vivo in mice with xenografts of bladder cancer.

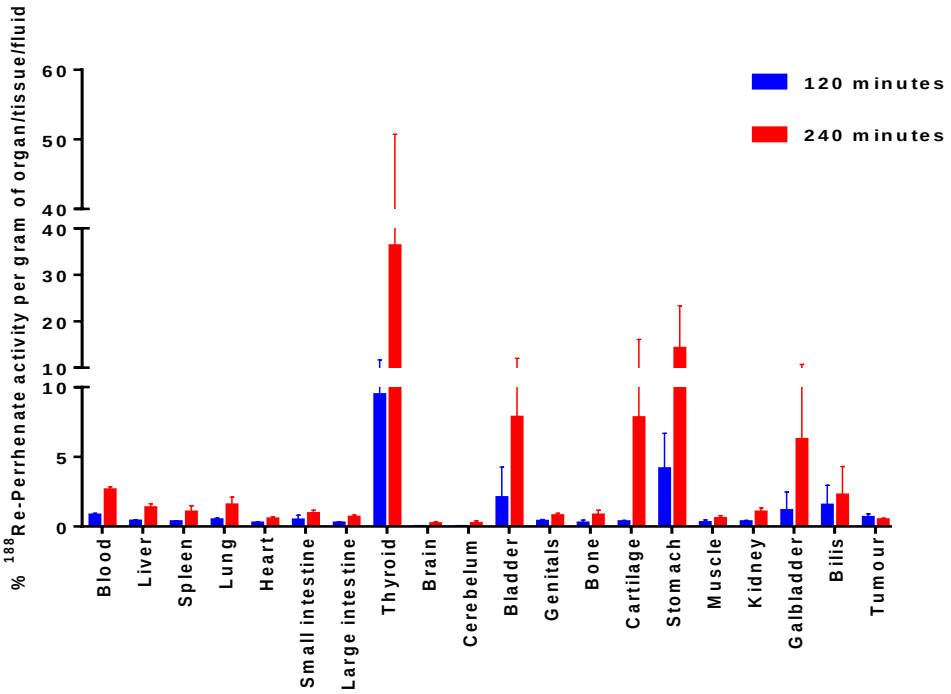

Figure 65. Biodistribution represented in percentage of activity per gram of organ/tissue/fluid, 120 and 240 minutes after the administration of ^{188}Re-Perrhenate and determined ex-vivo in mice with xenografts of osteosarcoma.

In addition, tumour/muscle, tumour/bladder, tumour/liver, tumour/lung and tumour/bone ratios were determined for all groups, with xenografts. Analysing the fig. 66, that shows the tumour ratios of mice with xenograft of bladder carcinoma and injected with ^{188}Re-Perrhenate, it's possible to visualize that tumour/muscle ratio is high comparing with the other tumour ratios. For 120 and 240 minutes after the administration, the tumour/muscle ratio was 2.92±0.55 and 2.80±0.51, respectively, demonstrating that the uptake by the tumour is higher than the muscle. Comparing these values with 1, that represents the equality between the tumour and muscle uptakes, the tumour/muscle ratio was statistically significantly higher at 120 minutes (p=0.024) and at 240 minutes (p=0.024). Tumour/bladder (0.45±0.27 at 120 min; 0.38±0.20 at 240 min) and tumour/lung (0.75±0.08 at 120 min; 0.73±0.18 at 240 min) ratios were always inferior to 1, demonstrating that the uptake by the tumour was inferior comparing to these organs. However these tumour ratios were only statistically significant lower for tumour/bladder at 240 minutes (p=0.032) and for

tumour/lung at 120 minutes (p=0.036). Tumour/liver (1.09±0.26 at 120 min; 1.11±0.19 at 240 min) and tumour/bone (1.90±0.53 at 120 min; 1.25±0.44 at 240 min) ratios were always superior to 1, demonstrating that the uptake by the tumour was superior comparing to these organs, however these ratios were not statistically significant. Considering these results, metastasis from a bladder carcinoma in lungs would appear as cold lesions, and metastasis in liver and bones would appear as hot lesions in nuclear medicine images. Therefore, if the goal was the therapy of bladder cancer metastases with ^{188}Re-Perrhenate, it wouldn't be possible taking into account the low selectivity of this radiopharmaceutical for metastatic tissue derived from a bladder carcinoma.

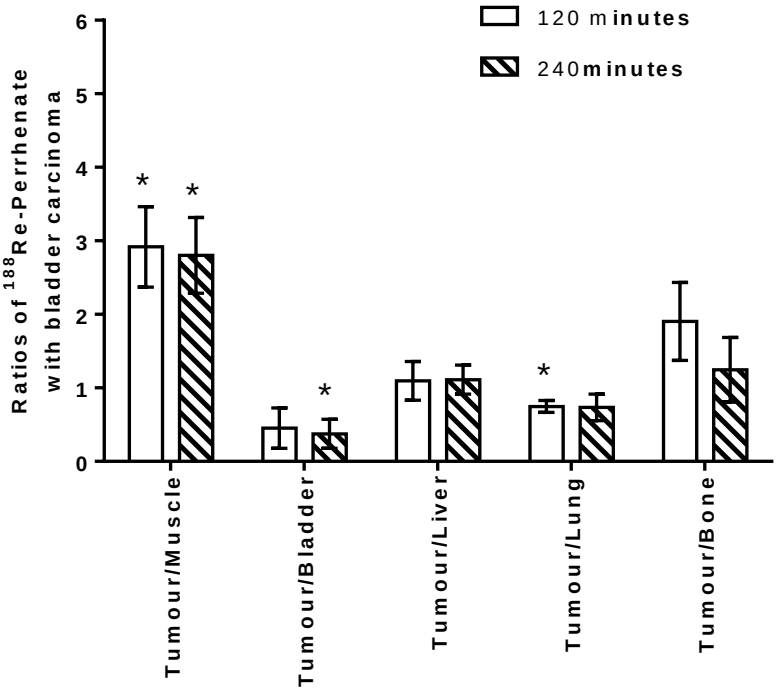

Figure 66. Tumour/muscle, tumour/bladder, tumour/liver, tumour/lung and tumour/bone ratios obtained for balb/c nu/nu mice with xenografts of bladder carcinoma after administration of ^{188}Re-Perrhenate.

Analysing the fig. 67, that represents the tumour ratios of mice with xenograft of osteosarcoma and injected with ^{188}Re-Perrhenate, it's possible to visualize that tumour/muscle ratio is high comparing with the other tumour ratios, however the difference between tumour/muscle ratio and tumour/bone ratio is smaller than

the others. For 120 and 240 minutes after the administration, the tumour/muscle ratio was 2.71±1.19 and 0.94±0.46, respectively, demonstrating that the uptake by the tumour is higher than of the muscle at 120 minutes and inferior or equal at 240 minutes. However comparing these values with 1, these tumour ratios were not statistically significant. Tumour/bladder ratio (0.62±0.38 at 120 min; 0.08±0.04 at 240 min) was always inferior to 1, demonstrating that the uptake by the tumour was inferior comparing with the bladder. However, tumour/bladder ratio was only statistically significant lower than unit at 240 minutes ($p<0.001$). Tumour/liver (1.61±0.47 at 120 min; 0.37±0.10 at 240 min), tumour/lung (1.35±0.33 at 120 min; 0.33±0.08 at 240 min) and tumour/bone (2.29±0.93 at 120 min; 0.64±0.22 at 240 min) ratios, were always superior to 1 at 120 minutes and inferior to one at 240 minutes. However these tumour ratios were only statistically significant lower for tumour/liver ratio at 240 minutes ($p=0.004$) and for tumour/lung ratio at 240 minutes ($p<0.001$). Considering these results, metastasis from an osteosarcoma in the liver, lung or bone at 120 minutes would appear as hot lesions and at 240 minutes would appear as cold lesions, in nuclear medicine images, after the administration of ^{188}Re-Perrhenate. Therefore, if the goal was the therapy of osteosarcoma metastases with ^{188}Re-Perrhenate, it wouldn't be possible taking into consideration the low selectivity of this radiopharmaceutical for metastatic tissue derived from a osteosarcoma.

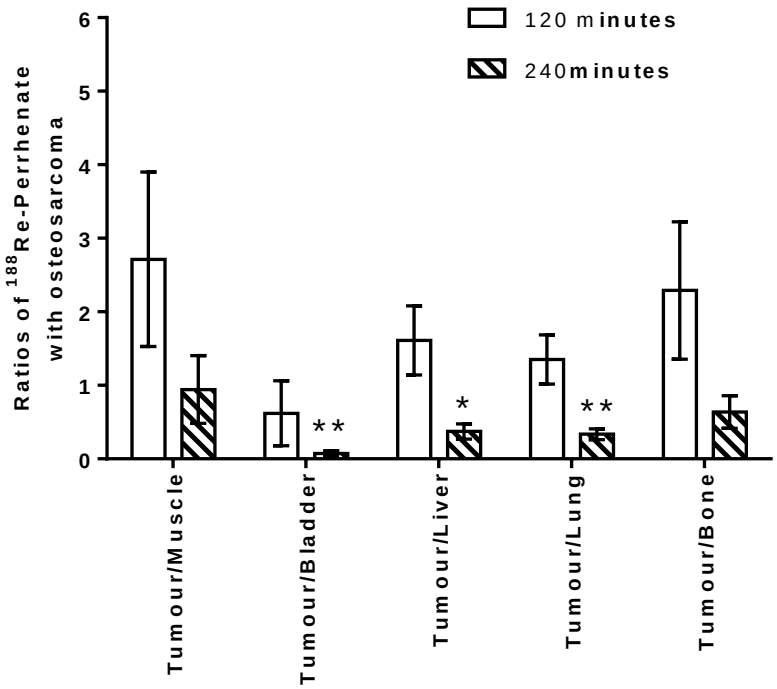

Figure 67. Tumour/muscle, tumour/bladder, tumour/liver, tumour/lung and tumour/bone ratios obtained for balb/c nu/nu mice with xenografts of osteosarcoma after administration of ^{188}Re-Perrhenate.

By analysing the fig. 68 that corresponds to the normal mice sacrificed 120 and 240 minutes after the administration of ^{188}Re-PEI-MP, it is possible to visualize a high uptake by the bladder wall and some uptake by the kidneys. These results support those obtained in the images of the biodistribution *in vivo* of ^{188}Re-PEI-MP in normal mice. As explained before this may indicate that ^{188}Re-PEI-MP is mainly excreted through the renal system. As explained before, the hydrophilicity of ^{188}Re-PEI-MP was not tested, however considering that ^{99m}Tc-PEI-MP is similar to ^{188}Re-PEI-MP it is expected that this complex is also hydrophilic and water soluble and the excretion should occur through the renal system. Considering that the bladder is carefully washed to remove any traces of urine, this uptake by the bladder wall demonstrates that ^{188}Re-PEI-MP as affinity for bladder cells, being this the primary reason to suspect that PEI-MP had some affinity to bladder carcinoma cells. Also it is possible to verify a high uptake by the lungs, supporting the results obtained in the *in vivo* images of normal mice. This could be explained by the fact that PEI-MP is a large

molecule, being trapped in the lung capillaries. Also the activity present at the liver and gallbladder, even being small, demonstrates that this polymer is also excreted through the hepatobiliary system. Being PEI-MP a polymer and a large molecule it is possible that ^{188}Re-PEI-MP is trapped by the Kupffer cells in the liver, that make part of the reticuloendothelial system. Considering the first propose of PEI-MP, that was for palliative therapy of bone metastases and also de results obtained in previous biodistribution studies [111], it's not surprising the uptake at bones. Moreover it is possible to visualize some retention of ^{188}Re-PEI-MP in the spleen, demonstrating that part of this complex is trapped by the reticuloendothelial system. The percentage of ^{188}Re-PEI-MP in blood is also high and seems to diminish over time.

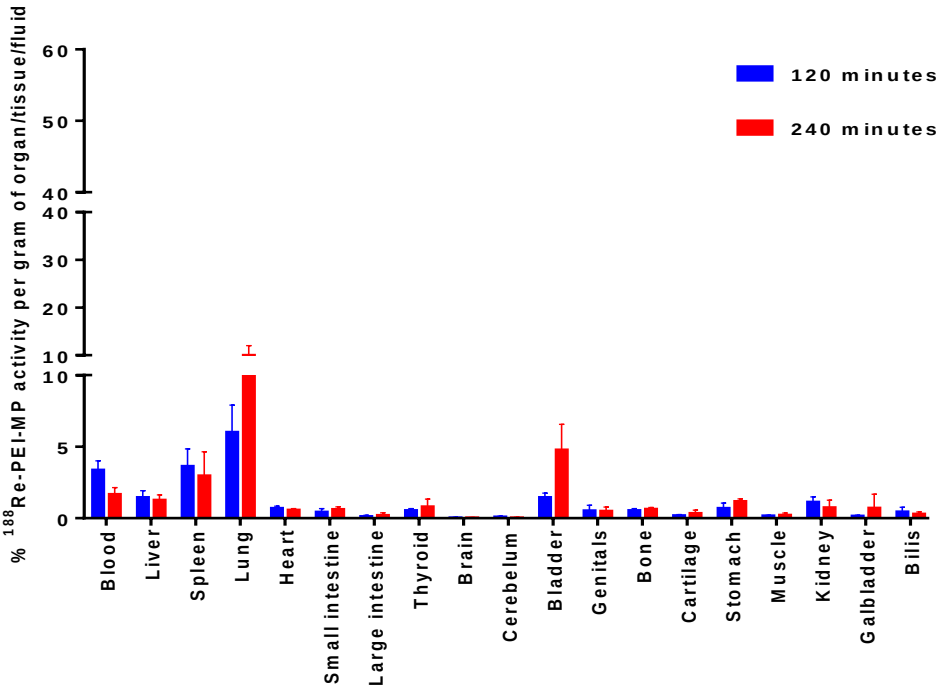

Figure 68. Biodistribution represented in percentage of activity per gram of organ/tissue/fluid, 120 and 240 minutes after the administration of ^{188}Re-PEI-MP and determined ex-vivo in normal mice.

By analysing the fig. 69 and fig. 70, which correspond to the mice with xenograft of bladder carcinoma and xenograft of osteosarcoma, respectively, sacrificed 120 and 240 minutes after the administration of ^{188}Re-PEI-MP, it is possible to visualize a high uptake by the bladder wall and kidneys. These results support

those obtained in the *in vivo* images of mice with xenografts of bladder carcinoma or osteosarcoma after the administration of ^{188}Re-PEI-MP, and are similar to the results of the biodistribution *ex vivo* in normal mice after the administration of ^{188}Re-PEI-MP. As explained before this may indicate that ^{188}Re-PEI-MP is mainly excreted through the renal system and that has an affinity for bladder cells. The uptake by the liver and gallbladder indicates, once again, that ^{188}Re-PEI-MP is also excreted through the hepatobiliary system, being possibly explained by the reasons discussed before. The activity in the liver diminished at 240 minutes. Also it is possible to verify some uptake by the lungs, supporting the results obtained in the *in vivo* images, and similar to the results of the *ex vivo* biodistribution in controls, being possibly explained by the reasons discussed before. In the same way as for *ex vivo* biodistribution studies in control mice after the administration of ^{188}Re-PEI-MP, it is possible to visualize some uptake by spleen and bone, possibly explained by the reasons discussed before. The percentage of ^{188}Re-PEI-MP in blood is also high and seems to decrease over time.

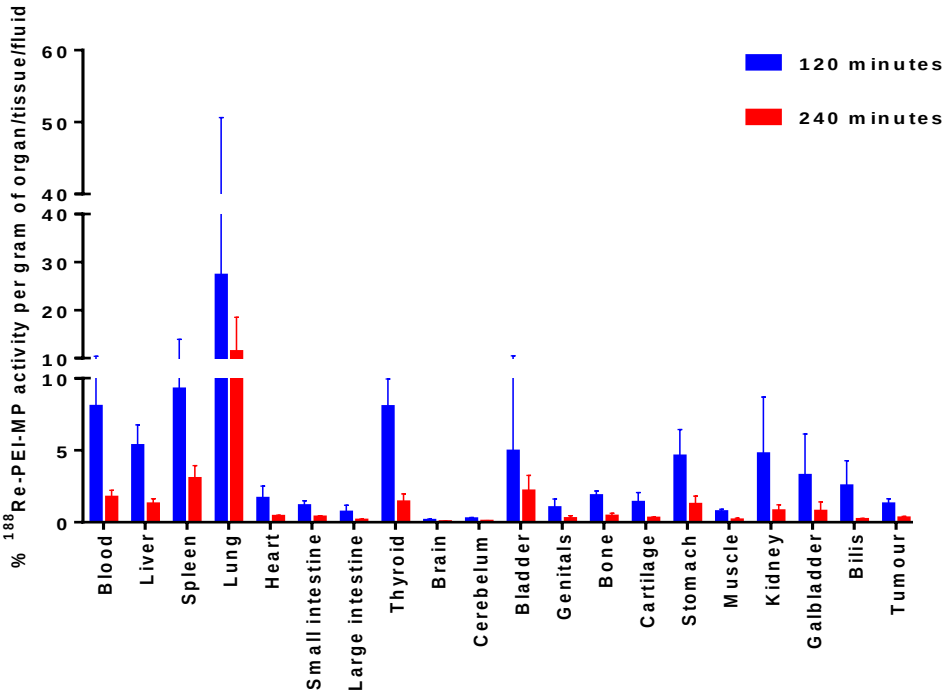

Figure 69. Biodistribution represented in percentage of activity per gram of organ/tissue/fluid, 120 and 240 minutes after the administration of ^{188}Re-PEI-MP and determined ex-vivo in mice with xenografts of bladder cancer.

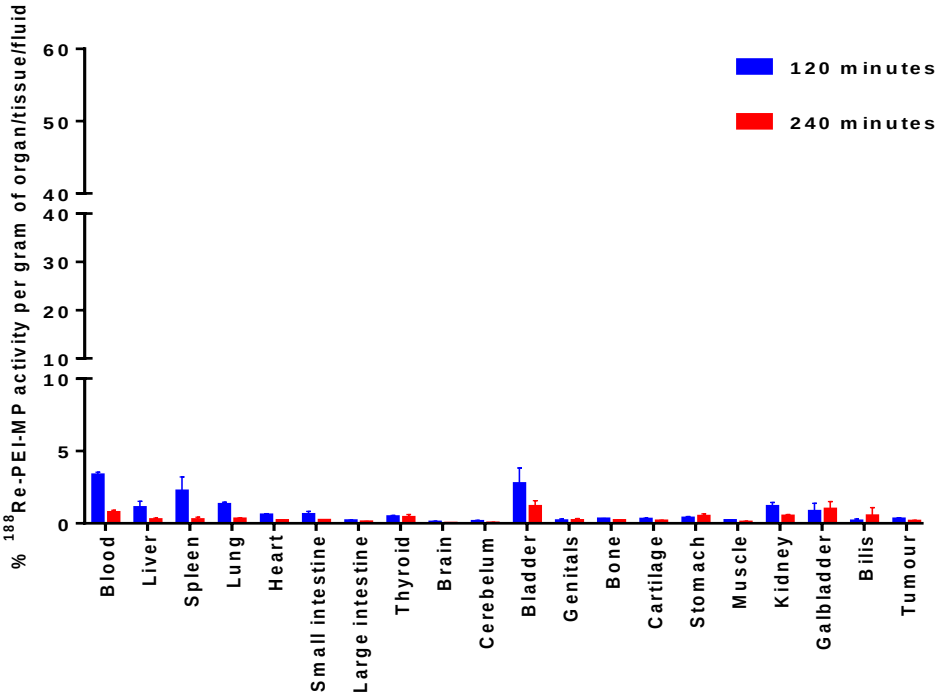

Figure 70. Biodistribution represented in percentage of activity per gram of organ/tissue/fluid, 120 and 240 minutes after the administration of ^{188}Re-PEI-MP and determined ex-vivo in mice with xenografts of osteosarcoma.

Analysing the fig. 71, that represents the tumour ratios of mice with xenograft of bladder carcinoma and injected with ^{188}Re-PEI-MP, it is possible to visualize that tumour/muscle ratio is high comparing with the other tumour ratios. For 120 and 240 minutes after the administration, the tumour/muscle ratio was 1.79±0.71 and 1.85±0.36, respectively, demonstrating that the uptake by the tumour is higher than the muscle. However comparing these values with 1, the tumour/muscle ratio was not statistically significantly higher at 120 or 240 minutes. Tumour/bladder (0.29±0.18 at 120 min; 0.17±0.06 at 240 min), tumour/liver (0.25±0.06 at 120 min; 0.24±0.03 at 240 min), tumour/lung (0.06±0.04 at 120 min; 0.09±0.15 at 240 min) and tumour/bone (0.70±0.21 at 120 min; 0.75±0.10 at 240 min) ratios were always inferior to 1, demonstrating that the uptake by the tumour was inferior comparing to these organs. However these tumour ratios were only statistically significant lower for tumour/bladder at 240 minutes ($p<0.001$), for tumour/liver at 120 minutes ($p<0.001$) and at 240 minutes ($p<0.001$), for tumour/lung at 120 minutes ($p=0.004$) and at 240

minutes (p=0.004). Considering these results, metastasis from a bladder carcinoma in liver, lung and bones would appear as cold lesions in nuclear medicine images, after the administration of ^{188}Re-PEI-MP. Therefore, the therapy of bladder cancer metastases with ^{188}Re-PEI-MP it wouldn't be recommended, since the irradiation of non-target tissues such as the liver, the lungs and bones would be higher than desirable, and can mean significant side effects, if this radiopharmaceutical was used. Also the uptake by these metastases would be too low so that the therapy with this radiopharmaceutical could be effective.

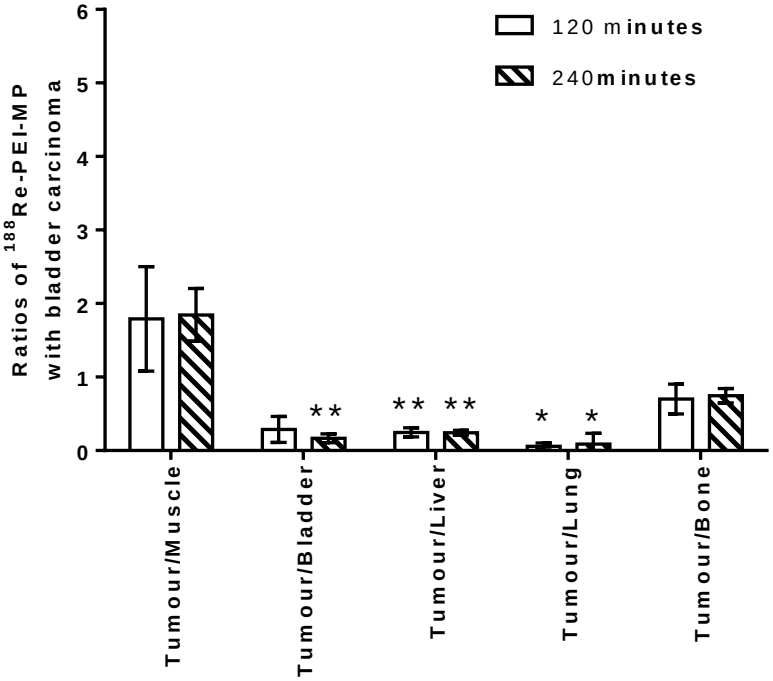

Figure 71. Tumour/muscle, tumour/bladder, tumour/liver, tumour/lung and tumour/bone ratios obtained for balb/c nu/nu mice with xenografts of bladder carcinoma after administration of ^{188}Re-PEI-MP.

Analysing the fig. 72, that represents the tumour ratios of mice with xenograft of osteosarcoma and injected with ^{188}Re-PEI-MP, it is possible to visualize that tumour/muscle ratio is high comparing with the other tumour ratios. For 120 and 240 minutes after the administration, the tumour/muscle ratio was 1.58±0.45 and 1.64±0.35, respectively, demonstrating that the uptake by the tumour is

higher than the muscle. However comparing these values with 1, the tumour/muscle ratio was not statistically significantly higher at 120 or 240 minutes. Tumour/bladder (0.14±0.08 at 120 min; 0.11±0.02 at 240 min), tumour/liver (0.32±0.15 at 120 min; 0.56±0.13 at 240 min), tumour/lung (0.25±0.09 at 120 min; 0.42±0.15 at 240 min) ratios were always inferior to 1, demonstrating that the uptake by the tumour was inferior comparing to these organs. However these tumour ratios were only statistically significant lower than one for tumour/bladder at 240 minutes ($p<0.001$), for tumour/liver at 240 minutes ($p=0.028$) and for tumour/lung at 240 minutes ($p=0.016$). Tumour/bone ratio (1.02±0.30 at 120 min; 0.60±0.17 at 240 min), was almost equal to one at 120 minutes and inferior at 240 minutes. However comparing these values with 1, these tumour ratios were not statistically significant. Considering these results, metastasis from an osteosarcoma in liver and lungs would appear as cold lesions, and in bones wouldn't be visible at 120 minutes and would appear as cold lesions at 240 minutes in nuclear medicine images, after the administration of ^{188}Re-PEI-MP. Therefore, if the goal was the therapy of osteosarcoma metastases with ^{188}Re-PEI-MP, it wouldn't be recommended because the irradiation of non-target organs like the liver, the lungs and bones would be higher than desirable, with significant side effects from the use of this radiopharmaceutical. Furthermore, the uptake by these metastases would be too low, and the treatment with this radiopharmaceutical wouldn't be effective.

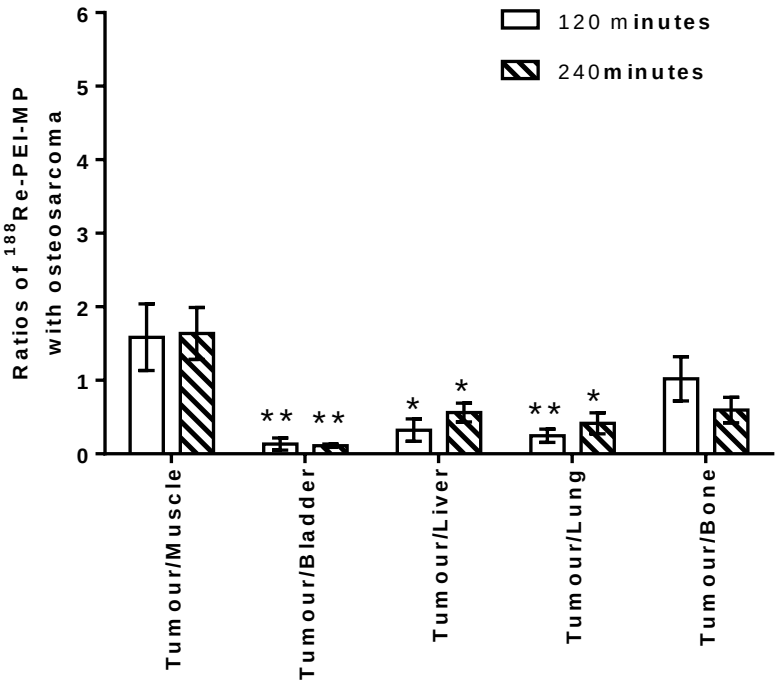

Figure 72. Tumour/muscle, tumour/bladder, tumour/liver, tumour/lung and tumour/bone ratios obtained for balb/c nu/nu mice with xenografts of osteosarcoma after administration of ^{188}Re-PEI-MP.

6.4. Section discussion

As mentioned before, since *in vitro* studies are conducted in a controlled environment, and knowing that a tumour is not only a set of tumour cells but a complex aggregate of tumour cells, supporting cells, nerves and vascular and lymphatic vessels, the *in vitro* results may not correspond to those obtained in a living organism. Therefore, it was imperative to conduct *in vivo* studies to analyse the potential of PEI-MP radiolabelled with ^{99m}Tc for early diagnosis and with ^{188}Re for therapy of bladder cancer, and to sustain the results obtained *in vitro*. The main purposes were to verify if the tumour cell uptake and retention of the referred complexes was maintained, to understand the biodistribution and biokinetics of these complexes *in vivo*, and identify the target organs, the routes of metabolism and excretion of ^{99m}Tc-PEI-MP and ^{188}Re-PEI-MP, by nuclear medicine imaging in a first approach and, after using animals for determination of the biodistribution for each organ. It was also an objective to compare the

potential of the referred complexes in osteosarcoma animal models. For the fulfil of all procedures involving animals, first it was obtained the approval by the Ethics Committee for Health of the Faculty of Medicine of the University of Coimbra and all the studies were performed according to their legislation.

The first step for carrying the *in vivo* and *ex vivo* studies was to choice a suitable animal tumour model. The animal tumour models chosen were the immunodeficient mice balb/c nu/nu with subcutaneous xenografts of bladder carcinoma or osteosarcoma. The balb/c nu/nu mice have genetic immune deficiencies, this is, has one or more mutations that minimize or prevent the rejection of the grafted tissues from other species [318]. These models have several advantages, namely, they are cost effective, provide a direct assessment of efficacy against a human cancer through calliper measurement of tumour size, and the tumour is accessible allowing the harvesting of tumour tissue [328-330]. The xenografts of osteosarcoma and bladder carcinoma developed well in 3 and 4 weeks, respectively, after the subcutaneous injection of a suspension of 5 million cells in the right axilla dug of the mice. The place chosen for the development of the xenografts demonstrated to be the best choice, given the fact that is contra lateral to the heart, is away from the liver, bladder and kidneys, avoiding the overlapping in the nuclear medicine images, once those organs can also be target of the administered radiopharmaceuticals. Also is a good area of expansion, and has a good vascularisation, which can explain the fast development of the xenografts, and is an area that allows a quick and easy excision of the tumour. Therefore for the planed experiments the animal tumour models chosen served its purpose. However it is important not to forget that human cells are placed in a murine environment, creating interactions that may not faithfully reflect the human disease process (e.g., differences in the local cell environment, cytokine, chemokine, and growth factor incompatibility, differences in immunologic state, etc.) [318]. Also, since for the development of these tumour models, immunocompromised animals are needed, and knowing that these animals are highly susceptible to viral, bacterial, and fungal infections, and that there are agents that can change the outcome and the reproducibility of the experiments, the animals must be

maintained in specific pathogen-free (SPF) environments, which increases the research costs [318].

Studies *in vivo* and ex-vivo using balb/c nu/nu mice with xenograft of bladder carcinoma and xenograft of osteosarcoma started when the tumour volumes reached 500-1000 mm^3, considered as sufficient for nuclear medicine imaging, taking into account the size of the mice. Also it is the maximum volume which will allow the least discomfort possible for the mice.

For nuclear medicine images it is important to maintain the mice immobilized, because if they move during the acquisition images, makes impossible the image analysis. The best way to immobilize a mouse is to anesthetize him. The anaesthesia was performed after the subcutaneous administration in the back of the mouse of a solution of ketamine 77% and chlorpromazine 23%. Ketamine is a rapid-acting general anaesthetic producing an anaesthetic stated characterized by profound analgesia, normal pharyngeal-laryngeal reflexes, normal or slightly enhanced skeletal muscular tone, cardiovascular and respiratory stimulation, and occasionally a transient and minimal respiratory depression. Has a wide margin of safety and short period of action, allowing several administrations to maintain the anaesthetic state. The chlorpromazine is a dopamine antagonist, possessing anti-cholinergic properties that cause sedation [337]. This solution demonstrated to be effective in producing an anaesthetic state without significant side effects to the mice. One of the side effects of the anaesthesia is the decrease of body temperature, therefore during the anaesthetic state, it was controlled [337]. For image acquisition, mice were placed in prone on top of the gamma-camera collimator, with the superior and inferior members kept away from the trunk. This position is appropriate so that the organs are closer to the detector without interference of the spine, and allows the tumour stay well-defined in the images.

Images started after the intravenous administration in the tail vein of the radiopharmaceuticals ^{99m}Tc-Pertechnetate, ^{99m}Tc-PEI-MP, ^{188}Re-Perrhenate or ^{188}Re-PEI-MP in mice without and with xenograft of bladder carcinoma and osteosarcoma. The dynamic images proved to be useful to confirm the injection and the distribution of the radiopharmaceuticals in the bloodstream of mice. The

static images obtained each 30 minutes following the administration of the radiopharmaceuticals proved to be adequate to obtain images with a better resolution and to follow the biodistribution along the time.

The images obtained with the ^{99m}Tc-Pertechnetate and ^{188}Re-Perrhenate are controls and show the normal biodistribution of these radiopharmaceuticals, but they can also be radiochemical impurities produced during the labelling process of PEI-MP kit with ^{99m}Tc-Pertechnetate or with ^{188}Re-Perrhenate. In these images is normal to obtain a high uptake in the thyroid, stomach, and choroid plexus. On another hand, if the radiochemical impurities exist the reduced/hydrolyzed technetium/rhenium species, it was expected to obtain a high uptake in the liver and the spleen. The biodistribution verified in the images will be a mirror of the radiochemical purity of the ^{99m}Tc-PEI-MP and ^{188}Re-PEI-MP, therefore is very important to control the radiochemical purity after radiolabelling. Images obtained after the administration of ^{99m}Tc-Pertechnetate and ^{188}Re-Perrhenate in normal mice, in mice with xenograft of bladder carcinoma and in mice with xenograft of osteosarcoma, demonstrated the expected biodistribution mentioned above. In the mice with xenografts of bladder carcinoma and osteosarcoma, it was verified a small uptake by the tumour. Since the images had low resolution, the uptake quantification was difficult, whereby it was important to obtain more quantitative data with the *ex vivo* studies.

After obtaining the images of the control mice without tumour and with xenografts of bladder carcinoma and osteosarcoma with ^{99m}Tc-Pertechnetate or ^{188}Re-Perrhenate, ^{99m}Tc-PEI-MP or ^{188}Re-PEI-MP were intravenously injected in the same animal models. By analysing the images obtained in these animal models mice, it was possible to visualize a high uptake in kidneys and bladder, indicating that these radiopharmaceuticals are excreted mainly through the renal system. In fact, taking in consideration the results of the partition coefficient demonstrated in Chapter V, clearly demonstrating that ^{99m}Tc-PEI-MP is a hydrophilic molecule, and therefore water soluble, it's not surprising that the main way of excretion is through the renal system and consequently eliminated through urine. This is an advantage because there are no retention in liver and fat tissue, and the faster kidney excretion allows for a higher target/background

ratio [273]. The hydrophilicity of the ^{188}Re-PEI-MP was not tested, however considering that ^{99m}Tc-PEI-MP is similar to ^{188}Re-PEI-MP it is expected that this complex is also hydrophilic and water soluble, what seems to be proved by the obtained images.

Also it was found a faint uptake by the lungs in the *in vivo* images that seem to decrease over time, especially after the intravenous administration of ^{188}Re-PEI-MP. This could be explained because the PEI-MP is a large molecule, being trapped in the lung capillaries, and as the ^{188}Re has a number of atomic mass bigger than the ^{99m}Tc, the complex ^{188}Re-PEI-MP may be larger than ^{99m}Tc-PEI-MP [61].

In mice with xenografts of bladder carcinoma and osteosarcoma was verified a small uptake of ^{99m}Tc-PEI-MP or ^{188}Re-PEI-MP by the tumour. Also the images had low resolution to be possible to quantify the uptake, therefore it was important to obtain more quantitative data with the *ex vivo* studies.

The evaluation of the biodistribution and biokinetics of ^{99m}Tc-PEI-MP and ^{188}Re-PEI-MP by *in vivo* imaging may not be enough to respond to all questions, given the low resolution of the conventional gamma-camera. Therefore, it was necessary to obtain the percentage of uptake of the radiopharmaceutical administered for each organ and tissue, as well as the uptake ratios of between the tumour and some organs, especially those where it is expected that have metastases from the tumours. This information was only gathered after the sacrifice of mice and the collection of every organs, tissue, fluid and tumour. The *ex vivo* studies performed after the administration of ^{99m}Tc-Pertechnetate and ^{188}Re-Perrhenate in mice without tumour and with xenografts of bladder carcinoma and osteosarcoma supports the results obtained in the *in vivo* images, being the target organs the thyroid, the stomach, and the choroid plexus. Also it was verified a small uptake by the tumours, supporting the results obtained in the *in vivo* images after the administration of ^{99m}Tc-Pertcehnetate and ^{188}Re-Perrhenate. The uptake by bladder carcinoma and osteosarcoma xenografts may be related with the blood supply to these xenografts, which is in accordance with the rich vascularisation of the axillary dug where the xenografts grew.

The *ex vivo* studies performed after the administration of ^{99m}Tc-PEI-MP and ^{188}Re-PEI-MP in mice without tumour and with xenografts of bladder carcinoma and osteosarcoma supports the results obtained in the *in vivo* images, where it is verified a high count rate in the kidneys and the bladder, demonstrating that these complexes are mainly excreted through the renal system. However, considering that the bladder was carefully washed to remove any traces of urine, this activity of the bladder wall demonstrates, once again, that ^{99m}Tc-PEI-MP or ^{188}Re-PEI-MP as affinity for bladder cells, being this the primary reason to suspect that PEI-MP could have some affinity to bladder cancer cells.

Supporting the results of the *in vivo* images it was possible to verify in the *ex vivo* studies, some uptake in lungs, possibly explained by reason referred before.

What was not possible to visualize in the *in vivo* images, but was verified in the *ex vivo* studies, for mice injected with ^{99m}Tc-PEI-MP or ^{188}Re-PEI-MP, was some uptake by the liver and the gallbladder demonstrating that, in part, these radiopharmaceuticals are also excreted through the hepatobiliary system. Being PEI-MP a polymer and being a large molecule, it is possible that these radiopharmaceuticals may be trapped by the Kupffer cells in the liver that make part of the reticuloendothelial system, are degraded and subsequently released in the gallbladder. Also it was possible to visualize some retention of ^{99m}Tc-PEI-MP and ^{188}Re-PEI-MP in the spleen, demonstrating that some percentage of this complex is trapped by the reticuloendothelial system.

Considering the first propose of PEI-MP, that was for palliative therapy of bone metastases and also de results obtained in previous biodistribution studies [111], it's not surprising the uptake of ^{99m}Tc-PEI-MP and ^{188}Re-PEI-MP by the bone.

Also, it was verified some uptake by the tumours, what supports results obtained in the images after the administration of ^{99m}Tc-PEI-MP and ^{188}Re-PEI-MP. The uptake by bladder carcinoma and osteosarcoma xenografts may be related not only with the good blood supply to these xenografts,, but also with the EPR effect associated to this polymer.

As discussed by Maeda *et al.* [169] and Seymour [170] the EPR effect, is the process in which water soluble macromolecules accumulate passively within tumour tissue, either primary or metastatic in nature, due to leaky blood vessels and poor lymphatic clearance. Therefore, theoretically, being PEI-MP a water soluble macromolecule it would follow this principle. Several studies were already conducted that assigns to PEI-MP this characteristic. For example, Dormehl IC *et al.* developed PEI-MP considering the EPR effect [111], and studied the biodistribution of several molecular sized PEI-MP radiolabelled with ^{99m}Tc. The results demonstrated that the smaller fraction of PEI-MP (10-30 kDa) had the best tumour uptake. In the same way Jansen D *et al*., demonstrated that ^{117m}Sn-PEI-MP, in the same fraction, also presented a higher affinity for tumour tissue [176]. Therefore it was expected that ^{99m}Tc-PEI-MP and ^{188}Re-PEI-MP, in the chosen fraction 10-30 kDa, would have a good uptake by the tumour tissue, which was confirmed by the *in vivo* and *ex vivo* studies. The retention of these complexes in the tumour, at least for 240 minutes, may be related with the EPR effect. As mentioned before tumour tissues have poor lymphatic drainage and slow venous return, allowing that macromolecules like PEI-MP are retained in the tumour, whereas extravasation into the tumour interstitium continues [171, 173]. The high period of retention of ^{99m}Tc-PEI-MP may be an advantage to perform diagnostic nuclear medicine images, to localize and delineate the tumour. Also for ^{188}Re-PEI-MP the tumour retention for a long period of time could be an advantage since gives time to deliver the high energetic β^- particles to the tumour cells, inducing tumour cell death [59]. Because the accumulation of macromolecules by the EPR effect is a progressive phenomenon, it is essential that the molecules are stable in the plasma for long periods [173]. In the *ex vivo* biodistribution studies was clear a high percentage of ^{99m}Tc-PEI-MP or ^{188}Re-PEI-MP in the blood, despite its reduction at 240 minutes after the administration. Owing to the prolonged retention of the polymeric complexes like ^{99m}Tc-PEI-MP or ^{188}Re-PEI-MP by the EPR effect and the enhanced plasmatic half-life, less frequent administrations would be needed, which is of great benefit to patients [173, 175].

However, the affinity of PEI-MP to bladder carcinoma or osteosarcoma is related not only with the vascularisation and the EPR effect, but also with the

fact that PEI-MP is a phosphonate derivative. Taniguchi M. *et al*. reported a case of a calcified transitional cell carcinoma of the bladder visualized in a bone scintigraphy performed with ^{99m}Tc-HMDP (a diphosphonate) and suggested possible uptake mechanisms. Calcification in uroepithelial tumours of the bladder is a rare radiographic finding and clearly characterized by a high concentration of calcium. As it is known, phosphonates has a particular affinity for calcium (Ca^{2+}) [102], hence its uptake. In the transitional cell carcinoma of the bladder, the most common location of calcifications is on the surface of the tumour epithelium creating incrustations. It is believed that the incrustation reflects a local interaction of pH related with urinary calcium and the tumour epithelium, since calcium precipitation is favoured by an alkaline urinary pH [338]. On the other hand, Moreno AJ *et al*. reported a case of transitional cell carcinoma of the kidney identified by imaging with ^{99m}Tc-MDP, that after histopathological examination it wasn't found any calcification in the tumour, suggesting several uptake mechanisms other than chemisorption, such as a possible selective binding of ^{99m}Tc-MDP with the tissue receptors or a hypervascularization [339]. Therefore, being PEI-MP a diphosphonate, the uptake of ^{99m}Tc-PEI-MP or ^{188}Re-PEI-MP by bladder carcinoma could be related with some of the factors mentioned by the referred authors. For osteosarcoma, the uptake is related with the presence of high concentrations of Ca^{2+} and with the strong affinity of phosphonates to the hydroxyapatite crystals, as already mentioned [102, 108].

In addition of calculating the percentage of activity per gram of organ/tissue/fluid, it was also determined the values of the tumour/muscle, tumour/bladder, tumour/liver, tumour/lung and tumour/bone ratios for all groups. Considering that, in case of metastases of a bladder carcinoma, the major target organs are the liver, lungs and the bone, and knowing that the bladder carcinoma has its origin in the bladder wall and in an initial stage the tumour will invade the muscle adjacent to this organ [184], is crucial to determine these tumour ratios, which can be done by nuclear medicine images. If the radiopharmaceutical uptake by the primary tumour or its metastases is equal to the uptake of the other organs, it's not possible to identify them, and therefore, the diagnosis could be inconclusive or negative to the tumour or to the

metastases. Also, the determination of those tumour/organ ratios is important, mainly when radionuclide therapy with ^{188}Re-PEI-MP in an option. In these circumstances, the main target should be the tumour and its metastases, and the non-target organs should be spared of high doses of ionizing radiation. If the radiopharmaceutical uptake by the tumour or its metastases is equal or lower to the uptake of the other organs, it is not possible to perform the therapy, since it would be the non-target organs the most affected by ionizing radiation and the therapy would not be effective, and possibly it would result in serious adverse effects.

For mice with xenografts of bladder carcinoma or osteosarcoma, after the administration of ^{99m}Tc-PEI-MP or ^{188}Re-PEI-MP, the tumour/muscle ratios were always superior to 1, demonstrating that the uptake by the tumour (bladder carcinoma or osteosarcoma) was bigger than muscle. The fact of the ^{99m}Tc-PEI-MP uptake by the tumour is higher than by the muscle, is an advantage and could allow to determine the degree of muscle invasion and could assist the surgery to determine how much muscle should be excised with the tumour and the bladder [188]. Also the high tumour/muscle ratio obtained with ^{188}Re-PEI-MP is an advantage for the therapy, allowing sparing the muscle from the action of high doses of ionizing radiation.

For the mice with xenografts of bladder carcinoma and osteosarcoma where ^{99m}Tc-PEI-MP were administered, tumour/bladder, tumour/liver, tumour/lung and tumour/bone was always inferior to 1 demonstrating that the uptake by the tumour was inferior to the quoted organs. Considering these results, the tumour of the bladder wall, and the metastases from a bladder carcinoma or osteosarcoma in liver, lung and bones would appear as cold lesions in nuclear medicine images, after the administration of ^{99m}Tc-PEI-MP. Therefore, it would be possible to identify the tumour and its metastases, in a non-invasive and in an effective way, after intravenous injection of ^{99m}Tc-PEI-MP, and the images must be acquired until 240 minutes after the radiopharmaceutical administration. Equally, for mice with xenografts of bladder carcinoma and osteosarcoma where ^{188}Re-PEI-MP were administered, tumour/bladder, tumour/liver, tumour/lung and tumour/bone was always inferior to 1 demonstrating that the uptake of the tumour was inferior comparing with these

organs. Considering these results, the primary tumour and its metastases from a bladder carcinoma or osteosarcoma in liver, lung and bones would appear as cold lesions in nuclear medicine images, after the administration of ^{188}Re-PEI-MP. Therefore, if the goal was the therapy of bladder carcinoma or osteosarcoma, and their metastases after the intravenous administration of ^{188}Re-PEI-MP, it wouldn't be possible taking into consideration that the irradiation of non-target tissue like the bladder wall, the liver, the lungs and the bones would be higher than desirable, and could present significant adverse effects from the use of this radiopharmaceutical. Also the uptake by these metastases would be too low, so that the therapy with this radiopharmaceutical could be non-effective.

Section IV. Discussion, Conclusions and Future Perspectives

Chapter 7.Final Discussion

Cancer is a serious disease and the bladder cancer (primary or secondary) is a catastrophic event for the patient and has a negative impact on quality of life and on social environment [67, 340]. As referred in Chapter 2, cancer is easier to treat and cure, if it is diagnosed early [35, 36]. Current diagnostic methods for bladder cancer are mainly morphologic imaging techniques like pyelography, ultrasonography, CT scanning, magnetic resonance imaging and cytoscopy, having each of these methods advantages and disadvantages [183, 194, 219-221]. The potential of functional imaging techniques is not being fully availed for this type of cancer. The advantage of being able to visualize physiopathological processes is based on the fact that they arise prior to morphological changes, which allows the diagnosis in a very early stage of the disease [183, 194, 219-221]. If we had a molecule with specificity affinity to a particular target of the bladder cancer, it could be used, if properly radiolabelled, to give information about the physiopathological processes through an image, helping to identify neoplastic masses of reduced size, and evaluate the eventual spread of bladder cancer, that could be impossible or very difficult to identify early with the diagnostic methods currently used. Until now, has not yet been developed a molecule with specific affinity for the bladder tissue.

Therefore, it seems urgent to identify new molecules that could be radiolabelled for diagnostic nuclear medicine imaging or for metabolic radiotherapy.

Non-invasive and early diagnosis of cancer is of crucial importance for effective treatment, and also would allow a more conservative management and therapy [35, 36]. Systemic treatment options for bladder cancer include surgery, chemotherapy, radiation, and immunotherapy. The choice on the therapeutic modality will depend on the tumour staging. In early stage of bladder cancer transurethral resection is a common surgical option while partial or radical cystectomy is performed for muscle-invasive and locally advanced bladder cancer [177]. Conservative management with organ preservation is now the

standard of care in numerous malignancies, and for bladder cancer patients it is imperative, because less surgery means no need for an urinary diversion, and the possibility of a normal sexual life [252]. Non-surgical treatment of invasive bladder cancer has been traditionally reserved for patients who are unfit for, or refuse radical cystectomy, but there are growing evidences that the evolution of radiotherapy (XRT) techniques and the availability of new chemotherapeutic protocols, have made bladder-saving treatment a competitive alternative to radical cystectomy in selected patients [198]. Historically, it is shown that local disease is controlled in only about 20% of patient treated with transurethral resection alone [253, 254] and 40% treated with XRT alone [255, 256]. Some studies have shown that combined transurethral resection with chemotherapy [230, 257] or XRT with chemotherapy [258, 259] can improve the treatment of the disease, but the best results are obtained using a trimodality strategy in which radiochemotherapy follows transurethral resection. As mentioned in Chapter 4 there is no reference to the use of radiopharmaceuticals for radiotherapy in bladder cancer. If we think in diagnose, the alliance of a radionuclide with a molecule with specific affinity to a particular cell or organ, gives specific functional information about that cell or organ. In terms of bladder cancer therapy, if we have a radiolabelled molecule with specific affinity to bladder tumour cells, it could improve the therapy of the primary tumour and its metastasis, enabling the delivery of high radiation doses to the target tissue with minimal side effects.

As described in Chapter 3, polyethyleneiminomethyl phosphonic acid (PEI-MP) was developed by Dormehl IC *et al.* for use in palliative therapy of bone metastases after suitable radiolabelling [67, 111]. Besides to be a bone-seeking agent, PEI-MP would accumulate in solid tumours due to the EPR effect [169, 170]. The studies that followed have established the biodistribution and pharmacokinetic properties of different complexes PEI-MP/metal radionuclides (^{99m}Tc, ^{117m}Sn and ^{186}Re) [129, 174, 267]. For any of the three complexes obtained and studied the dosimetric calculations have shown that the critical organ was consistently the bladder [111, 267]. The high count rate in the bladder wall with the different PEI-MP/metal radionuclides seems something that deserves to be further and better studied. As referred in Chapter 4, the

possibility of a high uptake of PEI-MP complexes by bladder tumour cells, and the EPR effect associated with this polymer [169, 170], assigns a high potential to the PEI-MP, if conveniently radiolabelled, for diagnosis and therapy of bladder cancer, more specifically, through the ^{99m}Tc-PEI-MP for diagnosis and ^{188}Re-PEI-MP for therapy of bladder cancer. As described in Chapter II, the technetium-99m (^{99m}Tc) is the most widely used radioisotope in diagnostic nuclear medicine due to its availability, its favourable physical properties and its versatile chemistry that allows the labelling of a great variety of ligands [55, 71], including the PEI-MP, making possible to apply this molecule for the diagnostic imaging. Also in Chapter 2, rhenium-188 (^{188}Re) is described as an excellent candidate for β^- particle therapy, particularly for large tumour masses given to the energy and tissue penetration of their β^- particles [66, 76-78, 81]. Other physical characteristics of ^{188}Re that constitute an advantage is its gamma ray emission that can be used for dosimetry purposes and to monitor biological distribution during therapy [61, 66, 76, 82, 83], and the relatively short physical half-life of 16.9 hours that allows the use of high activities and reduces the problem of radioactive waste handling and storage [82, 84]. The rhenium is a chemical congener of ^{99m}Tc, which means that ^{99m}Tc agents can be used as the "matched pair" for the corresponding ^{188}Re agent. This particularity associated with its physical characteristics of the rhenium makes feasible to obtain excellent diagnostic imaging, allowing pre- and post-assessment of patients treated with ^{188}Re radiopharmaceuticals [41]. According to these physic-chemical characteristics, the PEI-MP may also be radiolabelled with ^{188}Re, whereby it is possible to evaluate the potential of ^{188}Re-PEI-MP for therapy.

Therefore, the aim of this work was to verify the potential of PEI-MP radiolabelled with ^{99m}Tc for the early diagnosis, and radiolabelled with ^{188}Re for therapy of bladder cancer. Also, taking into account the initial purpose of PEI-MP the same studies were conducted in parallel for bone cancer [102, 111].

After a successful synthesis of the polymer and preparation of the kits, it was proceeded to labelling of the PEI-MP kits with ^{99m}Tc-pertechenetate and ^{188}Re-perrhenate, and radiochemical purity of the complexes was evaluated. The results of radiochemical purity showed to be better for ^{99m}Tc-PEI-MP (superior to 89%) than for the ^{188}Re-PEI-MP (superior to 85%). This high radiochemical

purity was maintained during at least 5 hours, revealing the stability of the kit formulation, and ensuring its use for a long period of time which is an advantage, since allows performing several experimental studies in the same day, which would also be an advantage for clinical use. To determine the radiochemical purity of these labelling kits the chromatographic systems chosen demonstrated to be adequate and efficient in separating the contaminant radiochemical species of ^{99m}Tc and ^{188}Re (free and reduced/hydrolyzed forms) [61, 71, 87].

Considering that during the experimental studies the complexes ^{99m}Tc-PEI-MP and ^{188}Re-PEI-MP would be exposed to cellular culture medium (DMEM) and to variations of room temperature (22 ºC to 45 ºC), radiochemical purity of ^{99m}Tc-PEI-MP complex was evaluated in those conditions. Given the impossibility of performing this experiment with ^{188}Re-PEI-MP, the results of radiochemical purity of this complex in cellular culture medium and at several temperatures, can only be extrapolated according to its similarities with ^{99m}Tc-PEI-MP complex. The results demonstrated that the exposure to temperatures of 22, 37 and 45 ºC didn't change significantly the radiochemical purity of ^{99m}Tc-PEI-MP during 5 hours. Similarly, the addition of cellular culture medium didn't change significantly the radiochemical purity, independently of the temperature, remaining superior to 85%. These results demonstrated that experimental studies could be performed without the worrying of loose the high radiochemical purity of ^{99m}Tc-PEI-MP, and certainly of ^{188}Re-PEI-MP.

The hydrophilicity and lipophilicity of a radiolabelled molecule has consequences on the biodistribution and biokinetics of the complex. Therefore the hydrophilicity of ^{99m}Tc-PEI-MP was evaluated over 4 hours after the radiolabelling. The results demonstrated that this complex was hydrophilic, and hence water soluble. Although it was not possible to perform these evaluations with ^{188}Re-PEI-MP, but considering their similarities, it would be expected the same hydrophilicity, which in turn was confirmed by the results obtained in the *in vivo* and *ex vivo* studies. These characteristic, perhaps means that the complexes would not be uptaked significantly by the liver or fat tissue, and would be eliminated very quickly through the renal system [273]. However,

these expected results didn't correspond totally with those obtained in the *in vivo* and *ex vivo* studies as it will be discussed after.

For diagnostic and therapeutic purposes PEI-MP should act only as a carrier and having no therapeutic or harmful effect. Therefore the cytotoxicity of PEI-MP was analysed through the evaluation of the inhibition of the cellular metabolic activity by MTT assay and the cell viability, the types of cell death, the production of peroxides and superoxide anion, and the expression of reduced GSH by flow cytometry. The results demonstrated that PEI-MP didn't inhibit the metabolic activity of bladder carcinoma or osteosarcoma cells, and the cell viability didn't decrease, there were no significant changes in the production of peroxides or superoxide anion that are harmful to cells [291, 293], and there were no significant changes in the expression of GSH, a major antioxidant that maintains a tight control of the redox status [295, 297]. Although the results have shown that the percentage of apoptosis has increased, and consequently decrease the mitochondrial membrane potential, these results should be carefully seen, since cellular viability did not change, as well as no changes were observed in the production of reactive oxygen species (ROS) or in the expression of GSH. In fact, the production of ROS and the depletion of GSH are associated with the induction of apoptosis [291, 295], and taking into account that none of these parameters was changed significantly, the result of the increased apoptosis seems not to be relevant. Therefore, PEI-MP would act as a carrier, not producing significant adverse effects to cells, thus it may be radiolabelled with ^{99m}Tc or ^{188}Re to study its potential for diagnosis (^{99m}Tc-PEI-MP) and for therapy (^{188}Re-PEI-MP) of bladder carcinoma and osteosarcoma.

As described before ^{99m}Tc not also emits gamma rays of low energy (140 keV), but also highly energetic auger electrons, that could represent a risk [59]. Additionally, as the objective is to use ^{99m}Tc-PEI-MP to perform safely diagnostic nuclear medicine images after its intravenous administration, is important to understand, if activities in the range of diagnostics represent or not a risk. Therefore it was evaluated the effects of equivalent doses until 20 mGy, (considering that the equivalent doses of most nuclear medicine diagnostic procedures varies between 0.3 and 20 mGy [303], after internal and external irradiation of bladder carcinoma and osteosarcoma cells. For this purpose, it

was analysed the ability of a cell to form a colony though the clonogenic assay, and it was also evaluated the cell viability, the types of cell death, the production of peroxides and superoxide anion, the expression of GSH, the changes in mitochondrial membrane potential and the cell cycle by flow cytometry. The results show that, for diagnostic equivalent doses, ^{99m}Tc didn't had any significant effects in the inhibition of cell growth, cell viability, cell death, and there were no changes in the production of ROS, in expression of GSH, and in mitochondrial membrane potential or cell cycle arrest. Therefore it is safe the use of ^{99m}Tc-PEI-MP for nuclear medicine imaging taking into account that the equivalent dose should not overcome the 20 mGy. The cytotoxicity of ^{188}Re doses was not determined, once again given the lack of a ^{188}W/^{188}Re generator, however considering the emission of high energetic β^- particles by the ^{188}Re, is possible to extrapolate the response of cells to its exposure, especially if internally irradiated where the cells were exposed to these particles and also to gamma photons of 155 keV. High energetic β^- particles may interact with cellular DNA and cause double or single-strand breaks and if these are not repaired correctly may lead to cellular death. This ionizing radiation may interact directly with the cellular DNA or indirectly with water molecules inside the cell, which may lead to an avalanche process in which are produced reactive oxygen species that, indirectly, will react with the cellular DNA and other cellular components producing damage [304, 306]. As consequence of the production of reactive oxygen species, the expression of GSH may be increased in order to control the redox status [295, 297]. Additionally, if the intrinsic pathway of apoptosis is activated, the mitochondria membrane potential goes eventually decrease [290, 304]. Therefore, the selection of ^{188}Re for therapy would be a good choice, but only if the selectivity for the target tissue is guaranteed.

For a radiolabelled molecule with diagnostic or therapeutic purposes it is important that the uptake and retention by the target tissue or organ is high and that at the non-target organs are as low as possible. Therefore, cellular uptake and retention studies were performed after adding ^{99m}Tc-PEI-MP or ^{188}Re-PEI-MP to bladder carcinoma or osteosarcoma cells in culture. The results showed that the uptake by cells of ^{99m}Tc-PEI-MP or ^{188}Re-PEI-MP was, during the 240 minutes of study, significantly higher than the uptake of ^{99m}Tc-Pertechnetate or

^{188}Re-Perrhenate, respectively. These results demonstrated clearly that PEI-MP has a particular affinity to cells of bladder carcinoma and osteosarcoma, and therefore can be an excellent carrier for ^{99m}Tc or ^{188}Re to perform diagnostic nuclear medicine images or therapy, respectively, in cases of bladder carcinoma or osteosarcoma. However, there are significant differences between the uptake of ^{99m}Tc-PEI-MP and ^{188}Re-PEI-MP, being the *in vitro* uptake of the last higher. A possible explanation is that ^{188}Re has a high atomic mass that makes ^{188}Re-PEI-MP a larger molecule than ^{99m}Tc-PEI-MP, and as mentioned before the tumour uptake of large molecules is dominated by the EPR effect. Related with this phenomenon, it is known that smaller molecules are cleared more rapidly and easier than larger molecules, and as a result the uptake and retention of larger molecules may be higher [169, 170, 341]. Schmidt M *et al.* [341] stated that smaller molecules require tighter binding to maintain significant tumour uptake than larger molecules, considering that larger molecules with some affinity to tumour cells (that is possibly the case of PEI-MP for bladder carcinoma and osteosarcoma cells) even losing the bound to the tumour cells, because they are cleared slowly, they have time to rebind to tumour cells. Therefore, the uptake and retention of larger molecules, like ^{188}Re-PEI-MP, would be higher than ^{99m}Tc-PEI-MP that is comparatively smaller. These results will be discussed again, when those obtained *in vivo* and *ex vivo* are analysed. Manual techniques for determining the cellular uptake and retention of ^{99m}Tc-PEI-MP and ^{188}Re-PEI-MP have some limitations like any other techniques. During the procedures is very difficult to maintain the cells at 37 ºC, being this the normal temperature in which the cells would be in real physiological conditions, once to obtain cell samples over time they must be removed from the incubator. Also the procedures are *per se* relatively aggressive to cells that may lead to changes in their behaviour. Therefore, as a future prospect, it would be interesting the study of cellular uptake and retention using a device such as the LigandTracer Yellow®. This instrument is equipped with a scintillator-based detector suitable for all nuclides used in PET/SPECT imaging, allowing for real-time detection of tracer cell-interactions [342]. With this equipment it would be less human interaction and the cells could be maintained at 37 ºC during all procedure.

After finished the *in vitro* studies it was proceeded to the *in vivo* studies. To animal tumour models it was chosen the balb/c nu/nu mice (immunodeficient mice) with xenografts of bladder carcinoma or osteosarcoma. As referred in the discussion of the Chapter 6, this type of animal tumour model has several advantages and disadvantages. The advantages of using this animal tumour model is the accessibility, the low costs, and as a first approach gives information about the behaviour of the administered radiopharmaceutical in an animal with a tumour implanted. However, as discussed before, this type of tumour model may not faithfully reflect the human disease process, because lacks some of the features of human cancer, such as, metastasis development to secondary sites, enabling only to understand the biodistribution of ^{99m}Tc-PEI-MP or ^{188}Re-PEI-MP. Spontaneous models of metastasis, like orthotopic models have several advantages over subcutaneous xerograph models. These advantages may include the development of differentiated structures within the tumour, such as vascular and lymphatic vessels, and possibility of metastatic spread, which turns the model more realistic [318]. Therefore, this type of animal models is very important for imagiologic nuclear medicine evaluation after the administration of ^{99m}Tc-PEI-MP and for therapy evaluation after administration of ^{188}Re-PEI-MP in cases of invasive and metastatic bladder carcinoma. However, tumour implantation for orthotopic models sometimes requires complex surgical procedures. Observation of tumour growth in internal organs typically needs the sacrifice of cohorts of animals because tumour acceptance and growth rates can be highly variable, as well as may be difficult and costly, to harvest tumour tissue for pathological analysis. These factors increase cost and decrease yield of the animal model [318].

Images obtained after the administration of ^{99m}Tc-PEI-MP or ^{188}Re-PEI-MP in control mice without tumour and with xenografts of bladder carcinoma and osteosarcoma, showed a high count rate in the kidneys and the bladder, results that were supported by the *ex vivo* studies. These results demonstrated that one of the main ways of excretion of these complexes is through the renal system, and therefore, eliminated with urine. Taking into account the results of the partition coefficient revealed in Chapter 5 and discussed before, demonstrating that ^{99m}Tc-PEI-MP is a hydrophilic molecule, and therefore water

soluble, it's not surprising that the main way of excretion is through the renal system. The same can be extrapolated to the ^{188}Re-PEI-MP due to their similarities. This characteristic, theoretically would mean a small liver and fat tissue uptake and a higher target/background ratio [273], however through the *in vivo* images and *ex vivo* studies it was possible to identify other target organs, such as the lungs, the liver and gallbladder, the spleen and the bone. Nevertheless, these results are not related to its hydrophilicity, but due to the fact that PEI-MP is a polymer, a large molecule and a phosphonate derivative, as discussed in the discussion section of the Chapter 6.

The uptake of ^{99m}Tc-PEI-MP or ^{188}Re-PEI-MP by bladder carcinoma or osteosarcoma xenografts is only faintly visible in gamma-camera images, especially in the ^{188}Re-PEI-MP images. This can be explained due to the different photonic flow of the two complexes. In fact, the photonic flow of 155 keV gamma rays from the ^{188}Re is low when compared with those from 140 keV coming from the ^{99m}Tc. This small photonic flow associated with the low resolution of the gamma camera detector, considering the animal size, justifies the reduced referred tumour visualization. This reduced visualization, turns very difficult or even impossible the quantification of the tumour uptake in relation to other organs. If there was the possibility to make precise measurements by *in vivo* imaging, and even perform measurements over time to better characterize the biokinetics of these radiopharmaceuticals, the number of sacrificed animals could be reduced greatly. A possible solution was to perform this nuclear medicine images in small animal dedicated gamma-cameras, equipment that would allow an higher spatial resolution and sensitivity [343].

The *ex vivo* studies also showed reduced uptake by the tumours of animals injected with ^{99m}Tc-PEI-MP or ^{188}Re-PEI-MP. As discussed previously the uptake by bladder carcinoma and osteosarcoma xenografts may be related not just with the xenografts blood perfusion, but also with the EPR effect associated to this polymer, besides being a phosphonate derivative. The EPR effect related with this polymer, would allow the accumulation within the tumour for a long period of time due to leaky blood vessels and poor lymphatic clearance of the tumour [169, 170]. In fact the results of the *ex vivo* studies demonstrated that the uptake of ^{99m}Tc-PEI-MP and ^{188}Re-PEI-MP (fraction 10-30 kDa) by the

xenografts of bladder carcinoma and osteosarcoma was relatively high and stable during 240 minutes. Because accumulation of macromolecules by the EPR effect takes time, it is essential that the molecules are stable in the plasma for long periods [173], what was found with the *ex vivo* biodistribution studies that clearly revealed a high percentage of ^{99m}Tc-PEI-MP or ^{188}Re-PEI-MP in the blood. The long period of retention of ^{99m}Tc-PEI-MP may be an advantage to perform diagnostic nuclear medicine images, to localize and delineate the tumour. Also for ^{188}Re-PEI-MP this high retention for a long period of time in the tumour could be an advantage to deliver the high energetic β^- particles to the tumour cells, causing tumour cell death [59]. Also the fact that PEI-MP be a phosphonate may explain its particular affinity to bladder carcinoma and osteosarcoma cells. Taniguchi *et al.* [338], had reported the diphosphonate ^{99m}Tc-HMDP uptake by a calcified transitional cell carcinoma of the bladder, relating this uptake with the particular affinity of phosphonates to calcium (Ca^{2+}) [102], that would be in abundance in a calcified tumour. On the other hand Moreno *et al.* [339], reported the diphosphonate ^{99m}Tc-MDP uptake by a non-calcified carcinoma of the kidney, and therefore it suggested that this uptake was possible due to the presence of selective tissue receptors or due to hypervascularity. Therefore being PEI-MP a diphosphonate, the uptake of ^{99m}Tc-PEI-MP or ^{188}Re-PEI-MP by bladder carcinoma could be related with some of the factors mentioned by the authors Taniguchi *et al.* and Moreno *et al.* For osteosarcoma this affinity is related with the presence of high concentrations of Ca^{2+} and with the strong affinity of phosphonates to the hydroxyapatite crystals, as mentioned many times before [102, 108]. Considering these possibilities, the high uptake and retention obtained in the *in vitro* studies, could be related with the uptake mechanism suggested by those authors, and demonstrates that PEI-MP has a particular affinity for bladder carcinoma and osteosarcoma cells. The same possible uptake mechanism, in addition to the EPR effect, may explain the fact that ^{188}Re-PEI-MP uptake and retention was significantly higher than ^{99m}Tc-PEI-MP. This difference is not visible in the *in vivo* and *ex vivo* studies, and is possibly related with the biodistribution upon intravenous administration, when much of ^{188}Re-PEI-MP is uptaken by other organs.

A manner of better characterize the biokinetics of ^{99m}Tc-PEI-MP and ^{188}Re-PEI-MP after intravenous administration it would be useful to choose more appropriate endpoints guided by functional imaging information. However, besides the eventual increase of animal number, what collides with the 3Rs principle, the obtained information would be much more rich and perhaps more clinically relevant.

The fact that the biodistribution of ^{99m}Tc-PEI-MP and ^{188}Re-PEI-MP remain with minor changes until 120 and 240 minutes after the intravenous administration, demonstrates the radiochemical stability of these complexes *in vivo*. This behaviour gives the guarantee that the nuclear medicine images show the biodistribution of the labelled PEI-MP and not the contaminant species after labelling break. Also for therapy it is important that ^{188}Re-PEI-MP has a high stability *in vivo*, to ensure the delivery of β^- particles of ^{188}Re to tumour tissue coupled to PEI-MP vehicle, and according to the principle of the EPR, the complex gradually would accumulate into the tumour. To support the results regarding the radiochemical stability of ^{99m}Tc-PEI-MP and ^{188}Re-PEI-MP *in vivo* blood sample collected over the time, and the radiochemical purity can be obtained, using the same quality control procedures. In order to avoid the sacrifice of more animals, these stability tests could be performed *in vitro* using human serum samples maintained at 37°C.

Considering that presence of metastasis of a bladder carcinoma, the major target organs are the liver, the lungs and the bone, and knowing that the bladder carcinoma has its origin in the bladder wall and in an initial stage the tumour can invade the muscle adjacent to this organ [184], to determine whether the tumour uptake of an administered radiopharmaceutical is higher or lower than the surrounding organs, is crucial to determine tumour/muscle, tumour/bladder, tumour/liver, tumour/lung and tumour/bone ratios. These results would be useful to clarify if it's possible to perform the diagnosis with ^{99m}Tc-PEI-MP and therapy with ^{188}Re-PEI-MP. For mice with xenografts of bladder carcinoma or osteosarcoma, after the administration of ^{99m}Tc-PEI-MP or ^{188}Re-PEI-MP, the tumour/muscle ratios were always superior to 1, demonstrating that the uptake by the tumour was superior to the muscle. The fact that the uptake of ^{99m}Tc-PEI-MP by the tumour is higher than the muscle, is

an advantage to determine the degree of muscle invasiveness, and could assist the surgeon in determine how much muscle should be excised along with the tumour and the bladder [188]. Also the high tumour/muscle ratio obtained for ^{188}Re-PEI-MP is an advantage for the therapy, allowing sparing the muscle from the action of high doses of ionizing radiation.

For mice with xenografts of bladder carcinoma and osteosarcoma where ^{99m}Tc-PEI-MP or ^{188}Re-PEI-MP were administered, tumour/bladder, tumour/liver, tumour/lung and tumour/bone ratios were always inferior to 1 demonstrating that the uptake of the tumour was inferior comparing with these organs. Considering these results, the tumour in the bladder wall, and the metastasis from a bladder carcinoma or osteosarcoma in liver, lung and bones would appear as cold lesions in nuclear medicine images, after the administration of ^{99m}Tc-PEI-MP. Therefore it would be possible to identify the tumour and its metastases, in an effective way, by intravenous administration of ^{99m}Tc-PEI-MP, in the late images. The results are not so good if the objective is the therapy with ^{188}Re-PEI-MP, because after the intravenous administration the irradiation of non-target tissues such as the bladder wall, the liver, the lungs and the bones would be higher than desirable, and can mean significant adverse effects. Also the uptake by its metastases would be too low for the therapy with this radiopharmaceutical could be effective. Thus, the use of ^{188}Re-PEI-MP for systemic therapy of bladder carcinoma and its metastasis by intravenous administration wouldn't be suitable. However, for the therapy of bladder carcinoma alone, direct instillation of ^{188}Re-PEI-MP to the bladder could be a viable option, considering the high uptake of this complex by the tumour cells. Nevertheless, with this option the bladder wall would also be exposed to radiation, whereby more studies should be conducted to review the feasibility of this hypothesis.

Section IV. Discussion, Conclusions and Future Perspectives

Chapter 8.Conclusions and Future Perspectives

The presented work, unique and innovative, allowed pre-clinical evaluation of the potential of ^{99m}Tc-PEI-MP to perform images in the scope of diagnostic nuclear medicine, and thus allowing to take a step for future clinical studies. Studies with ^{188}Re-PEI-MP were not fully completed, given the lack of an ^{188}W/^{188}Re generator, however the uptake and retention studies performed *in vitro* plus the biodistribution studies performed *in vivo* and *ex vivo*, allowed to draw preliminary conclusions regarding its potential.

In this work it was possible to develop a pharmaceutical formulation of the and constitute a reproducible cold kits that allows to obtain high radiochemical purity after labelling with ^{99m}Tc (>90%) or ^{188}Re (>85%). Also the *in vitro* stability was demonstrated to be high, ensuring the possible use of the labelling kit for a long period of time, being this an advantage for clinical application. Also the radiochemical stability of ^{99m}Tc-PEI-MP was not changed by the exposure to cellular culture medium or to room temperatures that could vary from 22 to 45 ºC when carrying out the *in vitro* studies. The same results would be expected for ^{188}Re-PEI-MP given the complexes' similarity. The chromatographic systems used to determinate the radiochemical purity demonstrated to be efficient, allowing calculating the different radiochemical species present in the labelling kits after adding ^{99m}Tc or ^{188}Re.

The polymer PEI-MP was confirmed to be a hydrophilic molecule, given the fact that partition coefficient was always inferior to -3. Also, PEI-MP demonstrated to be harmless to cells of bladder carcinoma and osteosarcoma, at least in terms of metabolic activity and cell viability. Therefore PEI-MP could be used as a carrier of ^{99m}Tc or ^{188}Re to target cells, tissues or organs.

Equivalent doses of ^{99m}Tc in the diagnostic range (0.3 to 20 mGy) to bladder carcinoma and osteosarcoma cells demonstrated that significant adverse effects were not produced, at least in terms of clonogenic activity and cell viability, whereby ^{99m}Tc-PEI-MP could be used for nuclear medicine imaging,

considering that the activity administered doesn't mean equivalent doses superior to 20 mGy.

In vitro studies demonstrated that the maximum uptake of ^{99m}Tc-PEI-MP was about 4 times the maximum uptake of the ^{99m}Tc-Pertechnetate in HT-1376 cell line, and approximately 5 times higher in the MNNG/HOS cell line. The minimum retention of ^{99m}Tc-PEI-MP was about 4 times the minimum retention of the ^{99m}Tc-Pertechnetate in HT-1376 cell line, and approximately 7 times higher in the MNNG/HOS cell line. The same studies demonstrated that the maximum uptake of ^{188}Re-PEI-MP was about 62 times the maximum uptake of the ^{188}Re-Perrhenate in HT-1376 cell line, and approximately 65 times higher in the MNNG/HOS cell line. The minimum retention of ^{188}Re-PEI-MP was about 194 times the minimum retention of the ^{188}Re-Perrhenate in HT-1376 cell line, and approximately 328 times higher in the MNNG/HOS cell line. These studies demonstrated that *in vitro* the uptake and retention of ^{99m}Tc-PEI-MP or ^{188}Re-PEI-MP was significantly higher than their controls, evidencing the specificity of PEI-MP.

In vivo and *ex vivo* studies demonstrated that ^{99m}Tc-PEI-MP and ^{188}Re-PEI-MP were mainly excreted through the renal system, possible explained by the fact that PEI-MP is a hydrophilic molecule. Also a small amount of ^{99m}Tc-PEI-MP and ^{188}Re-PEI-MP in the liver and gallbladder was confirmed by the *ex vivo* studies, demonstrating that a small part is excreted through the hepatobiliary system.

The *in vivo* and *ex vivo* studies confirmed the uptake of ^{99m}Tc-PEI-MP and ^{188}Re-PEI-MP by lungs, possible explained by the fact that these complexes are large molecules that could be trapped in the lung capillaries.

Some uptake was observed in xenografts of bladder carcinoma and osteosarcoma. This tumour uptake can be related not only with the blood perfusion to the tumour or the EPR effect associated with PEI-MP, but also with the presence of specific membrane receptors in the case of bladder carcinoma and high concentrations of Ca^{2+} in both tumour types.

The tumour/muscle ratio for ^{99m}Tc-PEI-MP and ^{188}Re-PEI-MP for both xenografts of bladder carcinoma and osteosarcoma was superior to 1. For nuclear medicine imaging, the high tumour to muscle ratio would ensure the tumour visualization and allows understanding of the degree of invasiveness of muscle and assisting the surgeon, especially for bladder carcinoma.

Tumour/bladder, tumour/liver, tumour/lung and tumour/bone ratios for ^{99m}Tc-PEI-MP and ^{188}Re-PEI-MP and for both xenografts of bladder carcinoma and osteosarcoma were always inferior to 1. These results demonstrated that for diagnostic nuclear medicine the tumour and its metastases would present as cold lesions allowing to identify them in the images. One the other hand the therapy of bladder carcinoma or osteosarcoma and its metastasis seem not to be feasible if administered intravenously, considering the high dosimetry to other organs.

In order to improve or complement the obtained results it would be interesting to complete the studies with ^{188}Re, namely determining the partition coefficient of ^{188}Re-PEI-MP, analysing the cytotoxicity of ^{188}Re and increasing the sample size of the studies already conducted.

Considering the limitations associated with the manual techniques for determining the cellular uptake and retention, and to overcome these limitations, it would be interesting to complete the cellular uptake and retention studies using the device LigandTracer Yellow®.

The xenograft model may not faithfully reflect the human disease process, because it lacks some of the features of human cancer development. The orthotopic models overcomes these limitations, therefore it would be interesting to conduct *in vivo* studies after the administration of ^{99m}Tc-PEI-MP or ^{188}Re-PEI-MP in orthotopic models of bladder carcinoma or osteosarcoma, to analyse more realistically the biodistribution and the pharmacokinetics of those complexes.

Using a gamma-camera that was built for human imaging to perform images of a small animal, turns it very difficult due to the resolution of this equipment that

is not highly enough for the small structures of a mouse. As a consequence it was not possible to quantify the tumour uptake in relation to other organs only in images, and therefore the need of sacrifying the animals. A possible solution was to perform this nuclear medicine images in small animal dedicated gamma-cameras, equipment that would allow a higher spatial resolution and sensitivity.

The uptake of ^{99m}Tc-PEI-MP and ^{188}Re-PEI-MP by the bladder cancer cells may be related not only with the blood perfusion or EPR effect, but also with the high concentration of Ca^{2+} if tumour microcalcifications are present as well as the expression of specific membrane receptors. Therefore it would be exciting the identification of these receptors and eventually associate them as one of the possible reasons for the high uptake of the radiolabelled PEI-MP by bladder tissue and bladder tumour tissue.

Considering the high uptake of ^{188}Re-PEI-MP by the bladder carcinoma xenograft, this complex could still be considered for therapy of bladder carcinoma, if administered directly by instillation to the bladder. However dosimetry to the bladder wall should be always considered. Nevertheless it would be attractive to conduct studies to confirm or not the feasibility of this hypothesis.

Section V. References

1. Hall EJ, Giaccia A: **Radiobiology for the Radiologist**, 6 edn: Lippincott Williams & Wilkins; 2006.
2. Passarge E: **Color Atlas of Genetics**, 2 edn: Georg Thieme Verlag; 2001.
3. Damjanov I: **Pathology for the Health-Related Professions**, 2 edn: W.B. Saunders Company; 2000.
4. McKinnell RG, Parchment RE, Perantoni AO: **The Biological Basis of Cancer**, 2 edn: Cambridge University Press; 2006.
5. Lodish H, Berk A, Matsudaira P, Kaiser CA, Krieger M, Scott MP, Zipursky L, Darnell J: **Molecular Cell Biology**, 5 edn: WHF Freeman; 2004.
6. Hanahan D, Weinberg RA: **Hallmarks of cancer: the next generation**. *Cell* 2011, **144**(5):646-674.
7. Hanahan D, Weinberg RA: **The hallmarks of cancer**. *Cell* 2000, **100**(1):57-70.
8. Weinberg RA: **The retinoblastoma protein and cell cycle control**. *Cell* 1995, **81**(3):323-330.
9. Datto MB, Hu PP, Kowalik TF, Yingling J, Wang XF: **The viral oncoprotein E1A blocks transforming growth factor beta-mediated induction of p21/WAF1/Cip1 and p15/INK4B**. *Molecular and cellular biology* 1997, **17**(4):2030-2037.
10. Schutte M, Hruban RH, Hedrick L, Cho KR, Nadasdy GM, Weinstein CL, Bova GS, Isaacs WB, Cairns P, Nawroz H *et al*: **DPC4 gene in various tumor types**. *Cancer research* 1996, **56**(11):2527-2530.
11. Adams JM, Cory S: **The Bcl-2 apoptotic switch in cancer development and therapy**. *Oncogene* 2007, **26**(9):1324-1337.
12. Lowe SW, Cepero E, Evan G: **Intrinsic tumour suppression**. *Nature* 2004, **432**(7015):307-315.
13. Rozan LM, El-Deiry WS: **p53 downstream target genes and tumor suppression: a classical view in evolution**. *Cell death and differentiation* 2007, **14**(1):3-9.

14. Harris CC: **p53 tumor suppressor gene: from the basic research laboratory to the clinic--an abridged historical perspective**. *Carcinogenesis* 1996, **17**(6):1187-1198.
15. Levine AJ: **p53, the cellular gatekeeper for growth and division**. *Cell* 1997, **88**(3):323-331.
16. Shay JW, Wright WE: **Senescence and immortalization: role of telomeres and telomerase**. *Carcinogenesis* 2005, **26**(5):867-874.
17. Hanahan D, Folkman J: **Patterns and emerging mechanisms of the angiogenic switch during tumorigenesis**. *Cell* 1996, **86**(3):353-364.
18. Veikkola T, Karkkainen M, Claesson-Welsh L, Alitalo K: **Regulation of angiogenesis via vascular endothelial growth factor receptors**. *Cancer research* 2000, **60**(2):203-212.
19. Nagy JA, Chang SH, Shih SC, Dvorak AM, Dvorak HF: **Heterogeneity of the tumor vasculature**. *Seminars in thrombosis and hemostasis* 2010, **36**(3):321-331.
20. Bergers G, Javaherian K, Lo KM, Folkman J, Hanahan D: **Effects of angiogenesis inhibitors on multistage carcinogenesis in mice**. *Science* 1999, **284**(5415):808-812.
21. Berx G, van Roy F: **Involvement of members of the cadherin superfamily in cancer**. *Cold Spring Harbor perspectives in biology* 2009, **1**(6):a003129.
22. Alberts B, Johnson A, Lewis J, Raff M, Roberts K, Walter P: **Molecular Biology of the Cell**, 5 edn: Garland Science; 2007.
23. Werb Z: **ECM and cell surface proteolysis: regulating cellular ecology**. *Cell* 1997, **91**(4):439-442.
24. Stetler-Stevenson WG: **Matrix metalloproteinases in angiogenesis: a moving target for therapeutic intervention**. *The Journal of clinical investigation* 1999, **103**(9):1237-1241.
25. Jones PA, Baylin SB: **The epigenomics of cancer**. *Cell* 2007, **128**(4):683-692.
26. DeBerardinis RJ, Lum JJ, Hatzivassiliou G, Thompson CB: **The biology of cancer: metabolic reprogramming fuels cell growth and proliferation**. *Cell metabolism* 2008, **7**(1):11-20.

27. Semenza GL: **HIF-1: upstream and downstream of cancer metabolism**. *Current opinion in genetics & development* 2010, **20**(1):51-56.
28. Semenza GL: **Defining the role of hypoxia-inducible factor 1 in cancer biology and therapeutics**. *Oncogene* 2010, **29**(5):625-634.
29. Kennedy KM, Dewhirst MW: **Tumor metabolism of lactate: the influence and therapeutic potential for MCT and CD147 regulation**. *Future Oncol* 2010, **6**(1):127-148.
30. Hardee ME, Dewhirst MW, Agarwal N, Sorg BS: **Novel imaging provides new insights into mechanisms of oxygen transport in tumors**. *Current molecular medicine* 2009, **9**(4):435-441.
31. Vajdic CM, van Leeuwen MT: **Cancer incidence and risk factors after solid organ transplantation**. *International journal of cancer Journal international du cancer* 2009, **125**(8):1747-1754.
32. Kim R, Emi M, Tanabe K: **Cancer immunoediting from immune surveillance to immune escape**. *Immunology* 2007, **121**(1):1-14.
33. Teng MW, Swann JB, Koebel CM, Schreiber RD, Smyth MJ: **Immune-mediated dormancy: an equilibrium with cancer**. *Journal of leukocyte biology* 2008, **84**(4):988-993.
34. AJCC: **What is Cancer Staging?** In.: American Joint Committee on Cancer; 2010.
35. WHO: **Treatment of cancer**. In.: World Health Organization; 2013.
36. WHO: **Cancer**. In.: World Health Organization; 2013.
37. Emole J: **Cancer Diagnosis and Treatment: An Overview for the General Practitioner**. In: *Primary Care at a Glance: Hot Topics and New Insights.* Edited by Capelli O: InTech; 2012: 175-186.
38. Sethi S, Ali S, Philip PA, Sarkar FH: **Clinical advances in molecular biomarkers for cancer diagnosis and therapy**. *International journal of molecular sciences* 2013, **14**(7):14771-14784.
39. Weissleder R, Mahmood U: **Molecular imaging**. *Radiology* 2001, **219**(2):316-333.
40. NCI: **Radiation Therapy of Cancer**. In.: National Cancer Institute; 2010.
41. Volkert WA, Hoffman TJ: **Therapeutic radiopharmaceuticals**. *Chemical reviews* 1999, **99**(9):2269-2292.

42. Oyen WJ, Bodei L, Giammarile F, Maecke HR, Tennvall J, Luster M, Brans B: **Targeted therapy in nuclear medicine--current status and future prospects**. *Annals of oncology : official journal of the European Society for Medical Oncology / ESMO* 2007, **18**(11):1782-1792.
43. Pacini F, Schlumberger M, Harmer C, Berg GG, Cohen O, Duntas L, Jamar F, Jarzab B, Limbert E, Lind P *et al*: **Post-surgical use of radioiodine (131I) in patients with papillary and follicular thyroid cancer and the issue of remnant ablation: a consensus report**. *European journal of endocrinology / European Federation of Endocrine Societies* 2005, **153**(5):651-659.
44. Berlin NI: **Treatment of the myeloproliferative disorders with 32P**. *European journal of haematology* 2000, **65**(1):1-7.
45. Berlin NI: **Polycythemia vera: diagnosis and treatment 2002**. *Expert review of anticancer therapy* 2002, **2**(3):330-336.
46. Witzig TE: **Radioimmunotherapy for B-cell non-Hodgkin lymphoma**. *Best practice & research Clinical haematology* 2006, **19**(4):655-668.
47. Davis TA, Kaminski MS, Leonard JP, Hsu FJ, Wilkinson M, Zelenetz A, Wahl RL, Kroll S, Coleman M, Goris M *et al*: **The radioisotope contributes significantly to the activity of radioimmunotherapy**. *Clinical cancer research : an official journal of the American Association for Cancer Research* 2004, **10**(23):7792-7798.
48. Chrisoulidou A, Kaltsas G, Ilias I, Grossman AB: **The diagnosis and management of malignant phaeochromocytoma and paraganglioma**. *Endocrine-related cancer* 2007, **14**(3):569-585.
49. Howman-Giles R, Shaw PJ, Uren RF, Chung DK: **Neuroblastoma and other neuroendocrine tumors**. *Seminars in nuclear medicine* 2007, **37**(4):286-302.
50. Scholz T, Eisenhofer G, Pacak K, Dralle H, Lehnert H: **Clinical review: Current treatment of malignant pheochromocytoma**. *The Journal of clinical endocrinology and metabolism* 2007, **92**(4):1217-1225.
51. Kwekkeboom DJ, Mueller-Brand J, Paganelli G, Anthony LB, Pauwels S, Kvols LK, O'Dorisio T M, Valkema R, Bodei L, Chinol M *et al*: **Overview of results of peptide receptor radionuclide therapy with 3 radiolabeled somatostatin analogs**. *Journal of nuclear medicine :*

official publication, Society of Nuclear Medicine 2005, **46 Suppl 1**:62S-66S.

52. Forrer F, Valkema R, Kwekkeboom DJ, de Jong M, Krenning EP: **Neuroendocrine tumors. Peptide receptor radionuclide therapy**. *Best practice & research Clinical endocrinology & metabolism* 2007, **21**(1):111-129.
53. Van Essen M, Krenning EP, De Jong M, Valkema R, Kwekkeboom DJ: **Peptide Receptor Radionuclide Therapy with radiolabelled somatostatin analogues in patients with somatostatin receptor positive tumours**. *Acta Oncol* 2007, **46**(6):723-734.
54. IAEA: **Radiopharmaceuticals: Production and Availability**. In: *Radiopharmaceuticals* 51st General Conference Documents: International Atomic Energy Agency 2007.
55. Cantone M, Hoeschen C: **Radiation Physics for Nuclear Medicine**: Springer; 2011.
56. Cherry S, Dahlbom M: **PET: Physics, Instrumentation, and Scanners**. In: *PET: Molecular Imaging and Its Biological Applications.* Edited by Phelps M: Springer; 2004: 1-124.
57. IAEA: **IAEA-TECDOC-1340, Manual for reactor produced radioisotopes**. In. Vienna, Austria; 2003.
58. IAEA: **Technical Reports Series No. 465, Cyclotron produced radionuclides: principals and practice**. In. Vienna, Austria; 2008.
59. Stigbrand T: **Targeted radionuclide tumor therapy**. New York: Springer; 2008.
60. Forshier S: **Essentials of Radiation Biology and Protection**, 2 edn: Cengage Learning; 2008.
61. Saha G: **Fundamentals of Nuclear Pharmacy**, 4 edn: Springer; 1998.
62. Eckelman WC, Coursey BM: **Special Issue - Technetium-99m - Generators, Chemistry and Preparation of Radiopharmaceuticals - Preface**. *Int J Appl Radiat Is* 1982, **33**(10):R5-R5.
63. Ell PJ, Gambhir SS: **Nuclear Medicine in Clinical Diagnosis and Treatment**, 3 edn: Elsevier; 2004.

64. Wessels BW, Meares CF: **Physical and chemical properties of radionuclide therapy**. *Seminars in radiation oncology* 2000, **10**(2):115-122.

65. Lattimer JC, Corwin LA, Jr., Stapleton J, Volkert WA, Ehrhardt GJ, Ketring AR, Anderson SK, Simon J, Goeckeler WF: **Clinical and clinicopathologic response of canine bone tumor patients to treatment with samarium-153-EDTMP**. *Journal of nuclear medicine : official publication, Society of Nuclear Medicine* 1990, **31**(8):1316-1325.

66. Volkert WA, Goeckeler WF, Ehrhardt GJ, Ketring AR: **Therapeutic radionuclides: production and decay property considerations**. *Journal of nuclear medicine : official publication, Society of Nuclear Medicine* 1991, **32**(1):174-185.

67. Ferreira S, Dormehl I, Botelho MF: **Radiopharmaceuticals for bone metastasis therapy and beyond: a voyage from the past to the present and a look to the future**. *Cancer biotherapy & radiopharmaceuticals* 2012, **27**(9):535-551.

68. O'Donoghue JA, Wheldon TE: **Targeted radiotherapy using Auger electron emitters**. *Physics in medicine and biology* 1996, **41**(10):1973-1992.

69. Palmedo H: **Radionuclid Therapy of Bone Metastases**. In: *Clinical nuclear medicine.* Edited by Biersack HJ, Freeman LM: Springer; 2007: 433-442.

70. Buchegger F, Perillo-Adamer F, Dupertuis YM, Delaloye AB: **Auger radiation targeted into DNA: a therapy perspective**. *European journal of nuclear medicine and molecular imaging* 2006, **33**(11):1352-1363.

71. Mallol J, Zolle I: **Preparation of Technetium ^{99m}Tc Pharmaceuticals**. In: *Technetium-99m Pharmaceuticals: Preparation and Quality Control in Nuclear Medicine.* Edited by Zolle I: Springer; 2007: 95-98.

72. Boyd RE: **Technetium-99m generators--the available options**. *The International journal of applied radiation and isotopes* 1982, **33**(10):801-809.

73. Richards P, Tucker WD, Srivastava SC: **Technetium-99m: an historical perspective**. *The International journal of applied radiation and isotopes* 1982, **33**(10):793-799.

74. Mazzi U: **Technetium in Medicine**. In: *Technetium-99m Pharmaceuticals: Preparation and Quality Control in Nuclear Medicine.* Edited by Zolle I: Springer; 2007: 7-46.
75. Mazzi U: **The coordination chemistry of technetium in its intermediate oxidation states**. *Polyhedron* 1989, **8**(13–14):1683–1688.
76. Boschi A, Bolzati C, Uccelli L, Duatti A: **High-yield synthesis of the terminal 188Re triple bond N multiple bond from generator-produced [188ReO4](-)**. *Nuclear medicine and biology* 2003, **30**(4):381-387.
77. Li S, Liu J, Zhang H, Tian M, Wang J, Zheng X: **Rhenium-188 HEDP to treat painful bone metastases**. *Clinical nuclear medicine* 2001, **26**(11):919-922.
78. Knapp FF, Jr.: **Rhenium-188--a generator-derived radioisotope for cancer therapy**. *Cancer biotherapy & radiopharmaceuticals* 1998, **13**(5):337-349.
79. Lisic EC, Phillips M, Ensor D, Nash KL, Beets A, Knapp FF: **Synthesis of a new bisphosphonic acid ligand (SEDP) and preparation of a (188)Re-(Sn)SEDP bone seeking radiotracer**. *Nuclear medicine and biology* 2001, **28**(4):419-424.
80. Knapp FF, Jr., Beets AL, Guhlke S, Zamora PO, Bender H, Palmedo H, Biersack HJ: **Availability of rhenium-188 from the alumina-based tungsten-188/rhenium-188 generator for preparation of rhenium-188-labeled radiopharmaceuticals for cancer treatment**. *Anticancer research* 1997, **17**(3B):1783-1795.
81. Wang SJ, Lin WY, Chen MN, Chen JT, Ho WL, Hsieh BT, Huang H, Shen LH, Ting G, Knapp FF, Jr.: **Histologic study of effects of radiation synovectomy with Rhenium-188 microsphere**. *Nuclear medicine and biology* 2001, **28**(6):727-732.
82. Chen FD, Hsieh BT, Wang HE, Ou YH, Yang WK, Whang-Peng J, Liu RS, Knapp FF, Ting G, Yen SH: **Efficacy of Re-188-labelled sulphur colloid on prolongation of survival time in melanoma-bearing animals**. *Nuclear medicine and biology* 2001, **28**(7):835-844.
83. Cherry S, Sorenson J, Phelps M: **Appendix C: Characteristics of Some Medically Important Radionuclides. Physics in Nuclear**

Medicine. In: *Physics in Nuclear Medicine.* 4 edn: Elsevier Saunders; 2012.

84. Liepe K, Kropp J, Runge R, Kotzerke J: **Therapeutic efficiency of rhenium-188-HEDP in human prostate cancer skeletal metastases**. *British journal of cancer* 2003, **89**(4):625-629.
85. Chiotellis E: **Lyophilization Technique for Preparing Radiopharmaceuticals Kits**. In: *Technetium-99m Pharmaceuticals: Preparation and Quality Control in Nuclear Medicine.* Edited by Zolle I: Springer; 2007: 99-102.
86. Spies H, Pietzsch H-J: **Stannous Chloride in the Preparation of ^{99m}Tc Pharmaceuticals**. In: *Technetium-99m Pharmaceuticals: Preparation and Quality Control in Nuclear Medicine.* Edited by Zolle I: Springer; 2007: 59-61.
87. Decristoforo C, Zolle I: **Quality Control Methods of ^{99m}Tc Pharmaceuticals**. In: *Technetium-99m Pharmaceuticals: Preparation and Quality Control in Nuclear Medicine.* Edited by Zolle I: Springer; 2007.
88. Zimmer AM, Pavel DG: **Rapid miniaturized chromatographic quality-control procedures for Tc-99m radiopharmaceuticals**. *Journal of nuclear medicine : official publication, Society of Nuclear Medicine* 1977, **18**(12):1230-1233.
89. Kindblom LG: **Bone Tumors: Epidemiology, Classification, Pathology**. In: *Imaging of Bone Tumors and Tumor-Like Lesions.* Edited by Davies AM, Sundaram M, James SJ: Hardcover; 2009.
90. ACS: **Bone Cancer**. In.: American Cancer Society; 2012.
91. NCI: **Bone Cancer**. In.: National Cancer Institute; 2008.
92. **The stages of bone cancer** [http://www.cancerresearchuk.org/cancer-help/type/bone-cancer/treatment/the-stages-of-bone-cancer]
93. Virk MS, Lieberman JR: **Tumor metastasis to bone**. *Arthritis research & therapy* 2007, **9 Suppl 1**:S5.
94. Coleman RE: **Clinical features of metastatic bone disease and risk of skeletal morbidity**. *Clinical cancer research : an official journal of the American Association for Cancer Research* 2006, **12**(20 Pt 2):6243s-6249s.

95. Paterson AH: **Bone metastases in breast cancer, prostate cancer and myeloma**. *Bone* 1987, **8 Suppl 1**:S17-22.
96. Jacobs SC: **Spread of prostatic cancer to bone**. *Urology* 1983, **21**(4):337-344.
97. Ye L, Kynaston HG, Jiang WG: **Bone metastasis in prostate cancer: molecular and cellular mechanisms (Review)**. *International journal of molecular medicine* 2007, **20**(1):103-111.
98. ACS: **Bone Metastasis**. In.: American Cancer Society; 2012.
99. Spangler JG: **Bone biology and physiology: implications for novel osteoblastic osteosarcoma treatments?** *Medical hypotheses* 2008, **70**(2):281-286.
100. Muller A, Homey B, Soto H, Ge N, Catron D, Buchanan ME, McClanahan T, Murphy E, Yuan W, Wagner SN *et al*: **Involvement of chemokine receptors in breast cancer metastasis**. *Nature* 2001, **410**(6824):50-56.
101. Nielsen OS, Munro AJ, Tannock IF: **Bone metastases: pathophysiology and management policy**. *Journal of clinical oncology : official journal of the American Society of Clinical Oncology* 1991, **9**(3):509-524.
102. Zeevaart JR, Louw WKA, Kolar ZI, Wagener JM, Jarvis NV, Claessens RAMJ: **A thermodynamic approach, using speciation studies, towards the evaluation and design of bone-seeking radiopharmaceuticals as illustrated for Sn-117m(II)-PEI-MP**. *J Radioanal Nucl Ch* 2003, **257**(1):83-91.
103. Besson JM, Chaouch A: **Peripheral and spinal mechanisms of nociception**. *Physiological reviews* 1987, **67**(1):67-186.
104. Mense S: **Sensitization of group IV muscle receptors to bradykinin by 5-hydroxytryptamine and prostaglandin E2**. *Brain research* 1981, **225**(1):95-105.
105. Franchi A: **Epidemiology and classification of bone tumors**. *Clinical cases in mineral and bone metabolism : the official journal of the Italian Society of Osteoporosis, Mineral Metabolism, and Skeletal Diseases* 2012, **9**(2):92-95.
106. **SEER Cancer Statistics Review 1975-2008** [http://seer.cancer.gov/archive/csr/1975_2008/]

107. **Statistics and outlook for bone cancer** [http://www.cancerresearchuk.org/cancer-help/type/bone-cancer/treatment/statistics-and-outlook-for-bone-cancer]
108. Bagi CM: **Targeting of therapeutic agents to bone to treat metastatic cancer**. *Advanced drug delivery reviews* 2005, **57**(7):995-1010.
109. Hayward JL, Carbone PP, Heuson JC, Kumaoka S, Segaloff A, Rubens RD: **Assessment of response to therapy in advanced breast cancer: a project of the Programme on Clinical Oncology of the International Union Against Cancer, Geneva, Switzerland**. *Cancer* 1977, **39**(3):1289-1294.
110. WHO: **Cancer pain relief and palliative care**. In. World Health Organization.; 1990.
111. Dormehl IC, Louw WK, Milner RJ, Kilian E, Schneeweiss FH: **Biodistribution and pharmacokinetics of variously sized molecular radiolabelled polyethyleneiminomethyl phosphonic acid as a selective bone seeker for therapy in the normal primate model**. *Arzneimittel-Forschung* 2001, **51**(3):258-263.
112. Jansen DR, Zeevaart JR, Kolar ZI, Djanashvili K, Peters JA, Krijger GC: **31P NMR study of the valence stability of tin in its 1-hydroxyethylene-diphosphonate (HEDP) and N,N′,N′-trimethylenephosphonate-polyethyleneimine (PEI-MP) complexes**. *Polyhedron* 2008, **27**(6):1779-1786.
113. ACS: **Immunotherapy**. In.; 2012.
114. Maisano R, Pergolizzi S, Cascinu S: **Novel therapeutic approaches to cancer patients with bone metastasis**. *Critical reviews in oncology/hematology* 2001, **40**(3):239-250.
115. Yoneda T, Michigami T, Yi B, Williams PJ, Niewolna M, Hiraga T: **Use of bisphosphonates for the treatment of bone metastasis in experimental animal models**. *Cancer treatment reviews* 1999, **25**(5):293-299.
116. Ridone S, Bonardi ML, Groppi F, Martinotti A, Alfassi ZB: **Paper radiochromatography for evaluation of radiochemical purity and stability of [186gRe]Re- HEDP in biological samples after human administration**. *J Radioanal Nucl Ch* 2008, **277**(1):117 - 123.

117. Hoskin PJ, Price P, Easton D, Regan J, Austin D, Palmer S, Yarnold JR: **A prospective randomised trial of 4 Gy or 8 Gy single doses in the treatment of metastatic bone pain**. *Radiotherapy and oncology : journal of the European Society for Therapeutic Radiology and Oncology* 1992, **23**(2):74-78.

118. Dearnaley DP, Khoo VS, Norman AR, Meyer L, Nahum A, Tait D, Yarnold J, Horwich A: **Comparison of radiation side-effects of conformal and conventional radiotherapy in prostate cancer: a randomised trial**. *Lancet* 1999, **353**(9149):267-272.

119. Hanks GE: **Conformal radiotherapy for prostate cancer**. *Annals of medicine* 2000, **32**(1):57-63.

120. Lewington VJ: **Targeted radionuclide therapy for bone metastases**. *European journal of nuclear medicine* 1993, **20**(1):66-74.

121. Porter AT, Ben-Josef E, Davis L: **Systemic administration of new therapeutic radioisotopes, including phosphorus, strontium, samarium, and rhenium**. *Current opinion in oncology* 1994, **6**(6):607-610.

122. Lin WY, Lin CP, Yeh SJ, Hsieh BT, Tsai ZT, Ting G, Yen TC, Wang SJ, Knapp FF, Jr., Stabin MG: **Rhenium-188 hydroxyethylidene diphosphonate: a new generator-produced radiotherapeutic drug of potential value for the treatment of bone metastases**. *European journal of nuclear medicine* 1997, **24**(6):590-595.

123. de Klerk JM, van Dijk A, van het Schip AD, Zonnenberg BA, van Rijk PP: **Pharmacokinetics of rhenium-186 after administration of rhenium-186-HEDP to patients with bone metastases**. *Journal of nuclear medicine : official publication, Society of Nuclear Medicine* 1992, **33**(5):646-651.

124. Nayak D, Lahiri S: **Application of radioisotopes in the field of nuclear medicine**. *J Radioanal Nucl Ch* 1999, **242**(2):423-432.

125. Thurlimann B, Morant R, Jungi WF, Radziwill A: **Pamidronate for pain control in patients with malignant osteolytic bone disease: a prospective dose-effect study**. *Supportive care in cancer : official journal of the Multinational Association of Supportive Care in Cancer* 1994, **2**(1):61-65.

126. Silberstein EB: **Systemic radiopharmaceutical therapy of painful osteoblastic metastases**. *Seminars in radiation oncology* 2000, **10**(3):240-249.
127. Rizkalla EN, Zaki MTM, Ismail MI: **Metal chelates of phosphonate-containing ligands—V Stability of some 1-hydroxyethane-1,1-diphosphonic acid metal chelates**. *Talanta* 1980, **27**(9):715-719.
128. Jurisson S, Berning D, Jia W, Ma D: **Coordination compounds in nuclear medicine**. *Journal Name: Chemical Reviews; (United States); Journal Volume: 93:3* 1993:Medium: X; Size: Pages: 1137-1156.
129. Botelho MF, Zeevaart JR, Dormehl IC, Louw WKA, Caramelo F, Metello LF, Gomes CM, Neves M, Sena C, Abrantes AM *et al*: **Dosimetric evaluation of the polyphosphonate; PEI-MP labeled with 117mSn, 186Re and 99mTc as potential diagnosis/therapeutic bone agents**. *European journal of nuclear medicine and molecular imaging* 2006, **33**:S309-S309.
130. Degrossi OJ, Oliveri P, Garcia del Rio H, Labriola R, Artagaveytia D, Degrossi EB: **Technetium-99m APD compared with technetium-99m MDP as a bone scanning agent**. *Journal of nuclear medicine : official publication, Society of Nuclear Medicine* 1985, **26**(10):1135-1139.
131. Louw WK, Dormehl IC, van Rensburg AJ, Hugo N, Alberts AS, Forsyth OE, Beverley G, Sweetlove MA, Marais J, Lotter MG *et al*: **Evaluation of samarium-153 and holmium-166-EDTMP in the normal baboon model**. *Nuclear medicine and biology* 1996, **23**(8):935-940.
132. Zeevaart JR, Jarvis NV, Louw WK, Jackson GE: **Metal-ion speciation in blood plasma incorporating the tetraphosphonate, N,N-dimethylenephosphonate-1-hydroxy-4-aminopropilydenediphosphonate (APDDMP), in therapeutic radiopharmaceuticals**. *Journal of inorganic biochemistry* 2001, **83**(1):57-65.
133. Bevan JA, Tofe AJ, Benedict JJ, Francis MD, Barnett BL: **Tc-99m HMDP (hydroxymethylene diphosphonate): a radiopharmaceutical for skeletal and acute myocardial infarct imaging. II. Comparison of Tc-99m hydroxymethylene diphosphonate (HMDP) with other technetium-labeled bone-imaging agents in a canine model**. *Journal*

of nuclear medicine : official publication, Society of Nuclear Medicine 1980, **21**(10):967-970.

134. Quilty PM, Kirk D, Bolger JJ, Dearnaley DP, Lewington VJ, Mason MD, Reed NS, Russell JM, Yardley J: **A comparison of the palliative effects of strontium-89 and external beam radiotherapy in metastatic prostate cancer**. *Radiotherapy and oncology : journal of the European Society for Therapeutic Radiology and Oncology* 1994, **31**(1):33-40.
135. Srivastava SC: **Bone-seeking therapeutic radiopharmaceuticals**. *Brazilian Archives of Biology and Technology* 2002, **45**:45-55.
136. Laing AH, Ackery DM, Bayly RJ, Buchanan RB, Lewington VJ, McEwan AJ, Macleod PM, Zivanovic MA: **Strontium-89 chloride for pain palliation in prostatic skeletal malignancy**. *The British journal of radiology* 1991, **64**(765):816-822.
137. Lewington VJ, McEwan AJ, Ackery DM, Bayly RJ, Keeling DH, Macleod PM, Porter AT, Zivanovic MA: **A prospective, randomised double-blind crossover study to examine the efficacy of strontium-89 in pain palliation in patients with advanced prostate cancer metastatic to bone**. *Eur J Cancer* 1991, **27**(8):954-958.
138. Blake GM, Zivanovic MA, McEwan AJ, Batty VB, Ackery DM: **89Sr radionuclide therapy: dosimetry and haematological toxicity in two patients with metastasising prostatic carcinoma**. *European journal of nuclear medicine* 1987, **13**(1):41-46.
139. Blake GM, Zivanovic MA, McEwan AJ, Ackery DM: **Sr-89 therapy: strontium kinetics in disseminated carcinoma of the prostate**. *European journal of nuclear medicine* 1986, **12**(9):447-454.
140. Robinson RG: **Strontium-89--precursor targeted therapy for pain relief of blastic metastatic disease**. *Cancer* 1993, **72**(11 Suppl):3433-3435.
141. Baziotis N, Yakoumakis E, Zissimopoulos A, Geronicola-Trapali X, Malamitsi J, Proukakis C: **Strontium-89 chloride in the treatment of bone metastases from breast cancer**. *Oncology* 1998, **55**(5):377-381.
142. Ogawa K, Kawashima H, Shiba K, Washiyama K, Yoshimoto M, Kiyono Y, Ueda M, Mori H, Saji H: **Development of [(90)Y]DOTA-conjugated**

bisphosphonate for treatment of painful bone metastases. *Nuclear medicine and biology* 2009, **36**(2):129-135.

143. Eary J, Brenner W: **Nuclear Medicine Therapy**. New York: Informa Healthcare USA; 2007.
144. Atkins HL, Mausner LF, Srivastava SC, Meinken GE, Straub RF, Cabahug CJ, Weber DA, Wong CT, Sacker DF, Madajewicz S *et al*: **Biodistribution of Sn-117m(4+)DTPA for palliative therapy of painful osseous metastases**. *Radiology* 1993, **186**(1):279-283.
145. Turner JH, Claringbold PG: **A phase II study of treatment of painful multifocal skeletal metastases with single and repeated dose samarium-153 ethylenediaminetetramethylene phosphonate**. *Eur J Cancer* 1991, **27**(9):1084-1086.
146. Farhanghi M, Holmes RA, Volkert WA, Logan KW, Singh A: **Samarium-153-EDTMP: pharmacokinetic, toxicity and pain response using an escalating dose schedule in treatment of metastatic bone cancer**. *Journal of nuclear medicine : official publication, Society of Nuclear Medicine* 1992, **33**(8):1451-1458.
147. Alberts AS, Smit BJ, Louw WK, van Rensburg AJ, van Beek A, Kritzinger V, Nel JS: **Dose response relationship and multiple dose efficacy and toxicity of samarium-153-EDTMP in metastatic cancer to bone**. *Radiotherapy and oncology : journal of the European Society for Therapeutic Radiology and Oncology* 1997, **43**(2):175-179.
148. Hsieh BT, Hsieh JF, Tsai SC, Lin WY, Wang SJ, Ting G: **Comparison of various rhenium-188-labeled diphosphonates for the treatment of bone metastases**. *Nuclear medicine and biology* 1999, **26**(8):973-976.
149. Serafini AN, Houston SJ, Resche I, Quick DP, Grund FM, Ell PJ, Bertrand A, Ahmann FR, Orihuela E, Reid RH *et al*: **Palliation of pain associated with metastatic bone cancer using samarium-153 lexidronam: a double-blind placebo-controlled clinical trial**. *Journal of clinical oncology : official journal of the American Society of Clinical Oncology* 1998, **16**(4):1574-1581.
150. Tian JH, Zhang JM, Hou QT, Oyang QH, Wang JM, Luan ZS, Chuan L, He YJ: **Multicentre trial on the efficacy and toxicity of single-dose samarium-153-ethylene diamine tetramethylene phosphonate as a**

palliative treatment for painful skeletal metastases in China. *European journal of nuclear medicine* 1999, **26**(1):2-7.

151. Collins C, Eary JF, Donaldson G, Vernon C, Bush NE, Petersdorf S, Livingston RB, Gordon EE, Chapman CR, Appelbaum FR: **Samarium-153-EDTMP in bone metastases of hormone refractory prostate carcinoma: a phase I/II trial**. *Journal of nuclear medicine : official publication, Society of Nuclear Medicine* 1993, **34**(11):1839-1844.
152. Deutsch E, Libson K, Vanderheyden JL, Ketring AR, Maxon HR: **The chemistry of rhenium and technetium as related to the use of isotopes of these elements in therapeutic and diagnostic nuclear medicine**. *International journal of radiation applications and instrumentation Part B, Nuclear medicine and biology* 1986, **13**(4):465-477.
153. Elder RC, Yuan J, Helmer B, Pipes D, Deutsch K, Deutsch E: **Studies of the Structure and Composition of Rhenium-1,1-Hydroxyethylidenediphosphonate (HEDP) Analogues of the Radiotherapeutic Agent (186)ReHEDP**. *Inorganic chemistry* 1997, **36**(14):3055-3063.
154. Weininger J, Ketring AR, Deutsch EA: **186Re-HEDP: a potential therapeutic bone agent**. *Nuklearmedizin Nuclear medicine* 1984, **23**(2):81-82.
155. Lin WY, Hsieh JF, Lin CP, Hsieh BT, Ting G, Wang SJ, Knapp FF, Jr.: **Effect of reaction conditions on preparations of rhenium-188 hydroxyethylidene diphosphonate complexes**. *Nuclear medicine and biology* 1999, **26**(4):455-459.
156. Eisenhut M: **Preparation of 186Re-perrhenate for nuclear medical purposes**. *The International journal of applied radiation and isotopes* 1982, **33**(2):99-103.
157. El-Mabhouh A, Mercer JR: **188Re-labeled bisphosphonates as potential bifunctional agents for therapy in patients with bone metastases**. *Applied radiation and isotopes : including data, instrumentation and methods for use in agriculture, industry and medicine* 2005, **62**(4):541-549.

158. Bryan JN, Bommarito D, Kim DY, Berent LM, Bryan ME, Lattimer JC, Henry CJ, Engelbrecht H, Ketring A, Cutler C: **Comparison of systemic toxicities of 177Lu-DOTMP and 153Sm-EDTMP administered intravenously at equivalent skeletal doses to normal dogs**. *Journal of nuclear medicine technology* 2009, **37**(1):45-52.

159. Das T, Chakraborty S, Unni PR, Banerjee S, Samuel G, Sarma HD, Venkatesh M, Pillai MR: **177Lu-labeled cyclic polyaminophosphonates as potential agents for bone pain palliation**. *Applied radiation and isotopes : including data, instrumentation and methods for use in agriculture, industry and medicine* 2002, **57**(2):177-184.

160. Hansen K, Khanna C: **Spontaneous and genetically engineered animal models; use in preclinical cancer drug development**. *Eur J Cancer* 2004, **40**(6):858-880.

161. Nilsson S, Larsen RH, Fossa SD, Balteskard L, Borch KW, Westlin JE, Salberg G, Bruland OS: **First clinical experience with alpha-emitting radium-223 in the treatment of skeletal metastases**. *Clinical cancer research : an official journal of the American Association for Cancer Research* 2005, **11**(12):4451-4459.

162. Henriksen G, Breistol K, Bruland OS, Fodstad O, Larsen RH: **Significant antitumor effect from bone-seeking, alpha-particle-emitting (223)Ra demonstrated in an experimental skeletal metastases model**. *Cancer research* 2002, **62**(11):3120-3125.

163. Kvinnsland Y, Skretting A, Bruland OS: **Radionuclide therapy with bone-seeking compounds: Monte Carlo calculations of dose-volume histograms for bone marrow in trabecular bone**. *Physics in medicine and biology* 2001, **46**(4):1149-1161.

164. Henriksen G, Fisher DR, Roeske JC, Bruland OS, Larsen RH: **Targeting of osseous sites with alpha-emitting 223Ra: comparison with the beta-emitter 89Sr in mice**. *Journal of nuclear medicine : official publication, Society of Nuclear Medicine* 2003, **44**(2):252-259.

165. Nilsson S, Franzen L, Parker C, Tyrrell C, Blom R, Tennvall J, Lennernas B, Petersson U, Johannessen DC, Sokal M *et al*: **Bone-targeted radium-223 in symptomatic, hormone-refractory prostate cancer: a**

randomised, multicentre, placebo-controlled phase II study. *The lancet oncology* 2007, **8**(7):587-594.

166. Parker C, Nilsson S, Heinrich D, O'Sullivan JM, Fossa SD, Chodacki A, Wiechno PJ, Logue JP, Seke M, Widmark A *et al*: **Updated analysis of the phase III, double-blind, randomized, multinational study of radium-223 chloride in castration-resistant prostate cancer (CRPC) patients with bone metastases (ALSYMPCA)**. *Journal of clinical oncology : official journal of the American Society of Clinical Oncology* 2012, **30**(18).
167. Parker C, Heinrich D, Helle SI, O'Sullivan JM, Fossa SD, Chodacki A, Demkow T, Logue JP, Seke M, Widmark A *et al*: **Overall survival benefit and impact on skeletal-related events for radium-223 chloride (Alpharadin) in the treatment of castration-resistant prostate cancer (CRPC) patients with bone metastases: A phase III randomized trial (ALSYMPCA)**. *Eur Urol Suppl* 2012, **11**.
168. Zeevaart JR, Louw WK, Kolar ZI, Kilian E, van Rensburg FE, Dormehl IC: **Biodistribution and pharmacokinetics of variously molecular sized 117mSn(II)-polyethyleneiminomethyl phosphonate complexes in the normal primate model as potential selective therapeutic bone agents**. *Arzneimittel-Forschung* 2004, **54**(6):340-347.
169. Maeda H, Wu J, Sawa T, Matsumura Y, Hori K: **Tumor vascular permeability and the EPR effect in macromolecular therapeutics: a review**. *Journal of controlled release : official journal of the Controlled Release Society* 2000, **65**(1-2):271-284.
170. Seymour LW: **Passive tumor targeting of soluble macromolecules and drug conjugates**. *Critical reviews in therapeutic drug carrier systems* 1992, **9**(2):135-187.
171. Hoste K, De Winne K, Schacht E: **Polymeric prodrugs**. *International journal of pharmaceutics* 2004, **277**(1-2):119-131.
172. Jansen DR, Krijger GC, Wagener J, Senwedi RM, Gabanamotse K, Kgadiete M, Kolar ZI, Zeevaart JR: **Blood plasma model predictions for the proposed bone-seeking radiopharmaceutical [(117m)Sn]Sn(IV)-N,N',N'-trimethylenephosphonate-**

poly(ethyleneimine). *Journal of inorganic biochemistry* 2009, **103**(9):1265-1272.

173. Iyer AK, Khaled G, Fang J, Maeda H: **Exploiting the enhanced permeability and retention effect for tumor targeting**. *Drug discovery today* 2006, **11**(17-18):812-818.
174. Zeevaart JR, Jansen DR, Botelho MF, Abrunhosa A, Gomes C, Metello L, Kolar ZI, Krijger GC, Louw WK, Dormehl IC: **Comparison of the predicted in vivo behaviour of the Sn(II)-APDDMP complex and the results as studied in a rodent model**. *Journal of inorganic biochemistry* 2004, **98**(9):1521-1530.
175. Uhrich KE, Cannizzaro SM, Langer RS, Shakesheff KM: **Polymeric systems for controlled drug release**. *Chemical reviews* 1999, **99**(11):3181-3198.
176. Jansen DR, Zeevaart JR, Denkova A, Kolar ZI, Krijger GC: **Hydroxyapatite chemisorption of N,N',N'-trimethylenephosphonate-poly(ethyleneimine) (PEI-MP) combined with Sn2+ or Sn4+**. *Langmuir : the ACS journal of surfaces and colloids* 2009, **25**(5):2790-2796.
177. Cote RJ, Datar RH: **Therapeutic approaches to bladder cancer: identifying targets and mechanisms**. *Critical reviews in oncology/hematology* 2003, **46 Suppl**:S67-83.
178. Lee R, Droller MJ: **The natural history of bladder cancer. Implications for therapy**. *The Urologic clinics of North America* 2000, **27**(1):1-13, vii.
179. Burger M, Catto JW, Dalbagni G, Grossman HB, Herr H, Karakiewicz P, Kassouf W, Kiemeney LA, La Vecchia C, Shariat S *et al*: **Epidemiology and risk factors of urothelial bladder cancer**. *European urology* 2013, **63**(2):234-241.
180. Eble JL, Sauter G, Epstein JI, Sesterhenn IA, World Health Organization., International Agency for Research on Cancer.: **Pathology and genetics of tumours of the urinary system and male genital organs**. Lyon: IARC; 2004.
181. Cheng L, Montironi R, Davidson DD, Lopez-Beltran A: **Staging and reporting of urothelial carcinoma of the urinary bladder**. *Modern*

pathology : an official journal of the United States and Canadian Academy of Pathology, Inc 2009, **22 Suppl 2**:S70-95.

182. Droller MJ: **Bladder cancer: state-of-the-art care**. *CA: a cancer journal for clinicians* 1998, **48**(5):269-284.
183. Jemal A, Siegel R, Xu J, Ward E: **Cancer statistics, 2010**. *CA: a cancer journal for clinicians* 2010, **60**(5):277-300.
184. **NCCN Clinical Practice Guidelines in Oncology - Bladder** [http://www.tri-kobe.org/nccn/guideline/urological/english/bladder.pdf]
185. Heney NM: **Natural history of superficial bladder cancer. Prognostic features and long-term disease course**. *The Urologic clinics of North America* 1992, **19**(3):429-433.
186. Shipley WU, Kaufman DS, Tester WJ, Pilepich MV, Sandler HM: **Overview of bladder cancer trials in the Radiation Therapy Oncology Group**. *Cancer* 2003, **97**(8 Suppl):2115-2119.
187. Hoglund M: **Bladder cancer, a two phased disease?** *Seminars in cancer biology* 2007, **17**(3):225-232.
188. NCI: **Bladder Cancer Treatment (PDQ®)**. In.: Nacional Cancer Institute; 2014.
189. Greene F, Page DL, Flemming I, Fritz A, Balch C, Haller D, Morrow M: **American Joint Committee on Cancer Staging Manual**, 6 edn: Springer-Verlag; 2002.
190. Edge SB, Byrd DR, Compton CC, Fritz AG, Greene FL, Trotti A: **AJCC Cancer Staging Manual**. In., 7 edn: Springer; 2010.
191. Miyamoto H, Miller JS, Fajardo DA, Lee TK, Netto GJ, Epstein JI: **Non-invasive papillary urothelial neoplasms: the 2004 WHO/ISUP classification system**. *Pathology international* 2010, **60**(1):1-8.
192. Angulo JC, Lopez JI, Grignon DJ, Sanchez-Chapado M: **Muscularis mucosa differentiates two populations with different prognosis in stage T1 bladder cancer**. *Urology* 1995, **45**(1):47-53.
193. Younes M, Sussman J, True LD: **The usefulness of the level of the muscularis mucosae in the staging of invasive transitional cell carcinoma of the urinary bladder**. *Cancer* 1990, **66**(3):543-548.
194. Amling CL: **Diagnosis and management of superficial bladder cancer**. *Current problems in cancer* 2001, **25**(4):219-278.

195. Knowles MA: **Identification of novel bladder tumour suppressor genes**. *Electrophoresis* 1999, **20**(2):269-279.
196. Billerey C, Chopin D, Aubriot-Lorton MH, Ricol D, Gil Diez de Medina S, Van Rhijn B, Bralet MP, Lefrere-Belda MA, Lahaye JB, Abbou CC *et al*: **Frequent FGFR3 mutations in papillary non-invasive bladder (pTa) tumors**. *The American journal of pathology* 2001, **158**(6):1955-1959.
197. Wu XR: **Urothelial tumorigenesis: a tale of divergent pathways**. *Nature reviews Cancer* 2005, **5**(9):713-725.
198. Caffo O, Veccia A, Fellin G, Russo L, Mussari S, Galligioni E: **Trimodality treatment in the conservative management of infiltrating bladder cancer: A critical review of the literature**. *Critical reviews in oncology/hematology* 2012.
199. Ferlay J, Parkin DM, Steliarova-Foucher E: **Estimates of cancer incidence and mortality in Europe in 2008**. *Eur J Cancer* 2010, **46**(4):765-781.
200. Parkin DM: **The global burden of urinary bladder cancer**. *Scandinavian journal of urology and nephrology Supplementum* 2008(218):12-20.
201. Kirkali Z, Chan T, Manoharan M, Algaba F, Busch C, Cheng L, Kiemeney L, Kriegmair M, Montironi R, Murphy WM *et al*: **Bladder cancer: epidemiology, staging and grading, and diagnosis**. *Urology* 2005, **66**(6 Suppl 1):4-34.
202. Freedman ND, Silverman DT, Hollenbeck AR, Schatzkin A, Abnet CC: **Association between smoking and risk of bladder cancer among men and women**. *JAMA : the journal of the American Medical Association* 2011, **306**(7):737-745.
203. Levin ML, Lilienfeld AM, Moore GE: **The association of smoking with cancer of the urinary bladder in humans**. *AMA archives of internal medicine* 1956, **98**(2):129-135.
204. Clavel J, Cordier S, Boccon-Gibod L, Hemon D: **Tobacco and bladder cancer in males: increased risk for inhalers and smokers of black tobacco**. *International journal of cancer Journal international du cancer* 1989, **44**(4):605-610.

205. Lower GM, Jr.: **Concepts in causality: chemically induced human urinary bladder cancer**. *Cancer* 1982, **49**(5):1056-1066.
206. Mommsen S, Barfod NM, Aagaard J: **N-Acetyltransferase phenotypes in the urinary bladder carcinogenesis of a low-risk population**. *Carcinogenesis* 1985, **6**(2):199-201.
207. Bartsch H, Caporaso N, Coda M, Kadlubar F, Malaveille C, Skipper P, Talaska G, Tannenbaum SR, Vineis P: **Carcinogen hemoglobin adducts, urinary mutagenicity, and metabolic phenotype in active and passive cigarette smokers**. *Journal of the National Cancer Institute* 1990, **82**(23):1826-1831.
208. Fernandez MI, Lopez JF, Vivaldi B, Coz F: **Long-term impact of arsenic in drinking water on bladder cancer health care and mortality rates 20 years after end of exposure**. *The Journal of urology* 2012, **187**(3):856-861.
209. Michaud DS, Kogevinas M, Cantor KP, Villanueva CM, Garcia-Closas M, Rothman N, Malats N, Real FX, Serra C, Garcia-Closas R *et al*: **Total fluid and water consumption and the joint effect of exposure to disinfection by-products on risk of bladder cancer**. *Environmental health perspectives* 2007, **115**(11):1569-1572.
210. Villanueva CM, Silverman DT, Murta-Nascimento C, Malats N, Garcia-Closas M, Castro F, Tardon A, Garcia-Closas R, Serra C, Carrato A *et al*: **Coffee consumption, genetic susceptibility and bladder cancer risk**. *Cancer causes & control : CCC* 2009, **20**(1):121-127.
211. Pelucchi C, Galeone C, Tramacere I, Bagnardi V, Negri E, Islami F, Scotti L, Bellocco R, Corrao G, Boffetta P *et al*: **Alcohol drinking and bladder cancer risk: a meta-analysis**. *Annals of oncology : official journal of the European Society for Medical Oncology / ESMO* 2012, **23**(6):1586-1593.
212. Palou J, Sylvester RJ, Faba OR, Parada R, Pena JA, Algaba F, Villavicencio H: **Female gender and carcinoma in situ in the prostatic urethra are prognostic factors for recurrence, progression, and disease-specific mortality in T1G3 bladder cancer patients treated with bacillus Calmette-Guerin**. *European urology* 2012, **62**(1):118-125.

213. Yee DS, Ishill NM, Lowrance WT, Herr HW, Elkin EB: **Ethnic differences in bladder cancer survival**. *Urology* 2011, **78**(3):544-549.
214. Datta GD, Neville BA, Kawachi I, Datta NS, Earle CC: **Marital status and survival following bladder cancer**. *Journal of epidemiology and community health* 2009, **63**(10):807-813.
215. Koroukian SM, Bakaki PM, Raghavan D: **Survival disparities by Medicaid status: an analysis of 8 cancers**. *Cancer* 2012, **118**(17):4271-4279.
216. Travis LB, Curtis RE, Boice JD, Jr., Fraumeni JF, Jr.: **Bladder cancer after chemotherapy for non-Hodgkin's lymphoma**. *The New England journal of medicine* 1989, **321**(8):544-545.
217. Boice JD, Jr., Engholm G, Kleinerman RA, Blettner M, Stovall M, Lisco H, Moloney WC, Austin DF, Bosch A, Cookfair DL *et al*: **Radiation dose and second cancer risk in patients treated for cancer of the cervix**. *Radiation research* 1988, **116**(1):3-55.
218. Turner AG, Hendry WF, Williams GB, Wallace DM: **A haematuria diagnostic service**. *British medical journal* 1977, **2**(6078):29-31.
219. Brown FM: **Urine cytology. It is still the gold standard for screening?** *The Urologic clinics of North America* 2000, **27**(1):25-37.
220. Heney NM, Ahmed S, Flanagan MJ, Frable W, Corder MP, Hafermann MD, Hawkins IR: **Superficial bladder cancer: progression and recurrence**. *The Journal of urology* 1983, **130**(6):1083-1086.
221. Barentsz JO, Witjes JA, Ruijs JH: **What is new in bladder cancer imaging**. *The Urologic clinics of North America* 1997, **24**(3):583-602.
222. Witjes JA, Compérat E, Cowan NC, De Santis M, Gakis G, Lebret T, Ribal MJ, Sherif A: **Guidelines on Muscle-invasive and Metastatic Bladder Cancer**. In.: European Association of Urology; 2013.
223. Duque JL, Loughlin KR: **An overview of the treatment of superficial bladder cancer. Intravesical chemotherapy**. *The Urologic clinics of North America* 2000, **27**(1):125-135, x.
224. Bouffioux C, Denis L, Oosterlinck W, Viggiano G, Vergison B, Keuppens F, De Pauw M, Sylvester R, Cheuvart B: **Adjuvant chemotherapy of recurrent superficial transitional cell carcinoma: results of a European organization for research on treatment of cancer**

randomized trial comparing intravesical instillation of thiotepa, doxorubicin and cisplatin. The European Organization for Research on Treatment of Cancer Genitourinary Group. *The Journal of urology* 1992, **148**(2 Pt 1):297-301.

225. Flamm J: **Long-term versus short-term doxorubicin hydrochloride instillation after transurethral resection of superficial bladder cancer**. *European urology* 1990, **17**(2):119-124.

226. Kurth K, Vijgh WJ, ten Kate F, Bogdanowicz JF, Carpentier PJ, Van Reyswoud I: **Phase 1/2 study of intravesical epirubicin in patients with carcinoma in situ of the bladder**. *The Journal of urology* 1991, **146**(6):1508-1512; discussion 1512-1503.

227. Kurth K, Tunn U, Ay R, Schroder FH, Pavone-Macaluso M, Debruyne F, ten Kate F, de Pauw M, Sylvester R: **Adjuvant chemotherapy for superficial transitional cell bladder carcinoma: long-term results of a European Organization for Research and Treatment of Cancer randomized trial comparing doxorubicin, ethoglucid and transurethral resection alone**. *The Journal of urology* 1997, **158**(2):378-384.

228. Lamm DL: **Long-term results of intravesical therapy for superficial bladder cancer**. *The Urologic clinics of North America* 1992, **19**(3):573-580.

229. Pawinski A, Sylvester R, Kurth KH, Bouffioux C, van der Meijden A, Parmar MK, Bijnens L: **A combined analysis of European Organization for Research and Treatment of Cancer, and Medical Research Council randomized clinical trials for the prophylactic treatment of stage TaT1 bladder cancer. European Organization for Research and Treatment of Cancer Genitourinary Tract Cancer Cooperative Group and the Medical Research Council Working Party on Superficial Bladder Cancer**. *The Journal of urology* 1996, **156**(6):1934-1940, discussion 1940-1931.

230. Prout GR, Jr., Shipley WU, Kaufman DS, Heney NM, Griffin PP, Althausen AF, Bassil B, Nocks BN, Parkhurst EC, Young HH, 2nd: **Preliminary results in invasive bladder cancer with transurethral resection, neoadjuvant chemotherapy and combined pelvic**

irradiation plus cisplatin chemotherapy. *The Journal of urology* 1990, **144**(5):1128-1134; discussion 1134-1126.

231. Kelly JF, Snell ME: **Hematoporphyrin derivative: a possible aid in the diagnosis and therapy of carcinoma of the bladder**. *The Journal of urology* 1976, **115**(2):150-151.
232. Walther MM: **The role of photodynamic therapy in the treatment of recurrent superficial bladder cancer**. *The Urologic clinics of North America* 2000, **27**(1):163-170.
233. Mitchell JB, McPherson S, DeGraff W, Gamson J, Zabell A, Russo A: **Oxygen dependence of hematoporphyrin derivative-induced photoinactivation of Chinese hamster cells**. *Cancer research* 1985, **45**(5):2008-2011.
234. Kamat AM, Lamm DL: **Immunotherapy for bladder cancer**. *Current urology reports* 2001, **2**(1):62-69.
235. Dalbagni G, Herr HW: **Current use and questions concerning intravesical bladder cancer group for superficial bladder cancer**. *The Urologic clinics of North America* 2000, **27**(1):137-146.
236. Malmstrom PU, Wijkstrom H, Lundholm C, Wester K, Busch C, Norlen BJ: **5-year followup of a randomized prospective study comparing mitomycin C and bacillus Calmette-Guerin in patients with superficial bladder carcinoma. Swedish-Norwegian Bladder Cancer Study Group**. *The Journal of urology* 1999, **161**(4):1124-1127.
237. Lamm DL, Blumenstein BA, Crawford ED, Montie JE, Scardino P, Grossman HB, Stanisic TH, Smith JA, Jr., Sullivan J, Sarosdy MF *et al*: **A randomized trial of intravesical doxorubicin and immunotherapy with bacille Calmette-Guerin for transitional-cell carcinoma of the bladder**. *The New England journal of medicine* 1991, **325**(17):1205-1209.
238. Hudson MA, Herr HW: **Carcinoma in situ of the bladder**. *The Journal of urology* 1995, **153**(3 Pt 1):564-572.
239. Herr HW, Laudone VP, Whitmore WF, Jr.: **An overview of intravesical therapy for superficial bladder tumors**. *The Journal of urology* 1987, **138**(6):1363-1368.

240. Herr HW, Badalament RA, Amato DA, Laudone VP, Fair WR, Whitmore WF, Jr.: **Superficial bladder cancer treated with bacillus Calmette-Guerin: a multivariate analysis of factors affecting tumor progression**. *The Journal of urology* 1989, **141**(1):22-29.
241. Cookson MS, Herr HW, Zhang ZF, Soloway S, Sogani PC, Fair WR: **The treated natural history of high risk superficial bladder cancer: 15-year outcome**. *The Journal of urology* 1997, **158**(1):62-67.
242. Ratliff TL: **Bacillus Calmette-Guerin (BCG): mechanism of action in superficial bladder cancer**. *Urology* 1991, **37**(5 Suppl):8-11.
243. Lattime EC, Gomella LG, McCue PA: **Murine bladder carcinoma cells present antigen to BCG-specific CD4+ T-cells**. *Cancer research* 1992, **52**(15):4286-4290.
244. Ratliff TL, Ritchey JK, Yuan JJ, Andriole GL, Catalona WJ: **T-cell subsets required for intravesical BCG immunotherapy for bladder cancer**. *The Journal of urology* 1993, **150**(3):1018-1023.
245. Lamm DL: **Complications of bacillus Calmette-Guerin immunotherapy**. *The Urologic clinics of North America* 1992, **19**(3):565-572.
246. Olsson CA, Chute R, Rao CN: **Immunologic reduction of bladder cancer recurrence rate**. *The Journal of urology* 1974, **111**(2):173-176.
247. Jurincic CD, Engelmann U, Gasch J, Klippel KF: **Immunotherapy in bladder cancer with keyhole-limpet hemocyanin: a randomized study**. *The Journal of urology* 1988, **139**(4):723-726.
248. Glashan RW: **A randomized controlled study of intravesical alpha-2b-interferon in carcinoma in situ of the bladder**. *The Journal of urology* 1990, **144**(3):658-661.
249. Stein JP, Lieskovsky G, Cote R, Groshen S, Feng AC, Boyd S, Skinner E, Bochner B, Thangathurai D, Mikhail M *et al*: **Radical cystectomy in the treatment of invasive bladder cancer: long-term results in 1,054 patients**. *Journal of clinical oncology : official journal of the American Society of Clinical Oncology* 2001, **19**(3):666-675.
250. Kaufman DS: **Challenges in the treatment of bladder cancer**. *Annals of oncology : official journal of the European Society for Medical Oncology / ESMO* 2006, **17 Suppl 5**:v106-112.

251. Zietman AL, Grocela J, Zehr E, Kaufman DS, Young RH, Althausen AF, Heney NM, Shipley WU: **Selective bladder conservation using transurethral resection, chemotherapy, and radiation: management and consequences of Ta, T1, and Tis recurrence within the retained bladder**. *Urology* 2001, **58**(3):380-385.

252. Henningsohn L, Wijkstrom H, Dickman PW, Bergmark K, Steineck G: **Distressful symptoms after radical cystectomy with urinary diversion for urinary bladder cancer: a Swedish population-based study**. *European urology* 2001, **40**(2):151-162.

253. Herr HW: **Conservative management of muscle-infiltrating bladder cancer: prospective experience**. *The Journal of urology* 1987, **138**(5):1162-1163.

254. Henry K, Miller J, Mori M, Loening S, Fallon B: **Comparison of transurethral resection to radical therapies for stage B bladder tumors**. *The Journal of urology* 1988, **140**(5):964-967.

255. Duncan W, Quilty PM: **The results of a series of 963 patients with transitional cell carcinoma of the urinary bladder primarily treated by radical megavoltage X-ray therapy**. *Radiotherapy and oncology : journal of the European Society for Therapeutic Radiology and Oncology* 1986, **7**(4):299-310.

256. Gospodarowicz MK, Hawkins NV, Rawlings GA, Connolly JG, Jewett MA, Thomas GM, Herman JG, Garrett PG, Chua T, Duncan W *et al*: **Radical radiotherapy for muscle invasive transitional cell carcinoma of the bladder: failure analysis**. *The Journal of urology* 1989, **142**(6):1448-1453; discussion 1453-1444.

257. Hall RR, Newling DW, Ramsden PD, Richards B, Robinson MR, Smith PH: **Treatment of invasive bladder cancer by local resection and high dose methotrexate**. *British journal of urology* 1984, **56**(6):668-672.

258. Shipley WU, Prout GR, Jr., Einstein AB, Coombs LJ, Wajsman Z, Soloway MS, Englander L, Barton BA, Hafermann MD: **Treatment of invasive bladder cancer by cisplatin and radiation in patients unsuited for surgery**. *JAMA : the journal of the American Medical Association* 1987, **258**(7):931-935.

259. Coppin CM, Gospodarowicz MK, James K, Tannock IF, Zee B, Carson J, Pater J, Sullivan LD: **Improved local control of invasive bladder cancer by concurrent cisplatin and preoperative or definitive radiation. The National Cancer Institute of Canada Clinical Trials Group**. *Journal of clinical oncology : official journal of the American Society of Clinical Oncology* 1996, **14**(11):2901-2907.

260. Dreicer R, Li H, Stein M, DiPaola R, Eleff M, Roth BJ, Wilding G: **Phase 2 trial of sorafenib in patients with advanced urothelial cancer: a trial of the Eastern Cooperative Oncology Group**. *Cancer* 2009, **115**(18):4090-4095.

261. Wulfing C, Machiels JP, Richel DJ, Grimm MO, Treiber U, De Groot MR, Beuzeboc P, Parikh R, Petavy F, El-Hariry IA: **A single-arm, multicenter, open-label phase 2 study of lapatinib as the second-line treatment of patients with locally advanced or metastatic transitional cell carcinoma**. *Cancer* 2009, **115**(13):2881-2890.

262. Petrylak DP, Tangen CM, Van Veldhuizen PJ, Jr., Goodwin JW, Twardowski PW, Atkins JN, Kakhil SR, Lange MK, Mansukhani M, Crawford ED: **Results of the Southwest Oncology Group phase II evaluation (study S0031) of ZD1839 for advanced transitional cell carcinoma of the urothelium**. *BJU international* 2010, **105**(3):317-321.

263. Gallagher DJ, Milowsky MI, Gerst SR, Ishill N, Riches J, Regazzi A, Boyle MG, Trout A, Flaherty AM, Bajorin DF: **Phase II study of sunitinib in patients with metastatic urothelial cancer**. *Journal of clinical oncology : official journal of the American Society of Clinical Oncology* 2010, **28**(8):1373-1379.

264. Sridhar SS, Winquist E, Eisen A, Hotte SJ, McWhirter E, Tannock IF, Mukherjee SD, Wang L, Blattler C, Wright JJ *et al*: **A phase II trial of sorafenib in first-line metastatic urothelial cancer: a study of the PMH Phase II Consortium**. *Investigational new drugs* 2011, **29**(5):1045-1049.

265. Hussain MH, MacVicar GR, Petrylak DP, Dunn RL, Vaishampayan U, Lara PN, Jr., Chatta GS, Nanus DM, Glode LM, Trump DL *et al*: **Trastuzumab, paclitaxel, carboplatin, and gemcitabine in advanced human epidermal growth factor receptor-2/neu-positive urothelial**

carcinoma: results of a multicenter phase II National Cancer Institute trial. *Journal of clinical oncology : official journal of the American Society of Clinical Oncology* 2007, **25**(16):2218-2224.

266. Hahn NM, Stadler WM, Zon RT, Waterhouse D, Picus J, Nattam S, Johnson CS, Perkins SM, Waddell MJ, Sweeney CJ: **Phase II trial of cisplatin, gemcitabine, and bevacizumab as first-line therapy for metastatic urothelial carcinoma: Hoosier Oncology Group GU 04-75**. *Journal of clinical oncology : official journal of the American Society of Clinical Oncology* 2011, **29**(12):1525-1530.
267. Botelho MF, Zeevaart JR, Jansen DR, Turtoi A, Abrantes AM, Kolar ZI, Neves MA, Schneeweiss FHA, Krijger GC, Dormehl IC: **Comparison of the sizes of the potencial therapeutic bone agents, the polyphosphonate PEI-MP labelled with 117mSn and 186Re**. *European journal of nuclear medicine and molecular imaging* 2007, **34**(2):S335.
268. Moedritzer K, Irani RR: **The Direct Synthesis of α-Aminomethylphosphonic Acids. Mannich-Type Reactions with Orthophosphorous Acid**. *The Journal of organic chemistry* 1966, **31**(5):1603–1607.
269. Dormehl I: **Novel phosphonate containing ligands for optimised targeted radiotherapy of neoplastic bone disease using animal models and scintigraphy**. *PhD.* North-West University Potchefstroom Campus; 2006.
270. Milner RJ: **Naturally occurring canine osteosarcoma in the dog animal model for research of targeted radiotherapy using beta-emitting radioisotopes with various ligands** *PhD.* University of Pretoria; 2013.
271. IAEA: **Technetium-99m Radiopharmaceuticals: Status and Trends**. In. IAEA Library: International Atomic Energy Agency; 2009.
272. Liu Y, Shen B, Liu F, Zhang B, Chu T, Bai J, Bao S: **Synthesis, radiolabeling, biodistribution and fluorescent imaging of histidine-coupled hematoporphyrin**. *Nuclear medicine and biology* 2012, **39**(4):579-585.

273. Fazaeli Y, Jalilian AR, Amini MM, Ardaneh K, Rahiminejad A, Bolourinovin F, Moradkhani S, Majdabadi A: **Development of a (68)Ga-Fluorinated Porphyrin Complex as a Possible PET Imaging Agent**. *Nuclear medicine and molecular imaging* 2012, **46**(1):20-26.
274. Strober W: **Trypan blue exclusion test of cell viability**. *Current protocols in immunology / edited by John E Coligan [et al]* 2001, **Appendix 3**:Appendix 3B.
275. Mosmann T: **Rapid colorimetric assay for cellular growth and survival: application to proliferation and cytotoxicity assays**. *Journal of immunological methods* 1983, **65**(1-2):55-63.
276. Mamede AC, Pires AS, Abrantes AM, Tavares SD, Goncalves AC, Casalta-Lopes JE, Sarmento-Ribeiro AB, Maia JM, Botelho MF: **Cytotoxicity of ascorbic acid in a human colorectal adenocarcinoma cell line (WiDr): in vitro and in vivo studies**. *Nutrition and cancer* 2012, **64**(7):1049-1057.
277. Brito AF, Abrantes AM, Pinto-Costa C, Gomes AR, Mamede AC, Casalta-Lopes J, Goncalves AC, Sarmento-Ribeiro AB, Tralhao JG, Botelho MF: **Hepatocellular carcinoma and chemotherapy: the role of p53**. *Chemotherapy* 2012, **58**(5):381-386.
278. Kerr JF, Wyllie AH, Currie AR: **Apoptosis: a basic biological phenomenon with wide-ranging implications in tissue kinetics**. *British journal of cancer* 1972, **26**(4):239-257.
279. Kroemer G, Dallaporta B, Resche-Rigon M: **The mitochondrial death/life regulator in apoptosis and necrosis**. *Annual review of physiology* 1998, **60**:619-642.
280. Williams JR, Little JB, Shipley WU: **Association of mammalian cell death with a specific endonucleolytic degradation of DNA**. *Nature* 1974, **252**(5485):754-755.
281. Savill J: **Phagocyte recognition of apoptotic cells**. *Biochemical Society transactions* 1996, **24**(4):1065-1069.
282. Riedl SJ, Shi Y: **Molecular mechanisms of caspase regulation during apoptosis**. *Nature reviews Molecular cell biology* 2004, **5**(11):897-907.
283. Timmer JC, Salvesen GS: **Caspase substrates**. *Cell death and differentiation* 2007, **14**(1):66-72.

284. Chipuk JE, Green DR: **Do inducers of apoptosis trigger caspase-independent cell death?** *Nature reviews Molecular cell biology* 2005, **6**(3):268-275.
285. Kim R, Emi M, Tanabe K: **Role of mitochondria as the gardens of cell death**. *Cancer chemotherapy and pharmacology* 2006, **57**(5):545-553.
286. Zong WX, Thompson CB: **Necrotic death as a cell fate**. *Genes & development* 2006, **20**(1):1-15.
287. Galluzzi L, Maiuri MC, Vitale I, Zischka H, Castedo M, Zitvogel L, Kroemer G: **Cell death modalities: classification and pathophysiological implications**. *Cell death and differentiation* 2007, **14**(7):1237-1243.
288. Aubry JP, Blaecke A, Lecoanet-Henchoz S, Jeannin P, Herbault N, Caron G, Moine V, Bonnefoy JY: **Annexin V used for measuring apoptosis in the early events of cellular cytotoxicity**. *Cytometry* 1999, **37**(3):197-204.
289. Abrantes AM, Serra ME, Goncalves AC, Rio J, Oliveiros B, Laranjo M, Rocha-Gonsalves AM, Sarmento-Ribeiro AB, Botelho MF: **Hypoxia-induced redox alterations and their correlation with 99mTc-MIBI and 99mTc-HL-91 uptake in colon cancer cells**. *Nuclear medicine and biology* 2010, **37**(2):125-132.
290. Kirkinezos IG, Moraes CT: **Reactive oxygen species and mitochondrial diseases**. *Seminars in cell & developmental biology* 2001, **12**(6):449-457.
291. Ozben T: **Oxidative stress and apoptosis: impact on cancer therapy**. *Journal of pharmaceutical sciences* 2007, **96**(9):2181-2196.
292. Shrivastava A, Kuzontkoski PM, Groopman JE, Prasad A: **Cannabidiol induces programmed cell death in breast cancer cells by coordinating the cross-talk between apoptosis and autophagy**. *Molecular cancer therapeutics* 2011, **10**(7):1161-1172.
293. Tan S, Sagara Y, Liu Y, Maher P, Schubert D: **The regulation of reactive oxygen species production during programmed cell death**. *J Cell Biol* 1998, **141**(6):1423-1432.
294. Halliwell B, Whiteman M: **Measuring reactive species and oxidative damage in vivo and in cell culture: how should you do it and what**

do the results mean? *British journal of pharmacology* 2004, **142**(2):231-255.

295. Ortega AL, Mena S, Estrela JM: **Glutathione in Cancer Cell Death**. *Cancers* 2011, **3**:1285-1310.
296. Zhao H, Joseph J, Fales HM, Sokoloski EA, Levine RL, Vasquez-Vivar J, Kalyanaraman B: **Detection and characterization of the product of hydroethidine and intracellular superoxide by HPLC and limitations of fluorescence**. *Proceedings of the National Academy of Sciences of the United States of America* 2005, **102**(16):5727-5732.
297. Franco R, Cidlowski JA: **Apoptosis and glutathione: beyond an antioxidant**. *Cell death and differentiation* 2009, **16**(10):1303-1314.
298. O'Connor JE, Kimler BF, Morgan MC, Tempas KJ: **A flow cytometric assay for intracellular nonprotein thiols using mercury orange**. *Cytometry* 1988, **9**(6):529-532.
299. Gottlieb E, Armour SM, Harris MH, Thompson CB: **Mitochondrial membrane potential regulates matrix configuration and cytochrome c release during apoptosis**. *Cell death and differentiation* 2003, **10**(6):709-717.
300. Yao J, Jiang Z, Duan W, Huang J, Zhang L, Hu L, He L, Li F, Xiao Y, Shu B *et al*: **Involvement of mitochondrial pathway in triptolide-induced cytotoxicity in human normal liver L-02 cells**. *Biological & pharmaceutical bulletin* 2008, **31**(4):592-597.
301. Munshi A, Hobb M, Raymond RE: **Clonogenic Cell Survival Assay**. In: *Chemosensitivity: In vitro assays.* Edited by Blumenthal RD, vol. 1: Humana Press; 2005: 21-28.
302. Tavares AA, Tavares JM: **(99m)Tc Auger electrons--analysis on the effects of low absorbed doses by computational methods**. *Applied radiation and isotopes : including data, instrumentation and methods for use in agriculture, industry and medicine* 2011, **69**(3):607-608.
303. Mettler FA, Jr., Huda W, Yoshizumi TT, Mahesh M: **Effective doses in radiology and diagnostic nuclear medicine: a catalog**. *Radiology* 2008, **248**(1):254-263.
304. Olive PL, Durand RE: **Apoptosis: an indicator of radiosensitivity in vitro?** *International journal of radiation biology* 1997, **71**(6):695-707.

305. Shinomiya N, Kuno Y, Yamamoto F, Fukasawa M, Okumura A, Uefuji M, Rokutanda M: **Different mechanisms between premitotic apoptosis and postmitotic apoptosis in X-irradiated U937 cells**. *International journal of radiation oncology, biology, physics* 2000, **47**(3):767-777.
306. Shinomiya N: **New concepts in radiation-induced apoptosis: 'premitotic apoptosis' and 'postmitotic apoptosis'**. *Journal of cellular and molecular medicine* 2001, **5**(3):240-253.
307. Merritt AJ, Allen TD, Potten CS, Hickman JA: **Apoptosis in small intestinal epithelial from p53-null mice: evidence for a delayed, p53-independent G2/M-associated cell death after gamma-irradiation**. *Oncogene* 1997, **14**(23):2759-2766.
308. Sak A, Wurm R, Elo B, Grehl S, Pottgen C, Stuben G, Sinn B, Wolf G, Budach V, Stuschke M: **Increased radiation-induced apoptosis and altered cell cycle progression of human lung cancer cell lines by antisense oligodeoxynucleotides targeting p53 and p21(WAF1/CIP1)**. *Cancer gene therapy* 2003, **10**(12):926-934.
309. Stuschke M, Sak A, Wurm R, Sinn B, Wolf G, Stuben G, Budach V: **Radiation-induced apoptosis in human non-small-cell lung cancer cell lines is secondary to cell-cycle progression beyond the G2-phase checkpoint**. *International journal of radiation biology* 2002, **78**(9):807-819.
310. Eriksson D, Lofroth PO, Johansson L, Riklund KA, Stigbrand T: **Cell cycle disturbances and mitotic catastrophes in HeLa Hep2 cells following 2.5 to 10 Gy of ionizing radiation**. *Clinical cancer research : an official journal of the American Association for Cancer Research* 2007, **13**(18 Pt 2):5501s-5508s.
311. Eriksson D, Joniani HM, Sheikholvaezin A, Lofroth PO, Johansson L, Riklund Ahlstrom K, Stigbrand T: **Combined low dose radio- and radioimmunotherapy of experimental HeLa Hep 2 tumours**. *European journal of nuclear medicine and molecular imaging* 2003, **30**(6):895-906.
312. Akagi Y, Ito K, Sawada S: **Radiation-induced apoptosis and necrosis in Molt-4 cells: a study of dose-effect relationships and their**

modification. *International journal of radiation biology* 1993, **64**(1):47-56.

313. Roninson IB, Broude EV, Chang BD: **If not apoptosis, then what? Treatment-induced senescence and mitotic catastrophe in tumor cells**. *Drug resistance updates : reviews and commentaries in antimicrobial and anticancer chemotherapy* 2001, **4**(5):303-313.
314. Ree A, Stokke T, Bratland A, Patzke S, Nome RV, Folkvord S, Meza-Zepeda LA, Flatmark K, Fodstad O, Andersson Y: **DNA Damage Responses in Cell Cycle G2 Phase and Mitosis – Tracking and Targeting**. *Anticancer research* 2006, **26**:1909-1916.
315. Pozarowski P, Darzynkiewicz Z: **Analysis of Cell Cycle by Flow Cytometry**. In: *Checkpoint Controls and Cancer.* Edited by Schönthal AH, vol. 1: Humana Press; 2004: 301-3011.
316. Mamede AC, Abrantes AM, Pires AS, Tavares SD, Serra ME, Maia JM, Botelho MF: **Radiolabelling of ascorbic acid: a new clue to clarify its action as an anticancer agent?** *Current radiopharmaceuticals* 2012, **5**(2):106-112.
317. Botelho F, Dormehl I, Louw W, Zeevaart JR, Gomes C, Kolar K, Abrunhosa A, Metello L, Milner R, de Lima J *et al*: **Polyethyleneiminomethyl phosphonate (PEI-MP) for selectively targeting bone malignancies**. *European journal of nuclear medicine and molecular imaging* 2003, **30**(2):S338.
318. Shields AF, Price P: **In Vivo Imaging of Cancer Therapy**: Humana Press; 2007.
319. Jackson RC: **The problem of the quiescent cancer cell**. *Advances in enzyme regulation* 1989, **29**:27-46.
320. Fidler IJ, Wilmanns C, Staroselsky A, Radinsky R, Dong Z, Fan D: **Modulation of tumor cell response to chemotherapy by the organ environment**. *Cancer metastasis reviews* 1994, **13**(2):209-222.
321. Killion JJ, Radinsky R, Fidler IJ: **Orthotopic models are necessary to predict therapy of transplantable tumors in mice**. *Cancer metastasis reviews* 1998, **17**(3):279-284.
322. Singh RK, Tsan R, Radinsky R: **Influence of the host microenvironment on the clonal selection of human colon**

carcinoma cells during primary tumor growth and metastasis. *Clinical & experimental metastasis* 1997, **15**(2):140-150.

323. Aamdal S, Fodstad O, Pihl A: **Human tumor xenografts transplanted under the renal capsule of conventional mice. Growth rates and host immune response**. *International journal of cancer Journal international du cancer* 1984, **34**(5):725-730.
324. Bogden AE: **The subrenal capsule assay (SRCA) and its predictive value in oncology**. *Annales chirurgiae et gynaecologiae Supplementum* 1985, **199**:12-27.
325. Custer RP, Bosma GC, Bosma MJ: **Severe combined immunodeficiency (SCID) in the mouse. Pathology, reconstitution, neoplasms**. *The American journal of pathology* 1985, **120**(3):464-477.
326. Bosma GC, Custer RP, Bosma MJ: **A severe combined immunodeficiency mutation in the mouse**. *Nature* 1983, **301**(5900):527-530.
327. Saxena RK, Saxena QB, Adler WH: **Defective T-cell response in beige mutant mice**. *Nature* 1982, **295**(5846):240-241.
328. Kerbel RS: **Human tumor xenografts as predictive preclinical models for anticancer drug activity in humans: better than commonly perceived-but they can be improved**. *Cancer biology & therapy* 2003, **2**(4 Suppl 1):S134-139.
329. Suggitt M, Bibby MC: **50 years of preclinical anticancer drug screening: empirical to target-driven approaches**. *Clinical cancer research : an official journal of the American Association for Cancer Research* 2005, **11**(3):971-981.
330. Voskoglou-Nomikos T, Pater JL, Seymour L: **Clinical predictive value of the in vitro cell line, human xenograft, and mouse allograft preclinical cancer models**. *Clinical cancer research : an official journal of the American Association for Cancer Research* 2003, **9**(11):4227-4239.
331. Decker S, Hollingshead M, Bonomi CA, Carter JP, Sausville EA: **The hollow fibre model in cancer drug screening: the NCI experience**. *Eur J Cancer* 2004, **40**(6):821-826.

332. Hall LA, Krauthauser CM, Wexler RS, Slee AM, Kerr JS: **The hollow fiber assay**. *Methods in molecular medicine* 2003, **74**:545-566.
333. Clarke AR, Hollstein M: **Mouse models with modified p53 sequences to study cancer and ageing**. *Cell death and differentiation* 2003, **10**(4):443-450.
334. Kwak I, Tsai SY, DeMayo FJ: **Genetically engineered mouse models for lung cancer**. *Annual review of physiology* 2004, **66**:647-663.
335. Kasper S, Smith JA, Jr.: **Genetically modified mice and their use in developing therapeutic strategies for prostate cancer**. *The Journal of urology* 2004, **172**(1):12-19.
336. Oppelt A: **Imaging Systems for Medical Diagnostics: Fundamentals, Technical Solutions and Applications for Systems Applying Ionizing Radiation, Nuclear Magnetic Resonance and Ultrasond**: Siemens; 2005.
337. Zutphen LFMv, Baumans V, Beynen AC: **Principles of laboratory animal science : a contribution to the humane use and care of animals and to the quality of experimental results**, Rev. edn. Amsterdam ; New York: Elsevier; 2001.
338. Taniguchi M, Tatsuta N, Yokota H, Ouguchi M, Higashi K, Okimura T, Yamamoto I: **Incrustation and uptake of skeletal imaging agent in transitional cell carcinoma**. *Journal of nuclear medicine : official publication, Society of Nuclear Medicine* 1997, **38**(8):1206-1207.
339. Moreno AJ, Toney MA, Griffith JC, Rodriguez AA, Turnbull GL: **Serendipitous finding of transitional cell carcinoma of the kidney on bone and gallium imaging**. *Clinical nuclear medicine* 1991, **16**(3):165-166.
340. Liotta LA: **An attractive force in metastasis**. *Nature* 2001, **410**(6824):24-25.
341. Schmidt MM, Wittrup KD: **A modeling analysis of the effects of molecular size and binding affinity on tumor targeting**. *Molecular cancer therapeutics* 2009, **8**(10):2861-2871.
342. AB RI: **LigandTracer for interaction analysis**. In., Revision E edn: Ridgeview Instruments AB.

343. Cunha L, Horvath I, Ferreira S, Lemos J, Costa P, Vieira D, Veres DS, Szigeti K, Summavielle T, Mathe D *et al*: **Preclinical imaging: an essential ally in modern biosciences**. *Molecular diagnosis & therapy* 2014, **18**(2):153-173.